

Alma Mater Studiorum – Università di Bologna

DOTTORATO DI RICERCA IN

Ingegneria Civile, Ambientale e dei Materiali

Ciclo XXVII

Settore Concorsuale di afferenza: 08/B1

Settore Scientifico disciplinare: ICAR/07

**MODELLING THE DYNAMIC RESPONSE
OF ROCKFALL PROTECTION BARRIERS**

Presentata da: Alessio Mentani

Coordinatore Dottorato

Alberto Lamberti

Relatore

Guido Gottardi

Correlatori

**Laura Govoni
Anna Giacomini**

Esame finale anno 2015

THESIS FORMAT

This thesis is presented as a series of journal and conference papers. The contributions of the candidate and co-author(s) for the papers comprising chapter 3, 4 and 5 are hereby set forth.

Journal Paper 1

The paper presented in Chapter 3 is co-authored by the candidate, first-authored by Dr. Cristina Gentilini and co-authored by Professor Guido Gottardi, Dr. Laura Govoni and Professor Francesco Ubertini, and is published as

Gentilini, C., Gottardi, G., Govoni, L., Mentani, A., Ubertini, F. (2013). Design of falling rock protection barriers using numerical models. *Engineering Structures*, 50: 96-106. DOI: 10.1016/j.engstruct.2012.07.008

Journal Paper 2

The paper presented in Chapter 4 is co-authored by the candidate, first-authored by Professor Stefano de Miranda, and co-authored by Dr. Cristina Gentilini, Professor Guido Gottardi, Dr. Laura Govoni and Professor Francesco Ubertini, and is published as

de Miranda, S., Gentilini, C., Gottardi, G., Govoni, L., Mentani, A., Ubertini, F. (2015). Virtual testing of existing semi-rigid rockfall protection barriers. *Engineering Structures*, 85: 83-94. DOI: 10.1016/j.engstruct.2014.12.022

Journal Paper 3

The paper presented in Chapter 5 is first-authored by the candidate and co-authored by Dr. Anna Giacomini, Professor Olivier Buzzi, Dr. Laura Govoni, Professor Stephen Fityus and Professor Guido Gottardi and has been submitted for publication as

Mentani, A., Giacomini, A., Buzzi, O., Govoni, L., Gottardi, G., Fityus, S. (2015). Numerical modelling of a low-energy rockfall barrier performance: new insight into the bullet effect. *Rock Mechanics and Rock Engineering*, submitted January 2015.

Conference papers

- ✓ de Miranda, S., Gentilini, C., Gottardi, G., Govoni, L., Mentani, A., Ubertini, F., (2011). *On the structural response of falling rock protection barriers*, in: Atti XX Congresso dell'Associazione Italiana di Meccanica Teorica e Applicata – AIMETA 2011, Conselice (RA), Publi&stampa, pp. 1-10.
- ✓ Gottardi, G., Govoni, L., Mentani, A., Ranalli, M., Strada, C. (2011). *The effectiveness of protection systems toward rockfall risk mitigation*. In: Geotechnical Safety and Risk (ISGSR 2011). Munich, Germany, June 2-3, 2011: 157-164.
- ✓ Gorlato, A., Gottardi, G., Govoni, L., Mentani, A., Ranalli, M., Strada, C. (2012). *The role of falling rock protection barriers in the context of landslide risk analysis and mitigation*. In Proceedings of: 12th Congress INTERPRAEVENT, Klagenfurt, International Research Society INTERPRAEVENT, April 23-26, 2012: 699-706.

-
- ✓ Gentilini, G., Gottardi, G., Govoni, L., Mentani, A., Ubertini, F. (2012). *Dynamic analysis of flexible falling rock protection barriers*. In Proceedings of: 7th International Conference on Computational Mechanics for Spatial Structures (IASS-IACM 2012), Sarajevo, Bosnia and Herzegovina, April 2-4, 2012: 112-115.

 - ✓ Gottardi, G., Govoni, L., Mentani, A., Gentilini, C., Ubertini, F. (2014) *Modelling for the design of passive protection measures against rockfall*. In Proceedings of: 8th International Conference on Physical Modelling in Geotechnics (ICPMG 2014), Perth, Australia, January 14-17, 2014, 2: 1179-85.

ABSTRACT

Mountainous areas are prone to natural hazards like rockfalls. Among the many countermeasures, rockfall protection barriers represent an effective solution to mitigate the risk. They are metallic structures designed to intercept rocks falling from unstable slopes, thus dissipating the energy deriving from the impact. This study aims at providing a better understanding of the response of several rockfall barrier types, through the development of rather sophisticated three-dimensional numerical finite elements models which take into account for the highly dynamic and non-linear conditions of such events.

The models are built considering the actual geometrical and mechanical properties of real systems. Particular attention is given to the connecting details between the structural components and to their interactions. The importance of the work lies in being able to support a wide experimental activity with appropriate numerical modelling. The data of several full-scale tests carried out on barrier prototypes, as well as on their structural components, are combined with results of numerical simulations. Though the models are designed with relatively simple solutions in order to obtain a low computational cost of the simulations, they are able to reproduce with great accuracy the test results, thus validating the reliability of the numerical strategy proposed for the design of these structures. The developed models have shown to be readily applied to predict the barrier performance under different possible scenarios, by varying the initial configuration of the structures and/or of the impact conditions. Furthermore, the numerical models enable to optimize the design of these structures and to evaluate the benefit of possible solutions. Finally it is shown they can be also used as a valuable supporting tool for the operators within a rockfall risk assessment procedure, to gain crucial understanding of the performance of existing barriers in working conditions.

ACKNOWLEDGMENT

I would like to express my special appreciation and thanks to my supervisor Prof. Guido Gottardi and co-supervisors Dr. Laura Govoni and Dr. Anna Giacomini for the support, help and guidance I received from them throughout this study. You always encouraged my research and allowed me to grow as a research scientist.

Prof. Olivier Buzzi and Prof. Stephen Fityus are sincerely acknowledged for the valuable advices and for having let possible my stay at the Centre for Geotechnical and Materials Modelling. The time spent at the Research Centre was a great experience and I am thankful to Prof. Scott Sloan and all the Department staff for their help and valuable suggestions.

At the same time I would sincerely thank Prof. Francesco Ubertini, Prof. Stefano de Miranda and Dr. Cristina Gentilini, their brilliant advices and contributions have been essential to fulfil this work.

The work here described is based on the data of experimental activities supported by Consorzio Triveneto Rocciatori (Belluno, Italy) and Officine Maccaferri (Bologna, Italy) in a cooperation established with DICAM Department of the University of Bologna. Data derived from the Australian Nationally Funded research project "Barriers for cost-effective rockfall hazard mitigation" (LP0989965) are also employed within this work. Part of the study has been carried out with the support of the Autonomous Province of Bolzano within the research activities of the European project PARAMount (imProved Accessibility, Reliability and safety of Alpine transport infrastructure related to MOUNTainous hazard in a changing climate). These supports are gratefully acknowledged. The author is particularly grateful to Dott. Claudia Strada for her contribution.

Finally, I wish to thank my family and all my friends for supporting and encouraging me during these years. I am not used to say them how much they are important to me.

TABLE OF CONTENTS

THESIS FORMAT

ABSTRACT

ACKNOWLEDGEMENTS

CHAPTER 1 – INTRODUCTION

1.1	Rockfall protection barriers.....	1
1.2	The need for further research.....	4
1.2.1	High-energy rockfall protection barriers	6
1.2.2	Low-energy rockfall protection barriers.....	9
1.3	Research aims.....	11
1.4	Thesis outline.....	13

CHAPTER 2 – BACKGROUND TO THE RESEARCH

2.1	Required numerical models for rockfall barriers analysis	15
2.2	Physical modelling of structural components.....	16
2.2.1	Testing of meshes	18
2.2.2	Testing of energy dissipating devices.....	26
2.3	Physical modelling of rockfall barriers.....	30
2.3.1	Procedures according to guidelines	31
2.3.2	Full-scale testing of rockfall protection barriers.....	34
2.4	Numerical modelling of rockfall protection systems	39
2.4.1	Modelling of meshes	40
2.4.2	Simplified models of rockfall protection barriers.....	47
2.4.3	Advanced models of rockfall protection barriers	51

CHAPTER 3 – NUMERICAL MODEL TO INVESTIGATE THE RESPONSE OF HIGH-ENERGY ROCKFALL BARRIERS

<i>Introduction</i>	55
<i>Background</i>	57
<i>Aims of the research</i>	62

Journal paper 1

3.1 Design of falling rock protection barriers using numerical models	64
<i>Abstract</i>	64
3.1.1 Introduction	65
3.1.2 Experimental details	67
<i>Impact tests on the interception structure</i>	67
<i>Full-scale impact tests on barrier prototypes</i>	68
3.1.3 The numerical approach	70
<i>Modelling of the supporting structures</i>	70
<i>Modelling of the connecting components</i>	71
<i>Modelling of the interception structures</i>	72
3.1.4 Model development and calibration	72
<i>Modelling details: interception structure</i>	73
<i>Modelling details: connecting components</i>	76
3.1.5 Model assessment	80
<i>Model response at the maximum energy level</i>	81
<i>Model response at the service energy level</i>	82
3.1.6 Use of the model as a design tool	85
3.1.7 Concluding remarks	88

Conference paper 1

3.2 Modelling for the design of passive protection measures against rock fall	89
<i>Abstract</i>	89
3.2.1 Introduction	90
3.2.2 Experimental testing	91

<i>Experiments on the interception structure</i>	91
<i>Experiments on barrier prototypes</i>	92
3.2.3 Numerical approach	94
<i>Modelling of the interception structures</i>	95
<i>Modelling of the energy dissipating devices</i>	97
3.2.4 Model assessment	99
<i>Model response at the maximum energy level</i>	99
<i>Model response at the service energy level</i>	99
3.2.5 Model predictions for design scenarios	100
<i>Impact of blocks with different shape</i>	100
<i>Impact on different areas of the barrier</i>	101
3.2.6 Conclusions	102

CHAPTER 4 – ANALYSIS OF EXISTING SEMI-RIGID ROCKFALL BARRIERS: A NUMERICAL APPROACH

<i>Introduction</i>	103
<i>Background</i>	104
<i>Aims of the research</i>	106

Conference paper 2

4.1 The role of falling rock protection barriers in the context of landslide risk analysis and mitigation	108
<i>Abstract</i>	108
4.1.1 Introduction	109
4.1.2 The falling rock protection barriers within the Autonomous Province of Bolzano	110
4.1.3 Modelling of falling rock protection barriers	112
4.1.4 Numerical modelling of the ANAS barrier type	114
4.1.5 Results of the numerical analyses on the ANAS barrier model	116
4.1.6 Concluding remarks	119

Journal paper 2

4.2	Virtual testing of existing semi-rigid rockfall protection barriers	121
	<i>Abstract</i>	121
4.2.1	Introduction	122
4.2.2	Semi-rigid rockfall protection barriers	124
4.2.3	Virtual testing of semi-rigid barriers	128
	<i>Numerical approach</i>	128
	<i>Testing programme</i>	131
4.2.4	Results	133
	<i>Tests in service condition (S)</i>	134
	<i>Tests in limit condition (L)</i>	138
	<i>Tests in failure condition (F)</i>	141
4.2.5	Concluding remarks.....	146

CHAPTER 5 – NUMERICAL MODEL OF A LOW-ENERGY ROCKFALL BARRIER

	<i>Introduction</i>	147
	<i>Background</i>	148
	<i>The bullet effect phenomenon</i>	151
	<i>Aims of the research</i>	158

Journal paper 3

5.1	Numerical modelling of a low-energy rockfall barrier performance: new insight into the bullet effect	159
	<i>Abstract</i>	159
5.1.1	Introduction	160
5.1.2	Details of the experiments on the barriers	161
	<i>Barrier models selected for the study</i>	162
	<i>Testing set up</i>	163
	<i>Tests performed on the barrier</i>	164
5.1.3	Numerical modelling	165

<i>Structural elements of the barrier</i>	165
<i>Double twist hexagonal wire mesh</i>	166
<i>Internal constraints and boundary conditions</i>	169
<i>Test block</i>	170
<i>Analyses</i>	170
5.1.4 Validation of the model	171
5.1.5 Investigation on the bullet effect	175
<i>Response of the double twist hexagonal mesh</i>	175
<i>Performance of the full barrier in relation to the bullet effect</i>	179
<i>Effect of intermediate longitudinal cables on the barrier response</i>	182
5.1.6 Concluding remarks.....	184

CHAPTER 6 – CONCLUDING REMARKS

6.1 Introduction.....	186
6.2 Original contributions and main findings	186
6.2.1 Development of advanced three-dimensional finite element models of high-energy rockfall protection barriers	186
6.2.2 Evaluation of performance of existing protective structure by means of a numerical approach to support rockfall risk assessment	187
6.2.3 Development of a numerical model of a low-energy rockfall barrier and investigation about the effectiveness of the energy criterion	189
6.4 CONCLUSION	190
REFERENCES	191

INTRODUCTION

1.1 ROCKFALL PROTECTION BARRIERS

Mountain areas cover about the 20% of all the European land and one-third of the European Countries have mountains on more than the 50% of the entire territory. The extreme environment makes mountain areas prone to natural phenomena such as landslides, rockfalls, mudslides, avalanches. Among these, rockfalls are very sudden, highly unpredictable and strongly influenced by weather events such as precipitations, freeze/thaw cycles and also wind, drought, fires and permafrost modification. According to the European Environment Agency, mountain areas have also seen considerable demographic change, and tourism has led to significant seasonal variation in the population make-up. As a result, populations and assets at risk have increased leading to enhanced rockfall risk.

Toward this risk different protection measures were developed over the last years and rockfall barriers represent one of the most commonly used passive systems. Rockfall barriers are metallic structures that represent efficient solutions to intercept and stop the blocks detached from an unstable slope.

Rockfall is a natural hazard which usually involves small areas and high velocities (Volkwein et al. 2011). It consists of free falling blocks of different volumes (ranging between 0.01 and 100 m³) which are detached from a steep rock wall or a cliff, after an initial block toppling or a local slide, associated with gravity, water pressure in the joints or adjacent block thrust (Giani 1992).

Rockfall hazard is a sudden and not easily predictable phenomenon, because of the several uncertainties in the estimation of the triggering factors that can lead to this event. If existing infrastructures need to be protected and the rockfall risk cannot be limited by zone planning of the area, then mitigation measures are required and a further level of investigation must be carried out in order to study the most probable propagation of the blocks falling along the slope.

Thus, the first problem in mitigating rockfall risk is to predict the motion of the falling bodies. Block mass and velocity, height of rebound and run-out distance are the typical outputs of numerical simulations carried out to identify the rock falling trajectory and to predict the most probable energy at impact.

Based on the estimation of the rockfall event properties, an adequate protective countermeasure must be designed to reduce the risk. These solutions are historically classified in two different technical-design approaches:

- *Active measures*, they prevent rocks from falling down the slope by stabilising or removing the located risk.
- *Passive measures*, they act during the event by intercepting and stopping the falling rock, therefore avoiding it from reaching the element at risk.

Among the many available passive protection systems, rockfall barriers represent an efficient solution. They are metallic structures designed to dissipate the kinetic energy deriving from the impact of the falling blocks. For this reason, the performance of a rockfall protection barrier is usually expressed in terms of the maximum energy capacity they are able to absorb. Since the dissipation of energy is accomplished through the accumulation of permanent deformations of the system, the rating of the barrier can be defined also in terms of its deformability. The greater is the barrier capacity, the higher its plastic compliance as reported in Fig. 1.1.

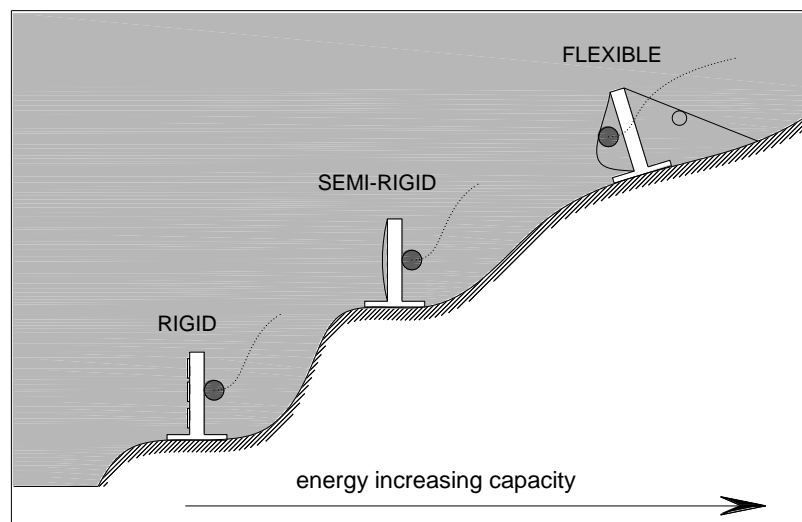


Figure 1.1 Scheme of the relevant typologies of rockfall barrier, absorbing capacity related to the system deformation (Gottardi et al. 2011).

Thus, it is common to talk about *high-energy* or *flexible barriers* when the system is able to dissipate high impacting energy value (up to 8000 kJ) by means of large irreversible deformations. On the contrary, if the system is less deformable with a comparatively minor absorbing capacity we refer to *low-energy* or *rigid* and *semi-rigid barriers* (few hundreds kilojoules).

The behaviour of a rockfall protection barrier is traditionally assessed referring to results of full-scale tests in which a prototype is subjected to the impact of block having a known mass and velocity. In Europe a guideline was recently developed (EOTA 2008) to supply a standard procedure to evaluate their performance through these experiments, in order to have a uniform assessment of the products made by different manufacturers.

A typical rockfall protection barrier is made of several identical functional modules installed in sequence for the required length. Each module is constituted by various components having different functions. Particularly, a functional module consists of three main parts plus the foundation system, as illustrated in Fig. 1.2. The parts have the following function:

- *Interception structure.* It is a metallic net of various mesh types. It has the function to intercept and stop the falling block. The mesh has to bear the direct impact of the impacting body, absorbing most of the kinetic energy deriving from the event by means of elasto-plastic deformations.
- *Supporting structure,* it is constituted by steel posts of different section types. They are designed to keep in position the interception structure and to transmit the forces resulting from the impact to the foundations.
- *Connecting components.* They are cables, energy dissipating devices, studs, clamps and other elements involved at the intersection nodes for the internal connection between the various constitutive elements. They have the function to connect the mesh to the supporting structure and transmit the stresses, resulting from the impact, to the foundations.

- *Foundation systems.* Generally they are designed as base plate for the post or anchoring system for the cables. They have to be suitably designed to distribute the impact loads to the ground without reaching failure, which could lead to overturning of the barrier.

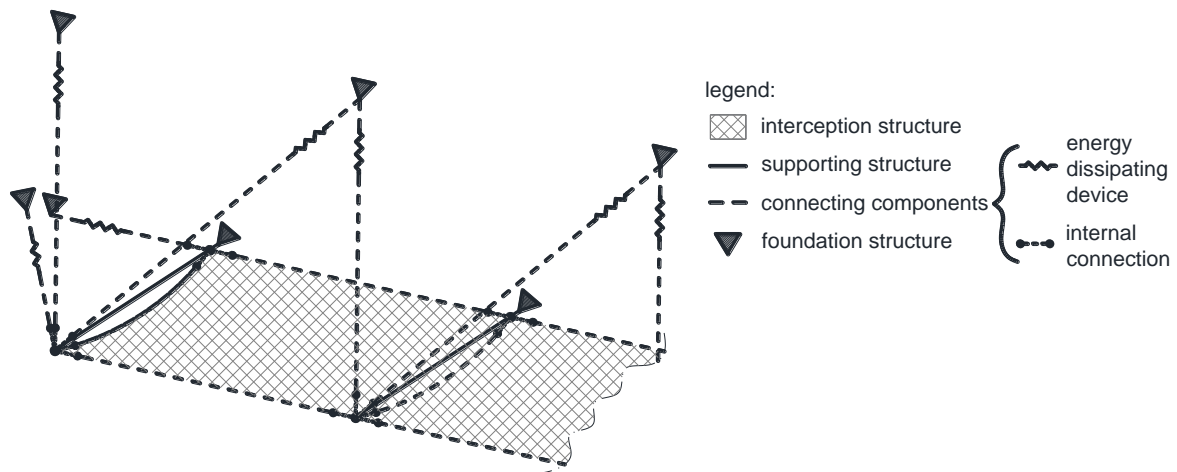


Figure 1.2 Scheme of the main components of a rockfall barrier functional module.

Recently, different authors have examined the outcomes of the existing research related to rockfall issues, producing a summary review of the worldwide contributions (Lambert and Nicot 2011; Volkwein et al. 2011, Turner and Schuster 2013; Duncan 2014). From the hazard assessment to the analysis of the protection measures used, all the relevant problematic were described highlighting the need for further research.

Within this context, the thesis aims at significantly advance the analysis of the performance of rockfall barriers by means of numerical methods. The response of protective systems having low to high energy absorption capacity towards dynamic loadings has been investigated. The different problematic relevant to the two systems type are extensively explained in next Section.

1.2 THE NEED FOR FURTHER RESEARCH

Rockfall protection barriers are designed by assembling many functional elements to withstand strongly dynamic impulsive events derived from falling blocks. It implies high non-linearity on the response at all the components, while the interactions

generated between them involve complex mechanisms that are not easy to be predicted. Further, the impact condition of a rockfall event on a protection barrier has a strong variability. Many parameters should be considered when an intervention project is planned, both in terms of design of the barrier (i.e. geometrical and mechanical characteristics) and prediction of the rockfall event (i.e. volume, velocity and trajectory of the impacting block).

Considering the existing rockfall protection barriers structures, the problem should be divided in two main branches:

- *High-energy barriers*, usually defined also as flexible (Fig. 1.3a), they allow the development of permanent deformation of the structure in order to dissipate elevate kinetic energy level (from few hundreds to thousands of kilojoules).
- *Low-energy barriers*, named rigid or semi-rigid for the characteristic of the system (Figs. 1.3b and c). The structure is similar to the flexible barrier but they present crucial differences in some constitutive elements and at their interconnections leading to a simplified design. Due to this modification of the structure the system is less deformable, thus influencing the overall energy absorption capacity which is generally lower than few hundreds kilojoules.



Figure 1.3 Rockfall protection barrier types (courtesy of the Autonomous Province of Bolzano): a) flexible; b) semi-rigid and c) rigid.

Though the problematic field is the same, they are hereinafter explained the different aims that need to be developed concerning the study of the two systems.

1.2.1 High-energy rockfall protection barriers

High-energy rockfall barriers are designed to arrest blocks moving along a slope by means of large plastic deformations. Several manufacturers produce different prototypes of barriers with energy absorption capacity that can range from few hundreds to thousands kilojoules. According to the deformation level they are able to perform, they are also defined as flexible barriers. Traditionally, the performance of high-energy barriers is assessed by means of empirical procedures based on full-scale tests of the prototypes and their components.

Nowadays, these full-scale experiments are carried out accordingly to standardised procedures (Gerber 2001; EOTA 2008) planned in order to gain a full knowledge of the structure response to withstand a given kinetic energy at the impact. Two main test site configurations are generally considered. An inclined test site where the barrier is installed along a slope and the block is guided to impact the fence by means of a trolley running along a track cable (Fig. 1.4a). Differently, in a vertical test site the block is lifted by a crane to a specific height and released to impact the prototype in a free-fall motion (Fig. 1.4b).

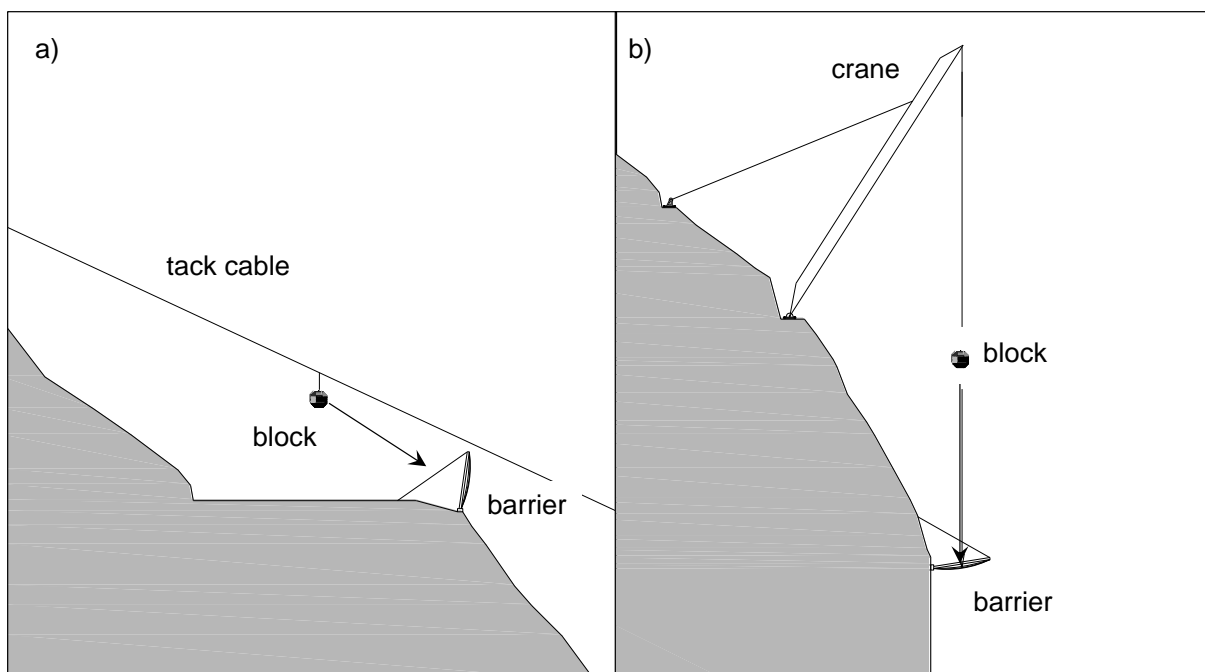


Figure 1.4 Full-scale procedures for testing rockfall protection barriers: a) inclined test site and b) vertical test site (Gottardi and Govoni 2010).

Test results are monitored through different measurement systems: high-speed camera or other suitable instruments to record the block velocity and displacement, load cells to evaluate forces acting at the foundation structure and additional direct measurements for other relevant data. In the standardised procedures the falling rock protection kit considered is made of three functional modules and impacted in the central panel in its geometrical centre. The barrier is tested using a concrete block of polyhedric shape and the test is conducted in order to gain a velocity at impact greater than 25 m/s. In this research, the outcomes of a series of full-scale tests carried out on different prototypes in a vertical drop test site are considered (Gottardi and Govoni 2010).

The performance assessment through a well-defined procedure represents a good opportunity to have a standardised definition of the reliability of different prototypes. On the other hand, it must be reminded that a rockfall event is variable and unpredictable; further the protection barrier in a real installation could have different geometrical and mechanical characteristics due to some restriction of the investigated area. For this reasons, when the results extrapolated from the full-scale tests are used for the design of a barrier installation, many safety factors need to be introduced. In order to assess its response to the variability of on-site impact condition, the experimental setup could be modified to perform various testing condition, but full-scale tests are cost expensive and time consuming procedures.

Despite the importance of the experimental testing assessments, in order to gain a real understanding of the performance of flexible barriers to the variability of the impact conditions and to reduce the costs of testing procedures, other instruments can be used. Over the last 20 years, numerical analyses have proved to be a valuable instrument to investigate the effect of highly non-linear dynamic events, like impact tests against metallic structures, like rockfall barriers.

Numerical modelling is a flexible tool, by modifying the submitted input results, different configuration can be obtained, ensuring the reliability of the obtained

outcomes if the model was well-validated. Data of full-scale tests carried out on the barrier prototypes are essential in order to assess the numerical model effectiveness by simulating retrospectively the experiments and compare the results. Thus, if a database of experiments is available, a numerical model of a rockfall barrier can be calibrated.

Some preliminary analytical and numerical models for these structures, with both finite and discrete elements methods, have been developed in the last few years to achieve such goal. There are simplified analytical models (Hearn et al. 1991; Peila et al. 1998; Cantarelli et al. 2008), two-dimensional FE model (Govoni et al. 2011) and complete three-dimensional FE and DE models (Nicot et al. 2001; Cazzani et al. 2002; Volkwein et al. 2005; Gentilini et al. 2012a) studying the phenomenon with different approaches. Though simplified models can be useful for a preliminary analysis of a prototype, in order to use subsequently the model as a predictive tool, an advanced three-dimensional numerical modelling technique is more suitable. It should be highlighted that to assembly advanced model of a rockfall barrier, a real understanding of all the constitutive components of the system is required. Therefore, gather information about their response under dynamic loading is a necessary step and experiments under dynamic conditions should be considered whenever possible.

The models already developed in literature have shown that there is a need of a better predictive numerical tool for the site-specific assessment of these structures. There is still a lack of information on the procedures for the assessment of the models already developed. Some details should be better explained and validated. The numerical tool developed must be able to reproduce the barrier behaviour of experimental results under various loading or design configurations, because only a well-calibrated model can be confidentially used as a design instrument. The availability of a wide database of full-scale tests carried out at different impact conditions on rockfall barriers and their components, allows to further enhance this study.

More accurate numerical models of these passive protection systems have been recently proposed by different group of research (Bertrand et al. 2012; Van Tran et al.

2013; Bourrier et al. 2014; Escallon et al. 2014; Moon et al. 2014) proving the relevant interest on this research topic during the last few years.

1.2.2 Low-energy rockfall protection barriers

Low-energy barriers are usually installed when rockfall events expected in the interested area involve low values of impacting energy. In many cases they are installed in condition of extreme urgency, without a specific structural design or comprehensive plan of countermeasures. Differences in the design, with respect to flexible barriers, can be found in the characteristics of some constitutive elements and at their internal connections, leading to a suitable structure. Constraints are restrictive and the system has lower deformability. Although some plastic deformations are likely to occur, semi-rigid barriers may be subjected to elastic deformation only. Their energy absorbing capacity has never been properly defined but they are generally considered able to withstand values from few to less than 300 kJ.

Although these barriers feature a simple structure, their performance was never quantified up to now. The European guidelines (EOTA 2008) were developed to define a methodology to assess the effectiveness of barrier having capacity greater than 100 kJ. As a consequence, the manufacturers were encouraged to analyse only the flexible system performance since full-scale testing is mandatory to gain a certification of the product. On the contrary, low-energy barriers were not studied experimentally and there is still a lack of information about their response to dynamic events.

Nevertheless the use of semi-rigid barrier is still worldwide requested. From Japan, as documented by Muraishi et al. (2005), where 68% of the monitored rockfall events involved energy lower than 100 kJ, to Australia where due to the nature of geological environments low energy levels are expected (Fityus et al. 2012, Spadari et al. 2013a). In mountainous areas, like the Alps in Europe or the Rocky Mountains in the US, greater values of kinetic energy are usually involved along the unstable slope and flexible barrier are the most demanded system. However, a recent study conducted by

the Autonomous Province of Bolzano (Italy) has shown a different scenario in the Alps territory (Gottardi et al. 2011). Within the context of the European project PARAMount (imPROved Accessibility, Reliability and safety of Alpine transport infrastructure related to MOUNTainous hazard in a changing climate) the Province has developed a tool to analyse the rockfall risk into the territory. In the process of the evaluation of the hazard assessment, a complete inventory of the existing passive countermeasures was achieved. A thousand of falling rock protection barriers, still in exercise in the province area, were identified of both low and high-energy type. Unexpectedly, about the 50% of the identified barriers belongs to the low-energy type. Reason for the wide use of these typologies can be various. First of all, in a forested area the expected energy at impact could be highly affected by the mitigating effect of the vegetation (Volkwein et al. 2011). Recent studies have shown that in the interaction between trees and falling blocks, the forest can be able to dissipate up to 200-500 kJ (Dorren and Berger 2006; Dorren et al. 2007; Jonsson 2007), leading to lower value of the expected energy obtained from rockfall trajectory models.

Further, due to their low deformability, semi-rigid barrier can be installed close to the road, railways or infrastructure they are called to protect and they are less expensive systems, easier to be installed especially in conditions of extreme urgency.

In order to evaluate the effectiveness of these structures against rockfall in a hazard assessment procedure, the energy absorption capacity of the system should be known. The absence of standards for an experimental assessment of semi-rigid barriers performance, stresses the need for improve the understanding of their dynamic behaviour and to assess a procedure to supply this lack of information. A suitable numerical investigation can be addressed to investigate the performance of these structures. Based on a well-defined numerical strategy and on detailed information of their design properties, a preliminary understand of the response of semi-rigid systems can be assessed.

Nowadays, due to the continuous request from public administration involved in the defence of the territory against rockfall risk, many manufacturers are developing the

study of new protection barriers for the low energy case. Recently Buzzi et al. (2013) at the CGMM (Centre for Geotechnical and Materials Modelling) of The University of Newcastle (Australia) have conducted an experimental campaign to analyse the structural response under dynamic conditions of newly developed prototypes having low-energy absorbing capacity.

A cooperation established with the group of research of the CGMM allowed the accessibility to such a wide database of full-scale tests, in order to define a numerical strategy also for these barrier types. Thus, as for the flexible systems, a numerical model opportunely calibrated to reproduce the test outcomes can be exploited to analyse the structure performance under different impact conditions.

1.3 RESEARCH AIMS

Full-scale impact tests are usually carried out to evaluate the performance of falling rock protection barriers under strongly dynamic events deriving from the impact of rock blocks, providing several details about the structure response. On the other hand the on-site conditions could be widely different from the standardised experimental setup and, in order to plan and design a barrier installation, many safety factors need to be considered.

The standard experimental configuration defined by the European Guideline does not take into account of the many other loading cases possible or geometrical configurations. Obviously, the physical model could be modified, but the full-scale tests are expensive solutions and the number of impact events, as well as the geometrical configuration of the system, can be unlimited.

Therefore, it is highly desirable to develop well-validated numerical models for the prediction of rockfall barriers response. Numerical models are reliable tool to gain understanding of non-linear dynamic analyses on metallic structures like rockfall protection barriers.

In order to develop a numerical strategy able to assess the performance of a system by varying its configuration, it is essential to study the singular component response in dynamic condition. Hence, the outcomes of experimental dynamic tests carried out on the single constitutive element should be considered.

Subsequently, the model of the barrier can be assembled, calibrated and validated, based on the results of full-scale tests. A database of experiments carried out at various impact conditions on the system should be preferred to enhance the ability of the numerical tools developed.

Once the reliability of the numerical model has been assessed, its use could be extended with the aim to predict its response to several impact configurations, using the model as a design tool.

A numerical approach that takes into account the composition and interrelation between the different constitutive elements of the structure and provides a reliable tool for the prediction of the performance of various barrier types is introduced in this thesis. Due to the importance of accurate modelling of the non-linear mechanical and geometrical characteristics of the elements involved, whenever possible the development of the numerical strategy here presented is strongly underpinned by extensive experimental data to calibrate the response of rockfall protection barriers.

In absence of these outcomes, as for the case of low-energy barriers already installed in the Autonomous Province of Bolzano, the well-defined numerical strategy developed for the other systems has been implemented to fill the lack of information.

Therefore to significantly advance three-dimensional numerical analysis of rockfall protection barriers, the aims of the research covered in this thesis are:

- 1- Analyse the behaviour of the single structural elements under dynamic loadings. Development of a strategy for three-dimensional numerical model for high-energy rockfall barriers. Validate the model reliability by reproducing retrospectively the outcomes of a database of results from full-scale tests carried out under several impact conditions.

- 2- Use the numerical model as a design tool, to evaluate the rockfall protection system performance under more realistic impact scenarios. Examine the potentiality of the created numerical tool to estimate the performance or to improve the design of a barrier, thus reducing the number of new experimental tests.
- 3- Develop a three-dimensional numerical model for low-energy rockfall barriers. In absence of experimental details use, the numerical strategy validated on high-energy barriers and, when experimental data are available, assess the model effectiveness through results comparison.
- 4- Implement the numerical strategy defined for low and high-energy protection barriers to evaluate the effectiveness of the existing barriers towards rockfall hazard mitigation.
- 5- Investigation of the dependence of the semi-rigid rockfall barrier performance to the variation of the impact conditions of the event or the geometric configuration of the structure through the numerical models.

1.4 THESIS OUTLINE

The thesis systematically works through the following steps in order to arrive at each of the research aims:

Chapter 2 provides background information to the areas concerning the physical and numerical modelling of rockfall protection barriers and single structural components.

In Chapter 3 a numerical FE three-dimensional model of a high-energy rockfall protection barrier is presented, further enhancing a numerical strategy previously developed. The effectiveness of the model is assessed by retrospectively simulate the experimental outcomes of several impact tests carried out at various energy level. The developed model capacity is then explored further using the model as a predictive

tool. The response of the rockfall barrier by varying the impact conditions or the structure design is addressed.

In Chapter 4 a thorough investigation is carried out to define the behaviour of several semi-rigid and rigid rockfall barriers installed within the Alps territory. Since no experimental evidences are available on the response of these structures, numerical models are developed accordingly to the strategy earlier defined. The model is employed to provide the system energy absorption capacity which represents the essential parameter to be assessed for a rockfall risk analysis. The barrier response is analysed assessing the performance in service and limit working conditions. The failure mechanism is also investigated to gain understand of the systems weakness. Finally, parametric simulations are carried out to define the response of the considered barrier in on-site configurations.

In Chapter 5 the numerical study of a specific low-energy barrier prototype is illustrated. The developed work combines extensive experimental testing of the system and its components with numerical FEM techniques. The designed model is calibrated and validated by comparing the simulations outcomes with results of several full-scale tests carried out on the barrier at The University of Newcastle (NSW, Australia). The numerical model is then exploited to estimate the influence of the block size on the barrier performance and new evidences about the so-called bullet effect are identified. Further, a different design, similar to realistic installation of the barrier, is studied to define pros and cons generated on the modified structure.

This leads to concluding remarks as well as recommendations for further research, which form Chapter 6.

BACKGROUND TO THE RESEARCH

2.1 REQUIRED NUMERICAL MODELS FOR ROCKFALL BARRIERS ANALYSIS

This thesis aims at advancing the analysis options available for the simulation of the response of passive protection system toward rockfall events through the development of techniques for the full three-dimensional numerical modelling of a rockfall barrier. The numerical strategy must be developed by comparing results of an integrated experimental study of the dynamic response of the barrier and its relevant constitutive elements considered alone.

A rockfall barrier is made of several identical modules, each of them composed of different parts: an interception structure, a supporting structure and connecting components. The performance of the system is assessed based on data deriving from a physical modelling of the event considering full-scale experimental tests carried out. In Europe the test on rockfall protection barriers have to be executed in accordance to standardised procedure defined in a guideline supplied by the authorities (EOTA 2008). In the overall response of a barrier to an impact event like rockfall, the constitutive elements of the system, in particular the interception structure composed by the mesh and the connecting elements such as energy dissipating devices, play a crucial role. Thus the components behaviour has to be investigated in a preliminary experimental analysis and then a numerical characterisation of their response can be obtained. Dynamic experiments may be preferred to static loading conditions since rockfall events can results in high dynamic impulsive loads on the structure. At a later stage the whole numerical model of the barrier can be assembled and assessed by comparing results with the outcomes of full-scale experimental tests.

The models introduced in this thesis provide a numerical strategy for the definition of the performance of these structures. For the different prototypes studied, the numerical

models were developed addressing to the same numerical strategy, which was defined to a similar level of sophistication. The numerical models predictability of the dynamic performance of the systems should be validated by comparing results of simulations with experimental tests.

In this chapter, physical and numerical modelling techniques used to date for the analysis of rockfall protection barriers and their components are discussed to provide background information to this thesis.

2.2 PHYSICAL MODELLING OF STRUCTURAL COMPONENTS

The typical arrangement of a protective rockfall barrier consists of many functional components. Different barrier prototypes can be designed by varying the type and characteristics of the elements used. Thus, to gain understand of the response of the whole system it is crucial to analyse individually the performance of each component. In fact, the role of each part is critical, since failure of any element may bring to failure the whole barrier system.

Basically, rockfall barrier performance is connected to the interception structure behaviour. It is a metallic mesh whose function is to intercept and arrest the block falling from the slope, acting as a surface along the area covered by the structure. The net absorbs most of the kinetic energy deriving from rock fall impacts by means of elasto-plastic deformations. Since it is the barrier component that is in direct contact with the impacting body, an appropriate knowledge of its behaviour is required. Many works in literature are about to gain definition of the performance of meshes through experimental tests under both dynamic and static conditions as fully explained in next Section.

Other important elements that contribute to the dissipation of the kinetic energy are the energy dissipating devices. Their use is generally restricted to barriers with high-

energy capacity, where they are frequently installed together with the cables acting as connecting elements in the whole system. Only a few works in literature consider their performance in dynamic condition, while results of static experiments are available and can vary with the design of the considered device. However, together with the interception structure they offer the greater contribution to the dissipative mechanism of the systems and their response to impulsive dynamic effects should be better investigated.

Of course, posts and cables are other important elements of a rockfall barrier. Cables can be found in many different configurations depending on the cross-section constructions, leading to a variation of the main mechanical properties. Tensile tests in laboratory are usually carried out on cables in order to determine their stress-strain constitutive law. Contributions in literature are available reporting results of quasi-static tensile test (Muhunthan et al. 2005; Castro-Fresno et al. 2008; Fontanari et al. 2009) and data can be furnished also by the manufacturers, but no dynamic test conditions are available. The function of posts in a rockfall barrier is to support the mesh and keep it in position and connected to the cables. They are not called to contribute to bear part of the impact energy in the whole barrier response. For this reason their behaviour is commonly considered only in the elastic range when a numerical approach of the barrier must be developed and to further investigate the dynamic response of these elements is negligible.

The barrier performance is related to the deformability of the structure, thus internal connections and resulting constraints between the different elements involved give a contribution to the overall system capacity. As an example, usually longitudinal cables are allowed to slide through eyelets placed at the head or base of the posts. However, there are not experiments carried out to analyse this aspect, also because it is not easy to investigate these sliding effect in such dynamic event. Tensile tests performed to analyse the internal connecting elements (i.e. clamps or bolts) used in the construction of the mesh are given in Castro-Fresno et al. (2012). The study shows that in a mesh constructed with these elements failure usually occur on cables and not in the

connecting clamps. For this reason they can be modelled with a simplified solution in a numerical model and no further experiments are required.

In the following, a literature review about different experimental tests carried out on relevant rockfall components like the interception structure and the energy dissipating devices is presented. The works presented were considered to develop part of the research reported in the thesis.

2.2.1 Testing of meshes

In a rockfall barrier, the mesh has the function to intercept and stop the falling block bearing the direct impact of the block. The mesh design has an important role in order to define the overall performance of the protection system and different types of metallic nets can be used as interception structure.

Figure 2.1 shows the typical mesh constructions used for rockfall barriers. Particularly, chain-wire, chain-link and double-twisted nets (Figs. 2.1 a, b and c) are light systems with wire diameter up to 4 mm, commonly used for low-energy barriers. When the prototype must be designed for higher energy levels these types of nets are no more reliable. They can be used as secondary meshes with the only function to intercept small fraction of blocks, but the principal mesh is made by strongly steel cables with larger diameters. The cables can be arranged to form a square grid net (Fig. 2.1 d) or interlaced ring mesh (Fig. 2.1 e). These mesh types have different geometrical characteristics (weight and dimension), and mechanical properties (strength and elongation). In order to characterise the mechanical behaviour of the mesh in a numerical model it is fundamental to have experimental test as reference. Many previous research take into account results of different experimental tests conducted on the mesh types illustrated (Nicot et al. 2001; Grassl et al. 2002; Muhunthan et al. 2005; Roth et al. 2007; Castro-Fresno et al. 2008; Bertolo et al. 2009).

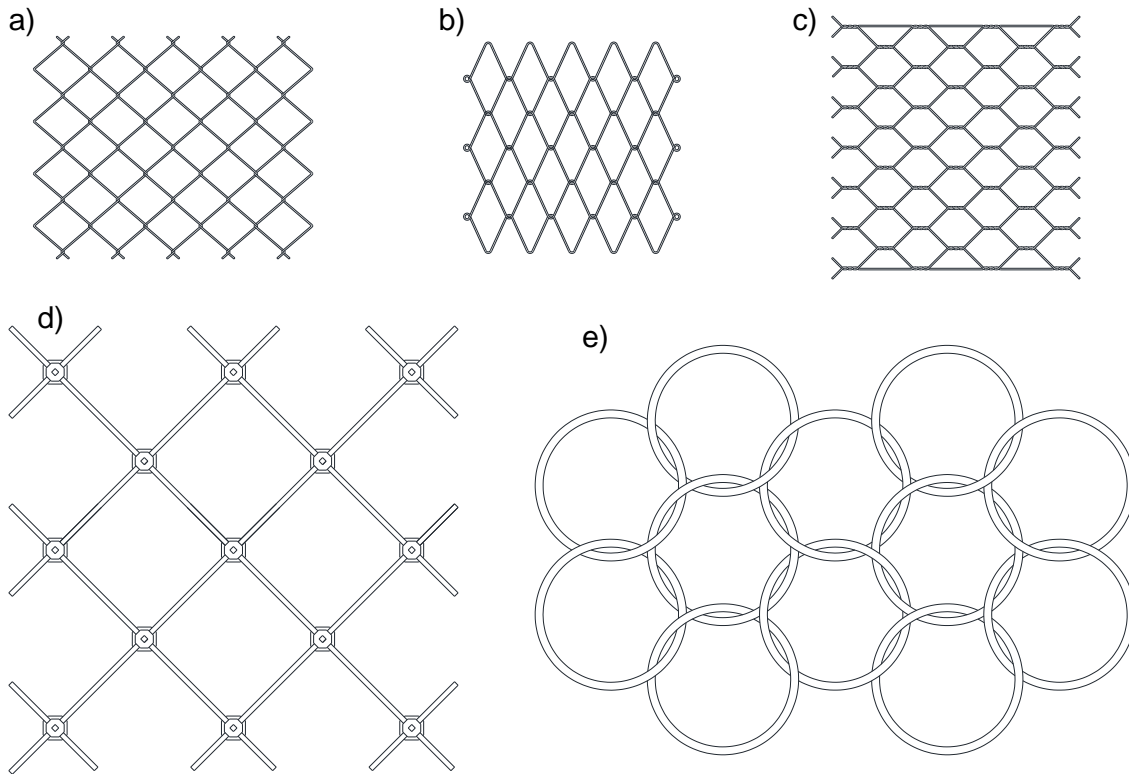


Figure 2.1 Rockfall mesh types (Spadari et al. 2013b): a) chain-wire, b) chain-link, c) double-twisted hexagonal, d) square grid cable and e) ring mesh.

The physical models adopted to study the mesh behaviour consider different scale approaches: from the singular wire or composing element, to a panel portion or a full-scale installed operating system. In the following, tensile test carried out in one of the two principal direction of the panel they are named in-plane test, while when the applied load is normal to the mesh surface we will talk about out-of-plane tests.

Surprisingly, results regarding dynamic tests on meshes are rather scarce in the existing literature and most of the works here presented concern quasi-static experimental procedure. One reason is that they are designed also as draped mesh systems, thus as active protective countermeasures for the stabilisation of slopes where static condition is the main characteristic of the phenomenon. On the contrary, for rockfall impact events, outcomes of strongly dynamic tests should be preferable. On the other hand, the execution of these experiments is more complex and the use of different instrumentation is required.

Another reason that leads to prefer static conditions, rather than dynamic, is that static tests are always carried out up to failure of the system and a full knowledge of the system response during the experiments is given. Further, the reproducibility of results is ensured. Differently, in a dynamic setup more than one test leading to rupture or not of the system should be provided. In fact, results in service and failure conditions are necessary to gain a full understand of the mesh response, also because similar tests can led to different outcomes due to the dynamic effects that can occur in the system. Further, it should be underlined that experiments carried out in service condition do not allow the necessary confidence to assess a numerical model with failure characteristics into the material properties.

Considering high-energy rockfall barrier, metallic ring-shaped mesh composed of rings (Fig. 2.1e) is the common solution for the interception structures.

Nicot et al. (2001) underlined that the behaviour of a ring mesh is complex because it depends on both geometrical and mechanical features of the rings. In the experiments, two scales approaches were considered: first a single ring alone (Fig. 2.2a) and then a small portion of mesh composed by seven rings interlaced with each other (Fig. 2.2b). The tests were performed in the in-plane direction in quasi-static condition. The tensile loading test carried out on the single ring showed two different domains of the ring shape evolution in a force-displacement graph (Fig. 2.2c).

In the first domain (OB) the ring changes its shape considerably developing a small rate of forces and high plastic strain. This phase is related to the geometric characteristics of the ring which modify its shape due to a small bending resistance. On the rockfall barrier, the developing of these deformations allows the mesh to dissipate a large amount of energy during the impact event.

Then, along the second domain (BC), the original circular shape of the ring is modified and it behaves like a cable subjected to a tensile loading test. Consequently, the forces rose to high value for small displacements with an elastic mechanism. In the second test concerning the mesh portion, four lateral rings were blocked vertically while the other two external rings were stretched in horizontal direction (Fig. 2.2b).

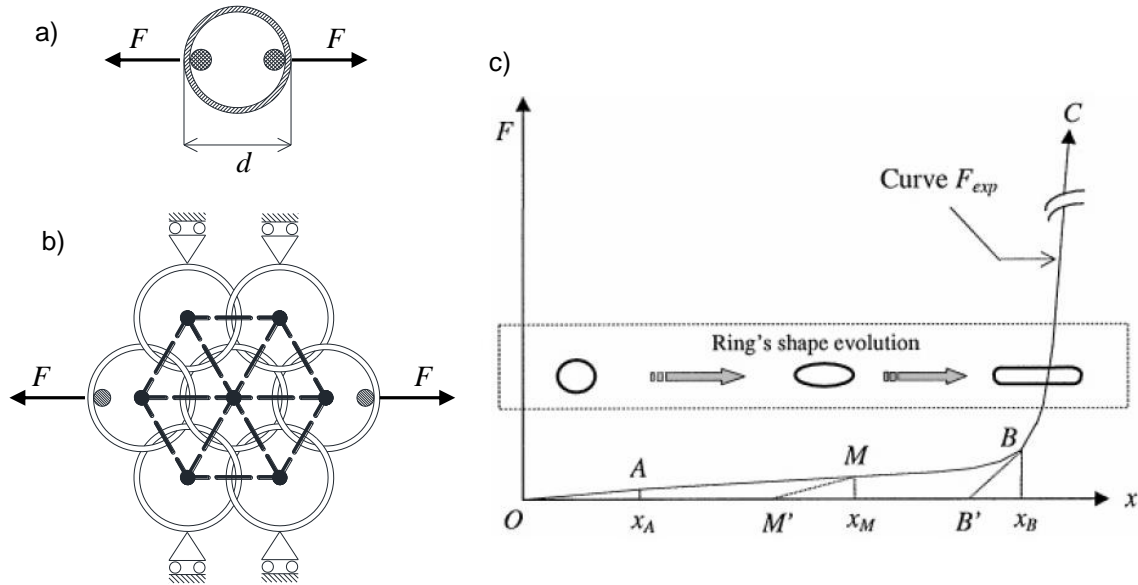


Figure 2.2 a) Tensile loading test performed on a single ring; b) tensile test on seven interlaced rings and equivalent DE model considered illustrated with dots and dashed lines; c) experimental behaviour of the single ring after Nicot et al. (2001).

Results obtained were evaluated in terms of force-displacement and then used to calibrate the numerical response of a discrete element model of the mesh. This is explained in Section 2.4.1.

The ring mesh behaviour was analysed experimentally also by a Swiss group of researcher (Grassl et al. 2002; Grassl et al. 2003; Volkwein 2005). Though the method was similar, some difference occurred compared to the work presented above. Quasi-static tensile tests were executed only on the single ring but concerning different initial boundary conditions, with two, three or four internal bolts used to stretch the ring as illustrated in Fig. 2.3a. The use of these configurations allowed to gain understands of the rings behaviour for different external constraints.

The mesh response was studied under dynamic condition with an out-of-plane impact test. The panel, a squared mesh portion of 4 m length, was connected to a rigid frame and tested dropping a concrete block by a crane from a known height (Fig. 2.3b).

Results were evaluated by monitoring the time history of acceleration and total energy of the block during the test, measured by means of high-speed cameras and accelerometers placed into the block.

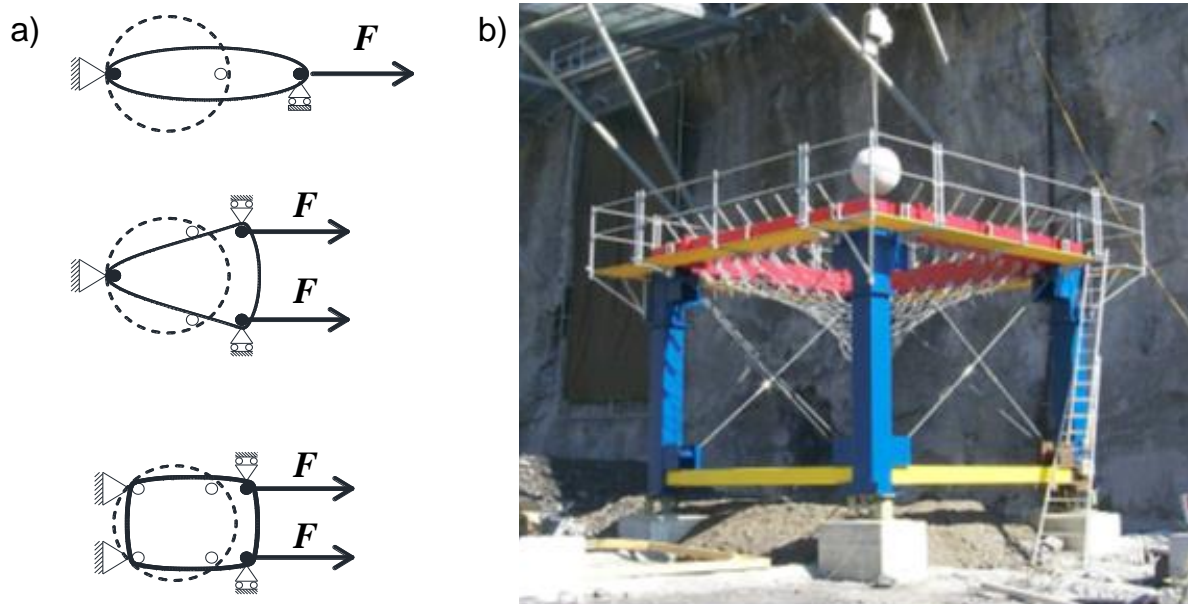


Figure 2.3 a) Tensile testing on single ring with two, three or four bolts; b) Rigid frame for impact test after Volkwein 2005.

This arrangement probably represents the best procedure to gain a full knowledge of the mesh performance in such dynamic conditions, because it behaves like the system installed on a real rockfall protection barrier. The weak point here is that no tests up to failure were considered in order to accurately determine the limit state of the material properties.

Concerning low to medium energy rockfall barriers, a lighter system is used as for interception structure. Chain-link and double-twisted mesh types (Figs. 2.1b and c) are installed on semi-rigid barriers, while cable nets (Fig. 2.1d) are generally used for high-energy prototypes fitted out for small amount of energy capacity (i.e. about 500 kJ). The latter mesh types are also used as drapery system, thus active protection systems for the stabilisation of slopes. For this reason, many works have investigated their performance in static condition, while no dynamic tests were carried out.

A comprehensive report was developed by Muhunthan et al. (2005) studying all the three mesh types experimentally. A series of quasi-static in-plane tests were carried out on square mesh panels of about 1 m length (Fig. 2.4a). The experiment was performed by means of a specific testing apparatus where one edge of the square sample was stretched keeping constrained the other side. Though the several data obtained, the different considered meshwork implied that their initial configuration

was not similar, thus the results were not comparable. However, the outcomes of the test campaign conducted allowed the evaluation of some relevant mechanical properties like the elastic modulus, the ultimate load and the tensile strength.

Another approach to investigate the performance of cable mesh leading to different outcomes was given by Castro-Fresno et al. (2008). The mesh was tested in quasi-static condition but the experiments were carried out in the out-of-plane direction. Results of two pull-out test type were evaluated: a concentrated load test where the load was applied in the centre of the mesh (Fig. 2.4b) and a distributed load test whit a pressure uniformly applied to the net sample (Fig. 2.4c). The net resistant capacity in terms of maximum deformation and forces developed on a square sample of 2 m length was estimated.

All the samples were tested up to failure that always occurred to the cables forming the mesh. This outcome was specifically investigated also with other tests, proving that the weakness of the system is not in the connecting clamps placed at the intersection of the wires, but at the cables themselves.

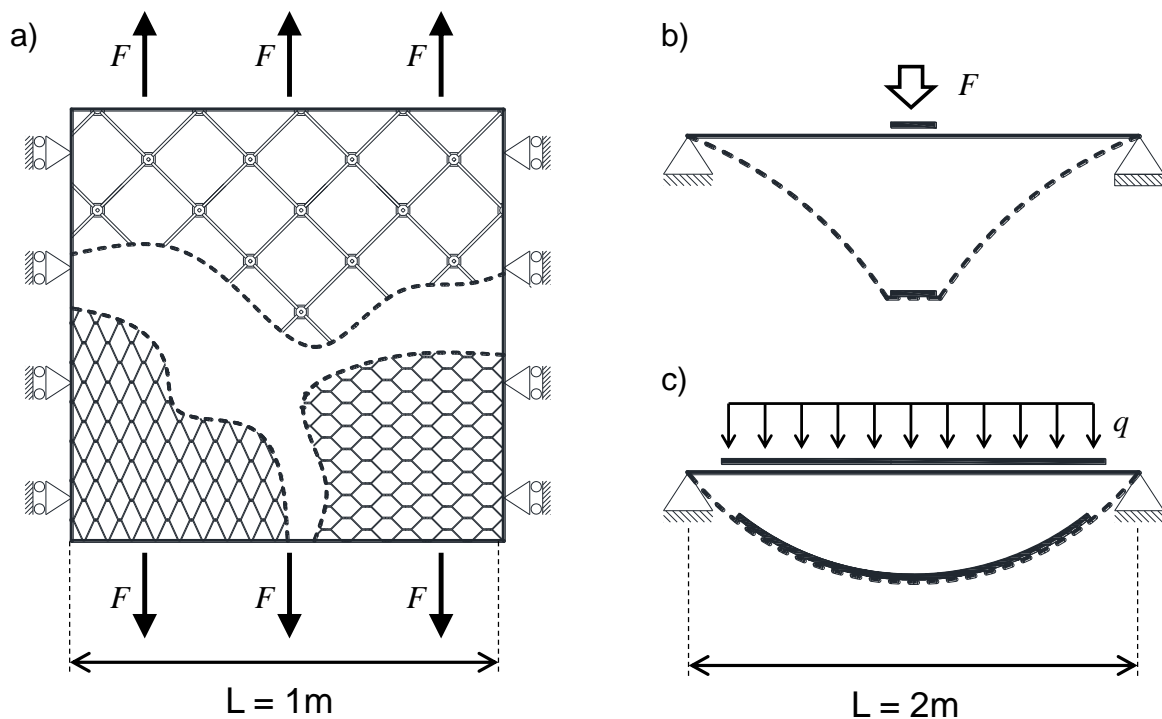


Figure 2.4 Quasi-static test on mesh panels: a) tensile in-plane test after Muhunthan et al. (2005); b) concentrated load out-of-plane test and c) distributed load out-of-plane test after Castro-Fresno et al. (2008).

Bertolo et al. (2009) proposed a similar experimental procedure. The authors pointed out that investigating the performance of the mesh only with local scale tests could be a limitation to the comprehension of the full-system response. Although partially representative of the real behaviour of the mesh, either in-plane or out-of-plane tests are greatly influenced by the adopted boundary conditions of using a frame of restricted dimension.

As a consequence, the authors decided to investigate the mesh response by means of a full-scale test suitably designed with the aim of analyse an installed draped mesh system performance. The physical model adopted is illustrated in Fig. 2.5, a square mesh of 6 m side installed on a vertical rock wall. A half-spherical cap-shaped load distributor of 1.5 m diameter was used to apply an out-of-plane force to the central surface of the mesh.

Tests were run till failure of the mesh or to maximum stroke of the loading system and results analysed for both displacement developed and forces acting on the cap. Load cells were also installed on the anchorages to investigate the distribution of forces along the system.

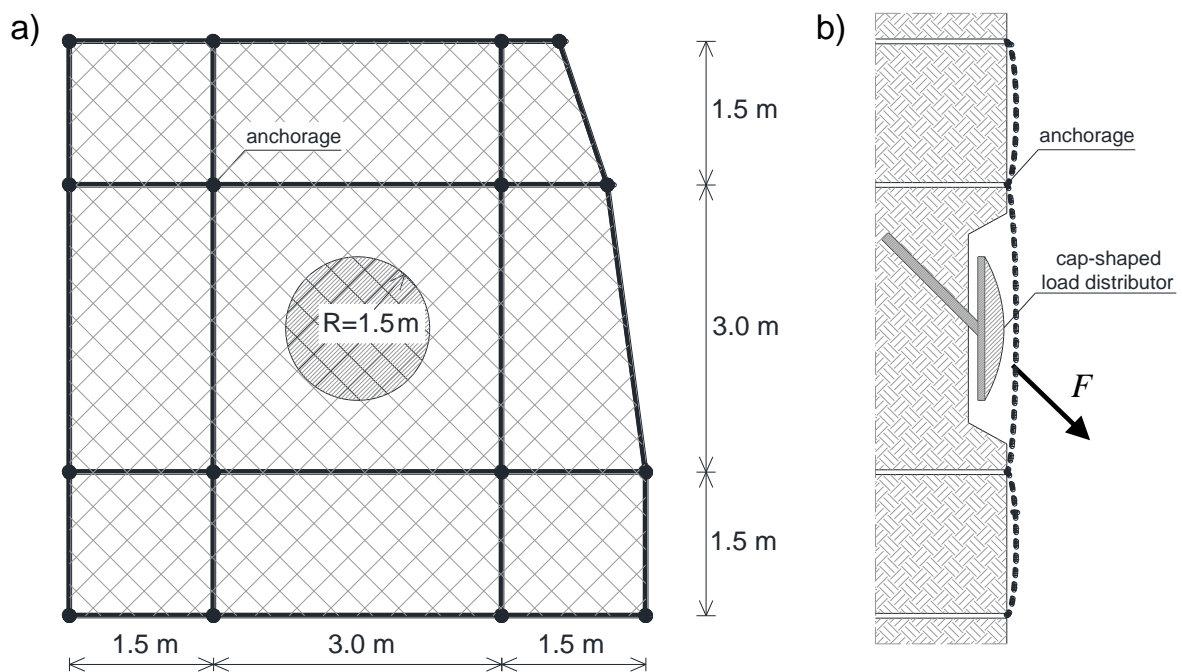


Figure 2.5 Schematic drawing of the full-scale field test adopted by Bertolo et al. (2009): a) front view; b) vertical section.

The experiments carried out showed that the constraints imposed in the laboratory test on mesh portion can led to different results compared to full-scale test. Thus, outcomes of experiments carried out on a small scale mesh can be useful to calibrate the response of the mesh in a numerical model, but full-scale test on the whole working system (i.e. the rockfall barrier) or experiments considering different boundary condition should be considered to have a full-knowledge of its behaviour.

Bertrand et al. (2008) investigated the double-twisted hexagonal mesh behaviour with a comprehensive experimental procedure. It is largely used on rockfall barriers with low energy absorption capacity. As defined by the authors, the double-twisted mesh is built by twisting continuous pairs of steel wires three half turns and by interconnecting adjacent wires to form hexagonal-shaped openings. Thus, two main section types must be considered in the constitutive elements of the mesh: the single wire and the double-twist which has double cross sectional area and behave differently. At a first stage uniaxial tensile tests were carried out to provide the mechanical behaviour of the single wire section. Then, in-plane and out-of-plane tensile tests in quasi-static conditions were carried out to investigate the performance of mesh samples (Fig. 2.6). Particularly, the in-plane test was carried out for different combination of mesh size of the hexagonal openings and single wire diameters. The out-of-plane test was performed on a square mesh of 3 m length where the external edges were fixed to a steel frame. It consisted of a punch test where a half-spherical body applied the loading at the centre of the panel. All the extracted data were used to calibrate and validate a DE model of the net that is widely illustrated in Section 2.4.1.

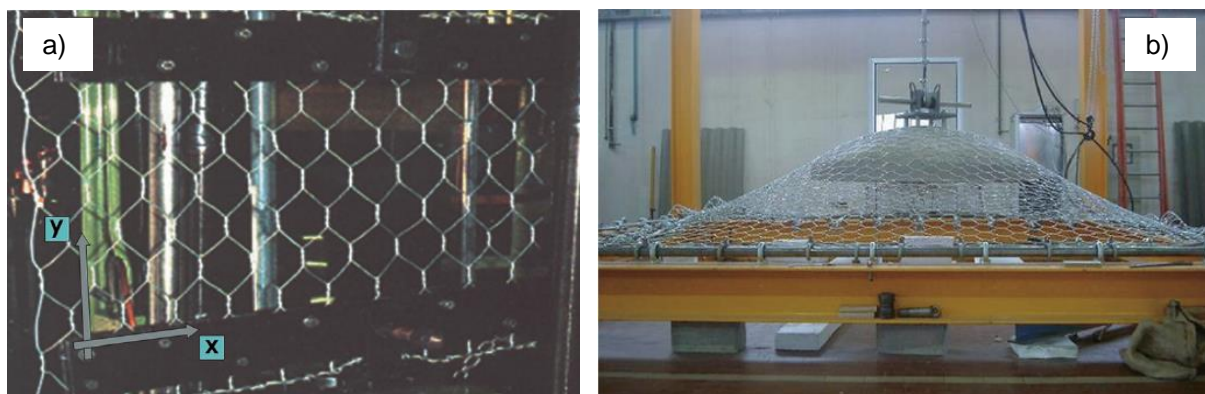


Figure 2.6 Quasi-static experiments carried out on double-twisted hexagonal mesh by Bertrand et al. (2008): a) tensile in-plane test; b) punch out-of-plane test.

Concerning the chain-link system, a series of quasi-static out-of-plane test were performed by Roth et al. (2007). The mesh was bolted to the ground in four points and pulled out by means of a square frame connected to a hydraulic jack. Experiments were conducted up to failure of the mesh that always occurred close to the area of the bolts representative of the boundary condition. It demonstrated that rupture for a chain-link system can be easily achieved for stress concentration where connections with other elements are involved.

Recently a full experimental analysis of the dynamic performance of a chain-link mesh was developed by Buzzi et al. (2014). Several impact tests were carried out by dropping blocks from a known height against a mesh fixed to a steel frame and the response of the net was analysed. The attention was focused to investigate the influence of the block size on the net performance. This effect is named “*bullet effect*” and it is better illustrated together with the paper details in Chapter 5.

2.2.2 Testing of energy dissipating devices

A rockfall protection barrier works dissipating the potential energy deriving from the impact of the rock by means of deformations of the structure. For barrier provided of high-energy absorbing capacity the introduction of energy dissipating devices is necessary in the design of the structure.

The configuration of these devices can be various as reported in Fig. 2.7. Generally they can dissipate energy by producing relevant plastic non-reversible deformation of their constitutive elements. Other typology are based on a friction criterion, they work transforming into heat the friction between two surfaces in contact.

Some research was carried out to investigate the behaviour of these devices, but usually their characteristics are supplied by the manufacturers and can vary depending on its construction design. The issue is that their performance is always assessed by means of quasi-static tensile test, while there is a lack of information about their behaviour in dynamic condition. It is due to the difficulty to perform a realistic test in this configuration.

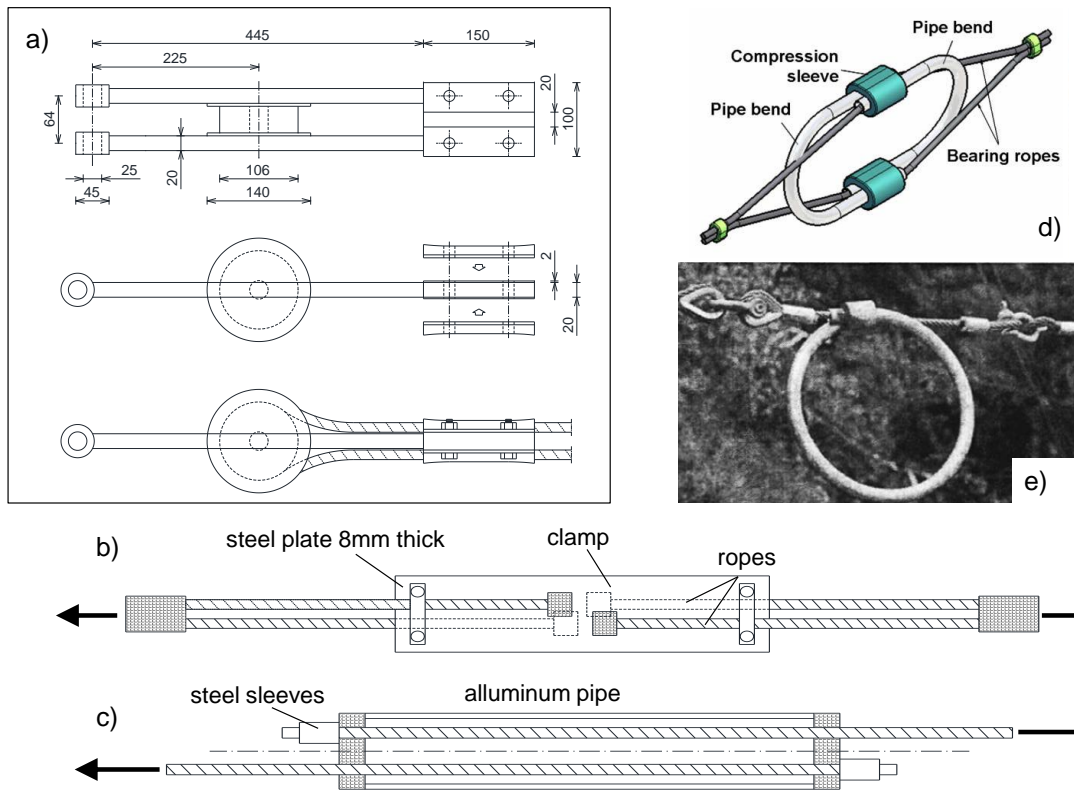


Figure 2.7 Energy dissipating devices: a) friction type (Giacomini et al. 2001); b) and c) friction and aluminium pipe type (Peila et al. 1998); d) U-shaped tubular double loop device (Castro-Fresno et al. 2009); e) ring-shaped type.

Quasi-static test on two type of energy dissipating devices were analysed by Peila et al. (1998). The type 1 develops energy by friction of wire sliding through the clamps (Fig. 2.7b), while the device named type 2 produces permanent plastic deformations of the constitutive aluminium pipe to dissipate energy (Fig. 2.7c). The experiments were carried out with the use of an electro-hydraulic machine to stretch the ropes attached to the system in one direction while keeping constrained the other. Tests on type 1 were performed by varying the bolt torque value at the clamps. Results were evaluated monitoring the evolution of the force-displacement curve, thus measuring the energy dissipated by the system. It was pointed out that the absorbed energy for type 1 is not directly associated with bolt torque and that the performance of the device could vary depending on this parameter. For type 2 only one test result was reported in terms of force-displacement measured.

Interestingly, Giacomini et al. (2001) carried out a series of tests considering static and dynamic condition and then compared the outcomes observed. The energy dissipating device studied is a “friction” type reported in Fig. 2.7a. The tests were conducted with different bolt torque value and outcomes analysed in terms of average braking force reached. For the dynamic experiments the scheme in Fig. 2.8a illustrates the adopted solution.

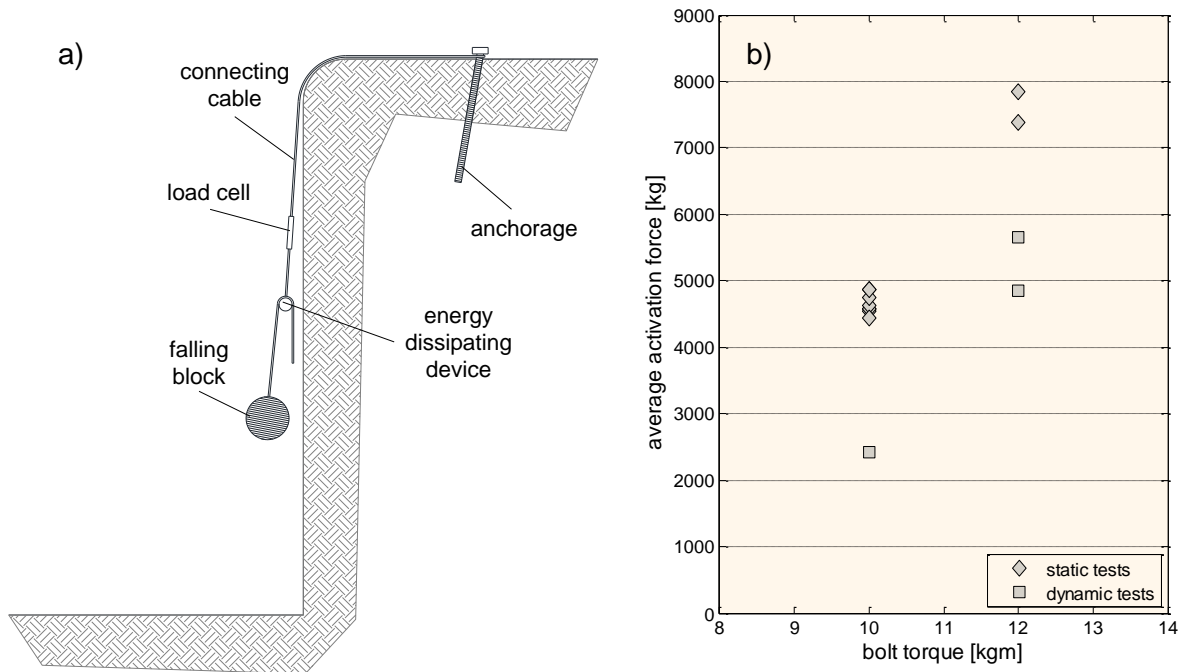


Figure 2.8 a) Schematic section of the dynamic test carried out by Giacomini et al. (2001) and b) comparison of the average activation forces measured from static and dynamic tests with different bolt torques.

The system was tested by dropping the block from a known height in a vertical free fall. The energy dissipating device was connected to a block in a side and fixed to a bolt anchorage to the other by means of a steel cable. During the event displacement and velocity of the block were monitored and force measured in a load cell placed in the upper cable. Two configurations of the brake system with different bolt torques applied were considered for the comparison. Figure 2.8b shows the results obtained for the two tests in terms of average activation force with the bolt torque applied. It was observed that the activation force was lower in the dynamic case, but, as stated by the authors, the small amount of data do not allow to identify a precise correlation between the two tests. Nevertheless it was proved that the response is different and

dynamic effect should be taken into consideration to study these important structural components.

A different approach to investigate the performance of an energy dissipating device was conducted by Castro-Fresno et al. (2009). It is a U-shaped tubular double loop device (Fig. 2.7d), a series of quasi-static tensile test were carried out by varying the tightening pressure on the compression sleeves which joined the two tubular steel loops. Figure 2.9 reports results in terms of force-displacement measured during the tests showing the different curves obtained for the tightening pressure considered. Further tests proved that, whit higher value of pressure, failure occurred at cables before the energy dissipating device could reach its plasticization. The excessive tightening pressure applied did not allow the sliding mechanism of the pipe bend through the compression sleeves. At a later stage the dynamic behaviour of the device was investigated with a virtual solution. A numerical model of the device was built with a finite element commercial code (i.e. ANSYS), non-linear dynamic simulations were run for two test types. First a symmetric tensile load test, where both ends were stretched with an applied velocity of 25 m/s; then one edge was fixed while the other subjected to a speed load of 50 m/s.

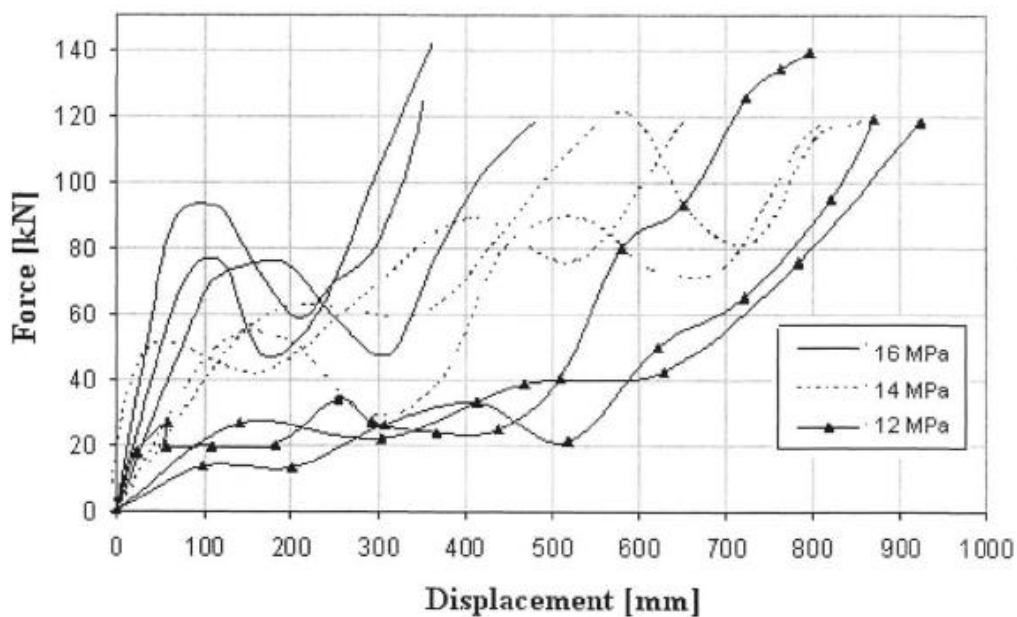


Figure 2.9 Force-displacement curve of sample tested with different tightening pressure (Castro-Fresno et al. 2009).

The simulations were performed considering different friction coefficients in the contact properties between the interfaces. The developed model was then used to estimate the behaviour of an improved version of the original design.

A complete description of the FE model of the device is reported by del Coz Diaz et al. (2010). Though the adopted procedure represents an interesting work, there is some lack of information on how the numerical model was calibrated since the comparison of results reported was made between static experiments and strongly dynamic simulations. Anyway, it confirms how the finite element method could be a suitable tool to analyse the response of this system to different loading configurations.

2.3 PHYSICAL MODELLING OF ROCKFALL BARRIERS

Rockfall protection barriers are complex systems whose performance is assessed with an energy criterion defined as the system capacity to absorb the kinetic energy derived from the impact of a falling body.

Nowadays different products are available, produced and designed by many manufacturers. The difficulty lies on assessing and comparing their performance uniformly, because the barrier configuration and the interaction mechanisms induced between the constitutive parts used can be various leading to different outcomes. Particularly, the geometrical and mechanical non linearity produced in the system during the strongly dynamic phenomenon are not easily predictable.

In order to gain an understanding of the whole system response under impact events it is essential to base the study on appropriate experimental analyses. Since any restriction to the physical model of the system can underestimate the real structure response to such complex event, full-scale tests had shown to be essential to assess the behaviour of a barrier prototype.

Over the last decade it was worldwide approved the importance of carrying out full-scale tests to assess their energy absorption capacity and to evaluate the response in terms of forces and deformations produced. Essentially, the test consists o the launch

of a block of known mass and velocity against the central panel of a prototype made of at least three functional modules (i.e. to obtain a symmetric response). The first outcome of the test is to observe if the barrier is able to withstand the impact. Then, the measure of displacements and forces produced within the system should be monitored. Many experimental setups have been proposed for full scale testing of rockfall protection barriers in the last few years (Smith and Duffy 1990, Hearn et al. 1995; Peila et al. 1998; Grassl et al. 2003; Arndt et al. 2009; Gottardi & Govoni 2010).

In Europe two important documents were recently developed (Gerber 2001; EOTA 2008). They defined a standardised assessment of a barrier performance. The documents provided the guidelines for the definition of the test methodology, the minimal requirements demanded during and after experiments and the approval procedure to obtain a certification of the product. After the endorsement of the guidelines testing rockfall protection barriers started to be compulsory in Europe leading to an improvement of the effectiveness of high-energy capacity systems. In the meanwhile, in other countries where no specific guideline was introduced, different passive protective countermeasures were tested similarly (Muraishi et al. 2005; Dhakal et al. 2011). It should be highlighted that the guidelines concern only flexible rockfall barrier with high energy capacity (i.e. assumed as more than 100 kilojoules), while no instruction are already given for low-energy systems even if they are widely used within mountain context.

In the following, after a brief introduction of the two guidelines, the relevant full-scale testing approach adopted in the last few years are described, showing the various assumptions made.

2.3.1 Procedures according to guidelines

In order to assess the main characteristics of a rockfall protection barrier by means of full-scale tests a well-defined methodology is required to ensure that different prototypes performance can be compared objectively.

Recently two important guidelines were developed for this purpose. The first document was published in Switzerland with the Swiss Guideline for the Approval of Rockfall Protection Kits (Gerber 2001). Then, in 2008 the European Organization for Technical Approval (EOTA) developed the Guideline for European Technical Approval of Falling Rock Protection Kits, otherwise known as ETAG 027 (EOTA 2008, Peila and Ronco 2009). The guidelines set out the minimum standards for the design and testing of rockfall protection systems having energy absorbing capacity greater than 100 kilojoules. They establish how the nominated Approval Bodies should evaluate the product suitability in order to approve its conformity and assign a certificate of its performance. In the documents, the rockfall barrier components and results to be measured during and after the impact test are identified providing the methodology to monitor these outcomes (Fig. 2.10a).

The guidelines do not specify a unique test configuration, various setups are allowed to test a prototype, accordingly to some restriction introduced.

The rockfall protection kit tested has to be arranged with at least three functional modules. The test consists on impacting the central module of the kit with a concrete polyhedric shaped block (Fig. 2.10b and c) having a minimal velocity of 25 m/s.

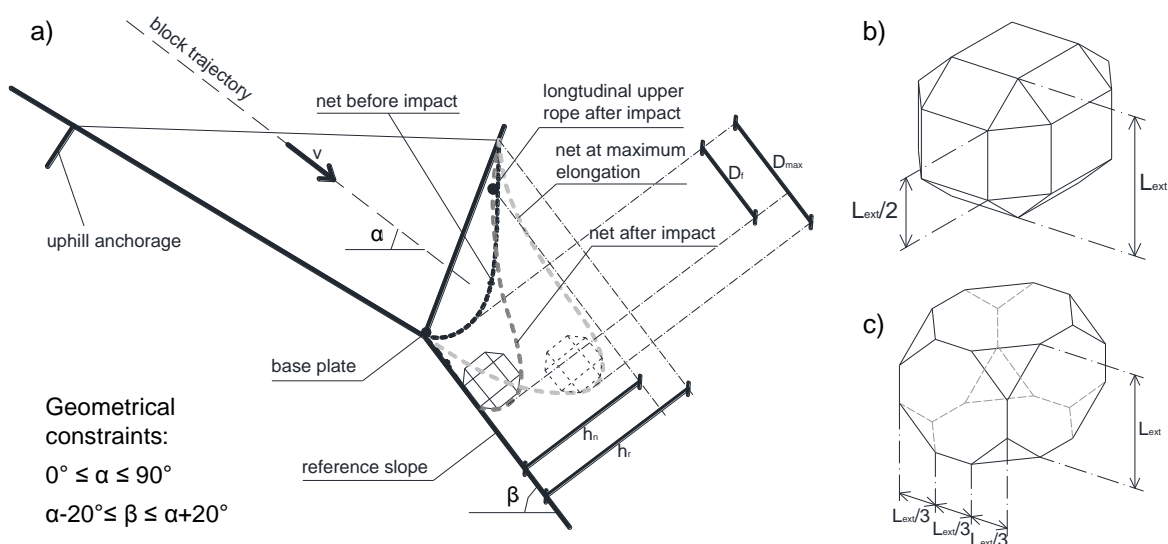


Figure 2.10 a) Rockfall barrier components after ETAG 027 (Peila and Ronco 2009). Shape of the testing block: b) ETAG 027 (EOTA 2008) and c) Swiss guideline (Gerber 2001).

In Switzerland a vertical test site facility (Fig. 1.2a) located in Walenstadt is managed by the Swiss Federal Institute for Forest, Snow and Landscape Research (WSL). In Europe both the two main test site configurations (Fig. 1.2) have been developed across the different countries. According to the guidelines, during the tests the rockfall protection kit must be able to stop the impacting block without a ground contact until the barrier reaches the maximum elongation. It means that the tested barrier has to absorb the full kinetic energy deriving from the impact. For this reason, vertical test site can be preferable avoiding any contact till the end of the test, when the complete stabilisation of the block is reached.

Two energy levels are considered: the maximum and the service energy levels (named MEL and SEL in the ETAG 027). The MEL is considered as the maximum energy absorbing capacity for what the prototype was designed. For the Swiss guideline the service level is 50% of the maximum, while ETAG considers it as 1/3 of MEL and the experimental launch of the block has to be repeated twice on the kit. When the test is carried out at the maximum level the barrier has to be able to arrest the block along with some specific restriction introduced by each guideline. Concerning the double impact test of SEL, during the first launch no rupture in the connection components is allowed, the block has to be removed and the second launch performed and arrested by the kit with no maintenance allowed between the two tests. Nine levels of classification of the rockfall barrier are defined in both the guidelines with different threshold values and measures limitation concerning the test results at the two energy levels.

The design of the foundation structure is not defined into the guidelines since they are not considered part of the rockfall protection kit. It is left to the discretion and responsibility of the designer, taking into account of specific national recommendations where defined.

As previously stated, only prototypes with high-energy capacity were contemplated into the guidelines. Consequently, in the last few years there was an important

improvement of the effectiveness of flexible barriers produced by different manufacturers leading to energy absorbing capacity up to 8000 kJ. However, it was proven that in many real case studies, the level of energy expected in the investigated area can be very low. In this configuration, low-energy barriers with semi-rigid characteristics of deformations can be more suitable and cost-effective. Into the guidelines there is a lack of information on how to assess these kinds of prototype even if they are still produced and frequently installed worldwide without a certification of their performance. Due to their low deformability these barriers work differently and cannot be tested following the same methodology introduced by the guidelines. The configuration of the test, the minimal velocity at impact of the block, the expected outcomes and other requirements and recommendations should be modified. In the absence of a document to regulate a certification procedure to assess the performance of these barriers in terms of maximum energy capacity, this value is unknown. Their design is still mainly based on the experience of the designer. In this legislative void, numerical procedure can be useful to preliminary evaluate the barrier performance but experimental test should be preferable to validate the model.

In the past low-energy barriers were tested considering different test setup, but results are unsuitable and poor, due to the old instrumentations used (Duffy and Haller 1993; Hearn et al. 1995). Furthermore, nowadays the configuration of these structures is changed and the old outcomes cannot be used to understand the modified system response. Recently Buzzi et al. (2013) have conducted a series of experimental full-scale test to analyse the performance of newly-developed low-energy protection kits. The methodology is proposed in Chapter 5 together with the numerical model developed as part of the research, accordingly to the available data.

2.3.2 Full-scale testing of rockfall protection barriers

In order to assess the rockfall protection barrier response to dynamic event full-scale test are necessary and mandatory to obtain a certification of the product performance in accordance to the guidelines recently introduced in Europe.

The first aim of the test is to assess whether a barrier prototype is effectively able to dissipate the kinetic energy deriving from the impact of falling blocks having energy up to the maximum designed level of the kit. A complete definition of the ultimate capacity of the prototype should require experiments conducted up to failure of the system, but it is beyond the scope of the guideline which aims to just verify the maximum level of performance of the barrier.

Concerning the analysis of results, full-scale test are useful to evaluate the maximum deformation of the mesh (D_{max}) obtained at a time named braking time (b_t) and the final value of the mesh elongation (D_f) achieved when the block is definitively stopped by the barrier. Another important quantity that has to be monitored at the end of the test is the residual height (h_r). It is the distance between the two longitudinal upper and lower ropes connecting the interception structure, that initially represents the nominal height (h_n) of the barrier (Fig. 2.10a). Furthermore, load cells installed at the base plate of the posts and at the anchorages of the cables can be installed to measure forces transmitted to the foundation structure.

A definition of methodology, limitation and expected results from a full-scale test on a barrier is now specified into the guidelines previously introduced, ensuring a good reproducibility of the obtainable results. In the following, an overview of the various approaches to execute full-scale test on rockfall barrier over the years is reported, underlying the pros and cons of the adopted procedures.

The first contribution to rockfall testing can be attributed to the Washington State Department of Highways where a research project was leading to monitor the rock motions along slopes and to observe the response of fence systems (Ritchie 1963). It was a pioneering study but it focused mostly to the analysis of the trajectory of the falling rock. A real approach to full-scale testing on barrier samples is dated to the mid-eighties when experiments were carried out just to examine the prototype response by means of a trolley system (Neri 1986). The barrier was installed vertically and to impart a horizontal speed against the central panel the impacting body was connected to a trolley running on a railway (Fig. 2.11a). It was a rudimentary method, the achievable velocity at impact was low and, in order to obtain high energy values,

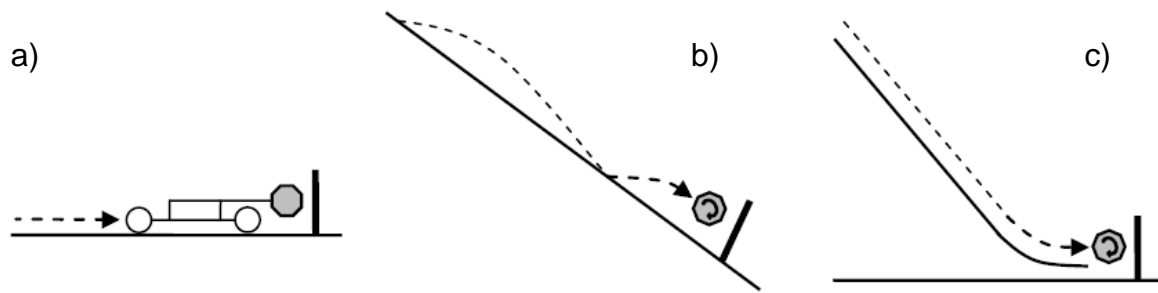


Figure 2.11 Experimental test setup developed over history (Spadari et al. 2013b): a) trolley system (Neri 1986); b) free motion along a slope (Smith and Duffy 1990; Hearn et al. 1991) and c) along a smooth ramp (Muraishi et al. 2005).

the considered mass had to be too big compared to the nominal height of the barrier. Though the adopted methodology led to a condition not representative of a typical rockfall event, it was an important breakthrough into the study of a rockfall barrier performance by means of full-scale testing.

More realistic testing methods were then developed in the US in the early nineties. The California Department of Transportation conducted full scale test on barriers built down a slope (Smith and Duffy 1990; Duffy and Haller 1993). A similar approach was also implemented by the Colorado Department of Highways testing a particular type of barrier named Flexpost fence (Hearn et al. 1991; Hearn et al. 1995). The block was left to roll along a natural slope in a free motion and to fall into a barrier sample (Fig. 2.11b). Over hundred tests were carried out on various prototypes. The observation of results was focused also to plan some modification to the system design. The barrier performance was tested with different configuration and also experiments up to failure were carried out. Therefore the experimental campaign was used with both the purpose to validate the performance and to improve the design of the structure. The physical model adopted was realistic, the effect of rotation and translation of the colliding block against the barrier were taken into account. The issue lies on the reproducibility of the test that could not be ensured since it was not easy to predict the motion of the falling bodies. The innovation introduced was the use of slow motion cameras for the analysis of the time-displacement evolution of the block during the impact. The obtained data were thought as a base to develop an analytical

model of the studied prototypes leading to the idea of studying the barrier behaviour by means of some virtual tool. The formulation proposed is quickly discussed in Section 2.4.3.

In order to obtain a more reproducible impact with a similar procedure, Muraishi et al. (2005) investigated the response of the barriers with a ramp system. In the present test method the block was a spherical body guided to collide against the barrier sample along a smooth ramp made of steel (Fig. 2.11c). As a consequence the impact location and speed was easily predicted and both the translational and rotational components were taken into account. The limitation of the method was that only low energy value could be reached. Thus, the adopted configuration can be considered as a notable example on how to test low-energy barrier systems. Recently this method was implemented also by Dhakal et al. (2011) to analyse the behaviour of a particular passive protection system mainly constitute by cables and net. Here the impacting body was able to achieve energies up to 400 kJ.

On the contrary, Peila et al. (1998) developed a testing method able to reach very high energy (i.e. mass of the block up to 7000 kg with achievable velocity of 34 m/s, leading to kinetic energy up to 4000 kJ). The setup consisted of an inclined test site where the barrier kit was installed at the bottom of the slope in a realistic condition. The impacting body was attached by a trolley to an aerial ropeway aligned with the slope and perpendicular to the barrier (Fig. 1.2b). The block was detached in order to impact the prototype directly, without any bounce on the ground before in accordance to ETAG. Three cameras filmed the event from different locations while the forces transmitted to the cable were monitored with dynamometers, giving results both in terms of acting forces and displacement or velocity of the block.

The advantage of this solution is that high-energy rockfall barrier can be tested in a very realistic way. Anyway, the impacting block has no rotational speed and the exact location of impact on the mesh is not easy to be predicted, therefore the reproducibility of the test cannot be absolutely guaranteed. As an example, a slight variation of the predicted impact location can cause a ground contact of the block

before maximum elongation of the mesh is reached, leading to test results that could not be taken into consideration.

To address this issue, vertical test site have shown to be the preferable solution. Firstly introduced by Gerber (2001) it allows the best control of impact velocity and location of the impacting body. The procedure consists of dropping concrete rocks by means of a crane into a rockfall barrier installed on a vertical rock wall (Fig. 1.2a). The block dimension, mass and dropping height are known, in order to predict the impact velocity. This configuration ensures the complete reproducibility of the test with any contribution of the ground to the dissipation of energy. High speed cameras and the use of multiple load cells for anchorages and base plate of posts allow to monitor all relevant measurements. The only limitation is that, as for the inclined test site with cableway, no rotation of the block is considered during the experiments. However, Arndt et al. (2009) showed that the rotational component of speed is negligible. Barrier prototypes performance was investigated in an inclined test site considering realistic value of rotational motion of the boulder used (Figure 2.10d). The outcomes showed that the overall performance of the barrier was not affected by the rotational motion and no cutting failures were observed during test conducted.

Nowadays vertical test site is the prevalent solution adopted to study the behaviour of high-energy rockfall protection systems. Recently, some work was produced considering outcomes carried out from these full-scale tests to develop numerical models of the studied barriers (Bertrand et al. 2012; Escallon et al. 2014).

In this thesis, data of full-scale tests carried out by Gottardi and Govoni (2010) on different high-energy barrier prototypes accordingly to ETAG were considered. The experiments were performed in a vertical test site located in Fonzaso (Italy). A comprehensive database of results investigating the barrier performance under several impact tests was produced. These data were used to develop the numerical models introduced in the presented research. Details and outcomes obtained are better explained in Chapter 3.

2.4 NUMERICAL MODELLING OF ROCKFALL PROTECTION SYSTEMS

An extensive introduction of the empirical methods followed to analyse the performance of rockfall protection barriers and their components has been reported. It was shown that, rockfall protection barriers in working conditions are subjected to high impact loads that produce geometrical and mechanical non linearity into the systems. Full-scale tests are essential to predict and assess the response of the system to such dynamic events. However, the real on-site installation of a rockfall barrier can be different from the prototype arrangement, as like as the impact condition can have high variability. Obviously, it is unrealistic to perform all the possible configurations experimentally, also because these investigations are expensive and time-consuming procedures.

Other instruments may be helpful to this aim. Analytical and numerical modelling provides a powerful tool to study such a complex phenomenon while reducing experimental costs. The use of these virtual approaches allows to simulate special load case or geometrical configuration of a prototype, as well as to estimate the performance of different construction design by varying the constitutive elements used. Up to now, some simplified analytical and numerical strategies have been developed in literature. It was pointed out that, if the aim is to use the developed model as a predictive tool, by varying the material and geometrical parameters of the barrier elements, the response of the single structural components must be correctly analysed before the whole system model is developed.

Thus, the effectiveness of a rockfall protection barrier model mostly depends on the attention given to characterise the behaviour of the constitutive elements involved, especially the mesh used as interception structure.

Further, it must be underlined that, regardless the numerical choice adopted to investigate the performance of a rockfall protection kit, the base model should always be validated by comparison with full-scale test results, whenever possible.

In the following, after a thorough introduction of numerical techniques adopted for the mesh types, a description of the modelling approaches employed to study the rockfall protection systems is presented. From the simplified analytical and numerical model to more sophisticated three-dimensional models developed by using either the Finite or Discrete Element Methods (i.e. FEM or DEM).

2.4.1 Modelling of meshes

The different mesh types generally used for rockfall barrier were introduced in Section 2.2 (Fig. 2.1). Based on the data produced, different approaches were adopted to simulate the mesh response, using both FE or DE methods and they are briefly illustrated hereinafter.

As for the ring mesh type, Nicot et al. (2001) analysed the experimental response of the net in two steps: first the single ring alone and then a small panel portion composed of seven rings (Fig. 2.2a and b). The numerical model was realised with the DE method. The adopted procedure was to model each ring as a particle placed at its centre and considering imaginary bars connecting the nodes to simulate the interaction between the adjoining rings. As a consequence, a simplified equivalent mesh with triangular shape of the openings was obtained avoiding to reproduce the entire ring shape (Fig. 2.2b). A force-displacement law was assigned to the connecting bars calibrated by comparing with the experimental outcomes of Fig. 2.2c. The model of the equivalent mesh was then validated reproducing the tensile loading test on the seven rings panel. The results of experiments and simulations were compared taking into account the forces and displacement developed in both vertical and horizontal directions. At a later stage, the model of the net was implemented on a full barrier model and details are reported in Section 2.4.3.

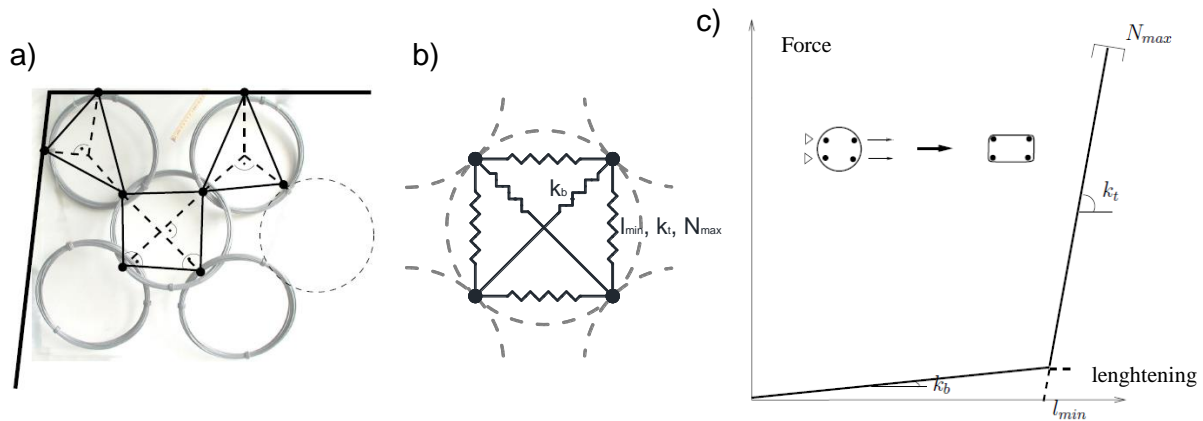


Figure 2.12 Definition of the equivalent mesh after Volkwein et al (2005): a) design with respect to the ring mesh; b) discretization with spring elements of a single ring; c) Force-displacement curve used to represent the ring response, until l_{min} is reached only the two internal springs work with k_b stiffness value, then the ring behave like a steel bar in tension with stiffness k_t of the external springs.

Grassl et al. (2002) carried out a similar experimental study on ring mesh, hence a numerical model was generated with a computer program named FARO based on the FE method. This software was developed by the Swiss Federal Research Institute (WSL) to specifically investigate the response of rockfall protection barriers (Anderheggen et al. 2002). An equivalent numerical mesh was built, each interaction node between the rings was connected with spring elements (Fig 2.12b). Thus, based on the number of external boundaries of the ring (i.e. adjoining rings or connection to other elements) it was modelled with two, three or four nodes connected to each other (Fig. 2.12a). The results of the tensile test carried out on the single ring (Fig. 2.3a) were used to assign the material properties to the spring elements. Initially the ring allowed high deformations with low stiffness (i.e. low resistance to bending of the ring) and only the two diagonal springs are working (Fig. 2.12c). When the sharp discontinuity is reached, the outside spring system take over the internal one, because the ring starts to behave like a steel bar in tension.

The equivalent mesh designed was then validated by reproducing the out-of-plane test performed and illustrated in Fig. 2.3 d. Good accordance between experimental results in terms of block deceleration and energy absorption confirms the calibration developed. The mesh model was then assembled on the whole barrier to simulate the response of the system to rockfall events as described in Section 2.4.3.

Whereas ring meshes are typical interceptive device for flexible barriers with very high energy absorbing capacity, wire meshes are commonly mounted on prototypes with minor dissipation capacity. This net is made of steel cables joined together to form a square grid with anti-slip clamps or bolts at the intersection nodes. Some numerical model was developed to analyse their response, considering the results of the experimental tests described in Section 2.2.1, and based on different approaches.

Sasiharan et al. (2006) analysed the behaviour of cable net numerically based on the data of experiments carried out by Muhunthan et al. (2005). The aim of the study was addressed to investigate the performance of active rockfall protection systems with a model of the mesh assembled with the finite element computer code ABAQUS. During the tensile test (Fig. 2.4a) the load-displacement behaviour of the mesh was determined. The data refer to the mesh portion considered as a unique system, while the behaviour of the constitutive cables was not investigated. The reason of this simplification lies on the choice to model the mesh as a three-dimensional membrane element, because the installed system works like a membrane. Hence, the data extracted from the test were used to set the material parameters of the membrane: the Young's modulus and yield stress parameters. The numerical model was then realised to analyse the built on-site configuration (Fig. 2.13).

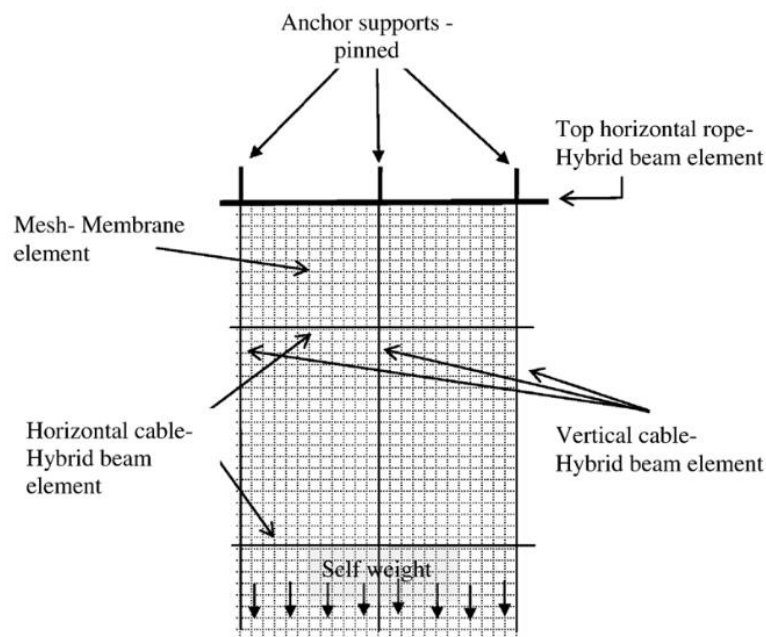


Figure 2.13 FE model and boundary conditions of the mesh adopted by Sasiharan et al. (2006).

The horizontal and vertical supporting cables were modelled with beam elements, the anchor nodes were assumed to be pinned, while the vertical and bottom external edge of the mesh were left free. Many considerations were made to establish the interface friction parameters with the rock wall, which played an important role since for this protection system.

The model reliability was assessed using some field test results but they are not entirely reported along the text. Once the model was validate, several analyses were executed by varying the configuration of the whole system (e.g. eliminating the horizontal top supporting rope, adding vertical cables, etc.) and outcomes examined. Thus, the numerical model was used as a supporting tool for the system design.

This method to simulate a cable mesh as a membrane was also used by Dhakal et al. (2011) to analyse a similar rockfall protection system. The structure had a similar construction design, acting like a hybrid passive system. The model was developed with the programme LS-DYNA that is based on the FE method and calibrated with experimental outcomes. Particularly, the mesh was modelled with shell elements having a non-linear stress-strain curve extracted by developing an out-of-plane numerical test on a wire panel. Though the assumptions made, the obtained results were quite satisfactory, showing that also this method could be taken into account to model a mesh system.

Castro-Fresno et al. (2008) followed a different approach to model a wire mesh. The numerical mesh was designed based on its real sketch with cable elements having spherical hinges at the intersection nodes instead of the clamps. The model was developed with the ANSYS computer program based on the FE method. The constitutive law of the cables was determined by means of quasi-static tensile tests carried out on a single wire. An elasto-plastic behaviour was assigned to the selected element type with no compression and bending moment resistance allowed. A model of the net with the laboratory test configuration was developed. The comparison of results in terms of force-displacement for the concentrated load case (Fig. 2.4b) had shown an excellent fit with experiment data. In the case of a distributed load over the

net (Fig. 2.4c), some difficulties occurred. The pressure during experiments was applied by means of gravel sacks and the realistic distribution of the load was not easy to be predicted. Therefore, in the simulations different load conditions were considered until a convergence of result was reached. This implies that the methodology used will always need a calibration with laboratory tests for other configuration of the mesh. On the contrary, the validated model with the concentrated load was used to investigate the influence of the mesh size and shape on its performance, for this case study (Fig. 2.14).

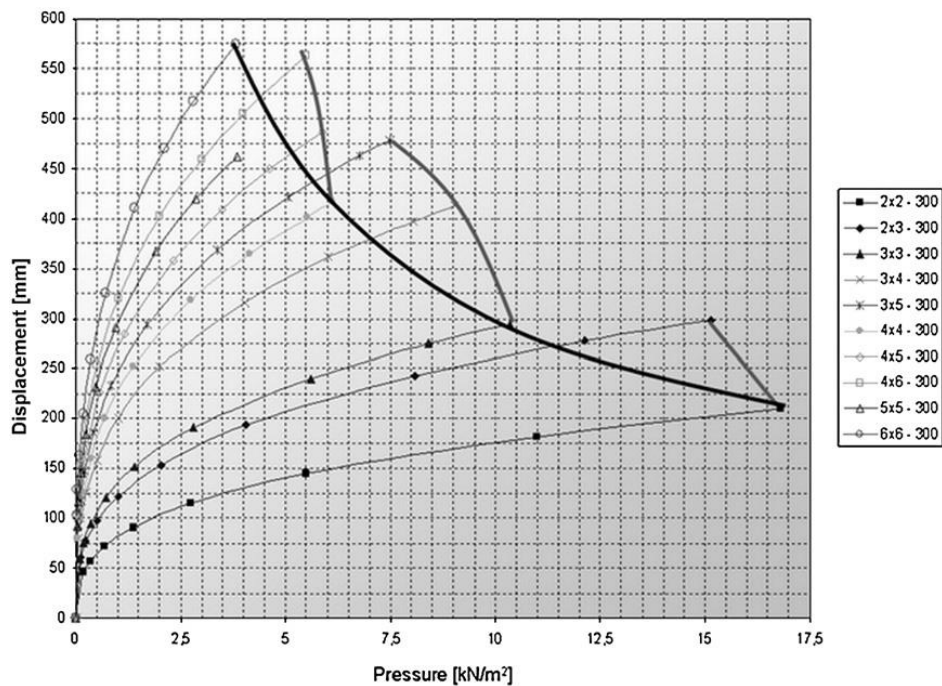


Figure 2.14 Displacement as a function of the applied pressure for a concentrated load towards the mesh (Castro-Fresno et al. 2008).

An important contribution to the research about rockfall interceptive device with wire meshes has been given by Cazzani et al. (2002). The FE commercial code ABAQUS was used to develop the numerical model of the mesh. The cables were modelled with truss element with an elastic-perfectly plastic behaviour, no bending stiffness and cut-off to compression stress. The clamps located at the intersection points were assumed as spherical hinges.

A first assumption that should be evidenced is that, despite strongly dynamic conditions were considered during the simulations, the material properties of cables

were assigned based on the outcomes of static tensile test. Thus, the definition of failure properties based on static condition could lead to wrong estimation of the outcomes. Further, no experimental data on the mesh were available and the performance of the numerical model developed was not perfectly validated. The idealised panel was designed with square shape of 5 m length with a grid of 25 cm size of the openings. The diameter of the constitutive cables was 8 mm and reinforcing cable at the perimeter with 16 mm diameter were considered. As for the boundary conditions, the panel was not fixed at the edges but connected at its vertices with four friction brakes aligned with the diagonals (Fig. 2.15 a). The brakes were modelled with truss element and a three-linear elasto-plastic constitutive law was adopted as from the typical static experimental results on these devices (Fig. 2.15 b).

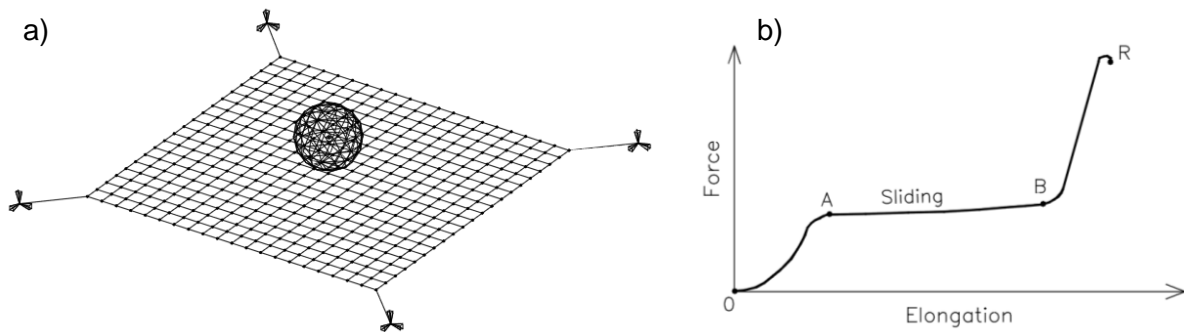


Figure 2.15 a) FE model of the cable mesh panel studied and b) constitutive law adopted for the friction brakes placed in the net corner (after Cazzani et al. 2002).

The dynamic performance of the net was estimated by simulating the impact of a spherical block against the panel. The mesh response was deeply analysed by running several simulations and considering different load conditions.

At a later stage the performance of an entire rockfall barrier FE model, assembled with this mesh type, was assessed by comparing results of simulations with experimental tests data (Peila et al. 1998). Details of the rockfall barrier model are described in next sections.

Typical meshes assembled on rockfall barriers with low energy capacity are the double-twisted and the chain-link systems. Consequently to the experimental campaign described, Bertrand et al. (2008) developed a DE model of the double-twisted hexagonal meshes. A spherical particle was located to each intersection point

and a concentrated mass assigned. A remote interaction model between the nodes was implemented with the mechanical properties of the metallic wire obtained from tensile laboratory tests. For the single wire a uniaxial elasto-plastic relation with work hardening, cut-off to compression stress and failure value, was defined accordingly to experimental outcomes. However, for this mesh type, two interaction models must be considered: the single wire and the double-twisted sections. The constitutive law of the double-twisted section was obtained considering two parameters to transform the single wire remote interaction model. One parameter was introduced to modify the lengthening at failure, while the other modifies the initial elastic stiffness. These parameters needed to be calibrated and the experimental in-plane test carried out on the mesh portion (Fig. 2.6a) was used to this aim. Considering the outcomes obtained from the test in terms of force-displacement, the parameters used in the simulations were modified in consecutive steps in order to find the best fit of results. Further validation of the model was done considering the simulation of the punch test (Fig. 2.6b). In this way also the out-of-plane loading path was investigated in static condition. The comparison of results of this case study showed some inconsistencies, the authors justified this variation by the difficulties to reproduce the stress concentration at the boundary conditions introduced in the experiments. Probably, the underestimation lies on the double-twisted section properties which are not defined experimentally but only with a numerical approximation.

The model response to dynamic conditions was then evaluated but only numerically. A particular rockfall protection system model was built and its capacity to withstand the collision of a rock falling against the net was investigated. The capability of a well-defined modelling strategy to be used as a design tool to study different test phenomenon was proved, although the dynamic tests should be validated by experimental data.

Recently Thoeni et al. (2013) have developed a more comprehensive study of this mesh type. They carried out tensile test on both the sections wire to determine the constitutive law experimentally, then dynamic out-of-plane tests on the panel were conducted to better validate the model of the system. The work has been considered to

the aim of developing part of this dissertation and it is extensively described in Chapter 5.

The chain-link mesh system was studied numerically by Roth et al. (2007). The model was realised using the FE software FARO; this code was specifically developed to study the behaviour of rockfall barrier made with a ring mesh. To analyse this mesh type, the equivalent model developed for the ring mesh was used, even if the meshwork of a chain-link system has a different design. The material properties were initially assigned to the elements and then modified considering four parameters. They were calibrated in order to obtain a similar response to the pull-out tests carried out experimentally. The model was then used to investigate the performance of the chain-link mesh to dynamic out-of-plane tests. Though this study represents an original work, the simulation results should be validated by experimental data. Further, the use of an equivalent mesh developed for another mesh type demonstrates that a better analysis should be considered for the chain-link system.

2.4.2 Simplified models of rockfall protection barriers

A first analytical solution to study the impact event against a rockfall barrier system was given by Hearn et al. (1991). Based on the wide experimental database of full-scale tests carried out for different configurations of a rockfall barrier named Flexpost fence, a FORTRAN program that considers non-linear dynamic analysis with large deformation was developed. The model was made by a set of nodes with lumped mass assigned to each node. During the analysis the node displacements and element forces were evaluated with a time-step approach of 0.01 s. The contact forces between the mesh and the block were computed during the analysis and distributed to the system. The model was able to estimate the elongation of the mesh, the rotation of the posts, and the reaction forces at the foundation nodes. The results were quite consistent with the field test data although the assumption made. Further, the program was refined to analyse the behaviour of other barrier configurations. Despite, the comparison with experimental data was not substantial, this work firstly proved the importance of using these instruments as predictive tool to define a barrier performance.

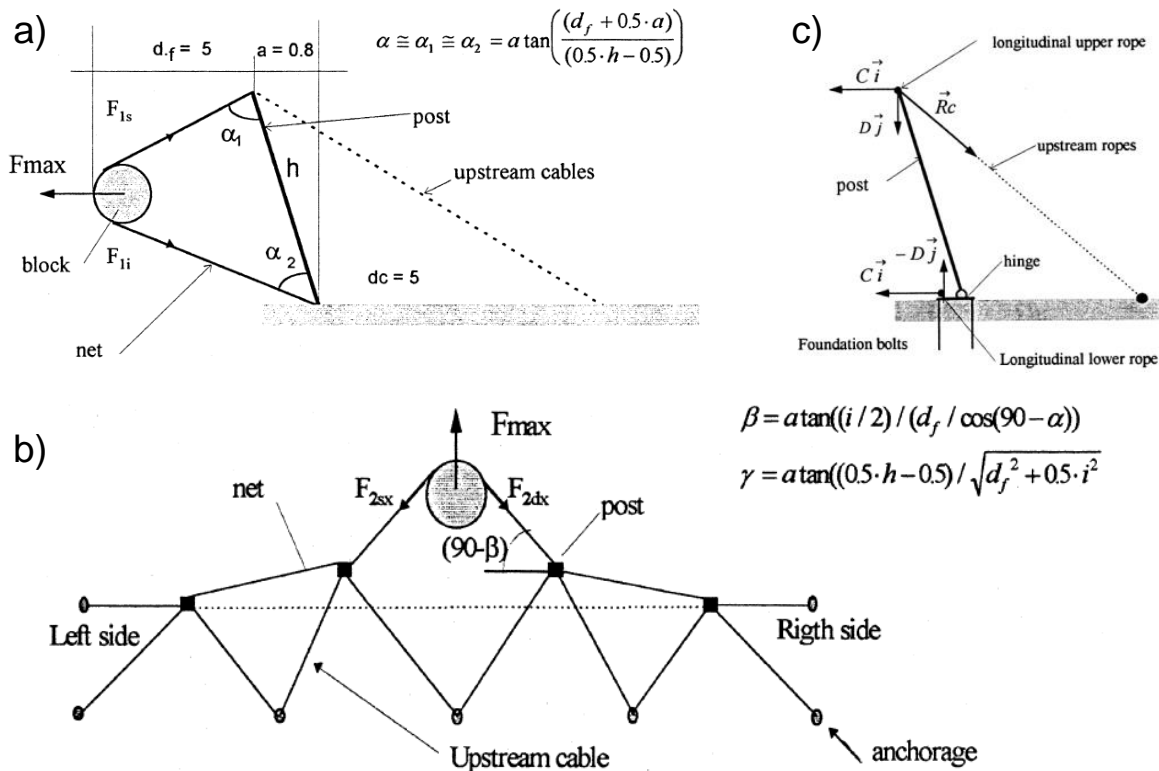


Figure 2.16 Geometry adopted as design scheme for the analytical formulation of Peila et al. (1998): a) transversal section; b) plan and c) scheme for the computation of the forces acting at uphill anchorage and post foundation.

A design procedure for rockfall barrier, adopting an equivalent static formulation was defined by Peila et al. (1998). The dynamic event was transformed into a static problem and solved with a simple redistribution of the acting forces. Two simplified schemes were used considering the deformed configuration of the barrier as illustrated in Fig. 2.16a and b. The design force (F_{max}) used in the problem was derived from the theoretical average force ($F_{average} = E_{kin}/D_{max}$) applying a safety factor of 2.5.

The following hypotheses were made to solve the analytical formulation:

- the block impacted the net orthogonally with no gravity;
- the design displacement considered in the adopted scheme was the maximum observed during experiments;
- the net was considered as a structure distributing the force uniformly.

The analytical model was able to compute the forces acting at the post foundation (Fig. 2.16c) and at the anchorages. It was validated based on the results of a full-scale test. The comparison of results was quickly illustrated and showed that the

approximations made were partially affecting the solution. However, the formulation proposed just wanted to represent a simple tool and to define a preliminary indication about the barrier outcomes.

A simplified analytical formulation to study rockfall protection barriers was also recently realised by Cantarelli et al. (2008). The model parameters were calibrated by comparing with the experimental outcomes obtained from different prototypes of barrier tested in a full-scale vertical test site (Gottardi and Govoni 2010). In the formulation, the initial time ($t_0 = 0s$) was assumed when the block, a lumped mass m , impacted the barrier with a vertical velocity (v_0). Considering the angle α as the barrier position with respect to the vertical direction (i.e. $\alpha = \pi/2$ for vertical test site) and the coefficient k to take into account the net elastic response, the simple harmonic motion equation was considered as:

$$\ddot{s} = g \sin \alpha - \frac{k}{m} s \quad (2.1)$$

Thus, by imposing $\frac{k}{m} = \omega^2$ and through opportune substitutions, the formulation that expresses the block motion after the impact can be written as:

$$s(t) = \frac{g \sin \alpha}{\omega^2} (1 - \cos \omega t) + \frac{v_0}{\omega} \sin \omega t \quad (2.2)$$

Eq. 2.2 combined with experimental outcomes can be used to estimate the elastic property of the barrier and to evaluate the braking time. It was proved that the equation was able to reproduce the experiment results quite well for a preliminary analysis. The validated model was then used to investigate the influence of the block characteristics on the rockfall barrier capacity by assuming some parameter to take into account for the block presence. This issue is further explained in Chapter 5.

Considering simplified analysis of rockfall barrier, some authors developed a two-dimensional numerical model to retrospective simulate the structure response to dynamic events (De Miranda et al. 2010; Govoni et al. 2011). The model was built with a FE code based on a time integration approach using the Newmark method to solve non-linear dynamic analyses. The aim was to reproduce the experimental full-

scale test carried out on several prototypes of high-energy rockfall barrier in a vertical test site (Gottardi and Govoni 2010). Due to the system configuration, the block was hitting the central point of the middle functional module with a normal trajectory, therefore the barrier response was considered symmetric with a uniform transmission of the derived forces to the structure. This assumption enabled a strong simplification in the model geometry, but still retaining its dynamic and highly non-linear nature. Thus, a two-dimensional model that considers a vertical cross-sectional plane located at the impact point was designed (Fig. 2.17a).

All the components were modelled with truss elements: one element as for the uphill cables, one for the posts and two for the mesh, while the block was modelled with an additional lumped mass placed at the central node of the net. Spherical hinges were assigned to the internal and external connection between the elements and the slope. The simulations fitted the experimental outcomes quite well for the different configuration of prototypes tested. Though a low computational effort required to solve the problem, the simulations were able to reproduce most of the first part of the impact test.

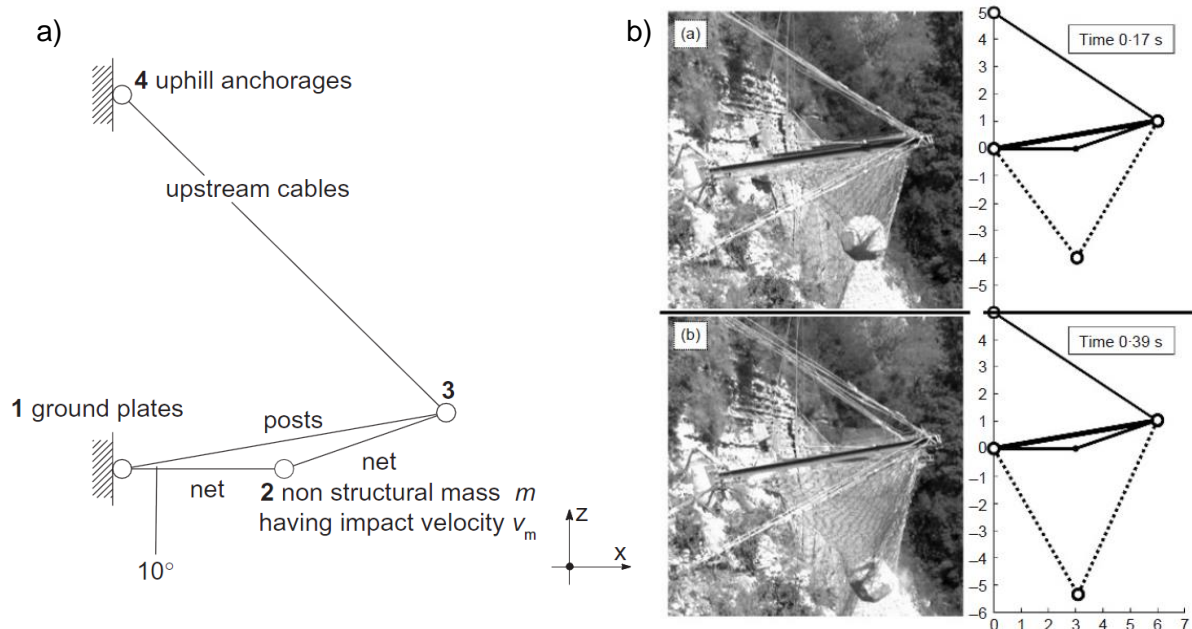


Figure 2.17 a) Two-dimensional model adopted by Govoni et al. (2011) and b) qualitative results of the deformation (experiments vs FE model).

Further, an excellent prediction of two important parameters, the maximum elongation (D_{max}) and the pertaining braking time (t_b) was achieved (Fig. 2.17b). The simplified FE model demonstrated to be a very practical tool to support for the design of these prototypes. However, it should be highlighted that the model data were strictly calibrated based on the full-scale test outcomes. Considering that the geometry of the system can vary for different manufacturers, the model should be re-validated with experimental data. Thus, to gain understand of different prototypes performance, a more realistic three-dimensional FE model should be developed.

2.4.3 Advanced models of rockfall protection barriers

If opportunely validated with experimental data, the simple two-dimensional analytical or numerical model described above, can be used as supporting tools for a preliminary estimation in the design of a barrier. Different impact condition (i.e. block size or velocity) or barrier configuration (i.e. barrier inclination or dimension) can be modified for simple parametric analyses. Anyway, to take advantage of the capacity of the numerical instruments and to gain accurate information of a prototype performance, the use of a complete three-dimensional model should be preferable.

Despite some work has been already carried out, the three-dimensional numerical models of rockfall barriers developed up to now should be enhanced.

This need has been underlined by the recent work developed to study the barrier by means of different numerical instruments (Bertrand et al. 2012; Van Tran et al. 2013; Bourrier et al. 2014; Escallon et al. 2014; Moon et al. 2014).

Nicot et al. (2001), after studying the mesh behaviour initialised a complete modelling of the system. Though it was a preliminary study, some important information were supplied. The model was developed with the DE method and the simulations were run through a software that used the explicit algorithm based on the finite differences method. In the creation of the model every material body was reproduced by nodes and linear elements, post were considered rigid elements as well as the spherical block. The energy dissipating devices were modelled with a plastic law but it was not

fully-explained in the text. The outcomes of full-scale testing on a rockfall barrier prototype were analysed and compared with the simulations. The problem is that no information about experimental results were recorded during the test, therefore only a qualitative comparison of the deformed shape as outcomes was done. The only available testing data were the final displacements of the energy dissipating devices, the comparison of these results showed a rather good agreement, although showing that the model dissipated less quantity of energy. As stated by the authors, the model should be better enhanced and validated. However, it proved the potentiality of a similar approach to gain a rapid understanding of many features that cannot be otherwise evaluated during an experiment or demand several tests to be estimated.

Similarly, Cazzani et al. (2002) investigated the dynamic response of a high-energy rockfall barrier after analysing the performance of the cable mesh. The studied barrier was subjected to full-scale tests in an inclined test site (Peila et al. 1998). The cables and the energy dissipating devices were modelled with truss elements as described for the mesh model, while beam elements with elastic-perfectly plastic relationship were selected for the posts. The trajectory parameters derived from the experiments were defined for the impacting block, but the angular velocity was neglected as well as the gravity acceleration. Other important approximation regarded the internal connections between the elements, the sliding mechanisms at the connections was simplified by joining the nodes with short rigid bar. Furthermore, the interaction with the ground, which happened during the experimental test, was not taken into account. The authors themselves highlighted the approximations made and the assumptions were justified by the purpose to develop a simple model with low computational cost. Due to the less flexible system obtained, as a consequence of the several assumptions made, the comparison of results showed that the model was underestimating the whole barrier performance. However, the work carried out represented a breakthrough on three-dimensional numerical modelling for rockfall protection barriers. It revealed the difficulties that need a further investigation to be overcome in order to develop a more reliable model of these structures. Particularly, the last part of the work was focused to

use the model to analyse the block size influence on the overall performance of the barrier and is illustrated in Chapter 5.

Up to now, one of the thorough works that developed a three-dimensional numerical model of rockfall barriers has been carried out by Volkwein (2005). The innovation here introduced regarded the modelling of the interaction between the different elements. Particularly, the attention was focused on the ring-cable connection. The sliding mechanism involved would require an investigation with high computational cost. The assumption made was to model the longitudinal cables as single tension-only springs with several nodes (Fig. 2.18a), allowing the movement of the internal nodes while keeping constraint the others (Fig. 2.18b).

In Volkwein et al. (2004) a comparison of results is shown, demonstrating the quite good accordance reached. However, while a lot of data were illustrated for the mesh modelling described in Section 2.2, only results of one test were reported for a prototype configuration. The model validity should be better validated also for other construction designs, or more experiments carried out at different impact condition. Though the numerical modelling technique is rather good, its flexibility to evaluate different case study was not proven and some uncertainties has been demonstrated.

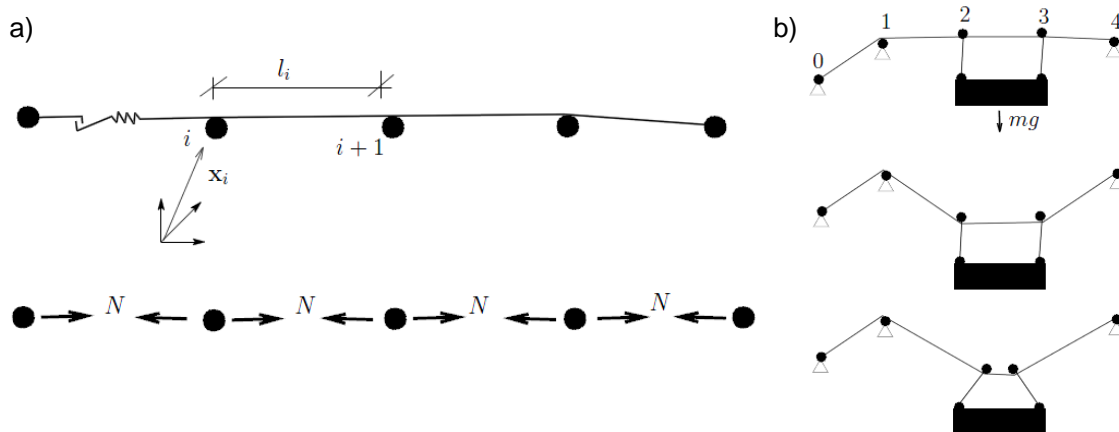


Figure 2.18 a) Modelling of the cable elements with springs and b) movement of the cable nodes during the dynamic event after Volkwein (2005).

Recently Gentilini et al. (2012a) have proposed a numerical strategy to realise three-dimensional numerical models of high-energy barrier prototypes. A well-defined procedure was assessed, considering data of impact tests carried out on barrier with different characteristics and construction designs. The numerical model produced by the authors has been further developed as part of this thesis, in order to reproduce the barrier response under different impact test conditions through an accurate comparison with experimental data. The work obtained is extensively described in Chapter 3.

CHAPTER 3

**NUMERICAL MODEL TO INVESTIGATE THE RESPONSE
OF HIGH-ENERGY ROCKFALL BARRIERS**

Introduction

High-energy rockfall barriers are complex systems designed to absorb the energy of blocks falling along an unstable slope by means of large plastic deformations of the structure.

Due to the high non-linearity engendered by the dynamic event, it is difficult to describe the decelerating process of the block, hence a typical barrier design is based on prototype testing (Volkwein et al. 2011). In 2008 the European Guideline were approved (EOTA 2008), outlining the testing procedures for rockfall barrier systems. Full-scale testing of these structures became mandatory for the manufacturers throughout the European countries in order to obtain a CE marking of their products. Thus, a continuous research of these systems has been encouraged leading to an improvement of their engineering design.

Consequently to a partnership between the Italian companies Consorzio Triveneto Rocciatori and Officine Maccaferri and the DICAM Department of the University of Bologna, a series of full-scale tests on several barrier prototypes were carried out. A comprehensive database of results was produced and most of the data obtained are described in Gottardi and Govoni (2010).

Based on these data, analytical and two-dimensional numerical solutions were developed (Cantarelli et al. 2008; de Miranda et al. 2010; Govoni et al. 2011). They supplied a simplified tool to gain a preliminary understanding of the barrier response. However, the several data available would allow for developing a more refined modelling of the prototypes in order to better analyse the structure behaviour.

Gentilini et al. (2012a) first realised advanced three-dimensional FE models of the different prototypes studied. The authors proposed a numerical strategy for the

definition of rockfall protection barrier models. The developed model was validated by reproducing retrospectively the experiments, however there were still some uncertainties in the definition of the behaviour of some constitutive elements. Moreover, the wide database at our disposal would allow to better assess the model reliability and then to further explore its potentiality.

In this research, the numerical approach devised by Gentilini et al. (2012a) has been further enhanced considering a rockfall protection barrier having energy absorbing capacity of 3000 kJ. The prototype was analysed by full-scale testing as described by Gottardi and Govoni (2010). The test results are used to assess the model effectiveness, by simulating, retrospectively, the experiments carried out at different energy levels. Then the barrier's model is used as a predictive tool to estimate the overall system performance by varying its construction design and the impact configurations.

In the following the details of the experimental database used to define the numerical model are briefly described. The numerical strategy previously developed is widely reported, highlighting the various weakness observed. A comprehensive background of this part of research has been given and finally, the chasing aims are illustrated.

After this introducing part, two papers produced are reported as part of the thesis. The first is a journal paper where the procedure followed to develop the FE model of the analysed barrier is widely described and the model has then been used as a supporting tool in the design of the structure. In the second, a conference paper, the potentiality of the model has been further explored to provide information about the barrier performance under different impact conditions. Other conference papers were developed about this issue outlining the model reliability but they are not reported here, their references are given in the first part of the thesis (de Miranda et al. 2011; Gentilini et al. 2012b).

Background

Typically found in territories interested by rapid slope movements, flexible barrier are metallic structures made of identical functional modules, installed in sequence for the required length. They are designed to withstand the impact of falling blocks producing large irreversible deformations of the system. For this reason their capacity is defined on an energy criterion, which is the kinetic energy owned by an impacting body that the barrier is able to absorb.

Gottardi and Govoni (2010) carried out a series of full-scale experiments on several prototypes of falling rock protection kits having energy absorbing capacity ranging from 500 to 5000 kJ. The tests were conducted as a consequence of the collaboration between the University of Bologna and two Italian firms: the Consorzio Triveneto Rocciatori and Officine Maccaferri. The first aim of the research was to investigate the response to impact events under various kinetic energy levels (SEL and MEL) of the different rockfall barrier configurations tested. The experiments were performed according to the European testing standard (ETAG 027) and a vertical drop test site located in Fonzaso (Italy) was used for the experimental campaign.

As described in Chapter 2, the vertical test setup allowed a series of advantages, above all the reproducibility of the tests. Further, it guarantees that all the energy is dissipated by the system, with any contact between the impacting body and the ground. In fact, the block was lifted by a crane to the requested initial height and then dropped, by means of an automatic quick release, to impact the centre of the middle functional module in a free vertical fall.

Five different configurations of barriers were tested, made of three functional modules of 10 m width and nominal height ranging from 3 to 6 m. Depending on the energy capacity of the system, the complexity of the design had some dissimilarities. The number of connecting cables and the energy dissipating devices mounted on them was varying on each tested prototype. As for the interception structure, a wire mesh was used for lower energy class barrier, while ring meshes were assembled on high-energy prototypes (i.e. more than 3000 kJ).

Concerning the relevant data obtained, different instrumentations were used to allow their supervision before, during and after each test. The initial configuration was measured with a precision surveying system, in order to have the right value of the initial block position with respect to the installed barrier and thus estimating the impact characteristics. Then, a laser sensor system located just above the barrier was used to monitor and verify the velocity at impact; while three front cameras and one lateral were recording the entire event allowing the extrapolation of the block displacement time-history.

All the anchorages of the connecting cables (i.e. lateral and uphill) were supplied with load cell instruments, able to record the resultant acting force evolution during the test. Only three prototypes were further investigated and equipped with load cells measuring all the components of the reaction forces at the post base. Note that all the foundation systems were provided with instrumentations to verify the symmetric response of the barrier to the impact test. Finally, at the end of the test the residual heights and the total shortening of the energy dissipation devices were taken with direct measurement.

The barriers were subjected to MEL test and some prototypes to the double launch of SEL impact test. Despite only part of the results were reported, all the test data were available to develop the research hereinafter described.

As stated by the authors, the experimental setup could be easily modified and different test conditions and configurations can be assessed but it would be a costly and time consuming procedure. Thus, the aim of the work was to supply a wide and rich database of experimental evidence on these structures, with the idea to support the development of an advanced numerical modelling of the systems.

In Section 2.4 the analytical and two-dimensional FE models proposed and calibrated with a back-analysis of these experimental data were introduced. The simple models have shown to be able to reproduce part of the relevant parameters design (i.e. elongation, braking time and average load distribution at the foundation structure). A preliminary understand of the barrier response was achieved, but a more advanced model was requested to further investigate the rockfall barrier performance.

Gentilini et al. (2012a), taking into account these broad experimental database, have developed a numerical strategy which aims to define a series of instruction to be followed in the design of numerical models of rockfall barriers.

Contrary to the researches previously described, the authors have assessed the models effectiveness taking into account data of three different prototypes tested under various impact conditions (i.e. SEL and MEL tests).

In the numerical approach, the commercial available computer program ABAQUS/Explicit was employed. In order to produce accurate simulations with a simple and computationally effective model, some assumption was made within reason of the structure complexity.

A first important approximation was taken in the modelling of the impacting body. It was simulated with a set of lumped mass placed in the mesh nodes of the impacted area. The equivalent mass of the block was distributed to the nodes and a vertical velocity input derived from the full-scale test was assigned. This solution allowed a strongly reduction of the computational cost of the simulations, even though the model had shown to be able to predict with accuracy only the first part of the test (i.e. till maximum elongation is reached).

All the cables were modelled with truss elements with an elasto-plastic constitutive law derived from the typical static tensile test outcomes, while for the posts, beam elements were used with a simplified linear elastic behaviour.

Differently, a three-linear stress-strain relation (Fig. 3.1a) was assigned to the cables endowed with an energy dissipating device. The curve was extrapolated through some assumptions of the results of the test carried out on the whole barrier. The authors analysed the force time-history recorded by an anchorage load cell where one cable equipped with the device was connected (Fig. 3.1b). After a first rapid increase of the force, a sort of plateau was noticed, before it grew again to the peak value.

It was suggested that the force at which the plateau was reached gave indication of the activation of the energy dissipation device. Thus, the almost horizontal branch of the constitutive law, which represents the device influence in the cable response, was identified and calibrated.

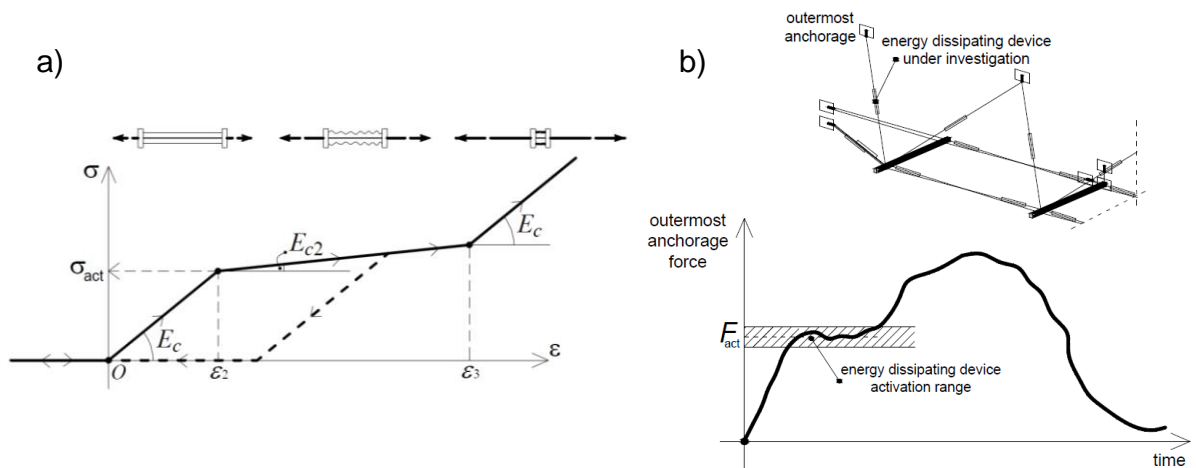


Figure 3.1 Energy dissipating devices properties after Gentilini et al. (2012a): a) constitutive law adopted and b) time-history recorded by the load cell and location of the node in the barrier.

Concerning the internal connection, a particular attention was focused to study the sliding mechanism of the longitudinal through special eyelets placed at the head and base of the posts. Figure 3.2a illustrates with a simplified scheme the effect: as a consequence of the impact, the cables tend to shift following the deformed shape, but the eyelets retain the vertical displacements allowing only horizontal movements. As pointed out in Section 2.4, it represents a problematic issue to be solved for these systems. A set of special link was used to model this mechanism in the simulations (Fig. 3.2b). Each link connected a master node (M) placed on the post centroid, to a slave node (S) located along the cable. The connector keeps constrained the vertical displacement of the S nodes to the initial value (y_0), while letting free the motion in the other directions. Further, when the cables slide till the so-called “detaching point”, the connector bond failed, allowing the S node to move also vertically, thus following the normal deformation derived from impact.

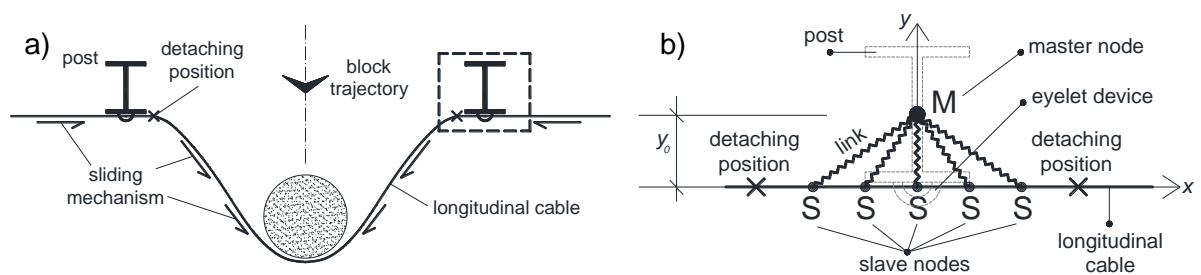


Figure 3.2 Details of the internal connection between post and the longitudinal cables after Gentilini et al. (2012a): a) sketch of the sliding mechanism and b) solution adopted in the numerical model.

This simple solution had shown able to well-describe the motion during the test, and it has been used also in the numerical models produced as part of this thesis and described hereinafter.

In order to investigate the rockfall protection barrier response to dynamic event, the interception structure is the most important component to be studied in the modelling approach. Two flexible barriers here analysed were built with a ring mesh type. An equivalent mesh made by truss element connecting each centre of the ring was realised following the approach proposed by Nicot et al. (2001). The stress-strain relationship assigned to the equivalent elements was calibrated through an identification procedure. Two quasi-static in-plane and out-of-plane tests were carried out on a panel made by rings and to the equivalent truss mesh (Fig. 3.3a). Results of the two tests are reported in Fig. 3.3b and c. As stated by the authors, no experimental evidence were available, hence the tests were performed only numerically.

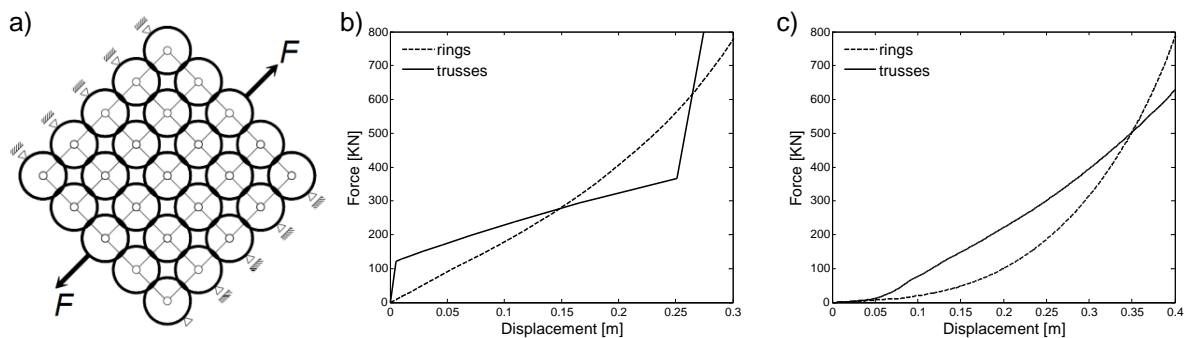


Figure 3.3 Identification procedure of the equivalent meshes (Gentilini et al. 2012a): a) ring mesh portion tested and equivalent truss mesh identified (lighter line); b) load-displacement curves obtained from the in-plane and c) out-of-plane tests.

Results of the model versus the experimental data were shown as time-history of the barrier elongation for all the tests analysed and a remarkably good agreement was observed both in terms of maximum value reached and general trend of the curves.

Concerning the forces measured at the anchorages and post foundations, only a comparison of one model at MEL impact test was illustrated proving the effectiveness of the numerical approach developed.

Though the method was well-validated by a wide confrontation with the experimental outcomes, there was still some lack of information on some details of the modelling that should be enhanced. Some of the approximations made in the modelling approach and highlighted above could be better solved.

Firstly, the model with lumped mass had proved to be not useful to predict the model response after the first peak or to run simulations of a second launch on the deformed barrier. Despite the possibility to model the impacting body with lumped mass is a good simplification, a three-dimensional model of the block can allow for further consideration.

Considering the method adopted for the energy dissipating devices, it obviously represents a good solution that can be easily implemented, but the problem is twice.

There is no evidence of test on a single brake system to validate the stress-strain curves adopted. Since the first aim of the work was to produce a model able to investigate the barrier performance by varying its configuration, it should not be possible to analyse the influence of using a different dissipating brake type. It leads to the second issue that, in order to define the behaviour of the dissipating device, this method need of test results on the entire barrier. Hence, a better investigation of this device should be carried out, both experimentally if possible, either by using the numerical method. The last assumption made was about the validation of the equivalent model of the mesh. The results obtained from the two tests (Fig. 3.4) proved that the response of the two models was not perfectly fitted. Further, the ring mesh behaviour should be validated with result of experimental test to assess the net performance, therefore a more accurate calibration should be developed.

Aims of the research

Up to now, a background of the relevant document proposed in literature, used to carry out this part of the thesis has been illustrated. The origin of the available experimental data was explained. The various problematic encountered in the definition of the numerical approach already defined were widely highlighted.

In the papers hereinafter reported, a numerical FE three-dimensional model of a rockfall protection barrier prototypes having energy absorbing capacity of 3000 kJ was developed and deeply investigated. For this protection kit, data of several impact tests carried out at various energy level, also on the deformed prototypes (i.e. double impact test of SEL) were available.

The starting aims of the produced works can be recapped in different point:

- Further investigation of the behaviour of some constitutive elements (i.e. the interception structure, the energy dissipating devices and the impacting body) by considering experimental data, if possible, or developing specific numerical analysis.
- Validation of the numerical model developed in a back-analysis confrontation by considering the outcomes of several impact test conditions. Especially, assess the model effectiveness to second launch tests carried out on the deformed structure.
- Use the model as a predictive tool to support the design of these structures. Investigate the performance of different construction design of the barrier, in order to assess the improvement of the new configuration by using the numerical model without recurring to costly full-scale tests.
- Use the model to analyse the response of the barrier to different impact test conditions.

JOURNAL PAPER I

3.1 DESIGN OF FALLING ROCK PROTECTION BARRIERS USING NUMERICAL MODELS

Abstract

A numerical approach has been recently devised by the authors for the modelling of falling rock protection barriers, metallic structures used as passive measures against rockfall. Following this approach, in this study a FE model of a specific barrier type is developed. The constitutive parameters of the model are calibrated employing the data of a series of experiments carried out onto the main barrier components such as the interception structure and the energy dissipating devices. Then, the ability of the FE model to reproduce the real barrier behaviour is explored by simulating, retrospectively, a set of experiments carried out onto real-scale prototypes of the barrier, under various impact conditions. The very good fit of the rather complex experimental and numerical results can assess the ability of the FE model to reproduce the prototype behaviour, so validating the reliability of the adopted numerical approach and giving further confidence to the use of such models as design tools. Therefore, based on the numerical results, the considered barrier model has been enhanced in terms of cost-effectiveness and on-site performance.

3.1.1 INTRODUCTION

Typically found in territories interested by very rapid slope movements, falling rock protection barriers are metallic structures, made of identical functional modules installed in sequence for the required length (Giani 1992). As depicted in Fig. 3.4, each module presents an interception structure kept in position by steel posts (supporting structure), while special connecting elements transfer the impact loads to the foundations. Easy to be installed and maintained, with relatively low environmental impact, the barriers are designed to intercept and stop the blocks moving along a potentially unstable slope, by developing large elasto-plastic deformations of the system and of the system components. Nowadays, several manufacturers produce different models of falling rock protection barriers which cover a wide range of energy absorption capacities, from less than 100 kJ to more than 5000 kJ.

Traditionally, these structures are designed using the results of full-scale tests in which prototypes are subjected to the impact of blocks having known mass and velocity. Since 2008, the testing methods and procedures have been provided by the European Guideline for the Technical Approval of Falling Rock Protection Kits – ETAG 27 (EOTA 2008). The data collected in the full-scale tests enable to assess the energy absorption capacity of a falling rock protection barrier and provide the relevant parameters for the barrier installation in-site, which include the deformation characteristics and the dynamic forces acting on the barrier anchorages and foundations.

In the last ten years, the results of full-scale tests were also employed to develop numerical models of specific types of commercially distributed falling rock protection barriers, using either FEM (Cazzani et al 2002; Volkwein et al 2009; Oggeri et al. [2006]; Govoni et al 2011) or DEM (Hearn et al. (1992); Nicot et al. 2001; Spadari et al. 2012; Bertrand et al. 2012) approaches.

Due to the complexity of the problem, the trustworthiness of numerical models as design tools relies upon a consistent procedure of calibration and assessment which must be based on experimental data, accurate in describing the complete barrier response in dynamic conditions. The database should also be diversified and relevant

to the response of these structures in different conditions, enabling the use of a set of data for the model development and calibration and the use of further results for the purpose of the model assessment.

Within this context, a numerical approach for the design and verification of flexible falling rock barriers has been recently proposed by the authors (Gentilini et al. 2012a). Rather than a single numerical model, the proposed procedure enables the definition of key numerical choices of general validity that enable the development of consistent numerical models of any type of falling rock protection barriers.

The main advantage of the approach is that, notwithstanding the complexity of the simulated phenomenon, it enables to produce comparatively simple models which accurately capture the highly non-linear response of these structures in dynamic conditions. The procedure was based on data of full-scale tests performed on various barrier prototypes of capacities ranging from 500 to 5000 kJ (Gottardi and Govoni 2010), under several values of impact energies, carried out in different conditions.

In this paper, a FEM model of a falling rock protection barrier of capacity 3000 kJ, hereinafter named barrier 3000, has been developed according to the above mentioned approach. The model is calibrated using the results of specific tests performed on the main barrier components and assessed using the experiments on full-scale prototypes. The reliability of the model as a predictive tool is then explored through a retrospective simulation of further full-scale tests executed on the same barrier prototypes. The model suitability to support the design of these structures is then investigated. In particular, guided by the reliable numerical results, few modifications in the tested prototype of barrier 3000 are introduced to enhance both its cost-effectiveness and on-site structural performance.

Impact analyses are then carried out onto the modified model of barrier 3000 to investigate its modified response in dynamic conditions. Results provide a useful guidance for the development of enhanced falling rock protection barriers.

In the paper details of the full-scale experiments are given in Section 3.1.2, referring to Gottardi and Govoni (2010) for further information; the numerical approach is

briefly described in Section 3.1.3, referring to Gentilini et al (2012a) for details; the development of a complete model of barrier 3000 is illustrated in Section 3.1.4. Results of retrospective simulations of full-scale tests on prototypes are then compared to the experimental data in Section 3.1.5, to enable a thorough assessment of the numerical model. The use of the model as a predictive tool has been finally investigated on an improved model of barrier 3000 in Section 3.1.6.

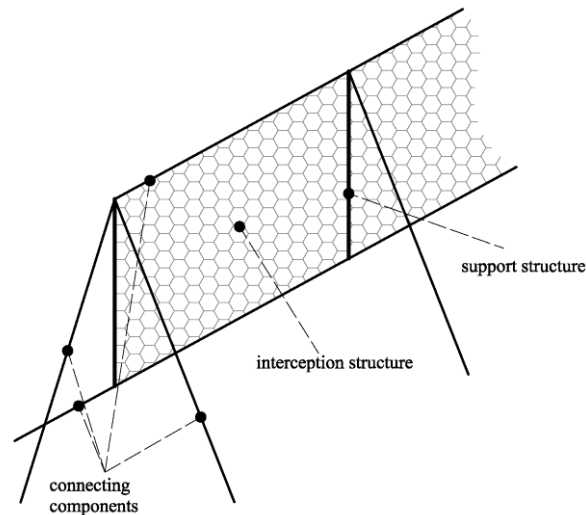


Figure 3.4 Scheme of the main components of a typical falling rock protection barrier.

3.1.2 EXPERIMENTAL DETAILS

In this Section, details of the experimental tests conducted on the interception structure and on full-scale barrier prototypes are described and discussed. These tests were carried out at the Fonzaso test site (Belluno, Italy) (Gottardi and Govoni 2010) and enable the development, calibration and assessment of the numerical modelling procedure described in the following Sections.

Impact tests on the interception structure

Impact tests were carried out onto samples of a type of ring net employed as an interception structure for various falling rock protection barriers of high energy absorption capacity (typically higher than 2000 kJ). The scope of the tests was to

evaluate the dynamic response of an individual net panel to the impact of a block of known mass, velocity and direction.

The tested net was made of 350 mm diameter rings completed by twisting six times the same 4 mm wire and arranged so that each ring is enclosed and loosely interlaced to other six. The sample, a 3040 mm x 2590 mm portion of such a net made up of 56 rings, was connected to the top of a rigid frame of structural steel beams, built on a concrete foundation as illustrated in Fig. 3.5a.

Employing a small crane, the test was carried out by lifting a concrete block of mass 1610 kg to the established position and then releasing it onto the net sample. Two video cameras, one on the front, one on the top of the frame, recorded the entire event. By varying the falling height of the block, two launches were performed at two distinct values of kinetic energy: 98 and 129 kJ, hereinafter called launch N1 and N2, respectively. At the end of each launch (Fig. 3.5b), the test block was removed and the net final maximum elongation was measured. Recorded values were 0.60 m and 0.67 m after launch N1 and N2, respectively. No failure occurred in the net after the two launches.

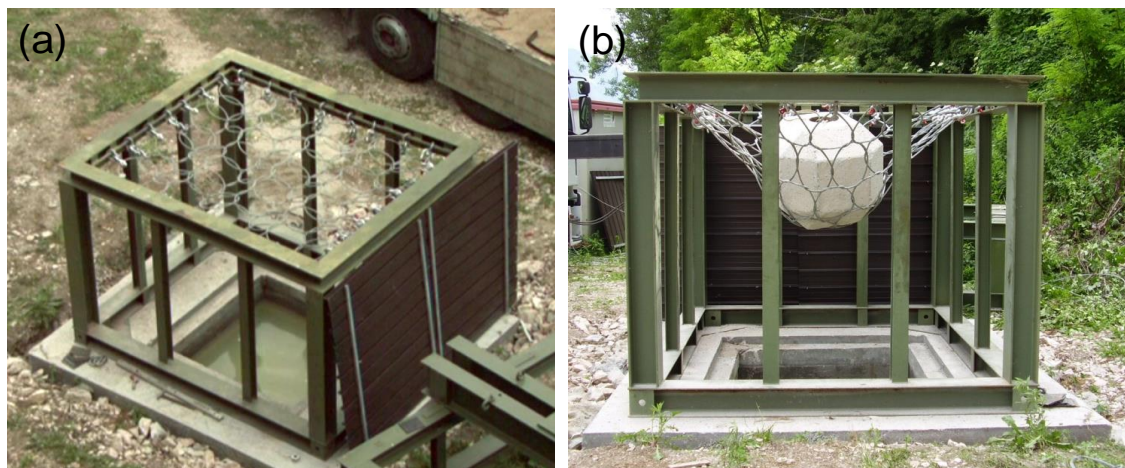


Figure 3.5 The experimental set up for impact tests on ring nets: a) before and b) after launch N1.

Full-scale impact tests on barrier prototypes

The Fonzaso test site is of one of the vertical-drop type, in which a three functional modules barrier, installed approximately normal to a sub-vertical rock wall, is subjected, in its centre, to the impact of a free falling test block.

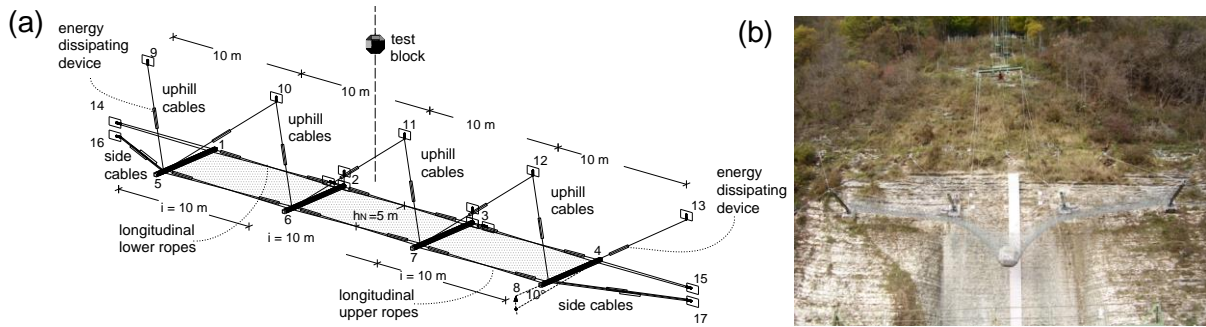


Figure 3.6 Barrier 3000 in the vertical-drop test site configuration: a) schematic drawing and b) picture taken after the maximum energy level impact test.

A scheme of barrier 3000 in the typical test-site configuration is given Fig. 3.6a, where the names of the principal elements, the positions of the load cells and node labelling are also indicated.

The interception structure is made of a steel ring mesh and the supporting structure of steel I posts, inclined at an angle of 10° with respect to the horizontal plane. The loads are transferred to the uphill anchorages through uphill cables. Two longitudinal upper and two longitudinal lower ropes connect, respectively, the heads and the bases of the four I beam posts. The lateral cables, two for each side, connect the heads of the external posts to the side anchorages. All cables are 20 mm in diameter and are provided with energy dissipating devices whose labelling and positions are illustrated in Fig. 3.7.

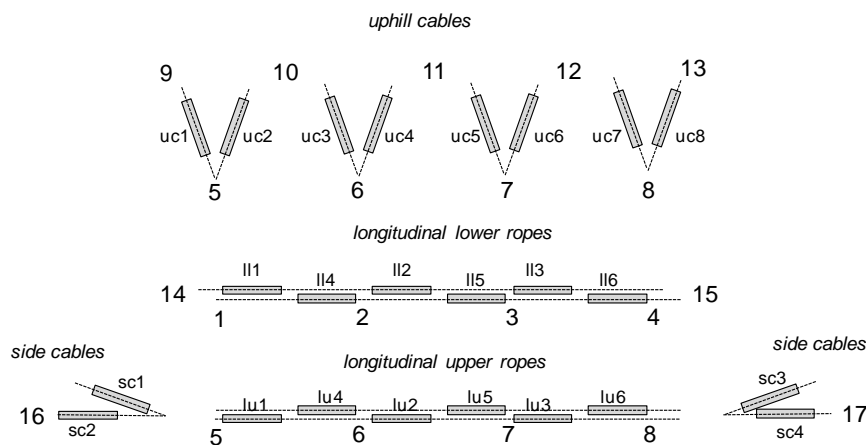


Figure 3.7 Barrier 3000 in the vertical-drop test site configuration: labeling and position of the energy dissipating devices on the uphill and side cables, on the longitudinal upper ropes and on longitudinal lower ropes.

The movements of the block, a concrete polyhedron, are controlled by a crane. The site is provided with precision instrumentation for the measurement, in the dynamic range, of the following relevant quantities: the barrier elongation (defined as the maximum downhill displacement of the net measured during the impact with respect to the initial position), the barrier residual height (defined as the minimum distance between the longitudinal ropes, measured after the impact orthogonally to the falling trajectory) and the forces acting at all the anchoring points and foundations. The braking time (defined as the interval between the instant of the first block-net contact and the instant in which the net elongation is maximum) is also evaluated during the test as well as the final shrinkage of all the energy dissipating devices (travel).

Three full-scale impact tests are considered in this study as follows. Maximum energy level test: a prototype of barrier 3000 was subjected, at its centre, to the impact of a block having energy higher than the design level (3000 kJ). Service energy level test: a prototype of barrier 3000 was subjected, at its centre, to the impact of a block having energy equal to one third of the maximum (1000 kJ). Following this launch, the prototype of barrier 3000 was subjected to a second launch at the same energy level (1000 kJ), to investigate the response of the barrier to subsequent launches. In Fig. 3.6b, a general view of barrier 3000 after the maximum energy level test is given.

3.1.3 THE NUMERICAL APPROACH

The FE model of barrier 3000 was developed according to an effective numerical approach for the modelling of falling rock protection barriers, recently developed by the authors. A concise description of the procedure is provided in this Section, referring to Gentilini et al. (2012a) for further details.

Modelling of the supporting structures

The supporting structures are the barrier posts made of structural steel S275. They can be modelled successfully with beam elements with a linear-elastic, perfectly plastic constitutive law described by the conventional steel elastic modulus ($E_p = 210$ GPa)

and yield strain threshold ($\varepsilon_1 = 0.0013$), as illustrated in Fig. 3.8a. Cylindrical hinges are also effective towards the modelling of the connection between the posts and the foundations. The posts are also provided with eyelets at the base and head which lead through the longitudinal lower and upper ropes. A translator type of connector which allows slave nodes located on the lower (upper) ropes to move along a specific direction while keeping a fixed distance from a master node located on the base (head) of the posts, was shown rather suitable to model these connections. The distribution of the impact force to the anchoring points and post foundations in the numerical analyses is rather accurate while a very low computational cost is ensured. Yet, numerical forces slightly above the experimental might be observed at some of the anchorages and post foundations, notably in presence of unloading-reloading cycles.

Modelling of the connecting components

The main barrier connecting elements are the uphill, side and longitudinal cables. These elements can be satisfactorily modelled by means of truss elements with no flexural rigidity and no ability to sustain compressive stresses. For cables, a bi-linear, elasto-plastic law with hardening can be used (Fig. 3.8b). The three parameters that characterize the constitutive curve are those typical of strands subjected to tensile loads and should be selected among those relevant for the considered type of cable (Fontanari et al. 2009; Castro-Fresno et al. 2008).

Typically, the cables are provided with energy dissipating devices to enhance the energy absorption capacity of the system by developing plastic deformation. These elements can be conveniently modelled using axial connectors provided with the three-linear force-displacement relationship illustrated in Fig. 3.8c. The first branch is intended to reproduce the linear-elastic (D_{d1}) response of the element prior to the activation. Following the activation displacement (s_1), the diagram flattens into a second linear branch (D_{d2}) along which large axial movements take place under low increments of force until the energy dissipating device is eventually smashed. At a displacement equal to s_2 , the response becomes comparatively stiffer (D_{d3}). In the next Section, an identification procedure to evaluate these parameters is illustrated.

Modelling of the interception structures

Truss elements are used to model the interception structures. In presence of a ring net, an identification procedure could be carried out, in order to provide a simpler equivalent truss mesh with a proper mechanical behaviour. Identification should be performed employing tests onto net samples. Experimental data would be preferable, but also numerical tests can be adopted for such a scope. A good agreement between the response of a ring net and the equivalent truss mesh could be achieved by assigning to the truss elements a three-linear, elasto-plastic hardening law (Fig. 3.8d) as it will be shown in the next Section, where details of the procedure employed to identify the five constitutive parameters (E_{n1} , E_{n2} , E_{n3} , ε_3 and ε_4), performed by means of both physical and numerical models, are provided with reference to the interception structure of the prototype of barrier 3000.

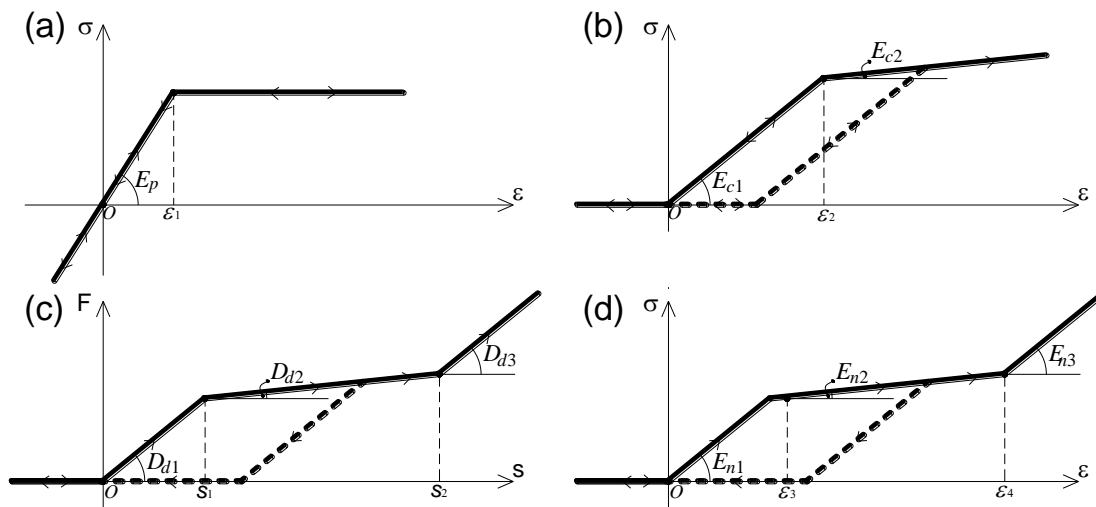


Figure 3.8 Constitutive laws adopted in the numerical approach for: a) steel posts; b) cables; c) energy dissipating devices and d) net truss elements.

3.1.4 MODEL DEVELOPMENT AND CALIBRATION

According to the procedure described in Section 3.1.3 and based on the data presented in Section 3.1.2, a FE model of barrier 3000 was developed. For the purpose, the

commercially available computer program ABAQUS/Explicit v. 6.9 (Hibbitt 1998) was employed. In this Section, details on the model development and calibration are given, with special emphasis to the identification procedure necessary to an effective modelling of the barrier interception structure and connecting components.

Modelling details: interception structure

The interception structure of barrier 3000 is made by ring elements, arranged so that each of them (diameter equal to 350 mm) is enclosed and loosely interlaced to other six. The numerical net was made of a triangular meshwork of truss elements, assembled so that the ends of each truss connect the centers of two adjacent rings (Nicot et al. 2001).

An identification procedure was performed on two net samples: one made of rings and the other one made of truss elements. The aim of the identification procedure is the selection of the mechanical parameters that characterize the three-linear constitutive law (as described in Section 3.1.3) of the truss elements such that the equivalent net has the same structural response of the ring net in loading conditions acting out and in the net plane.

To this purpose, two net panels were considered as illustrated in Figs. 3.9a and b. Following the testing conditions of the experiments described in Section 3.1.2, the ring sample was composed by 56 rings (Fig. 3.9a), restrained at the outermost points with spherical hinges. Rings were modelled by one-dimensional, two-node beam elements, obeying to a bilinear elasto-plastic hardening law. The parameters: the elastic ($E_{r1} = 150$ GPa) and hardening ($E_{r2} = 1$ GPa) slopes as well as the yield strain threshold ($\varepsilon = 0.008$) were calibrated on the base of static tensile tests recently performed on single rings (Cargnel 2011). The tests on the net panels were performed by impacting the sample centre with a three-dimensional deformable body of mechanical properties equal to those of high resistance concrete.

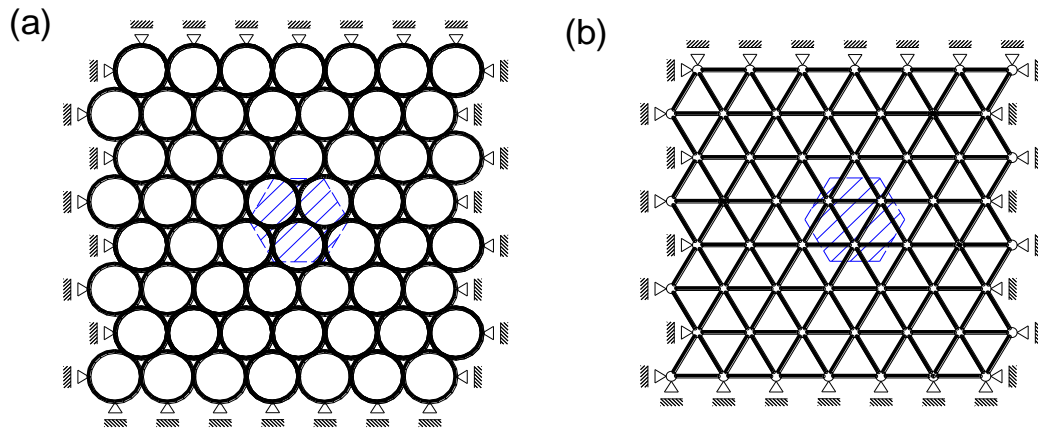


Figure 3.9 Out-of-plane test onto a) ring and b) equivalent truss samples.

Launches N1 and N2 were simulated onto two distinct samples of the same ring net. At the end of the simulations, the numerical elongations were 0.56 m and 0.60 m, respectively, in good agreement with the experimental results (0.60 m and 0.67 m, respectively).

The response of the ring sample in terms of total reaction force and elongation is found in Figs. 3.10a and b for launches N1 and N2, respectively. The results of the same, out-of-plane dynamic analyses, performed onto the truss sample (Fig. 3.9b) are also inserted in Fig. 3.10. With reference to the notation introduced in Section 3.1.3 (Fig. 3.8d), the constitutive parameters which ensured such response, essentially equivalent for the two samples, were: $E_{n1} = E_{n3} = 150$ GPa, $E_{n2} = 1$ GPa, and $\varepsilon_3 = 0.001$ and $\varepsilon_4 = 0.0015$.

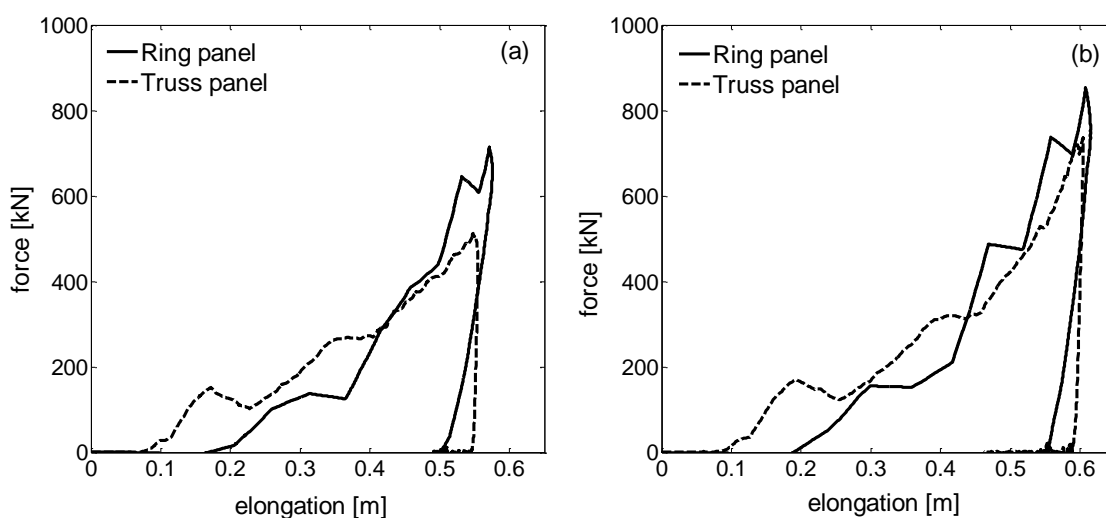


Figure 3.10 Out-of-plane test onto a) ring and b) equivalent truss samples.

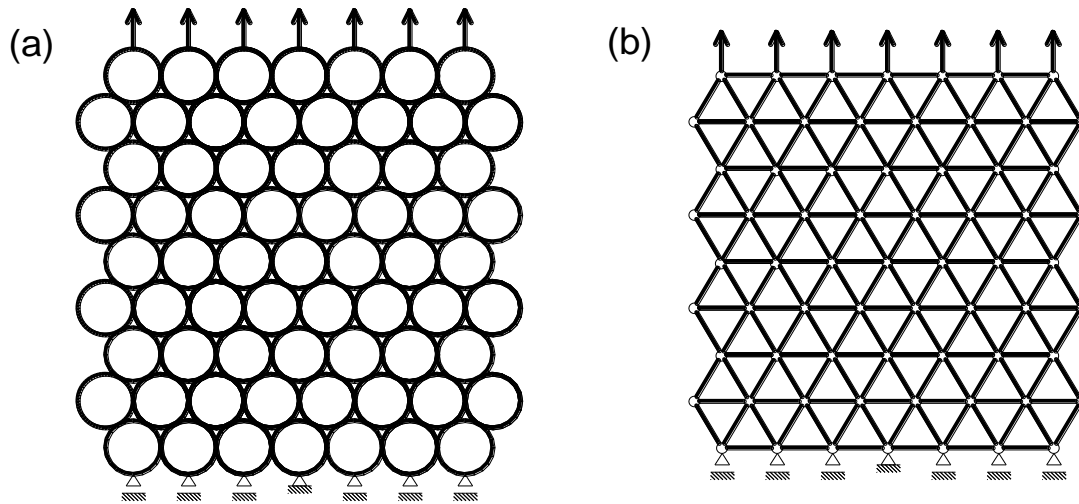


Figure 3.11 In-plane test onto a) ring and b) equivalent truss samples.

With the above mentioned parameters, the ring and truss samples were fully restrained at one side, while, at the opposite side, an incremental, in-plane, tensile load was applied, as depicted in Figs. 3.11a and b respectively.

Results of the numerical analyses are provided in Fig. 3.12 in terms of displacement and force mobilized throughout the test. As displayed the equivalent truss net is able to reproduce the in-plane response of the ring net rather accurately. After these tests, the identified parameters were thus implemented for the net in the whole barrier model.

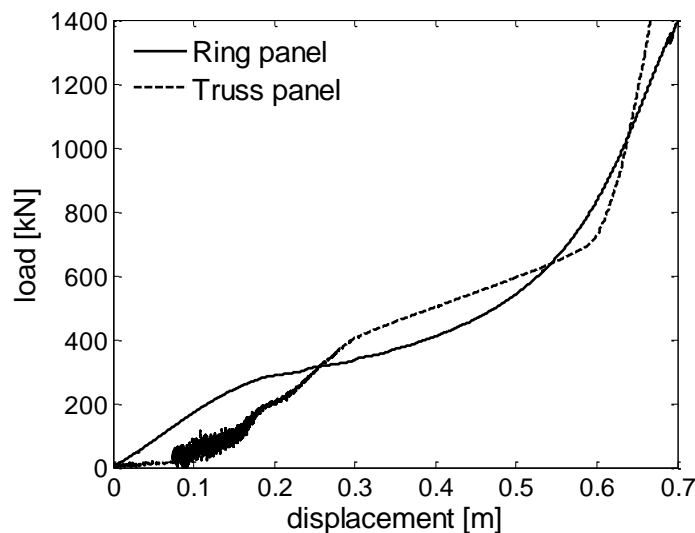


Figure 3.12 In-plane test results: total reaction forces versus displacements for the ring (solid line) and equivalent truss (dotted line) samples.

Modelling details: connecting components

The barrier cables were modelled with truss elements with no flexural rigidity and no ability to sustain compressive stresses. With reference to the notation introduced in Section 3.1.3 and in Figure 5b, the following mechanical parameters have been used: $E_{c1} = 150 \text{ GPa}$, $E_{c2} = 150 \text{ MPa}$ and $\varepsilon_2 = 0.006$. The diameter of all cables was 20 mm.

The energy dissipating devices of barrier 3000 (Fig. 3.13a) are made of two hollow pipes of length $L_d = 70 \text{ cm}$, made of structural aluminium connected at the ends by perforated plugs. As illustrated in Fig. 3.13b, the cables are assembled in the pipes in the inverse and symmetrical direction. As a result, when the cable undergoes a tensile force, the device shrinks and the entire cable elongates.

The energy dissipating devices were modelled using axial connectors (Section 3.1.3) having the force-displacement relationship of Fig. 3.8c. A procedure to identify the model parameters (D_{d1} , D_{d2} , D_{d3} , s_1 and s_2) is illustrated in this Section.

A one-dimensional and a three-dimensional model were used in the procedure. In fact, a three-dimensional model of a different type of energy dissipating device has been developed and tested in dynamic condition recently (Trad et al. 2011), encouraging the use of numerical models to explore the complex behaviour of these elements.

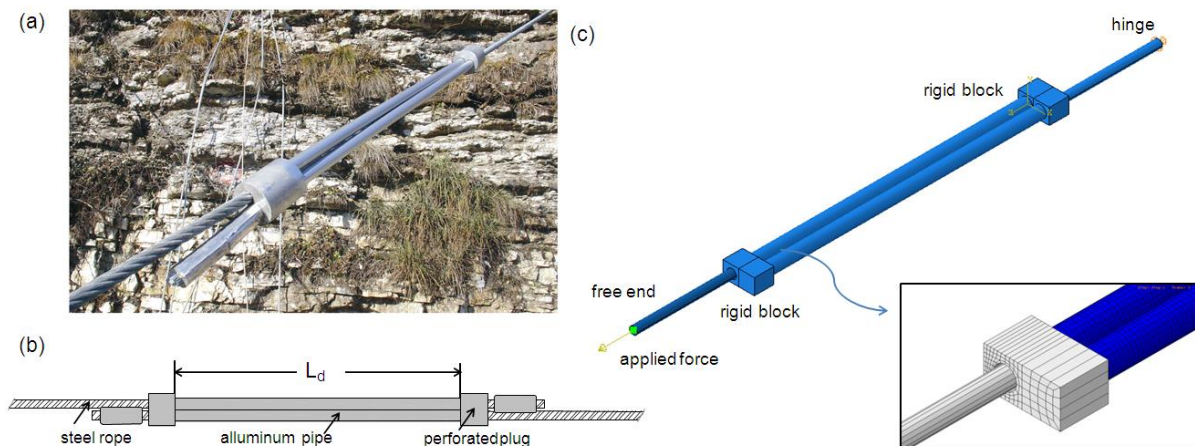


Figure 3.13 Energy dissipating device of barrier 3000: a) mounted on an uphill cable; b) simplified scheme; c) three-dimensional FE model.

The one-dimensional model of energy dissipating device was made of two truss elements with no flexural rigidity and no ability to sustain compressive stresses, connected through an axial connector of length L_d , and parameters D_{d1} , D_{d2} , D_{d3} , s_1 , s_2 . One model side was restrained using a spherical hinge.

The three-dimensional model was made of two hollow pipes connected by rigid, perforated, blocks at the ends, as shown in Fig. 3.13c. Each pipe was assembled about a cylindrical element which models the internal rope. Continuous homogeneous shells were used. The blocks and the internal ropes were assumed perfectly rigid, whereas a bi-linear, elasto-plastic law with hardening was assigned to the pipes with a Young modulus of 70 GPa, a yielding stress of 300 MPa and an ultimate stress of 550 MPa achieved at the 0.1 of strain. A frictional type of contact was assigned to the interface between the pipes and the internal ropes, between the ropes and the rigid blocks and between the two pipes.

As displayed in Fig. 3.13c, the model was restrained using a spherical hinge at one end.

The one-dimensional and three-dimensional FE models were subjected to a non-linear analysis in which a force equal to 500 kN was applied incrementally along the model axis. The results of the analyses are illustrated in Figs. 3.14 and 3.15. In particular, Fig. 3.14a shows the deformed shape of the three-dimensional model corresponding to a force equal to 200 kN.

In Fig. 3.14b, two pictures of a deformed energy dissipating device are also shown. The photographs were taken at the end of a full-scale impact test on a prototype of falling rock protection barrier. The deformed shape of the three-dimensional model is similar to that of the real energy dissipating device, exhibiting a significant localization of strains toward the ends of the element, where the ropes slide through the perforated plugs.

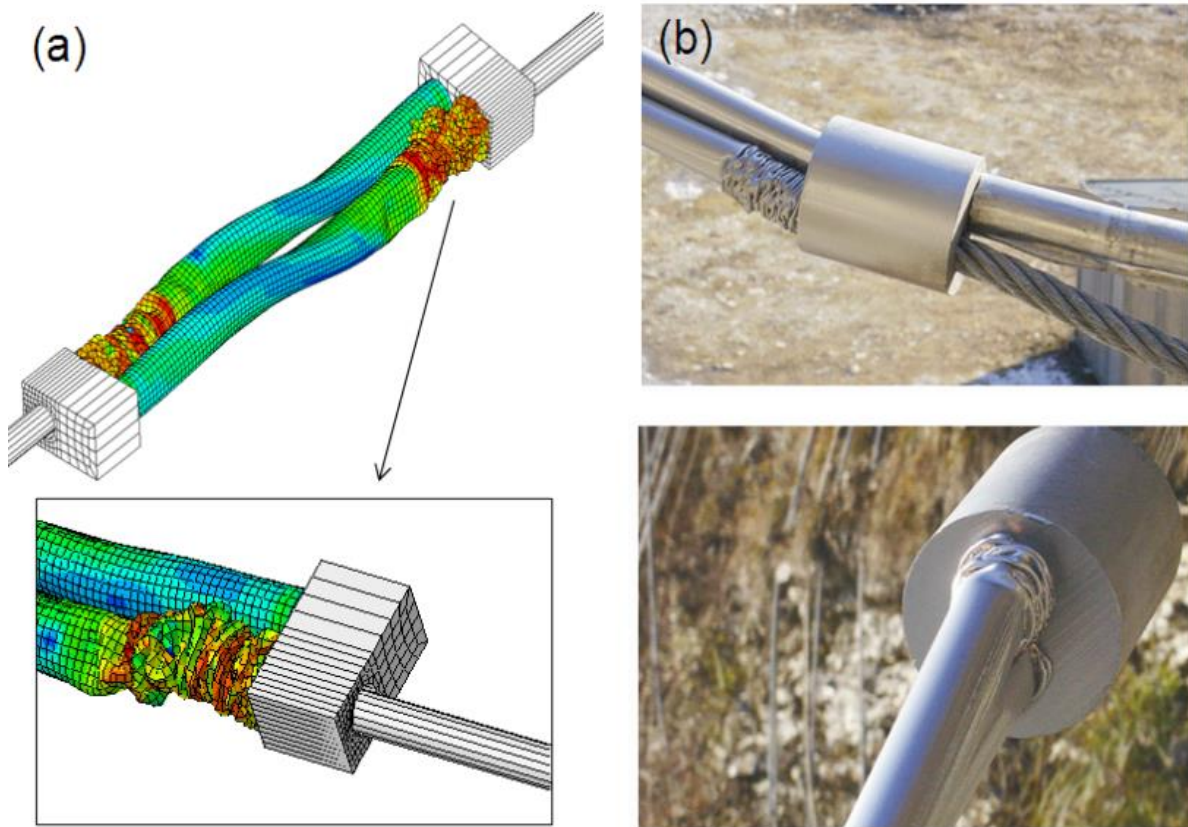


Figure 3.14 Deformation the energy dissipating device of barrier 3000: a) frame extracted from a numerical non-linear analysis and b) picture after a full scale test onto a barrier prototype.

Figure 3.15 displays the results of the analyses in terms of the reaction forces and the energy dissipated. As depicted in Fig. 3.15a, the three-dimensional model exhibits a steep and linear response prior to activation of the element, then the diagram flattens and large deformations take place under comparatively lower stress increments until the element is eventually smashed at about the 70% of deformation and a stiffer response is resumed prior to the achievement of the full-stroke (about 0.6 m). Such response is typical of this type of energy dissipating device in tensile static tests (Peila et al. 2006).

In Fig. 3.15b, the total energy dissipated during the test is also illustrated. For the three-dimensional model, the energy, dissipated by plastic deformation and friction, monotonically increases with the element length reduction up to a value of 130 kJ, recorded at a displacement of about 60 cm.

The results of the analyses performed onto the one-dimensional model are also inserted in Fig. 3.15. With reference to the notation introduced in Section 3.1.3 (Fig. 3.8c), the constitutive parameters which ensures the observed response, which is essentially equivalent for the two models, were: $D_{d1} = 20 \text{ MN/m}$; $D_{d2} = 580 \text{ kN/m}$, $D_{d3} = 1 \text{ MN/m}$; $s_1 = 0.002 \text{ m}$ and $s_2 = 0.5 \text{ m}$. The simple one-dimensional model well describes the response of the energy dissipating device and successfully predicts the activation, the pre-full-stroke behaviour and the amount of dissipated energy during the test.

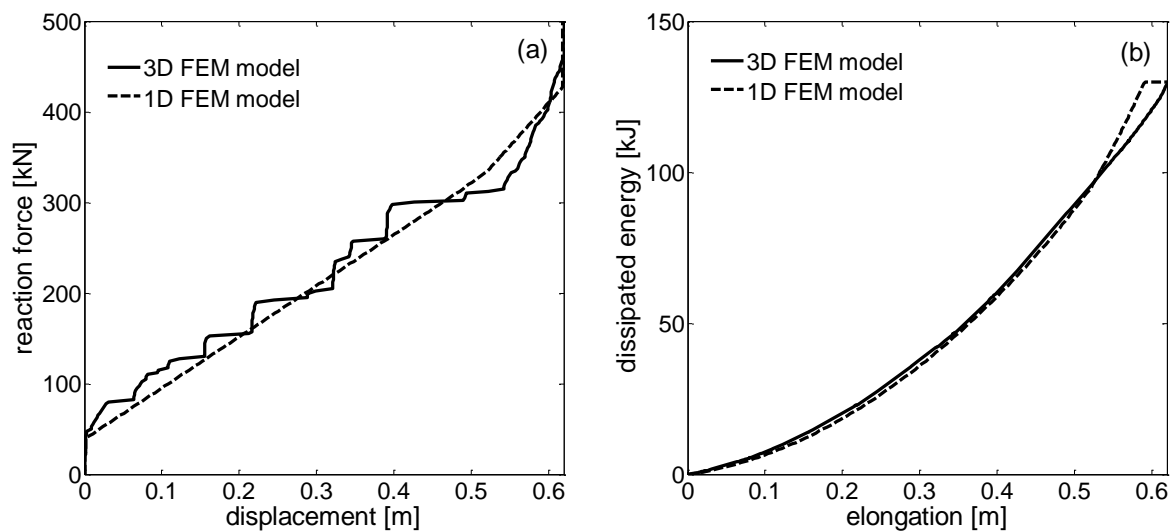


Figure 3.15 Non-linear static analysis of the three-dimensional and one-dimensional model of energy dissipating device: a) force versus displacement and b) dissipated energy versus displacement

A dynamic analysis was then carried out on the two models, in which the dynamic force recorded by the load cell 9 of the prototype of barrier 3000 (Fig. 3.6), during the maximum energy level test (Fig. 3.17a) was axially applied to the models. The force, which acted onto the energy dissipating device uc1 of Fig. 3.7, produced a travel of the element equal to 28 cm at the end of the test.

In Figure 3.16, the results of the analysis are shown in terms of the reaction forces and the energy dissipated

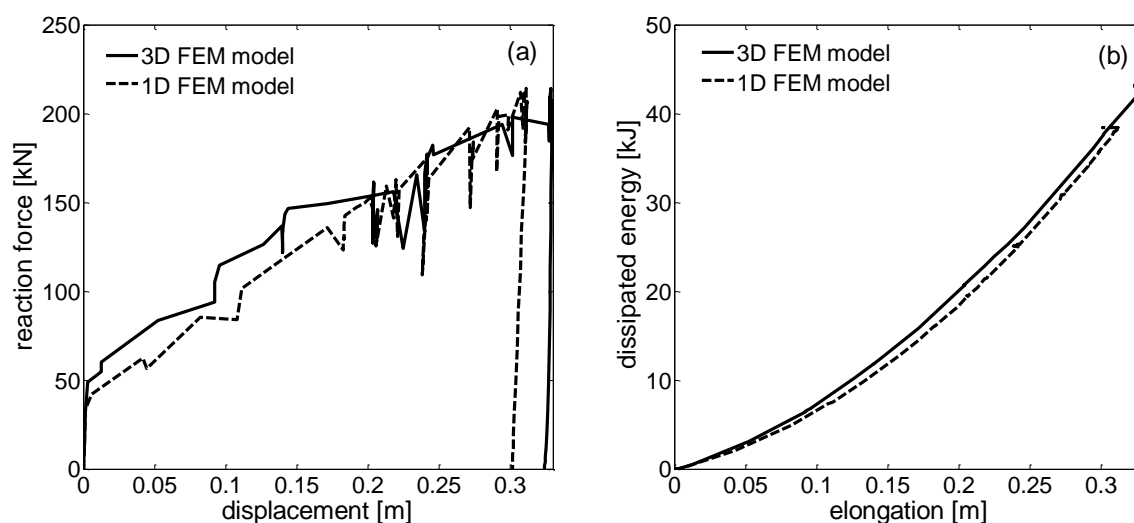


Figure 3.16 Non-linear dynamic analysis of the three-dimensional and one-dimensional model of energy dissipating device: a) force versus displacement and b) dissipated energy versus displacement.

With reference to Fig. 3.16a, the three-dimensional model, following the activation, reached at about 50 kN, continuously shrinks the force increases until a value of 200 kN is reached. Following this value, the element is completely unloaded. The final shrinkage (travel) is about 32 cm, in good agreement with the experimental measure.

In Figure 3.16b, the dissipated energy by the three-dimensional model is shown, increasing monotonically as the element displaces up to a maximum value of about 45 kJ.

The response of the one-dimensional model, also inserted in Fig. 3.16, describes the response of the energy dissipating device satisfactorily and successfully predicts the element travel (30 cm) and the dissipated energy in dynamic conditions. After these tests, the one-dimensional model of the energy dissipating device with the identified parameters was thus implemented in the whole barrier model.

3.1.5 MODEL ASSESSMENT

The model of barrier 3000 developed as described in Section 3.1.3, with the model parameters calibrated in Section 3.1.4, was subjected to retrospective simulations of the tests described in Section 3.1.2. Impact tests on a barrier model were simulated

using a three-dimensional deformable body as test block, with mechanical properties equal to those of high resistance concrete or in a simplified fashion (Gentilini et al. 2012a). With reference to Fig. 3.6a, the direction of the block was vertical in all the tests. In a first test, the block was conducted to impact the centre of the barrier model at the maximum energy level (3000 kJ). In a second test the model of barrier 3000 was subjected to two successive launches of a block impacting the barrier centre with energy equal to one third of the maximum (1000 kJ). In the following subsections, comparison with the experimental results is pursued to enable a thorough assessment of the model effectiveness.

Model response at the maximum energy level

The model of barrier 3000 was first subjected to the impact of a block having the maximum energy level (3000 kJ). Referring to Fig. 3.6a for the notation, the results of the analysis are illustrated in Fig. 3.17 along with the experimental data measured in the relevant full-scale test.

In particular, Fig. 3.17a shows the numerical and experimental time-history of the barrier maximum elongation. The model reproduces the downward displacement of the prototype throughout the test with good accuracy, mainly due to the ability of the equivalent truss net to model the behaviour of the actual ring net, in presence of in-plane and out-of plane loading conditions, as thoroughly assessed in Section 3.1.4.

In Figs. 3.17b to f, the numerical and experimental time-histories of the constraint forces at some representative load cells are found. In particular, Figs. 3.17b to d show the values of the forces mobilised at the uphill anchorages 9, 10 and 11, respectively, Fig. 3.17e the force acting at the side anchorage 14 and Fig. 3.17f the reaction force recorded at the post foundation 2, throughout the test. The numerical model captures the general trend of the forces with time, including the post-peak behaviour at all the anchoring points and post foundation with good precision, also providing a satisfactory estimation of the peak force values. A minor scatter is observed at the anchorages 11 and 14 (Figs. 3.17d and e).

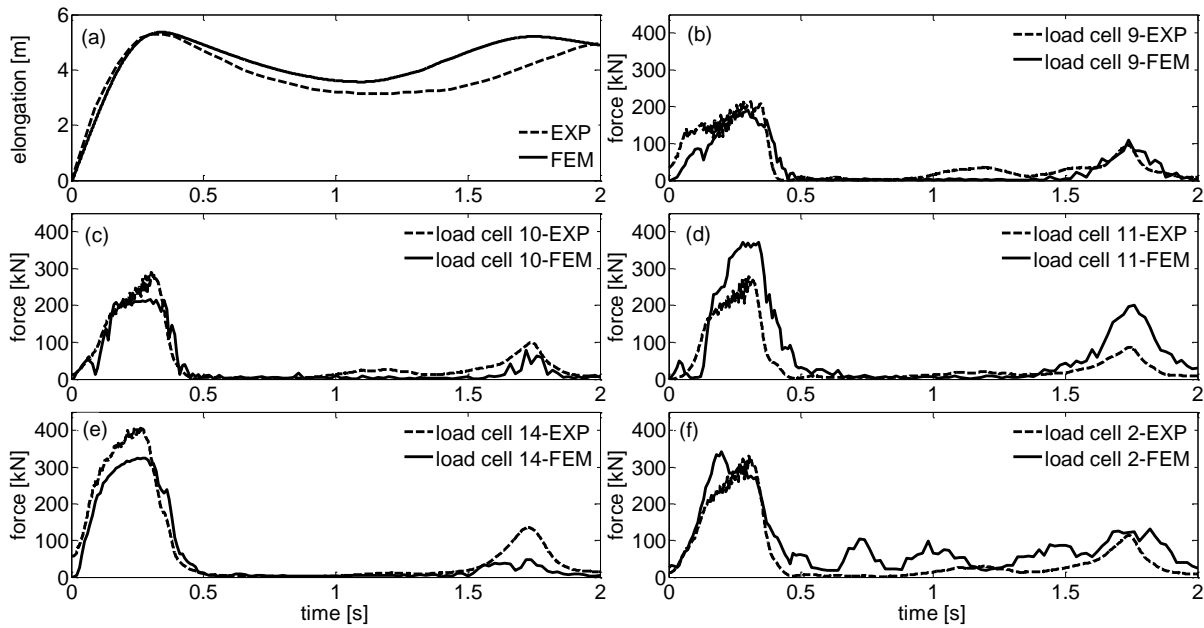


Figure 3.17 Numerical (FEM - solid line) and experimental (EXP - dotted line) results of the maximum energy impact test onto barrier 3000: a) maximum displacement versus time; forces versus time for b), c), d) uphill anchorages; e) lateral anchorage and f) post foundation.

As for the energy dissipating devices, referring to Fig. 3.7 for the notation, the uc2 and uc7 did not activate during the numerical analysis and no energy dissipating device reached the full-stroke, in agreement with the data collected on-site at the end of the impact test. The maximum numerical travel was 31 cm, recorded at the uc4 at the end of the analysis. The value is in agreement with the experimental measure (32 cm).

Model response at the service energy level

The model of barrier 3000 was also subjected to the impact of a block of energy level equal to one third of the maximum to investigate its response at low values of impact energy. The numerical results are shown in Fig. 3.18 along with the relevant data collected in the full-scale test. The numerical and experimental time-histories of the barrier maximum elongation are illustrated in Fig. 3.18a. Figures 3.18b to d display the values of the forces at the uphill anchorages 9, 10 and 11, respectively. In Figure 3.18e, the forces recorded at the side anchorage 14 are shown, whereas in Fig. 3.18f the reaction force recorded at the post foundation 2 is inserted. In general, the model

results well predict the general trend of the elongations and constraint forces, assessing the ability of the model to capture the major features of the barrier response at low energy values. In particular, the model reproduces the maximum experimental elongation accurately, validating further the effectiveness of the equivalent truss net toward the evaluation of the barrier displacements.

As for the reaction forces, the greater scatter is observed at the central uphill anchorage 11, at the side anchorage 14 and post foundation 2. These results are consistent with those obtained from the analyses carried out at the maximum energy level, though slightly augmented. These results are partly ascribable to the functioning of the translator connectors at the posts heads and bases, whose shortcomings were mentioned in Section 3.1.3.

With reference to Fig. 3.10 for the notation, the energy dissipating devices uc2 and uc7 did not activate during the numerical analysis. The maximum experimental travel was measured, at the end of the test, at the sc1 and sc2 (18 cm). The corresponding numerical travel was measured equal to 17 cm.

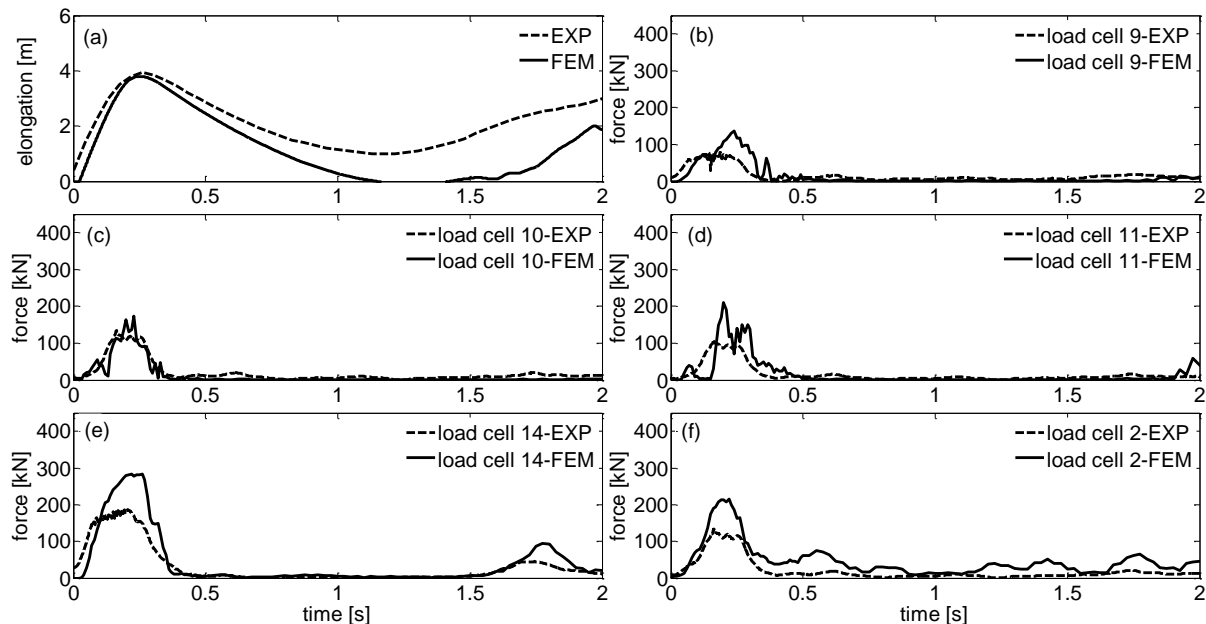


Figure 3.18 Numerical (FEM - solid line) and experimental (EXP - dotted line) results of the service energy impact (first launch) test onto barrier 3000: a) maximum displacement versus time; forces versus time for b), c), d) uphill anchorages; e) lateral anchorage and f) post foundation.

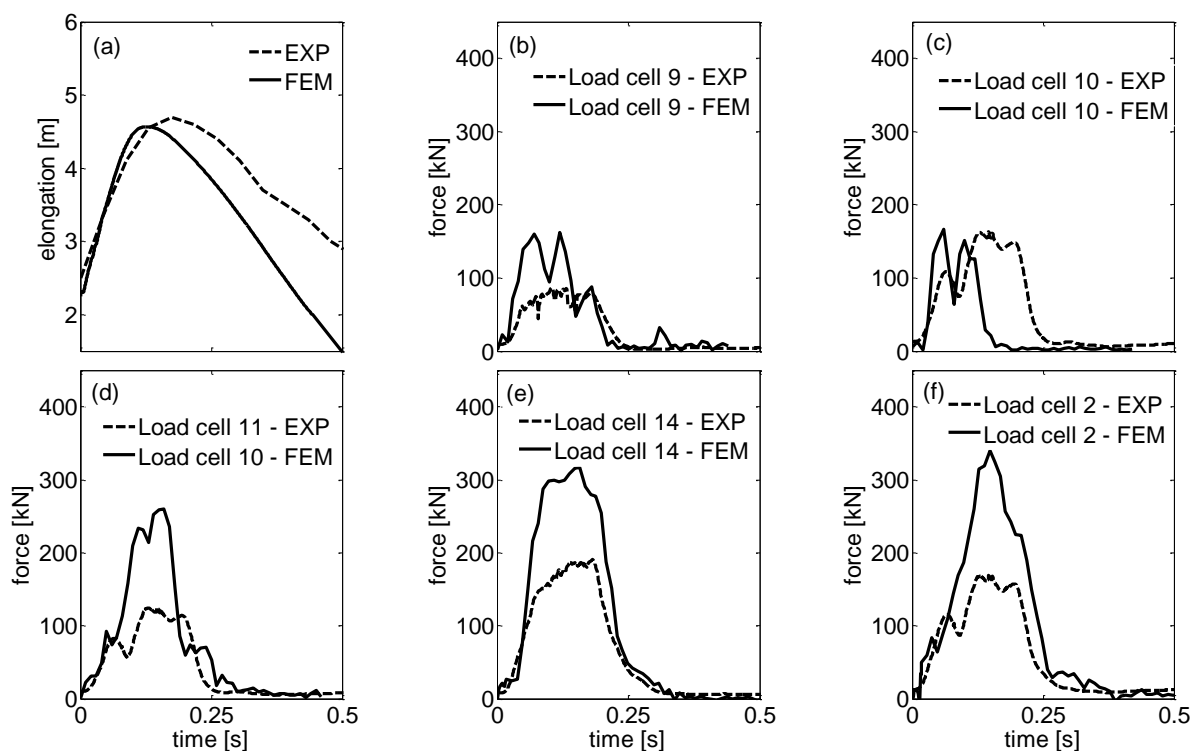


Figure 3.19 Numerical (FEM - solid line) and experimental (EXP - dotted line) results of the service energy impact (second launch) test onto barrier 3000: a) maximum displacement versus time; forces versus time for b) uphill anchorage 9, c) uphill anchorage 10, d) uphill anchorage 11, e) lateral anchorage 14 and f) post foundation 2.

After the launch, the block was removed and the deformed model of barrier 3000 was subjected to the impact of a further block of energy equal to one third of the maximum (1000 kJ). In this launch, the numerical forces at the anchorages and post foundations are expected to be affected by an overestimation, mainly ascribable to the use of the translator type of connectors which work with comparatively less accuracy during unload-reload cycles, as described in Section 3.1.3. However, due to the uncertainties related to the evaluation of the response of a deformed barrier, conservative results are rather welcome. The numerical results are shown, with the corresponding experimental data, in Fig. 3.19. The time interval considered was that relevant to the first bounce of the test block, which occurred within the first 0.5 seconds of test.

The time-histories of the numerical and experimental maximum elongations are compared in Fig. 3.19a. The origin of the two curves coincides with the final downward movement of the barrier prior to the second launch (final elongation). The good agreement between the numerical and experimental values of final elongation

confirms the capacity of the model to reproduce the prototype displacement response in unloading conditions. Such agreement is also observed when the barrier is re-loaded during the second launch, assessing the ability of the model to predict the time-displacement response of the prototype in presence of multiple launches.

In Figs. 3.19b to f the time-histories of the forces mobilised at the uphill anchorage 9, 10 and 11 and side anchorage 14, as well as the post foundation 2, are shown, respectively. The numerical results of the analysis are similar to those observed in the previous launch at low energy, since the stress-strain paths tracked by the barrier elements, rapidly enter the elasto-plastic branch (Fig. 3.8) where significant deformations are produced by small stress increments. As yet observed and expected the maximum scatter is found at the anchorages 11 and 14 and post foundation 2.

With reference to the travel of the energy dissipating devices measured at the end of the two subsequent launches, the energy dissipating devices uc2 and uc7 did not activate and none of the others reached the full stroke in agreement with the experimental data. The maximum numerical travel was recorded at uc7 (29 cm) well matching the experimental measure (30 cm). Overall, the model can be considered reliable toward the evaluation of forces and displacements of the prototype also in presence of subsequent launches

3.1.6 USE OF THE MODEL AS A DESIGN TOOL

The model of barrier 3000 proved to be able to reproduce satisfactorily the prototype behaviour in different conditions. These results assess the reliability of the numerical approach described in Section 3.1.3 and validate the procedure of parameters calibration illustrated and discussed in Section 3.1.4, so giving confidence to the use of well calibrated numerical models as predictive tools to support the design of these structures.

Guided by the numerical results, the suitability of the presented numerical approach to aid the design of these structures is investigated in this Section. In particular, few modifications were introduced in the model of barrier 3000. A modified model of barrier 3000, hereinafter called DESIGN 1, was completed by removing the 12 energy

dissipating devices from the longitudinal upper and longitudinal lower ropes, keeping the sole energy dissipating devices at the uphill and side cables, producing a lighter and more economical structure.

The numerical approach was then used to assess the response of DESIGN 1 which was subjected to an impact test at the maximum value of energy. The results were then compared with the data of the corresponding analysis performed onto the barrier 3000, described and discussed in Section 3.1.5.

No significant changes are observed in the response of the modified model in terms of maximum elongations as shown in Fig. 3.20a, where the time-elongation curve is illustrated for the two numerical models. As for the forces mobilised at the anchorages and post foundations, minor differences are observed at the lateral anchorages 14, as illustrated in Fig. 3.20b, where the time-history of the force mobilised at the anchorage 14 is shown for the two numerical models. In the modified model the force is consistently higher than in the original model, owing to the comparatively stiffer response of the longitudinal lower ropes now provided with no energy dissipating devices.

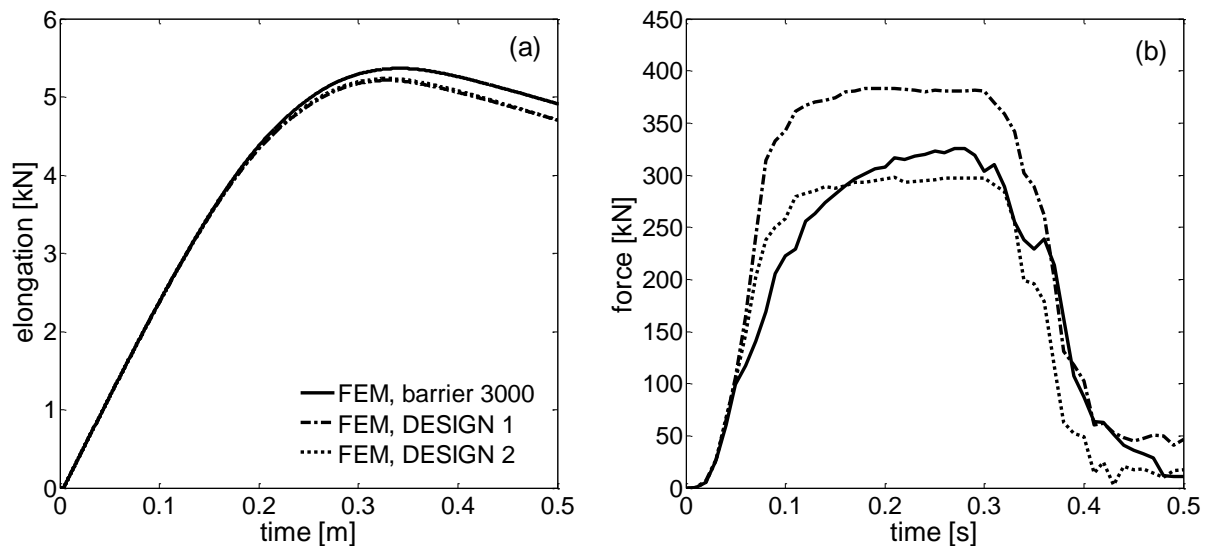


Figure 3.20 Results of the analysis carried out at the maximum energy level on the original model of barrier 3000, on the DESIGN 1 and on the DESIGN 2: a) elongation versus time and b) forces versus time for lateral anchorage 14.

With reference to Fig. 3.6 for the notation, the force at the side anchorages can be reduced, just adding two further energy dissipating devices at the longitudinal lower ropes, between node 14 and 1 and between node 4 and 15. The numerical approach was then used also to explore the response of this new version of barrier 3000, hereinafter called DESIGN 2. Subjected to an impact test at the maximum energy level, the model produced the results illustrated in Fig. 3.20. Specifically, no changes in the time-elongation response are observed (Fig. 3.20a). The time-history of the force mobilised at the anchorage 14 is given in Fig. 3.20b. The two additional energy dissipating devices enable to lower the constraint force to the original values, while no significant changes are produced in the other model quantities. Minor increments in the stresses mobilized within the model elements are also observed as shown in Fig. 3.21, where the stress mobilised within the model elements are found. The data illustrated refer to the element subjected to the highest stress value (located in the same position on the longitudinal lower ropes either for the original barrier and for DESIGN 2 version). As illustrated, the maximum stress remains within the admissible limits for the concerned ropes (1.8 GPa).

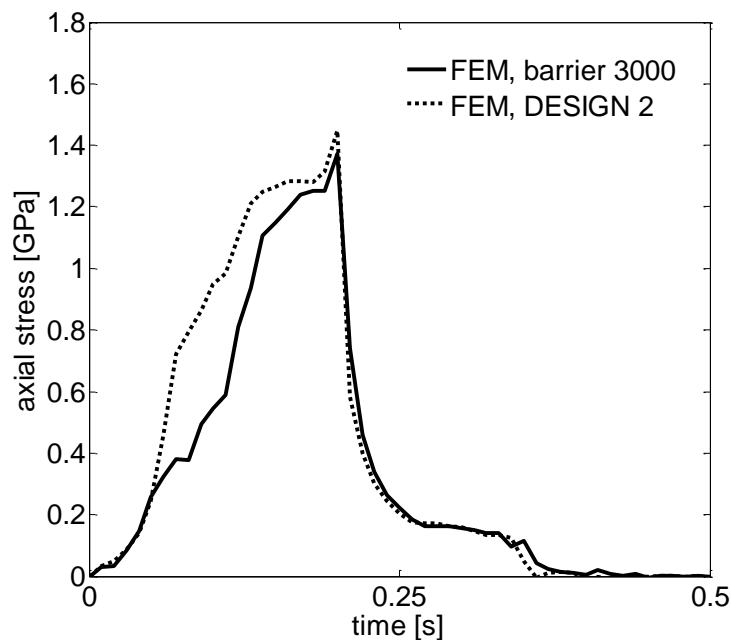


Figure 3.21 Results of the analysis carried out at the maximum energy level on the original model of barrier 3000 and on the DESIGN 2 : maximum stresses mobilised with time within the longitudinal ropes.

3.1.7 CONCLUDING REMARKS

The paper has presented a general numerical procedure for the modelling of falling rock protection barriers. Exploiting a rich set of experimental data, the procedure was applied to devise and calibrate a model of a high capacity falling rock protection barrier, called barrier 3000. The model development was described in the paper with special emphasis to the modelling of the barrier interception structure and the energy dissipating devices. The model ability in reproducing the prototype behaviour was then assessed by retrospectively simulating different full-scale tests. The model revealed to be able to perform successfully in terms of elongations and forces mobilized at the anchoring points and post foundations. The model suitability to support the design of these structures was then investigated. Guided by the numerical results, the suitability of the presented numerical approach to aid the design of these structures is investigated. In particular, few modifications were introduced in the model of barrier 3000 to improve its cost-effectiveness and performance on-site. The results have shown that the performance of barrier 3000 can be successfully improved by removing all the energy dissipating devices from the longitudinal ropes and adding just two of them at the outermost portion of the longitudinal upper ropes, next to the side anchoring points. The modification which ease the barrier installation process and cost effectiveness, produces no significant changes in the barrier response both in terms of maximum elongation, forces and stresses mobilized within the barrier elements. Results provide a useful guidance for the development and enhancement of falling rock protection barriers.

CONFERENCE PAPER 1

3.2 MODELLING FOR THE DESIGN OF PASSIVE PROTECTION MEASURES AGAINST ROCK FALL

Abstract

An increasing need of protecting the civil installations against natural hazards – like very rapid soil and rock movements – is due to the extensive mountain territories usage for infrastructures and residential areas. In this study, the so-called flexible falling rock protection barriers, which can be numbered among passive solutions against rock fall, are analysed in detail. These structures have been historically designed on the basis of full-scale impact tests on barrier prototypes. Based on a reliable experimental database, a numerical approach has been recently proposed for the modelling of these structures, which has proved to reproduce all the relevant quantities for the description of the barrier response with time. The very good fit of the experimental and numerical results can provide further confidence on the use of such models as predictive tools to support the design of flexible falling rock protection barriers under different scenarios.

3.2.1 INTRODUCTION

Typically found in areas subjected to very rapid slope movements, falling rock protection barriers are metallic structures made of identical functional modules installed in sequence for the required length. They consist of a metallic cable net, kept up-right by structural steel posts, with the function of intercepting falling blocks. Loads are transferred through special connecting elements to the foundations.

Easy to be installed and maintained, with relatively low environmental impact, the barriers are de-signed to intercept and stop the blocks moving along a potentially unstable slope. These structures dissipate high impact kinetic energies through the development of permanent deformations of the system. To this scope energy dissipating devices are often mounted on the connecting cables.

Traditionally, these structures have been designed and commercially distributed based on the results of full-scale tests on prototypes, now regulated, within the EU, by the European Guideline for Technical Approval of falling rock protection kit (EOTA 2008). The tests are intended mainly to verify if a full-scale barrier prototype, designed to absorb a given kinetic energy, is effectively able to arrest blocks having energy up to such value. These tests can provide the parameters (forces and deformations) relevant to the choice and installation of high capacity barriers within a more comprehensive planning of risk mitigation interventions along a potentially unstable slope. The availability of reliable experimental data on the higher capacity barriers has recently led to the development of analytical (Peila et al. 1998) and numerical models of these structures, simplified two-dimensional (de Miranda et al. 2010, Govoni et al. 2011) or more accurate three-dimensional ones (Cazzani et al. 2002, Volkwein et al. 2009).

In such context, the paper is aimed at presenting a numerical strategy for the optimization of the design of such structures, recently developed (Gentilini et al. 2012a, b, 2013) and based on a consistent experimental database of full-scale tests on several barrier prototypes featuring a variety of energy absorption capacity. Due to the complexity of the dynamic and highly non-linear phenomenon, the trustworthiness of numerical models as design tools relies upon a preliminary accurate procedure of

calibration. The numerical strategy is then applied to investigate the structure response under other impact conditions and scenarios.

3.2.2 EXPERIMENTAL TESTING

In this Section, details of the experimental tests carried out on the interception structure and on full-scale barrier prototypes are described and discussed. These tests (Gottardi and Govoni 2010) enabled the development, calibration and assessment of the numerical modelling procedure described in the following Sections.

Experiments on the interception structure

Different impact tests were carried out onto samples of a type of ring net usually employed for various falling rock protection barriers of high energy absorption capacity (greater than 2000 kJ). The scope was to evaluate the dynamic response of a single interception structure to the impact of a block of known mass, velocity and direction.

The tested net panel was made of 350 mm diameter rings, completed twisting 6 times the same 4 mm wire and arranged so that each ring is enclosed and loosely interlaced to other six. The panel had dimensions of 3040 mm x 2590 mm, made up of 56 rings. It was connected to the top of a rigid frame of structural steel beams, built on a concrete foundation as illustrated in Fig. 3.22a.

The test was carried out by lifting a concrete block of mass 1610 kg to the established position, then releasing it to impact the centre of the net panel. By varying the falling height of the block, three launches were performed at three distinct values of kinetic energy: 98, 129 and 136 kJ, named launch N1, N2 and N3, respectively. At the end of each launch (Fig. 3.221b) the test block was removed and the final maximum elongation measured. Recorded values were 0.60 m, 0.67 m and 0.77 m after launch N1, N2 and N3, respectively.

A ring failure occurred in the net after launch N3, so it will not be considered for the numerical identification described in Section 3.2.3.

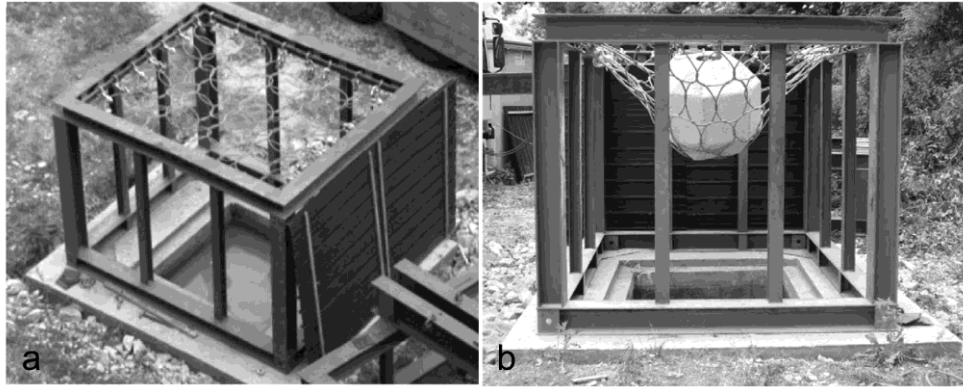


Figure 3.22 The experimental setup for impact tests on ring nets: a) before and b) after launch N1.

Experiments on barrier prototypes

The test site, located in Fonzaso (Belluno, Italy), was designed and developed by the Consorzio Triveneto Rocciatori together with the DICAM Department of the University of Bologna.

The Fonzaso test site is a vertical-drop type in which a concrete block in the shape of a polyhedron is lifted by a crane and then released to impact, with a velocity greater than 25 m/s, the kit middle functional module in its centre. The test site is provided with instrumentation for the measurement of the quantities relevant to the assessment of the barrier response. All anchorages and the two central posts are provided with load cells measuring the forces acting on the foundations.

This paper reports the results of impact tests carried out on a falling rock protection barrier of kinetic absorption capacity 3000 kJ, hereinafter named barrier 3000. A three-dimensional sketch of barrier 3000 in the typical test-site configuration is provided in Fig. 3.23a, where the principal elements are indicated.

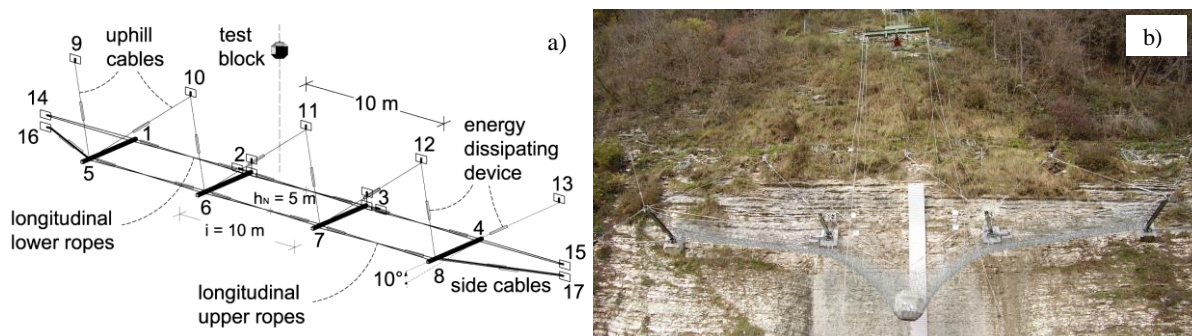


Figure 3.23 Barrier 3000 in the vertical-drop test site configuration: a) schematic drawing and b) picture taken after the maximum energy level impact test.

The interception structure is made of a steel ring mesh and the supporting structure of steel I-shaped posts. Two longitudinal upper and two longitudinal lower ropes connect the heads and the bases of the posts. The lateral cables connect the heads of the external posts to the side anchorages. All cables are 20 mm diameter and are provided with energy dissipating devices. Two full-scale impact tests are considered in this study on a prototype of barrier 3000. In the first test the prototype was subjected to the impact of a block having energy higher than the design level (maximum energy level, hereinafter called MEL test), while in the second test the impact energy was equal to one third of the maximum (service energy level, hereinafter called SEL test).

In Figure 3.23b a general view of barrier 3000 after the MEL test is given. In Figure 3.24, the relevant experimental maximum barrier elongations and forces acting on the anchorage 10 versus time are provided (dashed line).

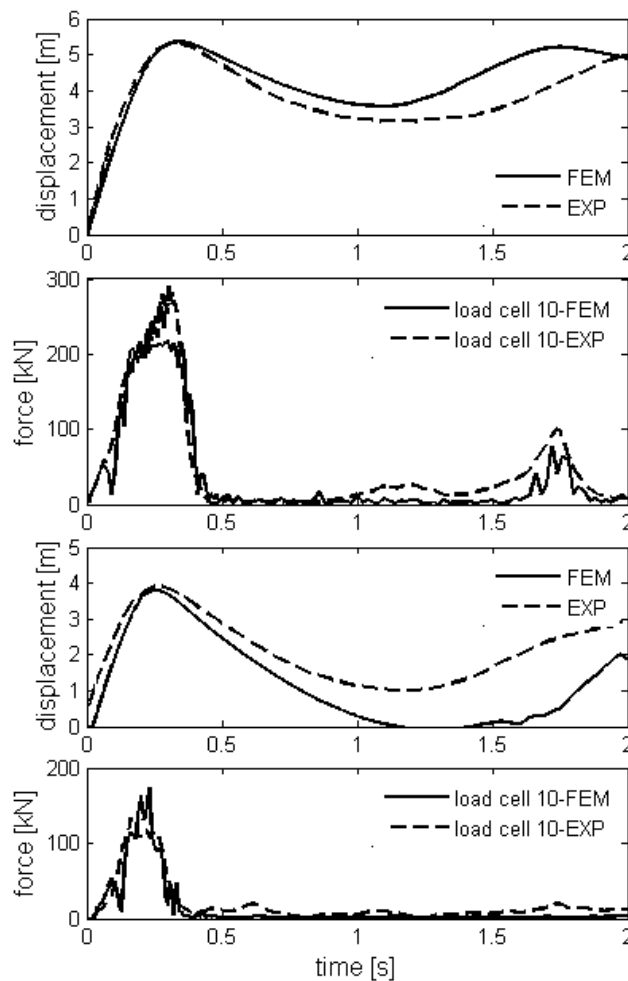


Figure 3.24 Numerical and experimental results vs. time of impact test onto barrier 3000: a) maximum displacement (MEL); b) uphill anchorage 10 (MEL); c) maximum displacement (SEL); d) uphill anchorage 10 (SEL).

The experimental set-up could be then modified to include more varied testing conditions, however such task is a costly and time consuming procedure. New testing scenarios could be equally well investigated by means of suitably developed numerical models as presented in the next Section.

3.2.3 NUMERICAL APPROACH

In this Section, the numerical strategy adopted for simulating the response of barrier 3000 to a rock impact is briefly illustrated. A complete description of the numerical approach can be found in Gentilini et al. (2013).

The steps of the approach have concerned first an identification procedure of the barrier components, based on the outcome of the experimental tests illustrated in Section 3.2.2, in order to match their real behaviour. According to the present procedure, a FEM model of barrier 3000 was then developed. For the purpose, the commercially available computer pro-gram ABAQUS/Explicit v.6.9 has been employed.

The Explicit package is well suited to perform and solve high-speed dynamic events, keeping the computational cost relatively low, even when a small time step is required in a simulation.

The barrier posts, made of I beams of structural steel S275, were modelled employing beam elements with a linear-elastic, perfectly plastic constitutive law represented in Fig. 3.25a with $E_p = 210$ GPa and yield strain threshold $\epsilon_l = 0.0013$. Cylindrical hinges were used at connection between the posts and the foundations. The posts have special eyelets at their heads and bases that guide the longitudinal upper and lower ropes. To model these connections a translator connector type was used. This connector type can be implemented relatively simply, while ensuring an accurate description of the post-cable relative motion with low computational costs (for details see Gentilini et al. 2012a, b).

The uphill, lateral and longitudinal cables were modelled by means of truss elements with no flexural rigidity and a tensile cut-off to compressive stresses. All cables were assumed to behave following the elasto-plastic, bi-linear behaviour depicted in Fig.

25b. The three parameters that characterise the constitutive law are those typical of strands subjected to tensile loads (Castro-Fresno 2008), the following values have been used: $E_{c1} = 150 \text{ GPa}$, $E_{c2} = 150 \text{ MPa}$ and $\varepsilon_2 = 0.006$.

Modelling of the interception structures

Modelling the entire barrier net by means of circular elements seems unnecessary sophisticated, especially if it can be shown that a simpler mesh of truss elements is able to reproduce the ring net behaviour. An identification procedure has been carried out, see for details Gentilini et al. (2012b). Identification has been performed considering tests onto the net panel described in Section 3.2.2.

The interception structure of barrier 3000 is made by ring elements, therefore the numerical model of the net was made of triangular meshwork of truss elements, assembled so that the ends of each truss connect the centres of two adjacent rings (Nicot et al. 2001). Two numerical samples of the net were thus considered: one actually made of rings (Fig. 3.26a), the other made by the equivalent trusses (Fig. 3.26b). Rings were modelled by one-dimensional, two-node beam elements, obeying a bilinear elasto-plastic hardening law (Fig. 3.25b). The constitutive parameters ($E_{c1} = 150 \text{ GPa}$, $E_{c2} = 1 \text{ GPa}$ and $\varepsilon_2 = 0.008$) were calibrated on the base of static tensile tests recently performed on single rings (Cargnel 2011). The tests were performed by impacting the net samples centre with a three-dimensional deformable body with mechanical properties of high resistance concrete.

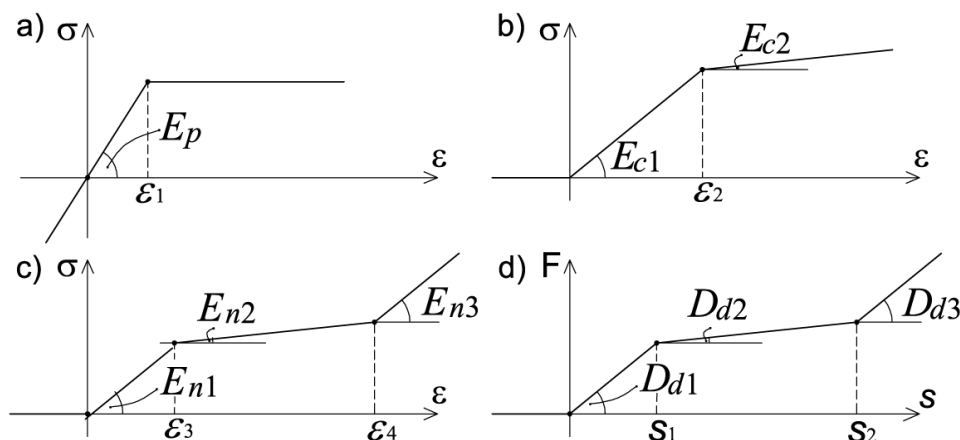


Figure 3.25 Constitutive laws adopted in the numerical approach for: a) steel posts, b) cables, c) net truss elements and d) energy dissipating devices.

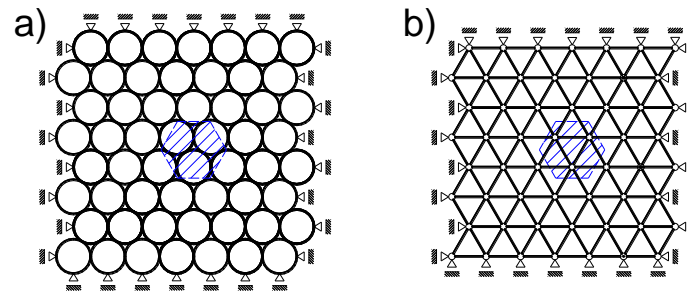


Figure 3.26 Out-of-plane test on panel samples: a) ring element and b) equivalent truss.

Launches N1 and N2 were simulated, at the end of the simulation the numerical elongations were 0.56 m and 0.60 m, respectively, in good agreement with experimental results (0.60 m and 0.67 m, respectively). The response of the two samples in terms of total reaction force and elongation is reported in Figs. 3.27a and b for launches N1 and N2, respectively. The identified constitutive parameters, which ensured such response for the truss panel, are $E_{n1} = E_{n3} = 150$ GPa, $E_{n2} = 1$ GPa, $\varepsilon_3 = 0.001$ and $\varepsilon_4 = 0.015$, see Fig. 3.25c.

With these parameters, two numerical nets were subjected to an in-plane tensile test. Results of the numerical analysis are similar between the models in terms of displacement and force mobilised through-out the test, assessing the ability of the truss net to reproduce both the out-of-plane and in-plane behaviour of the ring net. The identified parameters were thus implemented for the net in the whole barrier model.

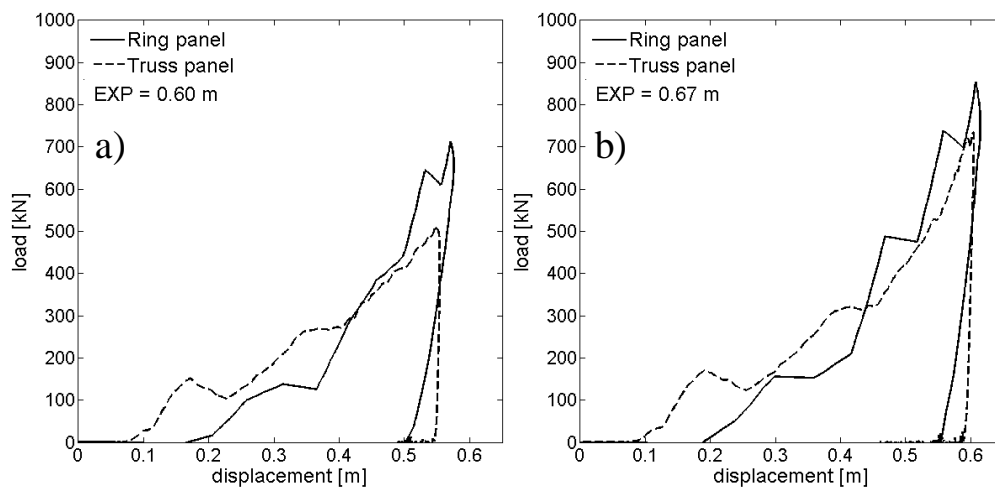


Figure 3.27 Out-of-plane test results, total reaction forces vs. displacement for the two samples: a) launch N1 and b) launch N2.

Modelling of the energy dissipating devices

The cables are provided with energy dissipating de-vices to enhance the energy absorption capacity of the system by developing plastic deformation. They are made of aluminum tubular hollow elements with perforated caps leading the steel ropes through as illustrated in Fig. 3.28.

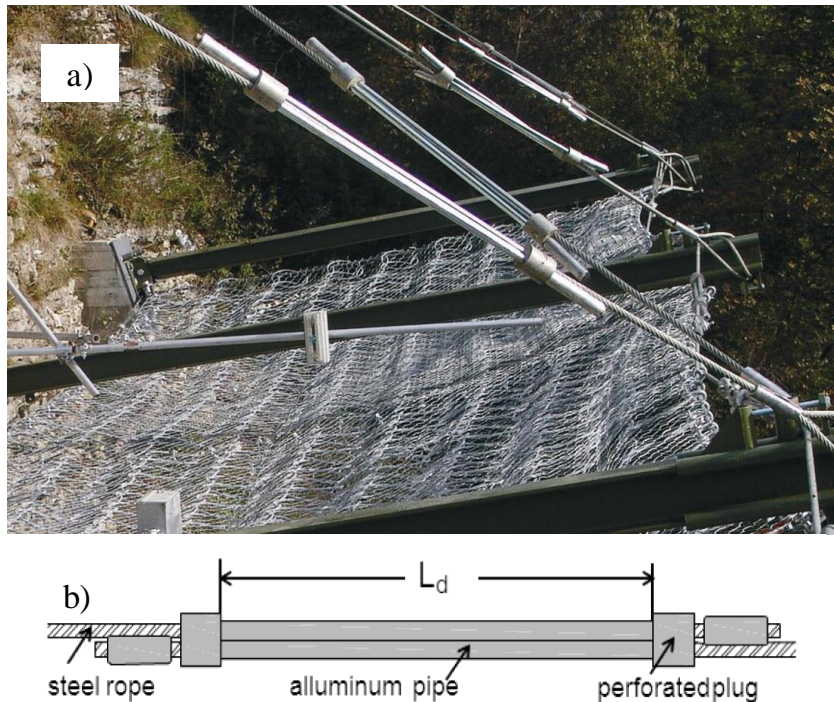


Figure 3.28 Energy dissipating devices in barrier 3000: a) along the uphill cables and b) simplified scheme.

A procedure to identify the model parameters is here reported. A one-dimensional and a three-dimensional model of the energy dissipating devices were used in the procedure. In the one-dimensional model, an axial connector type was used, having the force-displacement relationship represented in Fig. 3.25d. While the three-dimensional model was made of two hollow pipes connected by a rigid block at the ends. Continuous homogeneous shell elements with a bilinear elasto-plastic hardening law were used. A frictional type of contact was assigned to the correlated interfaces. The two models were subjected to a non-linear analysis in which a force equal to 500 kN was applied incrementally along the model axis.

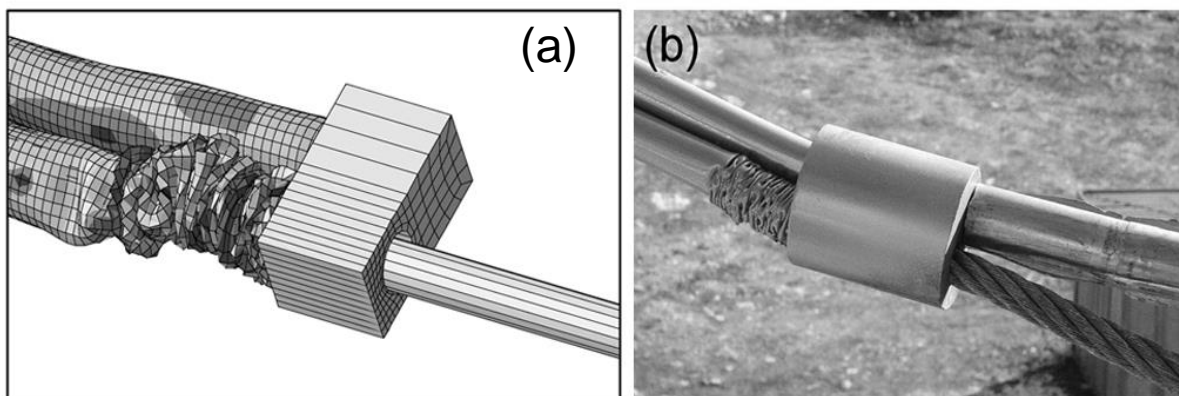


Figure 3.29 Deformation of the energy dissipating devices: a) frame from numerical model and b) picture after full-scale test.

A qualitative result of the analysis is illustrated in Fig. 3.29, which shows as the deformed shape of the three-dimensional model is similar to that of the real energy dissipating device. Fig. 3.30a displays the results of the analysis in terms of reaction force and displacement, while Fig. 3.30b represents the energy dissipated in the 1D model and in the 3D model. Both the models display the same behaviour in terms of force and dissipated energy. The constitutive parameters which ensure the observed response adopted for the 1D model are: $D_{d1} = 20 \text{ MN/m}$, $D_{d2} = 580 \text{ kN/m}$, $D_{d3} = 1 \text{ MN/m}$, $s_1 = 0.002 \text{ m}$ and $s_2 = 0.5 \text{ m}$, see Fig. 3.25d.

After these tests, the simple one-dimensional model of the energy dissipating device with the identified parameters was thus implemented in the whole barrier model.

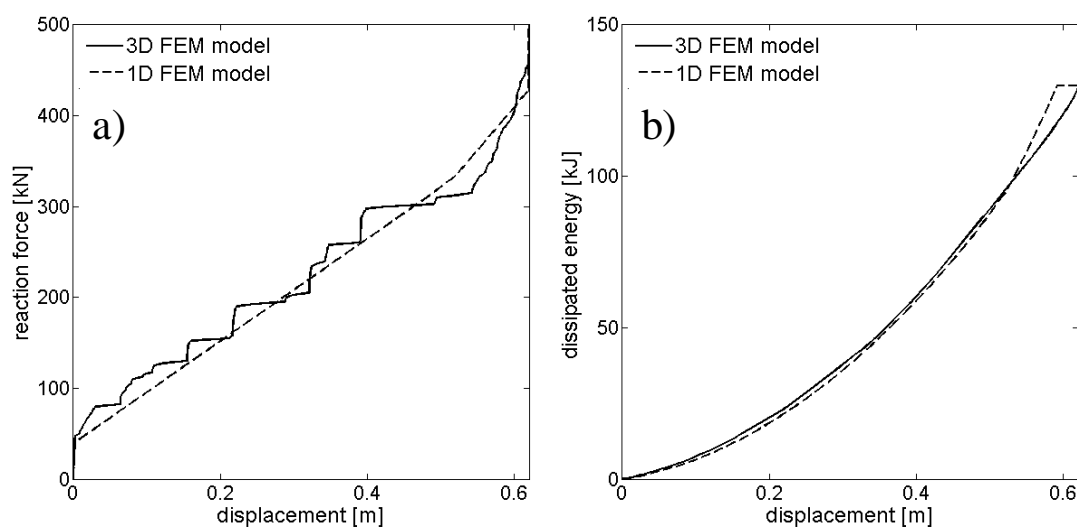


Figure 3.30 Non-linear static analysis of the three-dimensional and one-dimensional model of energy dissipating device: a) force vs. displacement, b) dissipated energy vs. displacement.

3.2.4 MODEL ASSESSMENT

The model of barrier 3000, developed as described in Section 3.2.3, was subjected to retrospective simulations of the tests described in Section 3.2.2. Impact tests on a barrier model were simulated using a three-dimensional deformable body as test block. In the following subsections, comparison with the experimental results of MEL and SEL tests are illustrated.

Model response at the maximum energy level

The model of barrier 3000 was first subjected to the impact of a block on its centre at the maximum energy level (3000 kJ). In Figs. 3.24a and b numerical results (solid line) are illustrated along with the data obtained in the relevant full-scale test (dashed line). A good agreement is shown between the numerical and experimental time histories of the barrier maximum elongation and of the resultant forces at anchorage 10, respectively, assessing the ability of the model to reproduce the time-displacement and the time-force response of the prototype.

In particular, the model reproduces the displacement of the prototype with good accuracy, mainly due to the ability of the equivalent truss net to model the behaviour of the actual ring.

Model response at the service energy level

The model of barrier 3000 was also subjected to the impact of a block at the service energy level (1000 kJ). The numerical results (solid line) are illustrated in Figs. 3c and d along with the data carried out in the relative full-scale test (dashed line). Also in this case the comparison of results shows an excellent match. It proves that the model is capable to investigate the barrier response at low energy values too, validating the effectiveness of the equivalent truss net. Although not all the load cells are reported here for brevity, good agreement of the numerical and experimental response in terms of time-force has been found (Gentilini et al. 2013).

3.2.5 MODEL PREDICTIONS FOR DESIGN SCENARIOS

The numerical strategy can be extended to the interpretation of the response of falling rock protection barriers to a variety of boundary and impact conditions, with the aim of improving their design.

More reliable design parameters to predict the on-site behaviour of the actual barrier can be obtained in addition to the data of the experimental tests carried out on the prototypes, typically used with suitable safety factors. However, in a full-scale test the response of a barrier to a central impact is solely explored, producing symmetrical forces and deformations. Thus in the following the barrier response is explored also under other impact conditions and scenarios.

In this study, retaining the maximum kinetic energy level and prototype configurations, analyses were run on the barrier model by changing the block shape and the impact location in order to investigate the structural response (Fig. 3.31).

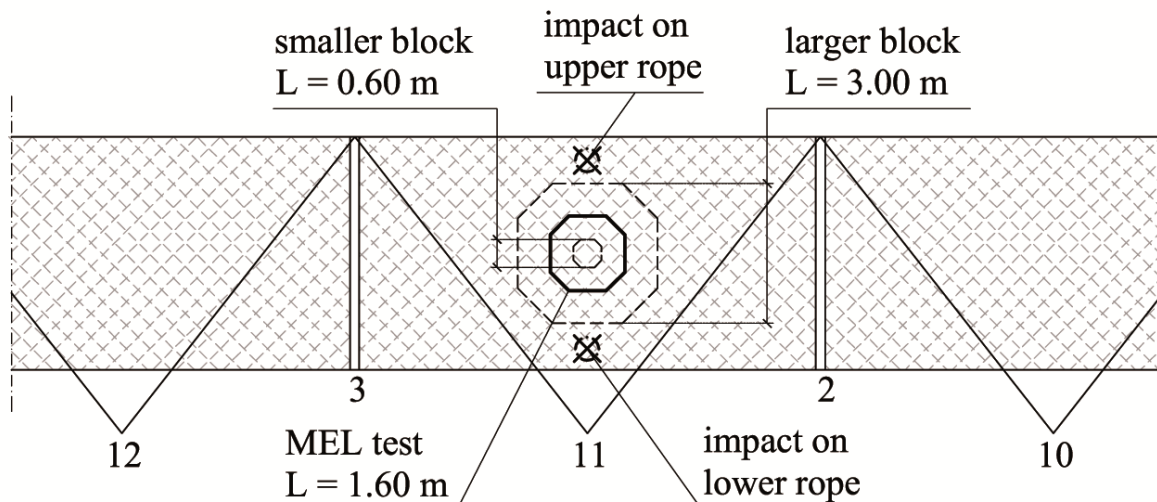


Figure 3.31 Scheme of the different impact conditions tested on the model of barrier 3000.

Impact of blocks with different shape

In order to investigate the effect of the block shape on the structural response, the barrier has been subjected to the launch of two blocks, one with a base dimension equal to 3 m and the other with a base dimension equal to 0.6 m. The total energy of the system has been kept the same of that of the MEL test. The time-displacement

responses of the model to the impact of the block of the MEL test (solid line), of the bigger block (dotted line) and of the smaller one (dashed line) are illustrated in Fig. 3.32a. The model predicts an increment of about 12% in the peak value of the maximum elongation for the block with a smaller base, due to the bullet effect (Cantarelli et al. 2008, Spadari et al. 2012). A decrement of 12% is registered for the block with a wider footprint. As expected, the force values at the anchorages and post foundations do not significantly differ from those observed in the MEL test and for this reason are not reported.

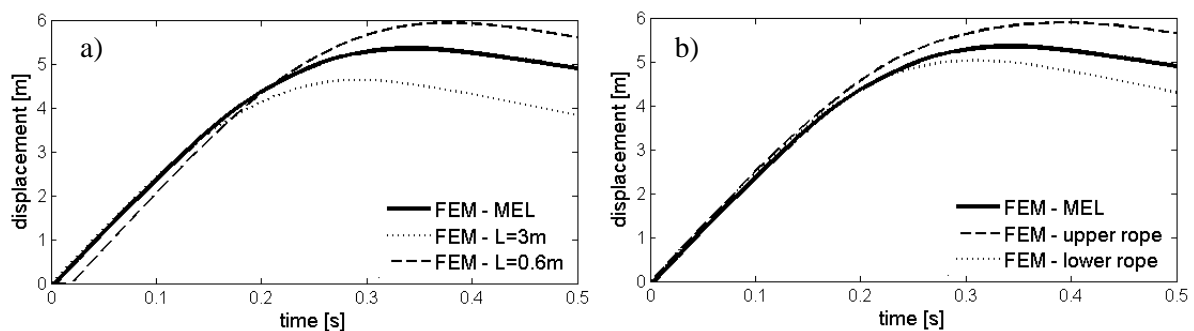


Figure 3.32 Numerical results of maximum elongation point for design scenarios: a) blocks with different shape, b) impacts on different areas.

Impact on different areas of the barrier

The time-displacement responses of the model to the MEL test (solid line), to a central impact near the upper longitudinal rope (dashed line) and near the lower one (dotted line) are illustrated in Fig. 3.32b, showing the trend of the maximum elongation point. The model predicts an increment of about 12% in the peak value of the maximum displacement when the block impacts on the upper part of the net panel, and a decrement of about 6% when it impacts on the lower part. In terms of force values, in the case of impact near the upper rope, an increment at the load cells in the lateral anchorages is registered. While the central post foundations are more unloaded with respect to the MEL test. The opposite occurs in the case of impact near the lower rope.

3.2.6 CONCLUSIONS

The design of falling rock protection barriers is typically based on the results of full-scale experimental tests carried out on relevant prototypes under standardized impact conditions. These may not represent the most severe conditions not only for the maximum elongation of the barrier but also for the forces transmitted to post foundations and ground anchorages.

Simplified or more advanced numerical models, if well calibrated and validated against the available database, can provide such fundamental information on the barrier response under more realistic impact scenarios, thus gaining confidence on the relevant parameters and enabling its design optimization.

CHAPTER 4

ANALYSIS OF EXISTING SEMI-RIGID ROCKFALL BARRIERS:

A NUMERICAL APPROACH

Introduction

Rockfall is a natural hazard that usually affects infrastructures located in mountainous areas. Within this context, existent roads and railways are often located close to unstable slopes prone to these events and they need to be maintained in safety conditions. Several falling rock protection barrier types have been already installed in these areas but most of them were designed in situations of emergency. It represents a problem in order to plan a rockfall risk management of the area, because they were built without a proper engineering design of the structure, hence their energy absorbing capacity is not defined. This is the case of rigid and semi-rigid rockfall barriers having low-energy absorbing capacity.

In fact, the rockfall barrier performance is assessed with an energy criterion as the ability of the protection system to arrest a block impacting with a given kinetic energy. This value is crucial in a rockfall risk assessment and mitigation procedure (Corominas et al. 2005; Mignelli et al. 2014). It is worldwide defined by means of full-scale testing of a prototype. In Europe a guideline (EOTA 2008) provides the requirements to assess the barrier capacity through these experiments, but only system having energy level greater than 100 kJ are considered.

Recently the Autonomous Province of Bolzano (PAB) has developed a database of the existing passive and active protection countermeasures. The inventory includes a catalogue of the rockfall barriers already installed and about a half of them are low-energy systems (<100 kJ) but they are not provided of an exhaustive behavioural documentation.

Since there was a lack of experimental evidence, in order to gain understands of the barrier performance a procedure to supply such becomes necessary. Here the numerical strategy developed for flexible barriers, described in previous Chapter, can

be usefully followed to realise numerical FE model of low-energy barriers. The model is used as a predictive tool to evaluate the effectiveness of the existing structures toward rockfall events. The outcomes obtained represent a reliable parameter in order to enable an assessment of rockfall hazard within the PAB's area.

A preliminary analysis of these systems has been already developed by the author (Gottardi et al. 2011) and is briefly described hereafter as part of the background of the research. Particularly, the hazard assessment method proposed by the PAB is introduced, together with a definition of the inventory. The work was then further developed and has been reported as part of the thesis with two publications produced. The first is a conference paper where a set of FE models of these barriers were developed and outcomes investigated. Then a further study was carried out leading up to comprehensive remarks about the structural performance of semi-rigid barriers; it has been reported in a journal paper which concludes the Chapter.

Background

Mountainous areas are prone to natural phenomenon like landslides, among these rockfall represents a high geological risk especially in Alpine space. In these territories, the extensive urban expansion has increased the interferences between infrastructures and these events. Hence, the development of appropriate tools for landslide risk analysis and management became a crucial issue for the local administrations in charge of protecting the territory (Lee and Jones 2004).

A method to assess the rockfall risk has been developed by the Autonomous Province of Bolzano (PAB) within the context of the European project PARAMount (improved Accessibility, Reliability and safety of Alpine transport infrastructure related to MOUNTainous hazard in a changing climate). In a rockfall mitigation analysis each existent protection structure offers a specific response that affects the intensity of the risk on the area and the hazard assessment method proposed by the PAB wanted to take in due consideration their presence.

In the procedure, the natural slope hazard (H) is modified to account for the presence of protection systems (H^*). The modified hazard is evaluated by means of the charts reported in Fig. 4.1. Three relevant parameters describing the installed protection measure are used in the analysis: the *design*, *location* and *conditions* of the structure. The combination between the design and location parameters defines the *utility of the protection system*, which represent the ability of the barrier to stop the rock falling along the unstable slope. The determined value is then combined with the *condition* parameters, which take into account the actual effectiveness of the structure, to assess the *priority of the protection system maintenance*. The modified hazard (H^*) is finally evaluated by matching the latter parameter obtained with the hazard of the natural slope (H). This value can remain unvaried or be reduced depending on the effectiveness of the rockfall barrier in its working condition.

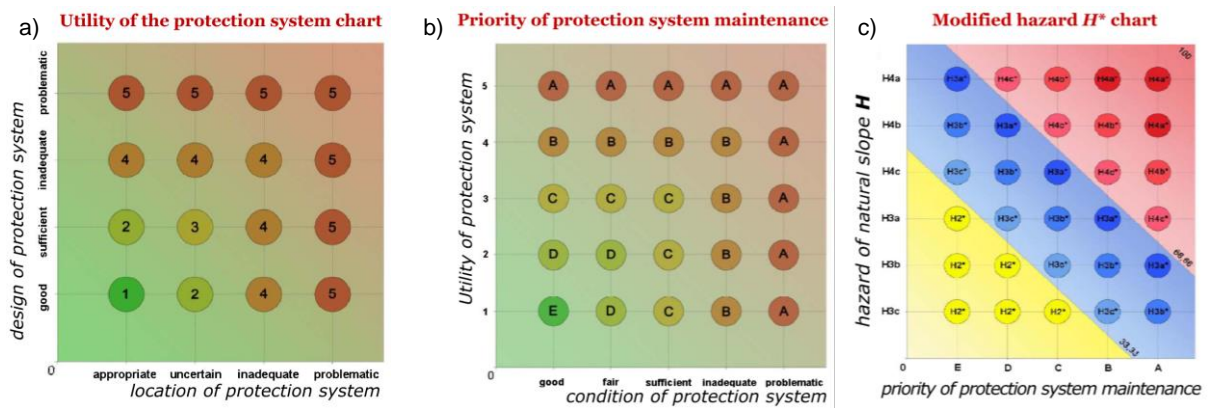


Figure 4.1 Procedure for the evaluation of the modified hazard H^* : a) chart for the assessment of the protection system *utility*; b) chart for the *protection system maintenance priority* and c) chart for the evaluation of the modified hazard H^* .

Clearly, in the described procedure the three parameters of the current rockfall protection barrier must be provided to be successfully applied. The main sources for the acquisition of these data were: on-site direct surveys, documentations provided by National or Federal Agencies in charge of protecting the relevant road stretches and Manufacturer Companies. Thus, the PAB developed a thorough inventory of the existing active and passive protection countermeasure. In the database, named VISO, more than a thousand of several rockfall barrier types were identified and about halves are low-energy structures. For each item the information relevant to the position, the

geometry, the principal components and corresponding materials, data on barrier certifications as well as technical or design reports were included. Details were also collected on the barrier state of maintenance with a proper photographic documentation. In particular, a capacity expressed in terms of kinetic energy absorption was associated to each catalogue item. However, these data were available only for a small selection of all the inventoried barriers and scarce or sometimes none information was recoverable for semi-rigid barriers. Specifically, for about a tenth of the inventoried barriers this data was available and they were all belonging to the flexible category.

Since there was a lack of testing evidence and it was not possible to develop an experimental campaign to study the barrier behaviour in dynamic conditions, a preliminary numerical analysis was addresses to solve the problem. Two selected types of barriers were modelled to estimate the parameter for the hazard assessment method. In the FE analysis developed the barrier was tested with the typical design of ETAG test: three functional module and impact in vertical direction of a polyhedric block. By varying the block velocity, the simulations were carried out observing the barrier response to increasing values of kinetic energy up to admissible stress in the elements was reached, thus defining the maximum absorbing capacity. The final data obtained provided the *design* parameter for the hazard assessment procedure. The designed models were further enhanced and described in the papers presented.

Aims of the research

A comprehensive introduction to gain useful information about the developed work reported in the following has been given. The available data and the method to be implemented in a rockfall risk assessment analysis have been explained. The various problematic and the need for further research concerning the study of low-energy rockfall barrier are highlighted.

In the papers reported, a set of FE models of the relevant semi-rigid and rigid barrier types installed within the Alps territory were realised in order to predict the response of the systems. The numerical approach widely defined in Chapter 3 for flexible barriers was used to develop the models. In absence of a standardisation procedure for these barrier types, the testing approach defined by ETAG has been followed in the numerical study.

The following aims are investigated in this part of research:

- Determine the energy absorbing capacity allowed by the low-energy barriers under dynamic events by considering also a test at service energy level to be repeated twice without going to failure of the elements.
- Investigate the failure mechanism of the studied prototypes in a vertical-drop testing configuration.
- Analyse the system performance by varying the construction design of the structures through parametric tests.

CONFERENCE PAPER 2

**4.1 THE ROLE OF FALLING ROCK PROTECTION BARRIERS IN THE
CONTEXT OF LANDSLIDE RISK ANALYSIS AND MITIGATION**

Abstract

In this paper, the authors investigate the behaviour of the falling rock protection barrier at present installed within the territory of the Autonomous Province of Bolzano (PAB). Information relevant to the description of these structures are found in the complete inventory of all rockfall protection works, recently developed by PAB (VISO). Based on these data, suitably integrated with the available technical documentation and in situ surveys, a set of FE models was developed to predict the response of such structures to the impact of blocks of known kinetic energy. The models were designed so that the results could be interpreted to evaluate the effectiveness of existing barriers toward any possible rockfall event, in terms of structure deformation and forces developed at the foundations and anchoring points. This study forms part of the research activities of the European project PARAMount: imProved Accessibility, Reliability and safety of Alpine transport infrastructure related to MOUNtainous hazard in a changing climate.

4.1.1 INTRODUCTION

Falling rock protection barriers are metallic structures used as passive measures against rockfall, with the aim of intercepting and stopping the blocks moving along an unstable slope.

As illustrated in Fig. 4.2a, these structures are made of a series of identical functional modules installed in sequence up to the desired length. Each functional module generally features an interception structure, kept in position by support structures. Connecting components join the barrier elements and transfer the loads to the foundations. Falling rock protection barriers are able to intercept the blocks moving along a slope and stop them by developing elasto-plastic deformations of the system and its components: the higher the structure compliance, the greater the barrier energy absorption capacity from few to more than 4500 kJ (Descouedres et al. 1999), as it is schematically illustrated in Fig. 4.2b. Available in a variety of models, these structures are widely used since they are light, versatile, easy to be maintained and particularly effective towards rockfall risk mitigation.

The Autonomous Province of Bolzano has recently catalogued about one thousand falling rock protection barriers installed on its territory: approximately more than a half are of low capacity (lower than 100 kJ).

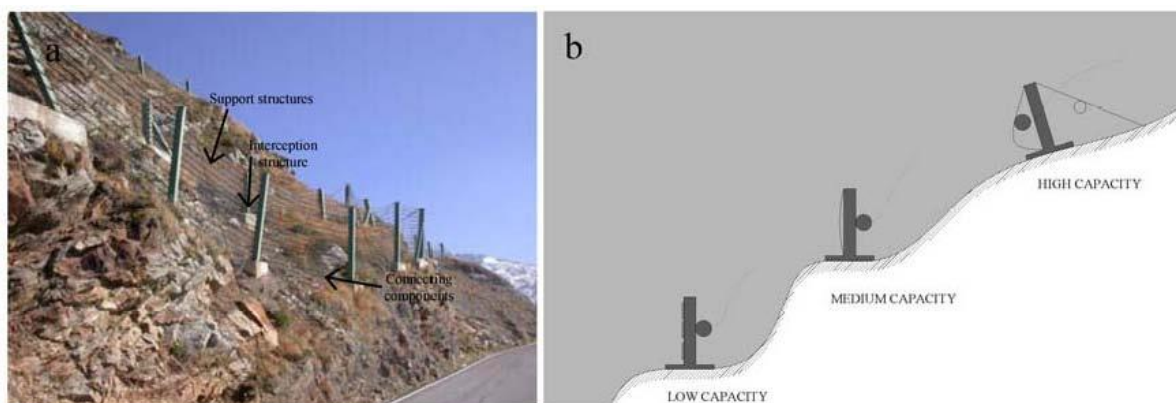


Figure 4.2 Falling rock protection barrier: a) functional modules and structural components; b) compliance and capacity.

In order to evaluate the effectiveness of these structures against rockfalls, the position and the behaviour under dynamic conditions should be known and compared with the data relevant to the description of predicted rockfall events (Giani 1992; Corominas et al. 2005; Oggeri and Tosco 2005, Peila and Guardini 2008). The dynamic behaviour of a falling rock protection barrier is traditionally evaluated by means of full-scale tests, in which the ability of the system to stop blocks having energies up to the nominal value is assessed on prototypes. However, experimental evidences are not available for all the existing falling rock protection barriers and a relevant procedure becomes necessary.

Within such context the paper presents a numerical procedure for the investigation of the behaviour of falling rock protection barriers in dynamic conditions. The procedure has been developed and assessed on the basis of high quality experimental results of flexible falling rock protection barriers (Gottardi and Govoni 2010) and has shown to be of general validity (Gentilini et al. 2012a), as it is able of producing a very accurate description of the response of various types of flexible systems to a wide range of impact kinetic energies. The procedure is herein extended to predict the behaviour of barriers for which experimental data are not available. Numerical analyses enable to predict the parameters relevant to the evaluation of the effectiveness of existing barriers against rockfall events.

4.1.2 THE FALLING ROCK PROTECTION BARRIERS WITHIN THE AUTONOMOUS PROVINCE OF BOLZANO

A complete database of the falling rock protection barriers at present installed within the Autonomous Province of Bolzano has been recently developed. The starting point was found in VISO, a thorough inventory of the protection works now installed within the Province area. With reference to the specific hazard events and threatened items, passive systems such as ditches, wire nets, earth dams, sheds and falling rock protection barriers have been registered within the inventory. Information included in VISO have been mostly acquired by direct inspections carried out over the last few

years and essentially concerns the position, typology and principal dimensions of each protection work, along with relevant photographs and remarks on the state of maintenance.

With reference to the sole falling rock protection barriers, including those of low (Figs. 4.3a and b) and high (Fig. 4.3c) energy absorption capacity, further data were collected in order to provide each item with a complete structural description. These data, generally collected from the available technical documentation along with suitably carried out in-situ surveys, enable both geometry and mechanical properties of the barrier functional module to be accurately depicted.

Since the goal of the database is to provide the information necessary to investigate the response of such structures, technical reports on relevant full-scale tests were included in the catalogue. Experimental results were available for only about one tenth of the inventoried works (all high capacity barriers) and no behavioural data were found for the rest of the structures.

Barriers were then grouped according to their functional module, providing the identification of a set of falling rock protection barriers types. Each type features a specific interception structure, support structure and connecting components and has been, in general, distributed by a single manufacturer.

Although barriers belonging to a given type might feature minor differences among each other (e.g. dimensions, special components), they are expected to exhibit a similar response to block impacts.



Figure 4.3 Falling rock protection barriers within the Autonomous Province of Bolzano: a) and b) low capacity systems, c) high capacity systems.

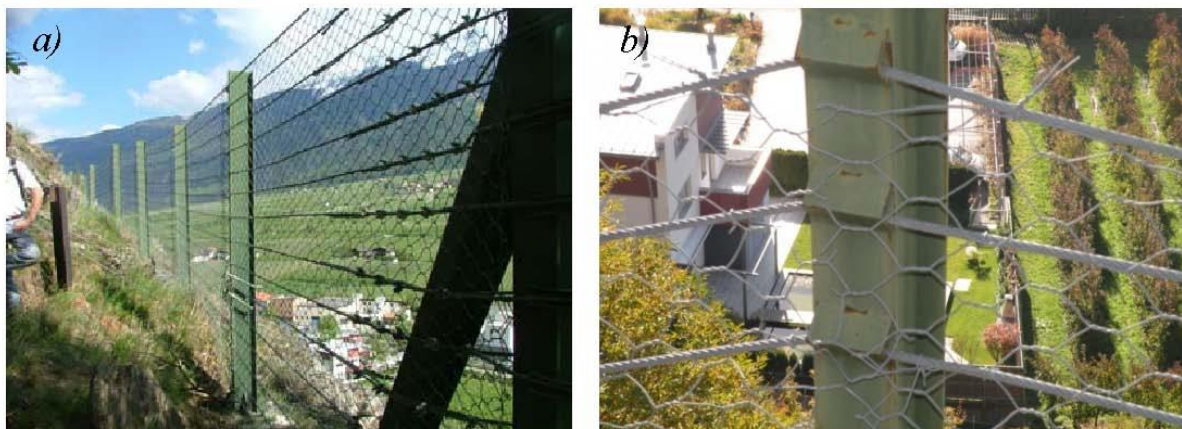


Figure 4.4 The ANAS barrier type: a) general view and b) details of the connecting components.

Therefore, behavioural studies were carried out for each barrier type and results were considered as reference data for all the barriers belonging to the group.

In Figure 4.4, pictures of the ANAS barrier type are shown. The functional module of this barrier type features: equally spaced longitudinal ropes, steel I-beam posts, side cables and special eyelets which let the longitudinal ropes slide horizontally through the posts while no vertical movement are enabled.

Several barrier types are currently under investigation. However, for brevity the study is presented and discussed in the following Section with reference to the ANAS barrier type only.

4.1.3 MODELLING OF FALLING ROCK PROTECTION BARRIERS

The dynamic behaviour of a falling rock protection barrier is traditionally evaluated by means of full-scale tests on prototypes and experiments are generally carried out at test sites (Fig. 4.5) suitably instrumented for the measurement of the quantities relevant to the description of the structure response to block impacts, such as displacements and forces mobilised at the anchorages. In a test site as such, a barrier prototype, made of three functional modules, is subjected to the impact of blocks of known kinetic energies into the middle functional module. Results of the tests provide the complete time histories of the force-displacement response of the barrier and enable the assessment of its energy absorption capacity (the nominal capacity).

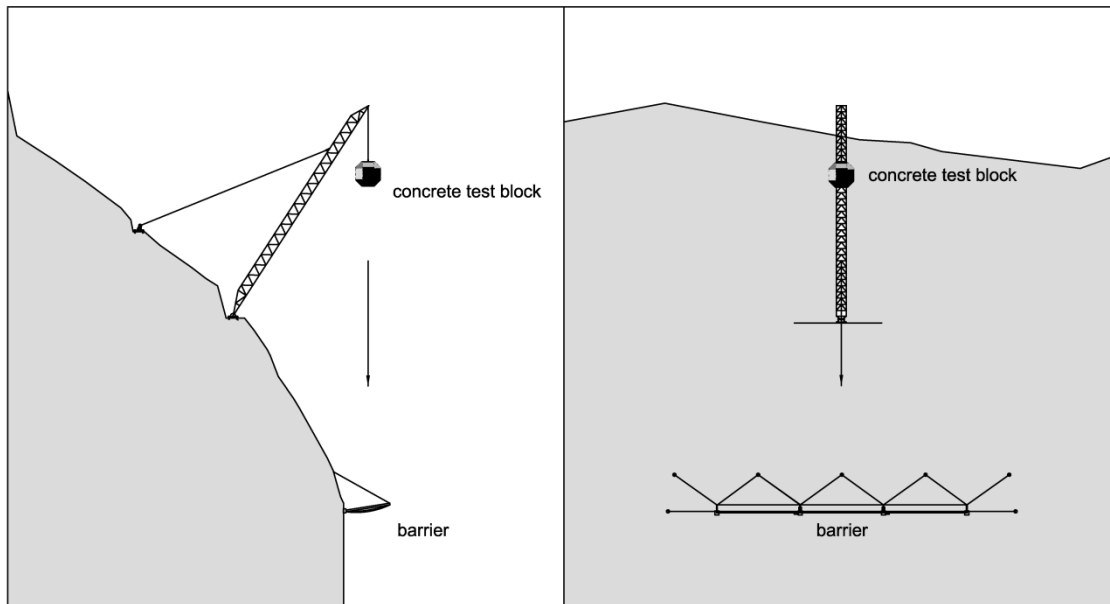


Figure 4.5 Full-scale testing procedures on a three functional modules prototype at a vertical-drop test site.

According to the recently published Guideline for the European Technical Approval of falling rock protection kits, ETAG 27 (EOTA, 2008), full-scale testing is now mandatory for high capacity falling rock protection barriers. The Guideline, which has recently come into effect, provides all the requirements which a barrier should meet for being classified and distributed with a CE marking, as a proper construction product kit.

Over the last few years, significant improvements in testing set-ups and procedures have been made to meet the instructions included in the ETAG 27 and accurate and reliable experimental data on the behaviour of these structures in dynamic conditions have now become available (Gottardi and Govoni 2010). Based on these data, a comprehensive strategy for the numerical modelling of falling rock protection barriers have been recently developed. The numerical procedure was designed on a set of numerical solutions for the modelling of the barrier structural components and impact conditions, which enable simple and effective models to be implemented (Govoni et al. 2011; Gentilini et al. 2012a). Finite element, non linear, dynamic models of different high capacity barrier types were developed according to such procedure and analyses were run under various levels of impact kinetic energy using commercially available FEM codes.

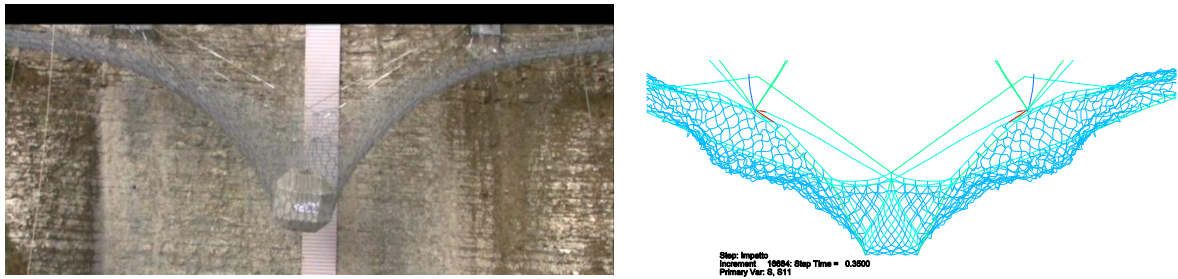


Figure 4.6 Physical and numerical modelling of a falling rock protection barrier prototype in a vertical-drop test site.

All the models have shown to be able to accurately reproduce the experimentally observed behaviour, thus assessing the general validity of the numerical procedure. Such accuracy can be qualitatively appreciated in Fig. 4.6, where the response of a model of a high capacity barrier type to a central impact is compared to the response of the corresponding prototype. Further details and results of the procedure are found in Gentilini et al. (2012a). The findings would encourage the use of such numerical procedures to predict the response of any barrier type to any impact condition.

4.1.4 NUMERICAL MODELLING OF THE ANAS BARRIER TYPE

According to the data collected in the above described database of the falling rock protection barriers of the Autonomous Province of Bolzano, there is no experimental evidence of the response to block impacts of the ANAS barrier type.

In order to evaluate the effectiveness of this structure against possible rockfall events, a numerical study has been carried out, which can yield information on the behaviour that this structure would exhibit in full-scale testing conditions. Results of such analyses enable a thorough investigation of the structure force-displacement response along with an estimate of its nominal energy absorption capacity.

To this end, a prototype of ANAS barrier was devised, as schematically illustrated in Fig. 4.7, according to typical full-scale testing conditions, i.e. a prototype made up of three functional modules and each module featuring an interception structure, a support structure and special connecting components.

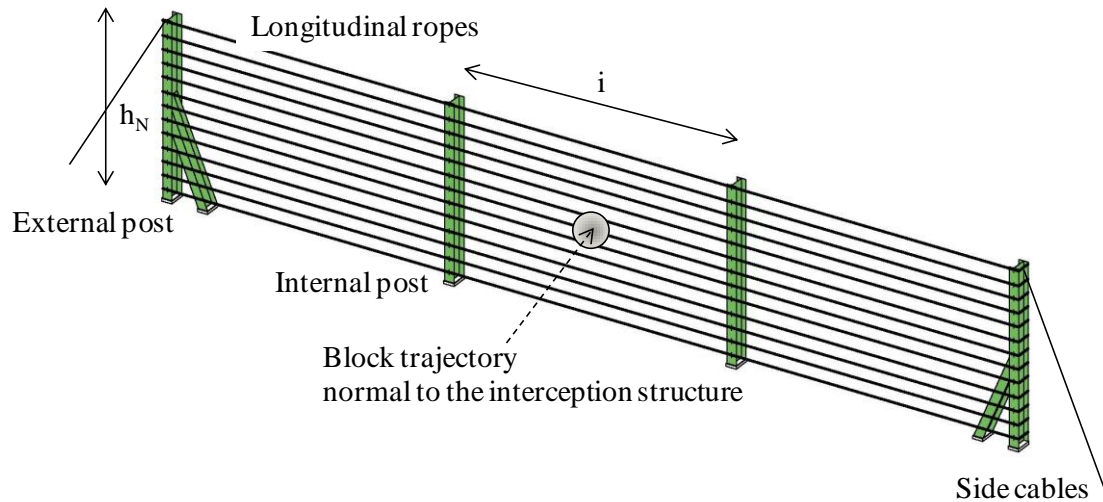


Figure 4.7 FE Model of the ANAS type of semi-flexible falling rock protection barrier: geometry and impact conditions.

The interception structure is made of 12 mm longitudinal ropes, equally spaced; the support structures are made of two internal and two external I-beams; the connecting components are two side cables, each 18 mm in diameter. Eyelets let the ropes move through the posts while vertical movements are prevented. The dimensions of the module are described by the barrier height, defined as the distance between the top and the bottom longitudinal ropes ($h_N = 3.2$ m) and the post spacing ($i = 5$ m). Posts are fully restrained at their base.

A FE model of the prototype has been then developed according to the model proposed by Gentilini et al. (2012a): the interception structure was modelled with one-dimensional truss elements and no flexural rigidity. For the side cables, truss elements were used as well. For the posts, one-dimensional beam elements were adopted with flexural rigidity. The one-dimensional constitutive behaviour assigned to these elements is schematically shown in Fig. 4.8, in terms of stress-strain and moment-curvature. In particular, an elastic perfectly plastic behaviour was introduced for the I-beams (Fig. 4.8a). All the ropes were assumed to have a simple bi-linear, elastic hardening-plastic behaviour with no ability to sustain compressive stresses (Fig. 4.8b), as it is observed on cables in conventional tensile tests (Fontanari et al. 2009; Castro Fresno et al. 2008).

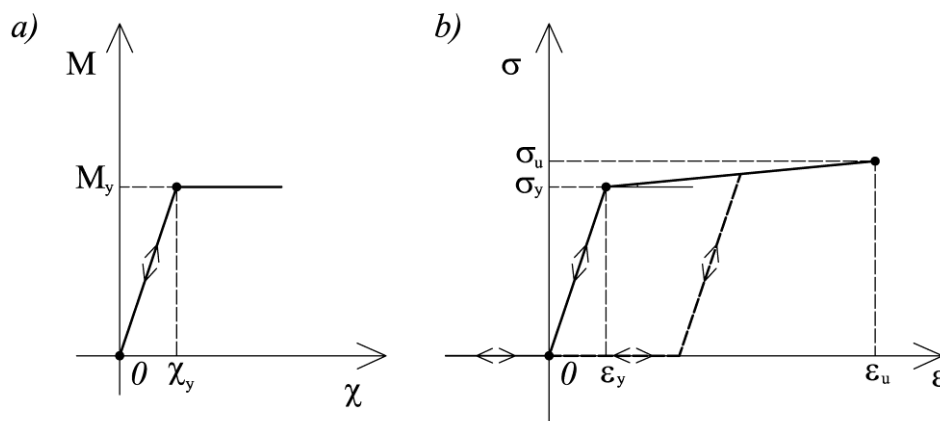


Figure 4.8 FE Model of the ANAS type of semi-flexible falling rock protection barrier: material properties a) posts and b) interception structure.

4.1.5 RESULTS OF THE NUMERICAL ANALYSES ON THE ANAS

BARRIER MODEL

Analyses were run following the procedures of vertical-drop test site: the impact of the test block, normal to the centre of the middle functional module, was simulated by a set of lumped masses (311 kg) distributed on the impact area. A velocity was assigned to the masses in the direction normal to the interception structure plane. Such procedure has been proved effective onto other barrier types (Gentilini et al. 2012a).

Results of the analyses enable the behaviour of a given falling rock protection barrier type to be described. In particular, the simulations allow for the identification of a collapse mechanism for the investigated prototype, obtained by observing the development of plastic hinges within the structural components.

As it is illustrated in Fig. 4.9, with reference to the ANAS barrier type, in response to a central impact, plastic zones start to develop at the external posts and then move to the base of the internal posts. Such mechanism was previously observed and used in simplified analytical procedures for the investigation of the behaviour of this structure type (Paronuzzi and Coccolo 1998).

A set of analyses was performed by varying the intensity of the velocity vectors in order to identify a threshold level after which the model no longer converges. Such velocity level, combined with the applied mass value, provides the maximum kinetic energy that the model is able to absorb prior to fail. Such value was taken as the barrier type nominal capacity, in the case of the analysed ANAS barrier type 50 kJ.

Results provide also information on the system maximum displacements. The time-history of the barrier elongation, given by the movement of the impact points in the direction normal to the interception structure, is given in Fig. 4.10a. The peak value on the curve (1 m for the ANAS barrier type), when compared with the in-situ minimum distance between the barrier and the protected items, gives a further crucial information on the barrier effectiveness against rockfall.

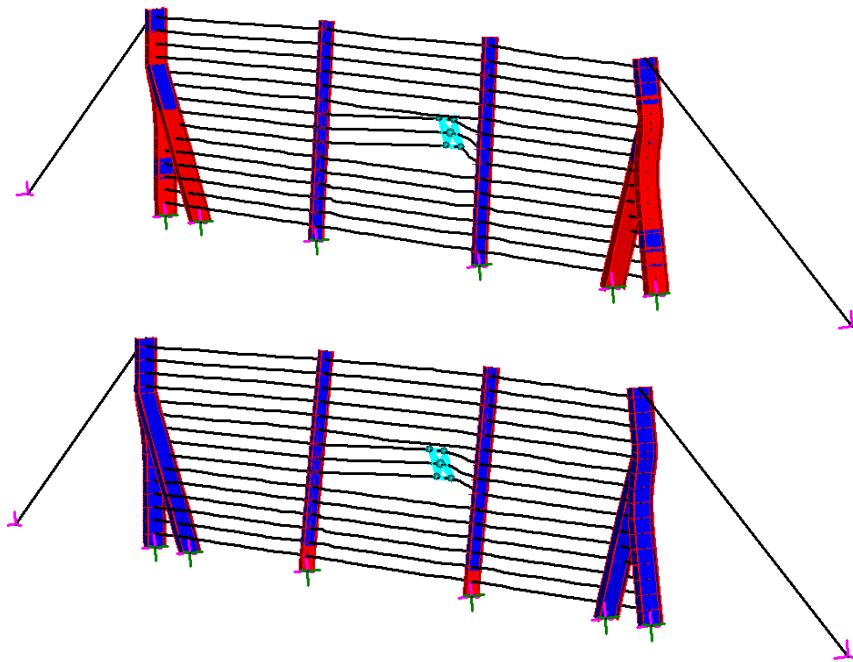


Figure 4.9 Results of FE analyses of the ANAS type of falling rock protection barrier: failure mechanism.

Other relevant results are those concerning the reaction forces developed at the foundations. Again, the peak value on the curve can be suitably used to verify the adequacy of such foundation design. For the ANAS prototype, the tensile force developed at the side anchorages is given in Fig. 4.10b, while the time histories of the

force and moment resultants mobilised at the internal post foundations are shown in Figs. 4.10c and d.

These results provide the reference data for all the barriers installed within the Autonomous Province of Bolzano and catalogued in the ANAS barrier type group. Since these barriers can be found on the Bolzano territory in several geometrical (post spacing, nominal height) and mechanical (posts and rope sections) configurations, parametric analyses were run to investigate their influence. Noting that parameter values in *italic* are those of the reference model, results of the simulations are summarised in Table 4.1, with relation to the capacity values and maximum forces and moments acting on the foundations.

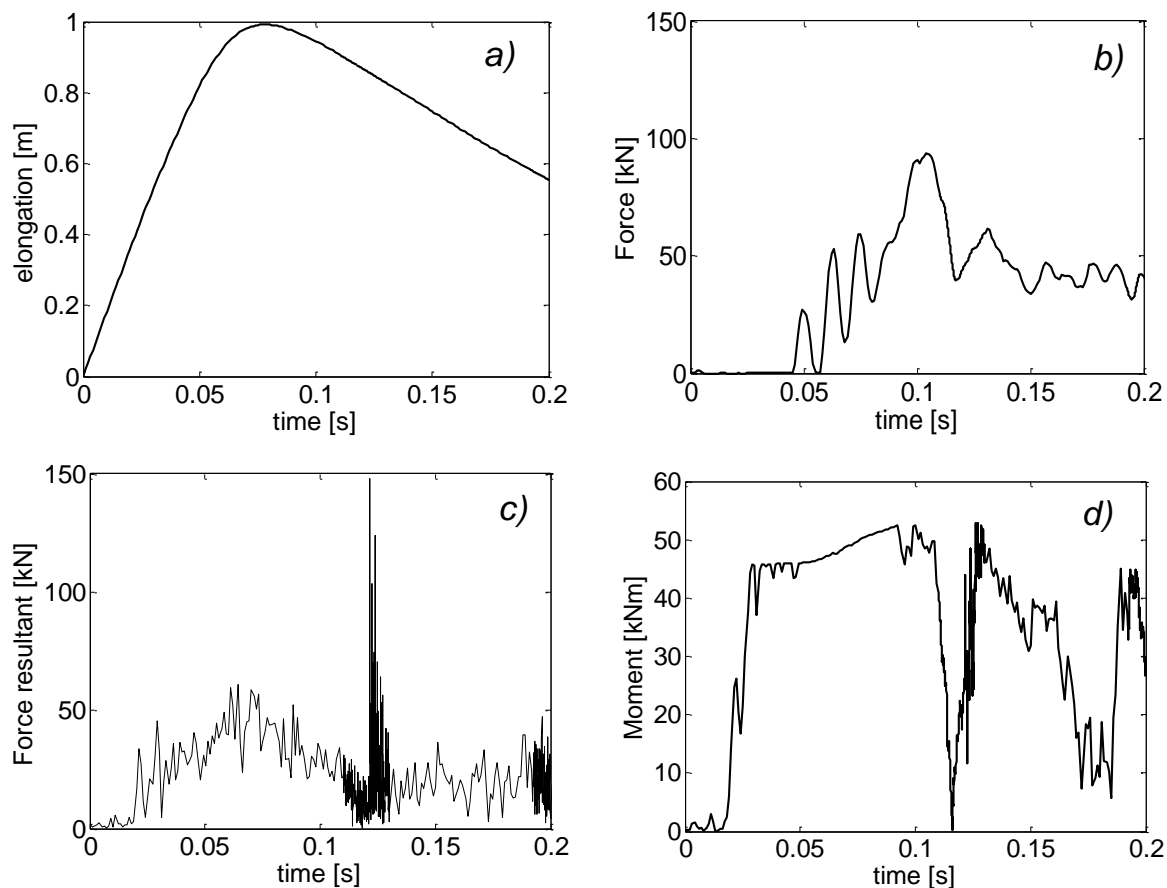


Figure 4.10 Results of FE analyses of the ANAS type of falling rock protection barrier: time histories of a) the barrier elongation, b) the tensile force at one side anchorage, c) the force resultant at one internal post foundation and d) the resultant moment at one internal post foundation.

Results were obtained by varying one parameter at time on the reference barrier model. A preliminary parametric study was also carried out to investigate the effects of the impact location and results are also reported in Table 4.1. In particular, the structure response was studied for impacts onto the top longitudinal rope (top) and side span (lateral). More details can be found in Gorlato (2011).

As it can be observed, the barrier capacity increases with its dimensions, both in terms of post spacing and height. Higher posts sections produce higher capacities, whereas larger rope diameters produce lower capacities. The capacity of this barrier type, as predicted by numerical analyses, is found between 30 and 90 kJ. It is also worth noticing that non standard and symmetric impact conditions can significantly reduce the barrier capacity.

Parameters		Capacity [kJ]	Max reaction force [kN]	Max reaction Moment [kNm]
Post spacing i	3.5 m	40	600	50
	5 m	50	600	50
	6.5 m	70	500	55
Nominal height h_N	2 m	40	500	55
	3.2 m	50	600	50
	4 m	70	400	50
Internal posts diameter	IPE 200	50	600	50
	IPE 220	70	600	60
	IPE 240	90	700	80
External posts diameter	IPE 270	40	550	50
	IPE 300	50	600	50
Longitudinal rope diameter	12 mm	50	600	50
	16 mm	30	600	50
	18 mm	30	700	50
Impact conditions	central	50	600	50
	top	30	350	50
	lateral	30	600	45

Table 4.1 Parametric analyses on the ANAS type of semi-flexible falling rock protection barrier.

4.1.6 CONCLUDING REMARKS

The paper has presented a procedure to investigate the behaviour of the falling rock protection barriers at present installed within the territory of the Autonomous Province of Bolzano. The procedure has been developed from the information collected in a database of all the barriers catalogued within the inventory of all the protection works

of the Province territory. The aim of the study is to provide the data relevant to the description of the effectiveness of these special structures toward possible rockfall events. The data enabling the description of the behaviour of these structures in dynamic conditions are generally available only for high-capacity falling rock protection barriers, as they are typically subjected to suitably developed full-scale tests, while no experimental evidences on the response to block impacts of lower capacity falling rock protection barriers are currently available. A FE procedure, recently developed and assessed, has been then applied to investigate numerically the response of such low capacity barriers in conditions similar to those encountered in a test site. The procedure has been applied to various barriers and presented in the paper with reference to the widely used ANAS type. Results of the simulations provide parameters relevant to the evaluation of the effectiveness of this structure type against rockfall, such as the barrier absorption capacity, deformation and force mobilised at the foundations. Results of specific parametric analyses were also briefly presented. This study forms part of the research activities of the European project PARAMount: imProved Accessibility, Reliability and safety of Alpine transport infrastructure related to MOUNtainous hazard in a changing climate.

JOURNAL PAPER 2

4.2 VIRTUAL TESTING OF EXISTING SEMI-RIGID ROCKFALL PROTECTION BARRIERS

Abstract

Semi-rigid rockfall protection barriers are steel structures constituted by a principal interception structure made of cables mounted on structural steel posts fully restrained to the ground. Traditionally, they are assigned a low capacity value which ranges from few to less than 300 kJ. Over the last decades, semi-rigid rockfall protection barriers have been installed along areas interested by rockfall events, often in conditions of extreme urgency, without a specific structural design. As a result, they are found in a variety of subtypes, most of them lacking the essential structural information, such as the energy absorption capacity, crucial for a reliable application of procedures for quantitative risk assessment. To fill this gap, and considered the lack of experimental data on semi-rigid barriers, in the present study a numerical investigation of the most common barrier subtypes is developed. In the absence of standards for this kind of barriers, the barriers are virtually tested in conditions inspired by the essential prescriptions included in the European Guideline for flexible barriers (ETAG 27). Results allow to: i) investigate the performance of the barriers in service condition; ii) provide an estimate of the barrier capacity and iii) explore the barrier failure mode.

4.2.1 INTRODUCTION

The development of rockfall mitigation strategies often concerns areas which have been subjected to former protection actions. These actions commonly involved the installation of structural rockfall protection systems such as barriers, embankments, ditches or galleries (Volkwein et al. 2011; Lambert and Nicot 2011; Duncan 2014).

In many cases, the structures still rest on the area, identifying its actual protection scenario. Each existent structure offers a specific response to impact that affects the intensity of a rockfall risk on the area (Corominas et al. 2005; Agliardi et al. 2009; Lambert et al. 2013; Mignelli et al. 2014).

A special type of rockfall mitigation structure, hereinafter named semi-rigid rockfall protection barrier, has been extensively employed as a convenient passive countermeasure being cost-effective, versatile, easy to be installed and maintained. Semi-rigid rockfall protection barriers are steel structures made of the repetition of a single functional module. Generally, each module is constituted by a principal interception structure made of cables mounted on structural steel posts fully restrained to the ground. The use of connecting components, such as further cables or clamps, produces a variety of barrier subtypes. Semi-rigid rockfall protection barriers are usually less than four meters high and can be several meters long.

The capacity of a falling rock protection barrier is identified with a kinetic energy value, associated to the maximum energy possessed by a block that the barrier is expected to arrest, and may range from few up to 8000 kJ. Semi-rigid rockfall protection barriers are also described as low-energy barriers. Although there are no experimental evidences, they are traditionally assigned capacity values ranging from few to less than 300 kJ (Descoedres et al. 1999).

Semi-rigid barriers are typically found just above road stretches and railways, installed directly to the ground or on gravity retaining walls to arrest the blocks at the very end of their fall.

Recently, the Autonomous Province of Bolzano (Italy) has counted on its territory about a thousand working falling rock protection barriers. About a half was recognized to belong to the semi-rigid type, installed in a variety of subtypes during the last two decades (Gottardi et al. 2011). The barriers are typically installed without

specific design instructions and often used as a fast response in condition of emergency. As a result, the essential structural information are missing. Further, this type of barrier received only little attention up to now (Cazzani et al. 2001; Muraishi et al. 2005; Bourrier et al. 2014; Kwan et al. 2014).

In response to the lack of data, a numerical study offers a suitable alternative to carry out a complete description of the response to impact of semi-rigid rockfall protection barriers.

The base of the study is provided by a FE strategy, devised by the authors, which provides all the elements for the development of simple structural models of falling rock protection barriers (Gentilini et al. 2012a). The strategy was assessed using results of full scale tests carried out on various prototypes of flexible falling rock protection barriers (Gottardi and Govoni 2010). Rather than a single model, the proposed procedure enables the definition of key numerical choices of general validity that enable the development of reliable numerical models of any type of falling rock protection barriers. Two-dimensional (de Miranda et al. 2010; Govoni et al. 2011) and three-dimensional non-linear, dynamic models made of one-dimensional FE elements of all the tested prototypes were devised according to that strategy, with special emphasis on the modelling of the components, such as the net panel and energy dissipating devices (Gentilini et al. 2013).

The strategy was shown to be effective independent of the barrier type and impact energy, encouraging its use as a predictive tool (Gottardi et al. 2014). In the last two decades, other studies have confirmed that numerical models based on finite elements, or discrete elements, certainly are a powerful tool to investigate the dynamic behaviour of highly flexible barriers (Nicot et al. 2001; Volkwein 2005; Bourrier et al. 2011; Shi et al. 2013; Van Tran et al. 2013; Moon et al 2014), establishing a consolidated numerical research environment.

Within this context, the main objective of the research is to investigate the response of semi-rigid rockfall protection barriers, widely used but narrowly studied. In response to the lack of experimental evidences, the study presents the results of a virtual testing program conducted on four semi-rigid rockfall protection barrier types developed according to the above mentioned strategy. In particular, the most commonly installed

barriers along the Alps are considered. Models are kept as simple as possible, with truss and beam elements to represent the components of the barriers, focusing on the connection between the elements.

In absence of specific instructions for semi-rigid rockfall protection barriers of energy lower than 100 kJ, the essential instructions included within the European Guideline, ETAG 27 (EOTA 2008) for comparatively higher capacity barriers were used as a guide in developing the virtual testing program. Thus, barrier models are made of three functional modules and are subjected to the central impact of a concrete block of known mass and velocity. Vertical-drop testing conditions were considered. In order to investigate the structural behaviour of the barriers in service condition, the models are subjected to two subsequent launches at the same energy level, verifying that the barrier was able to arrest the block. Based on the service energy threshold, limit state was associated to a value of kinetic energy of the impacting block equal three times the service energy, ensuring that the barrier was still able to stop the block. Then, the barriers are taken to failure increasing in constant steps the kinetic energy of the block, detecting the failure energy and failure mode of each barrier type.

The paper is organized as follows. In Section 4.4.2, the main features of the four types of barriers under study are presented. In Section 4.2.3, the numerical procedure and the virtual testing program are shown. Results of the study are discussed in Section 4.2.4.

4.2.2 SEMI-RIGID ROCKFALL PROTECTIONS BARRIERS

Semi-rigid rockfall protection barriers are steel structures made of the repetition of a single functional module. Each module consists in an interception structure, a supporting structure and various connecting components. In many cases, the interception structure is made of evenly spaced longitudinal cables of various diameters and a secondary steel hexagonal meshwork. Steel posts such as I-beams or flange beams are the supporting structure. Connecting components are all the further cables (uphill cables, lateral cables, etc.), studs or clamps resulting in a variety barrier subtypes. A typical semi-rigid rockfall protection barrier, located within the territory of the Autonomous Province of Bolzano (Italy), is depicted in Fig. 4.11.



Figure 4.11 A typical semi-rigid rockfall protection barrier installed in the Autonomous Province of Bolzano (Italy).

Semi-rigid and flexible barriers, though quite alike in the essential features, present crucial differences which influence the deformation mode and the energy absorption capacity.

The posts of semi-rigid rockfall protection barriers are fully restrained to the ground, so that both the supporting and interception structure bear the impact loads. Semi-rigid rockfall protection barriers are generally not provided with energy dissipating devices and are used where rockfall events are expected to be of low intensity, while flexible barriers are used when boulders would fall with energy comparatively higher (from few hundreds to more than 5000 kJ).

In a flexible barrier, this function is primarily fulfilled by the interception structure made of highly deformable net panels and connecting components such as energy dissipating devices and the posts are provided with hinges at the base.

Flexible barriers have been studied thoroughly within the last ten years and their design is supported and regulated by international and national standards and guidelines. On the contrary, the structural behaviour of semi-rigid rockfall protection barriers, is still not adequately characterised.

This study attempts to fill this gap considering four types of semi-rigid rockfall protection barriers, selected among those most frequently encountered along the Alps. These barriers, identified hereinafter with the labels SF1, SF2, SF3 and SF4, are illustrated from Figs. 4.12 to 4.15, respectively.

In particular, barrier SF1 is illustrated in Fig. 4.12. The nominal height h_N of the barrier is 3.2 m and the post spacing is equal to 5 m. The principal interception structure is made of longitudinal steel cables of 12 mm diameter. Internal posts, I-beams of European type IPE 200, are provided with special eyelets to let the longitudinal cables of the interception structure pass through. External posts are steel beam IPE 300, provided with a further beam as a trestle support and suitably modified to accommodate the ending loops of each longitudinal cable. The barrier is provided with side cables of 18 mm diameter.

Semi-rigid barrier SF2, Fig. 4.13, has the same dimensions of barrier SF1, but it is provided with a secondary hexagonal meshwork, made of twisted steel wires of 2.7 mm diameter, attached with clamps or steel threads to the uppermost and lowermost longitudinal ropes. This barrier configuration is the most frequently installed.

Barrier SF3 features a set of steel clasps mounted on the principal interception structure. Each clasp of 12 mm diameter retains two successive longitudinal cables defining the regular pattern represented in Fig. 4.14.

Barrier SF4, shown in Fig. 4.15, features three couples of cross cables mounted on the interception structure and four uphill cables. The diameter of the cross and uphill cables is 12 mm. The principal dimensions of barriers SF3 and SF4 are those of barrier SF1.

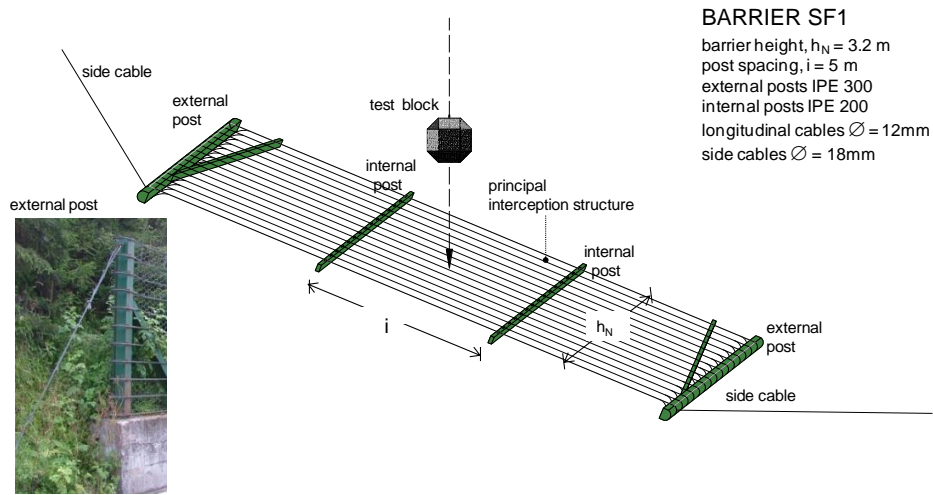


Figure 4.12 Model of semi-rigid barrier SF1, in vertical drop test site configuration.

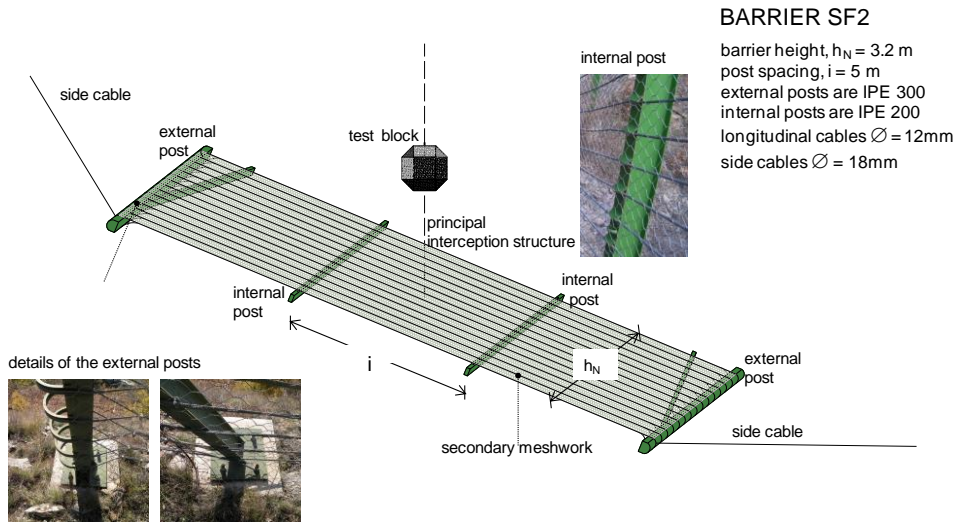


Figure 4.13 Model of semi-rigid barrier SF2, in vertical drop test site configuration.

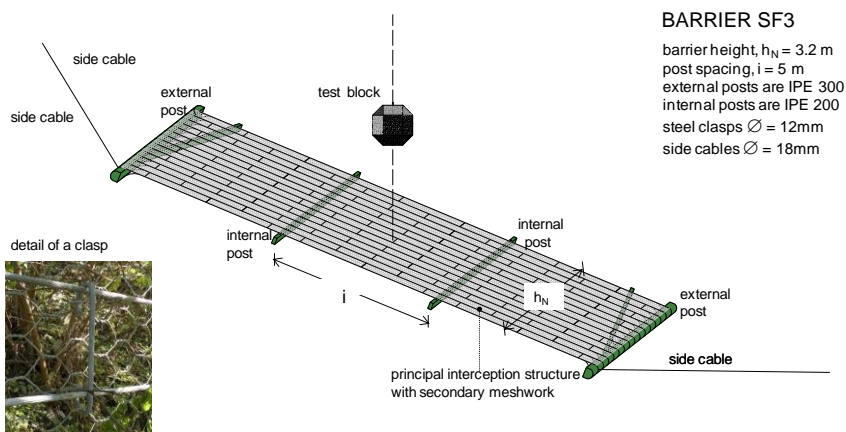


Figure 4.14 Model of semi-rigid barrier SF3, in vertical drop test site configuration.

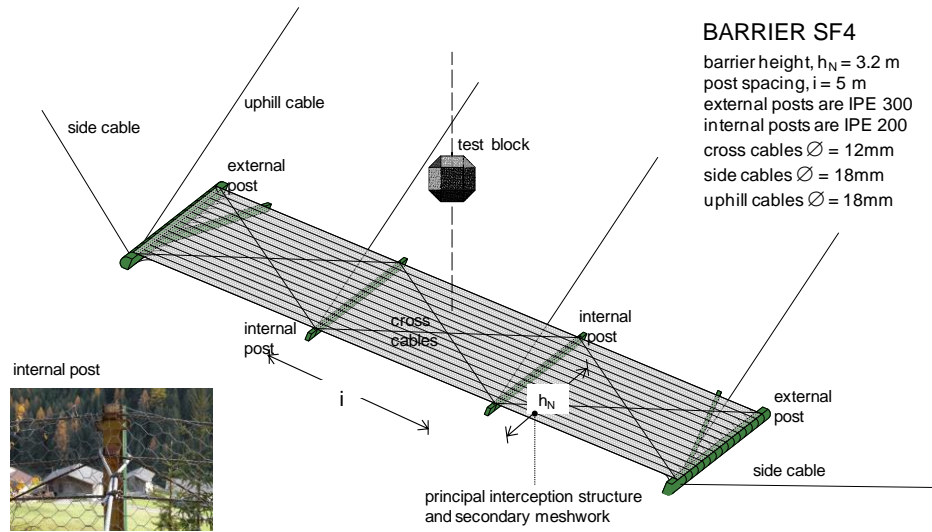


Figure 4.15 Model of semi-rigid barrier SF4, in vertical drop test site configuration.

4.2.3 VIRTUAL TESTING OF SEMI-RIGID BARRIERS

In this Section, the virtual testing program adopted for simulating the response of the barrier types described in details in Section 4.2.2 is described in detail.

In the numerical analyses, the commercially available computer program ABAQUS/Explicit v. 6.11 has been employed (Hibbitt 1998).

Numerical approach

In response to the lack of experimental instructions for the testing of these barrier types, the present study refers to the recently published European Guideline, ETAG027 for experimental details, measured quantities and data interpretation. Although the guideline specifically applies to flexible falling rock protection barriers with high energy absorption capacity, it is herein extended to investigate the response of semi-rigid barriers, being the two barrier types adequately alike, as described in Section 4.2.2.

For the numerical procedure, a simple and effective FE strategy developed in recent years for the investigation of the mechanical behaviour of flexible barriers is followed. Referring to Gentilini et al. (2012a and 2013) for further details, the strategy was

tuned on results of full scale tests carried out in a vertical drop test site onto different flexible barrier prototypes at different energy levels. The experimental database was particularly rich and consistent, thus enabling the calibration and assessment of both two-dimensional and three-dimensional FE barrier models as well as an accurate modelling of the main components, such as the interception structure and energy dissipating devices. The very good fit between the experimental and numerical results assessed the capability of the FE model to represent the barrier behaviour, reproducing accurately the barrier deformation, the elongations and the forces developed at the anchoring points. Once the reliability of the strategy was validated, this has given confidence to the use of such models for studying other types of barriers in standardized testing conditions.

According to the established numerical procedure, three-dimensional FE models of the semi-rigid barriers object of the present study are carried out. All the cables are modelled using 2-node, truss elements with no flexural rigidity and unable to withstand compressive forces. Secondary meshwork and the connecting components are modelled with truss elements as well. The posts are modelled using 2-node, beam elements.

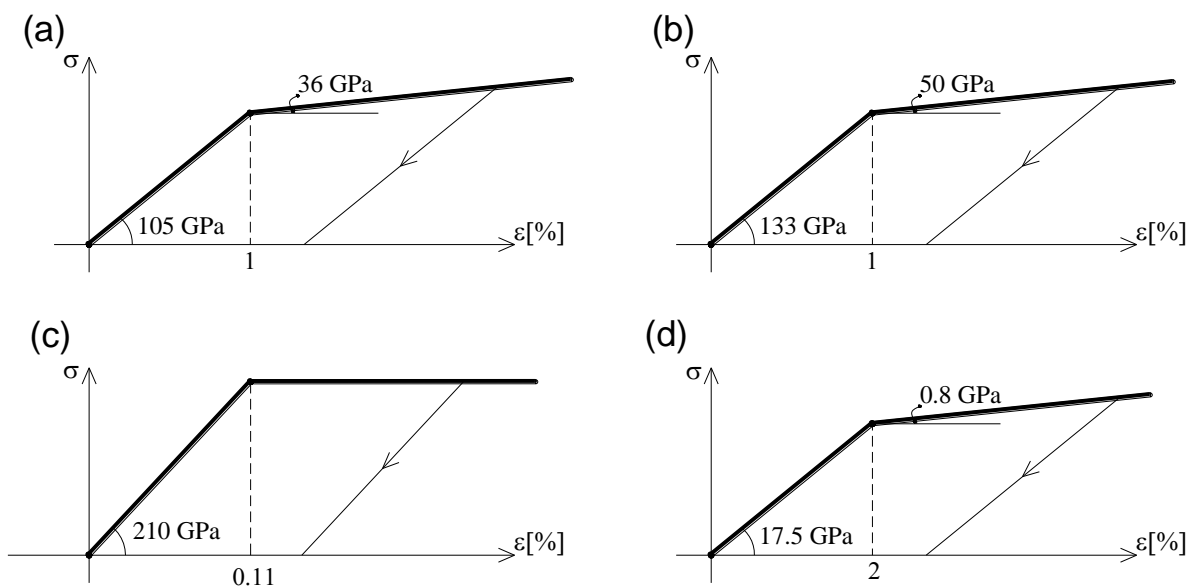


Figure 4.16 Constitutive behaviour of: a) $\phi 12$ cable; b) $\phi 18$ cable; c) posts and d) steel wires of the secondary net.

An elastic-plastic constitutive law is adopted for the description of the mechanical behaviour of all the elements. The constitutive parameters are selected according to those used for flexible barriers, as they ensured a good prediction of the experimental response. A tensile failure strain equal to 20% has been adopted for the posts elements and 2% for the cables. In Fig. 4.16, the constitutive laws adopted for the cables, the posts and the secondary net are schematically represented.

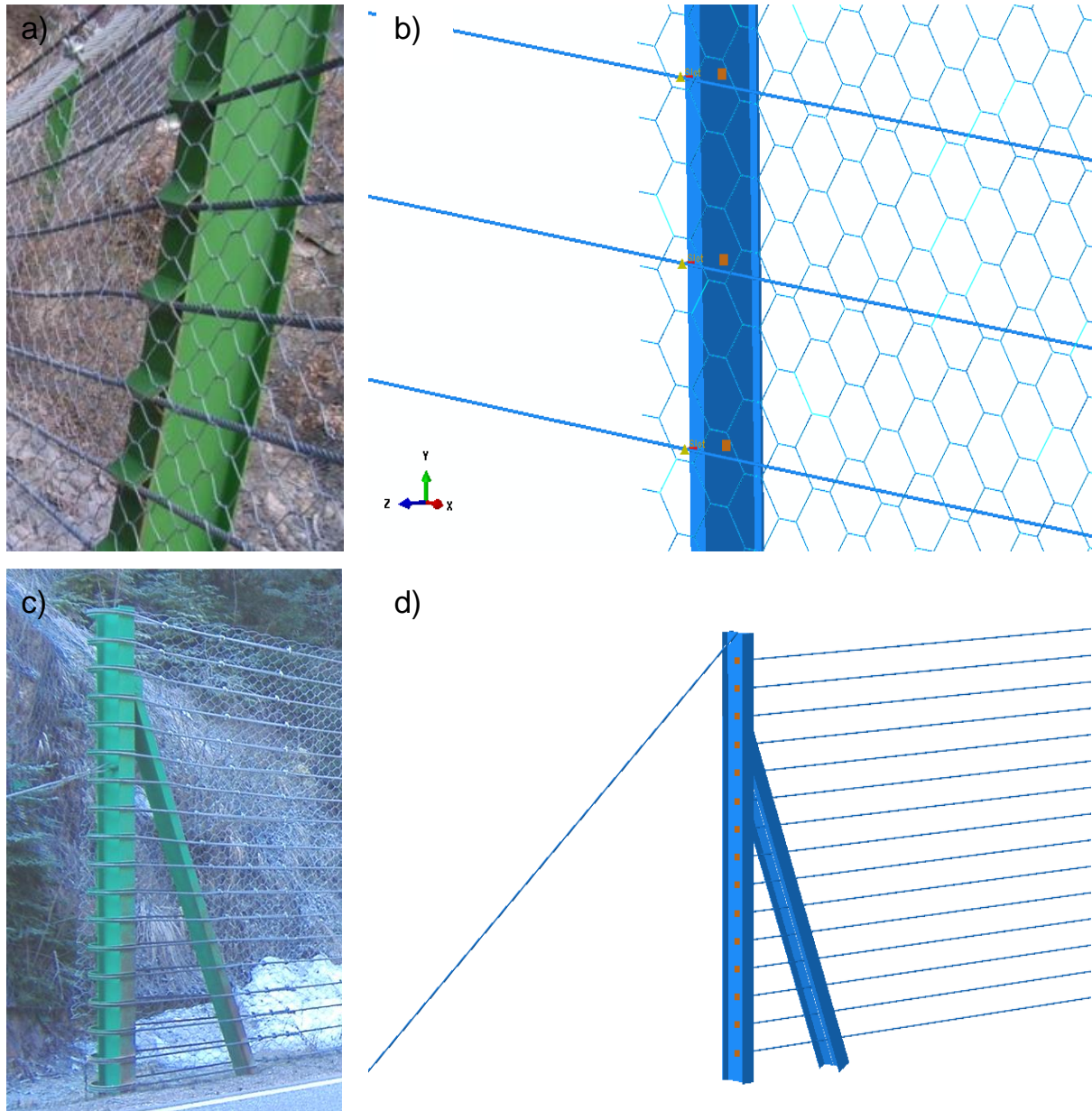


Figure 4.17 Details of the connection between the posts and the longitudinal cables. a) Longitudinal cables can slide through metallic eyelets on the internal post and b) in the numerical model the relative motion between the cable and the internal post is modeled by means of special connectors (SLOT). c) Longitudinal cables show a loop termination at the external posts locked by a set of several clips and d) in the numerical model the cables are hinged to the external post.

Details about the connections between the posts and the longitudinal cables are shown in Fig. 4.17. In particular, the longitudinal cables can slide through metallic eyelets on the internal posts, Fig. 4.17a. In order to reproduce this important mechanism, the special connection type SLOT available in Abaqus is adopted, Fig. 4.17b. This device allows the sliding between one-dimensional elements. At the external posts, longitudinal cables show a loop termination locked by several clips, Fig. 4.17c. To the authors' knowledge, sliding through the cable clips is not documented. For this reason, in the numerical model a hinge like connection between the cables and the external posts is adopted, Fig. 4.17d.

Following the experimental vertical drop test site condition, the numerical testing procedure provides that the barrier prototype is placed horizontally and a concrete block impacts the centre of the middle functional module with known initial velocity (v_0), Figs. 4.13 to 4.15. The test block has a 1 m side and mass equal to 1700 kg. The block is simulated with a three-dimensional body that is shaped as a polyhedron, made of high-resistance concrete. The dimensions of the block are chosen so that the impact involves three consecutive longitudinal ropes, ensuring a barrier height greater than three times the block side. The contact between the test block and the net has been simulated with a standard contact algorithm, namely GENERAL CONTACT available in Abaqus, that allows a simple definition of the contact between a three-dimensional body and truss elements. The dynamic friction coefficient is chosen equal to 0.4, since this value, used in previous works, was shown to reproduce accurately the contact between the block and the net.

Testing programme

The FE tests are carried out by varying the block's initial velocity v_0 , such that the response of each barrier type to different intensity energy levels is explored. Small velocity increments are considered (2 m/s) for impact energy values ranging within the typical interval of capacity of these barrier types, from few to more than 200 kJ.

The assessing method is based on the amount of kinetic energy the barrier is able to absorb in the impact tests. Three threshold levels of kinetic energy are considered: the service energy level (hereinafter labelled with S), the limit energy level (hereinafter labelled with L) and the failure energy level (hereinafter labelled with F).

In particular, to identify the service energy level (E_{kS}), the barrier prototypes are subjected to two subsequent launches, S1 and S2, performed using the same test block and initial velocity. In the first launch, it is assessed that the block is arrested with no rupture or significant deformation in the model elements. In the second launch, performed on the barrier model following the first launch, after the block is removed, the assessment only concerns the barrier model ability to stop the test block still.

Based on the ETAG, the limit energy level, E_{kL} , is defined as three times the service energy level ($E_{kL} = 3E_{kS}$). Assessment methods concern again the verification that the barrier models arrest the block impacting with the limit energy level, E_{kL} . Finally, it is assumed that failure coincides with the barrier loss of capacity in arresting the impacting block.

In order to study the failure mechanisms of each barrier, starting from E_{kL} , the kinetic energy of the block has been increased in constant steps, till reaching the minimum amount of energy corresponding to which the barrier model is no longer able to arrest the block. This threshold energy level is identified with E_{kF} .

During each test, specific quantities are monitored: the vertical component of the displacement and velocity measured at the centre of the test block, as well as the vertical force F acting on the block:

$$F = m a \tag{4.1}$$

where m is the block mass and a is the vertical component of the block acceleration. In the following, it is assumed that F is positive if acting upward.

The deformation of the barrier during each test is documented by means of a selection of relevant frames.

4.2.4 RESULTS

In this Section, the numerical results of the testing campaign on the four barriers are discussed. According to the procedure described in Section 4.2.3, the obtained threshold levels E_{kS} , E_{kL} and E_{kF} , as well as the initial block velocities v_0 , are listed in Table 4.2 for each barrier. The interval of variation of the initial velocities for all the barriers in service, limit and failure conditions varies between 5.5 m/s and 17.2 m/s. These values are similar to the velocities observed in similar barriers, reported in (Buzzi et al. 2013).

Barrier name	Service Condition (S)		Limit Condition (L)		Failure Condition (F)	
	v_0 [m/s]	E_{kS} [kJ]	v_0 [m/s]	E_{kS} [kJ]	v_0 [m/s]	E_{kS} [kJ]
SF1	5.5	26	9.7	80	10.8	100
SF2	6.9	40	12.4	130	13.7	160
SF3	7.7	50	13.3	150	14.3	175
SF4	8.7	65	15.3	200	17.2	250

Table 4.2 Threshold energy values and initial block velocities for the barriers.

The energy value E_{kL} offers a reasonable estimate of the barrier's capacity, ranging between 80 kJ to 200 kJ for the four barrier models. The lowest value is associated to barrier SF1. The addition of the secondary net in barrier model SF2 leads to an increment of about 60% in E_{kL} , with respect to barrier SF1, while the contemporary addition of the secondary net and the hooks between the cables allows to obtain an increment of about 80% in terms of E_{kL} with respect to barrier SF1. The capacity is more than doubled when uphill cables are inserted in the barrier model.

The numerical results revealed that for the barriers analysed within this study, the ratio between E_{kF} and E_{kL} is always included in the interval 1.2-1.25.

In the following, the results of the analyses carried out in the service, limit and failure conditions are illustrated in detail.

Tests in service condition (S)

The results of the tests performed at service condition for the different barrier models are reported in Figs. 4.18 and 4.19. In particular, Fig. 4.18 depicts the configuration of all the barriers after test S1 when the test block has been removed. The elements which show plastic deformations are in a lighter colour. No failure occurred in any of the components of the barrier and only few elements (such as the cables interested by the impact and part of the posts) underwent permanent deformations, always within admissible values.

In Fig. 4.19, the vertical displacement and velocity of the block are displayed versus time as well as the dynamic force acting on the block, calculated according to Eq. (4.1), is shown against the vertical displacement of the block both for the S1 and S2 launches. The time history of the displacement is recorded until two seconds from the beginning of the test in order to observe two subsequent block rebounds, Fig. 4.19a. The block reaches the maximum displacement at the braking time then bounces back. The response of barrier models SF1, SF2 and SF4 is essentially elastic, with the greatest part of displacement recovered after the rebound. Barrier model SF3 dissipates part of the impact energy as shown in the second rebound of the test block with a second peak lower than the first.

Data on maximum displacements and braking times are inserted in Table 4.3. As it can be observed, maximum displacements lie within 0.89 m and 1.18 m, and braking times between 0.16 s and 0.33 s. According to the data, the greatest displacement is shown by barrier SF3, which also features the longest braking time, while barrier SF4 exhibits the smallest values for displacement and braking time.

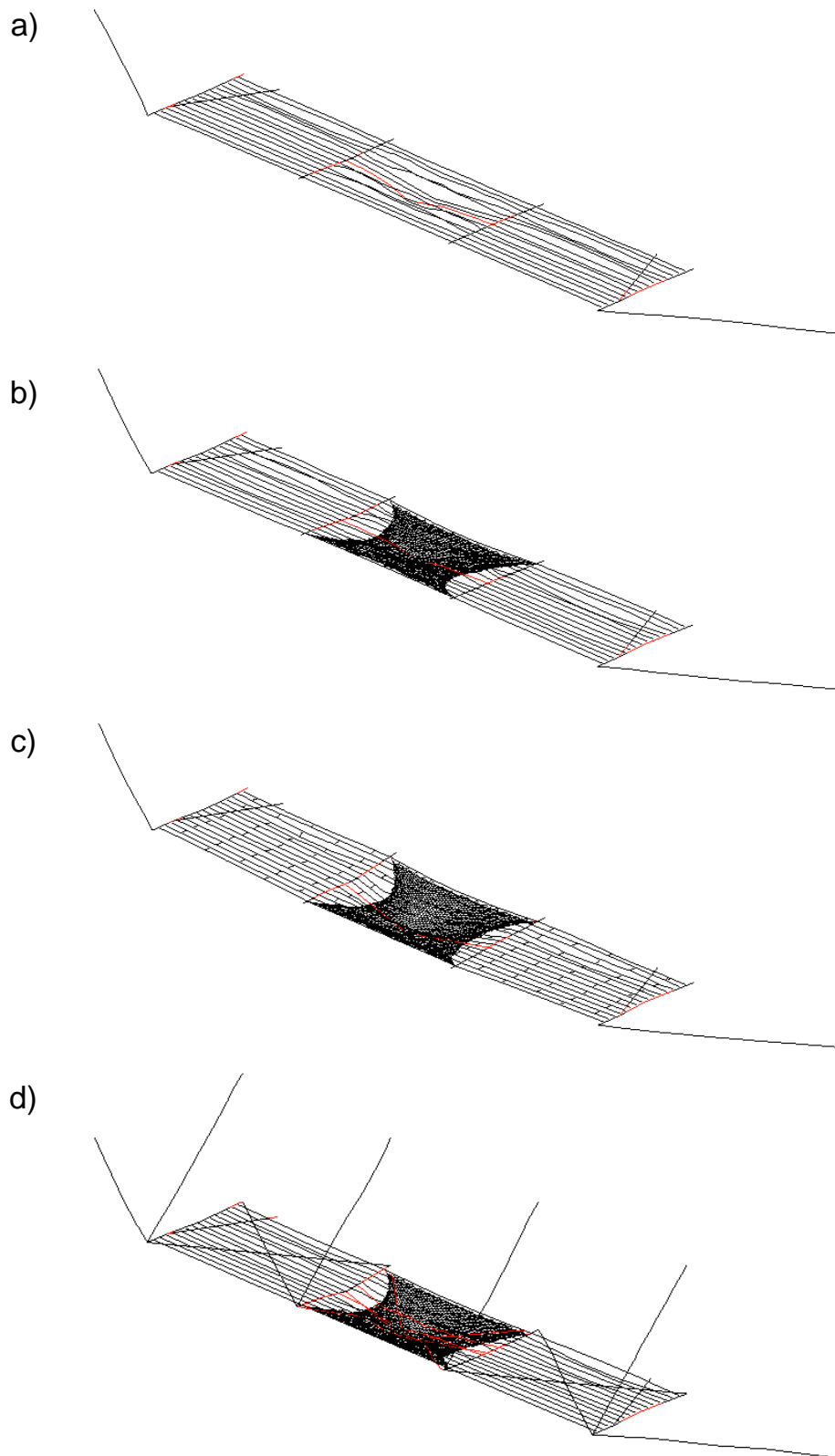


Figure 4.18 3D view of barrier models after the first launch (S1) carried out in service condition once the block has been removed: a) SF1; b) SF2; c) SF3 and d) SF4.

Block velocities with time for launch S1 are represented in Fig. 4.19c. The velocity initially increases until the full block to barrier contact has been achieved, then decreases up to a value of around -2.5 m/s and oscillates till to 2 m/s, as observed for all the barrier models.

In Fig. 4.19e, the force acting on the block is shown with the displacement for all the barriers. After some initial oscillations, barrier SF4 shows the steepest slope, thus indicating a highest rigidity for this barrier, while SF3, as seen before, is the most deformable displaying greater displacements for equal force values. After attaining the maximum displacement, the curves show a loop termination, i.e. decreasing displacements for constant values of the force, that indicates the block is being arrested.

At the end of the test, once the block has been removed, residual heights for the barriers are registered and collected in Table 4.3. It should be noted that the residual heights are always greater than 70% of the nominal height h_N .

After S1, the second launch S2 is performed impacting the already deformed barrier with a block with the same initial velocity. Data relevant to S2 are given in Figs. 4.19b, d and f. As expected, the block displacements are greater than those observed in the first launch, Fig. 4.19b, and velocity curves are similar to those in S1, Fig. 4.19d. Also for S2, the block has been stopped by the barriers, as it can be seen in Fig. 4.19f, where the force is shown versus displacement.

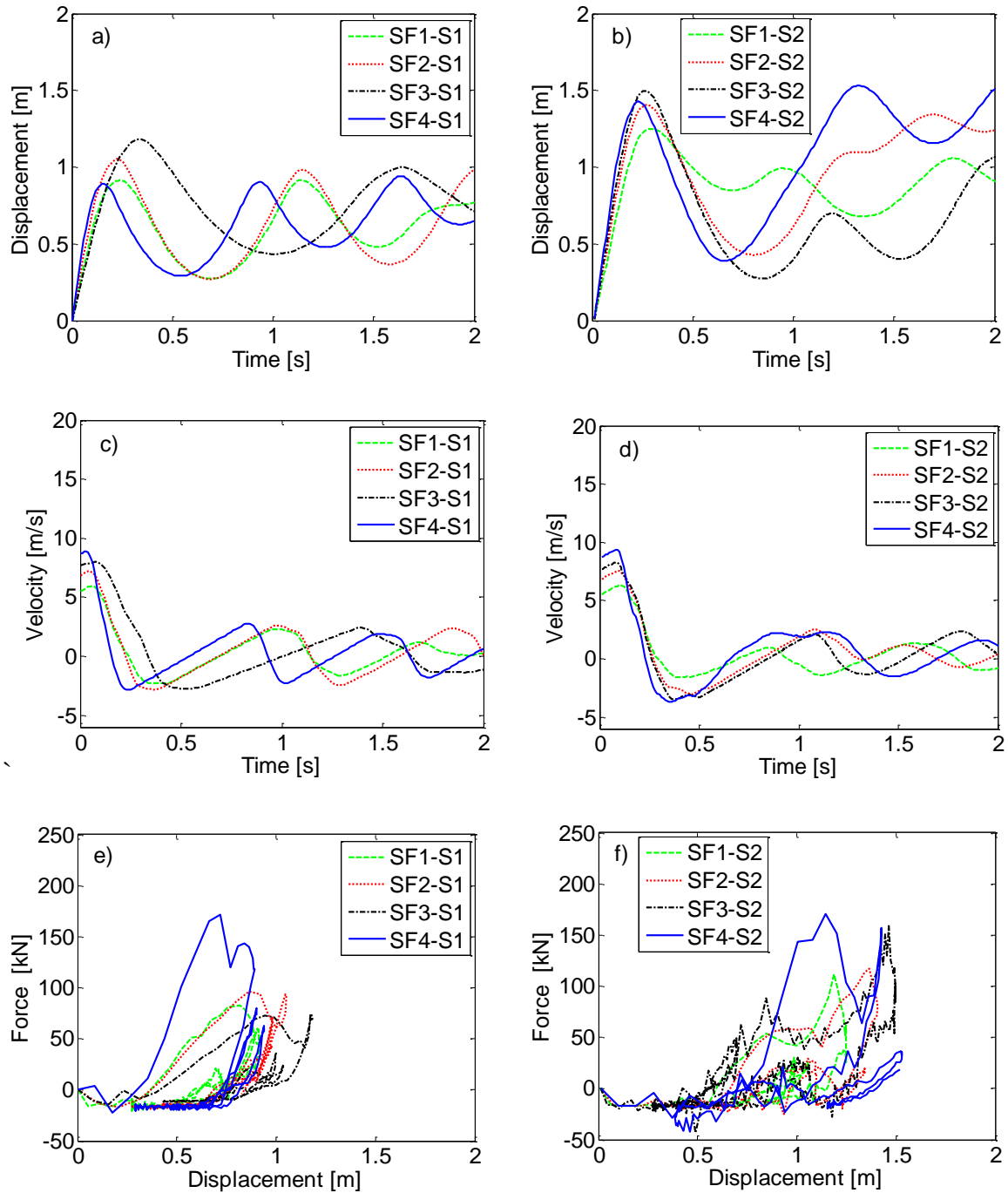


Figure 4.19 Results of the tests in service condition, first launch (S1) on the left and second launch (S2) on the right: a) and b) block displacement versus time; c) and d) block velocity versus time and e) and f) force acting on the block versus block displacement.

Relevant parameters (maximum displacement, braking time and residual height) registered in the second launch for all the barriers are inserted in Table 4.3.

Barrier name	Test Name	Energy level [kJ]	Maximum displacement (block) [m]	Braking time [s]	Residual height [m]
SF1	S1	26	0.91	0.24	2.76
	S2	26	1.25	0.29	2.70
	L	80	1.37	0.22	2.56
SF2	S1	40	1.05	0.22	2.68
	S2	40	1.40	0.27	2.60
	L	130	1.85	0.43	2.40
SF3	S1	50	1.18	0.33	2.65
	S2	50	1.50	0.26	2.47
	L	150	1.95	0.30	2.43
SF4	S1	65	0.89	0.16	2.73
	S2	65	1.43	0.23	2.48
	L	200	1.84	0.22	2.24

Table 4.3 Results of the tests in service (S1 and S2) and limit (L) conditions: maximum displacements, braking times, residual heights.

Tests in limit condition (L)

Results for the tests carried out in limit condition are collected in Figs. 4.20, 4.21a, 4.21c and 4.21e. In particular, in Fig. 4.20 the three-dimensional view at the braking time for all the barrier models is reported on the left as well as the corresponding lateral view on the right. It can be observed that the posts show a meaningful deflection towards the barrier centre interested by the impact, and show plastic deformations (lighter colour in the figure).

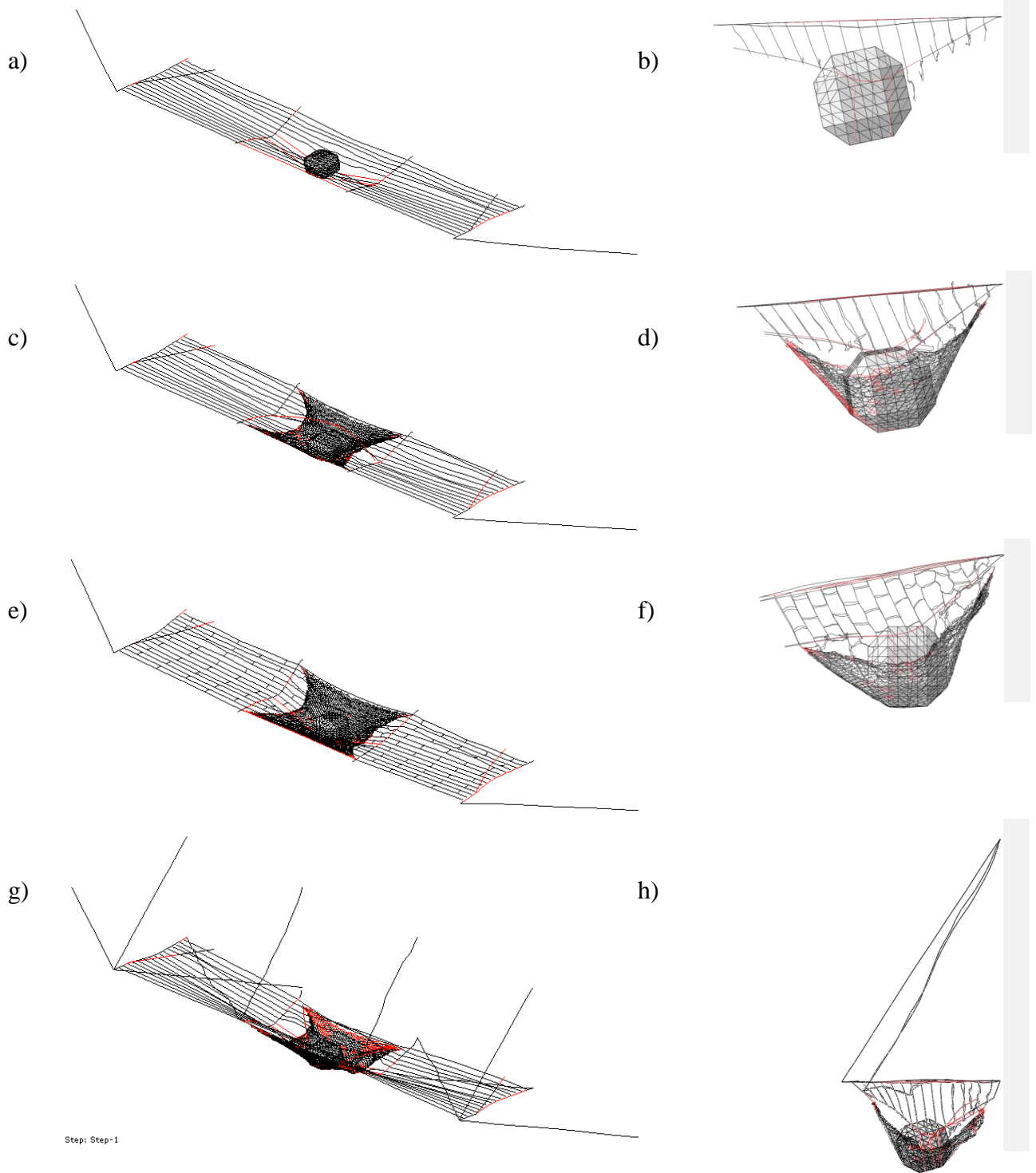


Figure 4.20 3D and lateral view of the barrier models at the braking time for the tests carried out in limit condition: a) and b) SF1; c) and d) SF2; e) and f) SF3; g) and h) SF4.

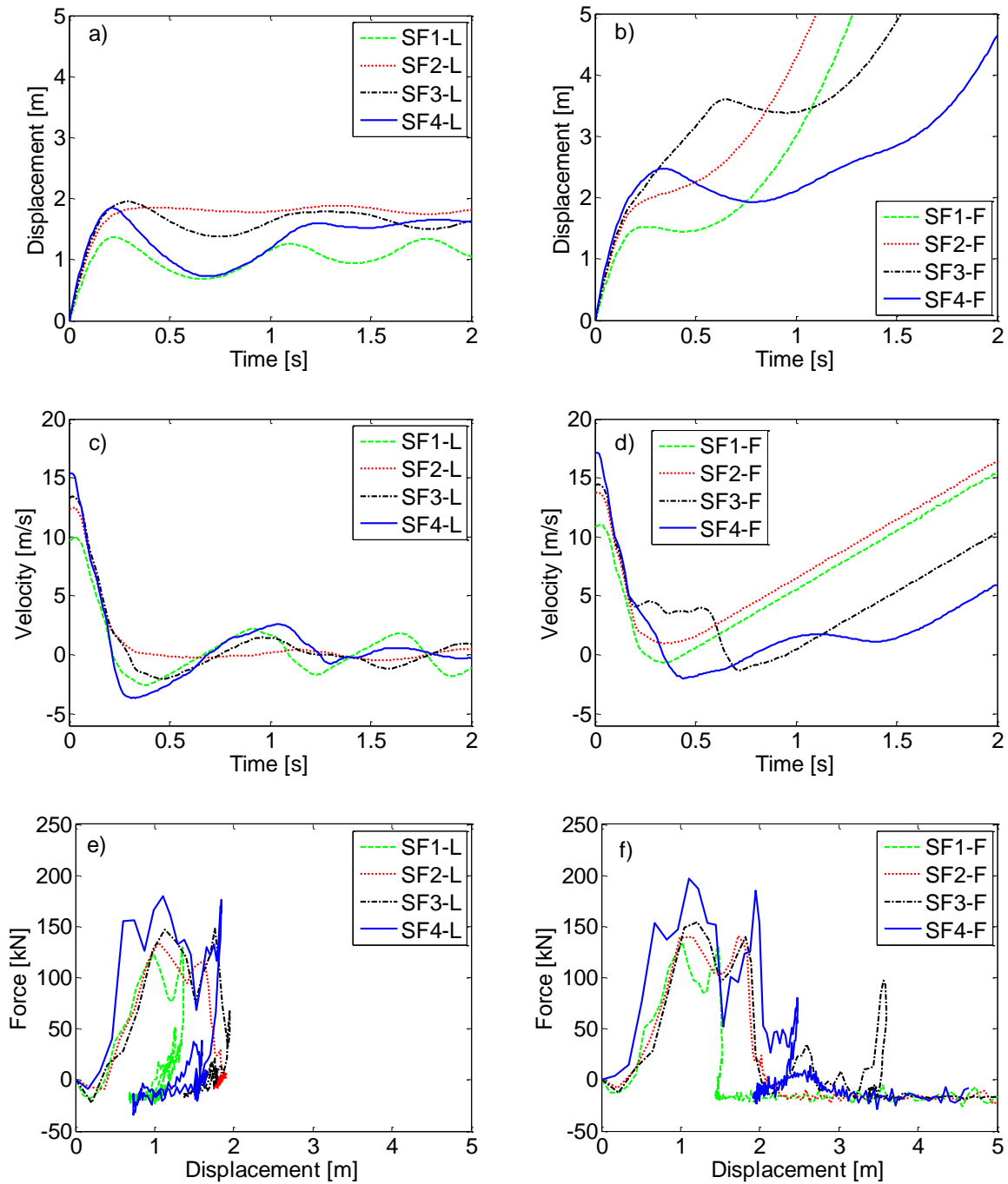


Figure 4.21 Results of the tests in limit (L) on the left and failure conditions (F) on the right: a) and b) block displacement versus time; c) and d) block velocity versus time; e) and f) force acting on the block versus block displacement.

Curves of the block displacement versus time (Fig. 4.21a) show that, after the barriers attain the maximum displacement, the rebound is not fully elastic as it was observed in the service tests. In particular, for SF2 once the block maximum displacement is reached, it remains almost constant throughout the test. This aspect is confirmed also

in the time histories of the velocity, Fig. 4.21c, where, after the initial drop, the block velocity for SF2 is around zero. The first part of the force-displacement curves, Fig. 4.21e, confirms the higher stiffness of barrier SF4. While the last part of curves reveal, with decreasing displacements and constant values of force, that the barriers are still able to arrest the test block.

Maximum displacements, braking times and residual heights for all the barriers in limit condition are reported in Table 4.3.

Tests in failure condition (F)

Failure tests are carried out onto each model in order to investigate the corresponding barrier's mode of failure, with reference to this specific testing condition. As indicated in Table 4.2, the minimum block's kinetic energy which produces failure is: 100 kJ, 160 kJ, 175 kJ and 250 kJ for barrier SF1, SF2, SF3 and SF4, respectively.

In Fig. 4.22, relevant frames describe the failure mode of barrier model SF1 where the elements which show plastic deformations are in lighter colour. As it can be noted, failure is due to an excessive deformation of the longitudinal ropes, Figs. 4.22a and b. In particular, Figs. 4.22c to f show that the block passes the interception structure just upon the three impacted cables, after about 0.3 s from the test beginning.

A different response is exhibited by barrier model SF2. In Fig. 4.23, six frames illustrate the barrier failure mode under an impact energy level of 160 kJ. In particular, the deformed shape of the barrier model prior to failure, at 0.25 s and 0.37 s from the test start is illustrated in Figs. 4.23a and c (with the corresponding lateral views in Figs. 4.23b and d), respectively. The deformed shape at failure is shown in Figs. 4.23e and f, which depict the barrier model at 0.55 s from the test beginning. After about 0.3 s, the block starts rolling on the net, eventually stepping over it, through the principal interception structure and the secondary net. Comparing results of barriers SF1 and SF2 highlights the role of the secondary net, which contributes to slow down the block, absorbing part of the block kinetic energy.

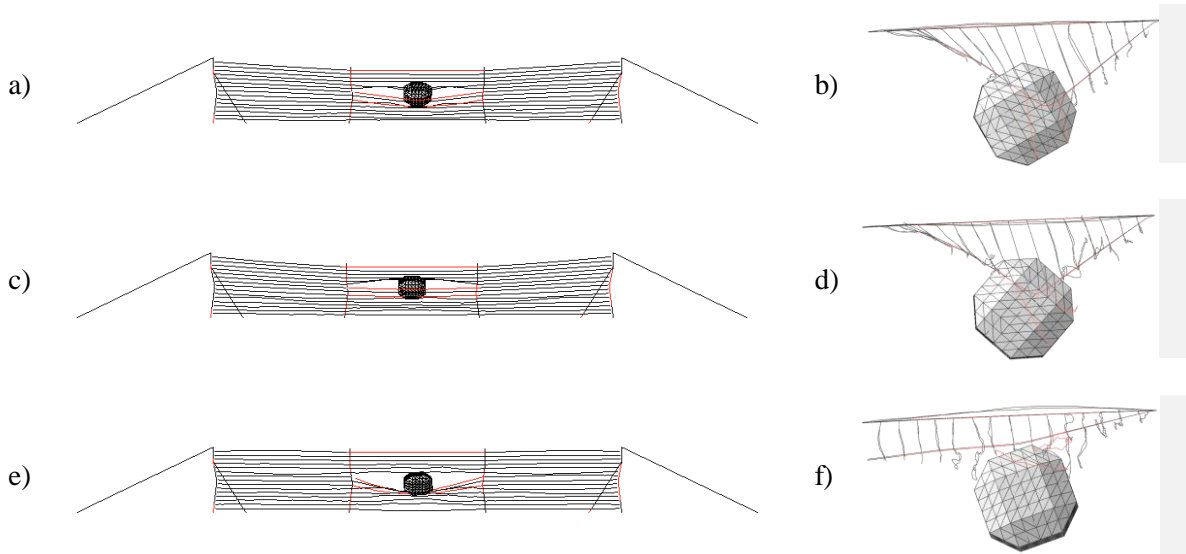


Figure 4.22 Selection of frames from failure test ($E_{kF} = 100$ kJ) on model SF1, bottom and lateral view at a) and b) 0.25 s; c) and d) 0.30 s; e) and f) 0.43 s.

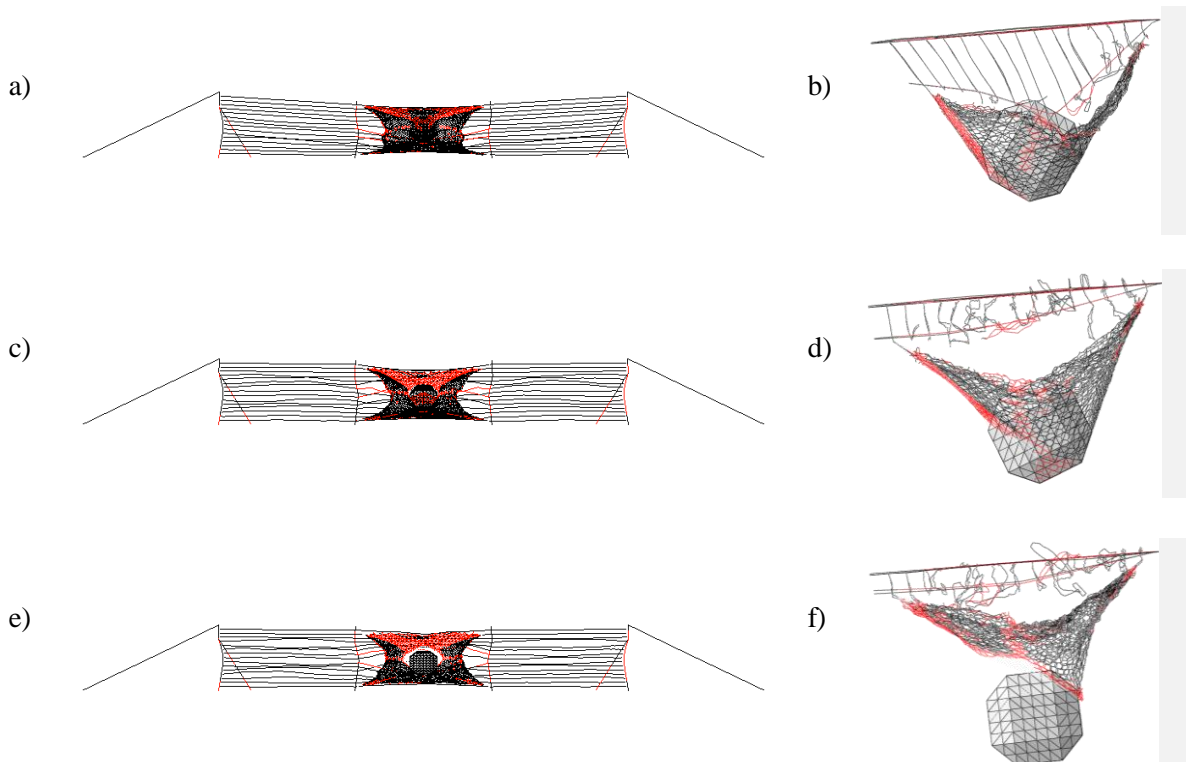


Figure 4.23 Selection of frames from failure test ($E_{kF} = 160$ kJ) on model SF2, bottom and lateral view at a) and b) 0.25 s; c) and d) 0.37 s; e) and f) 0.55 s.

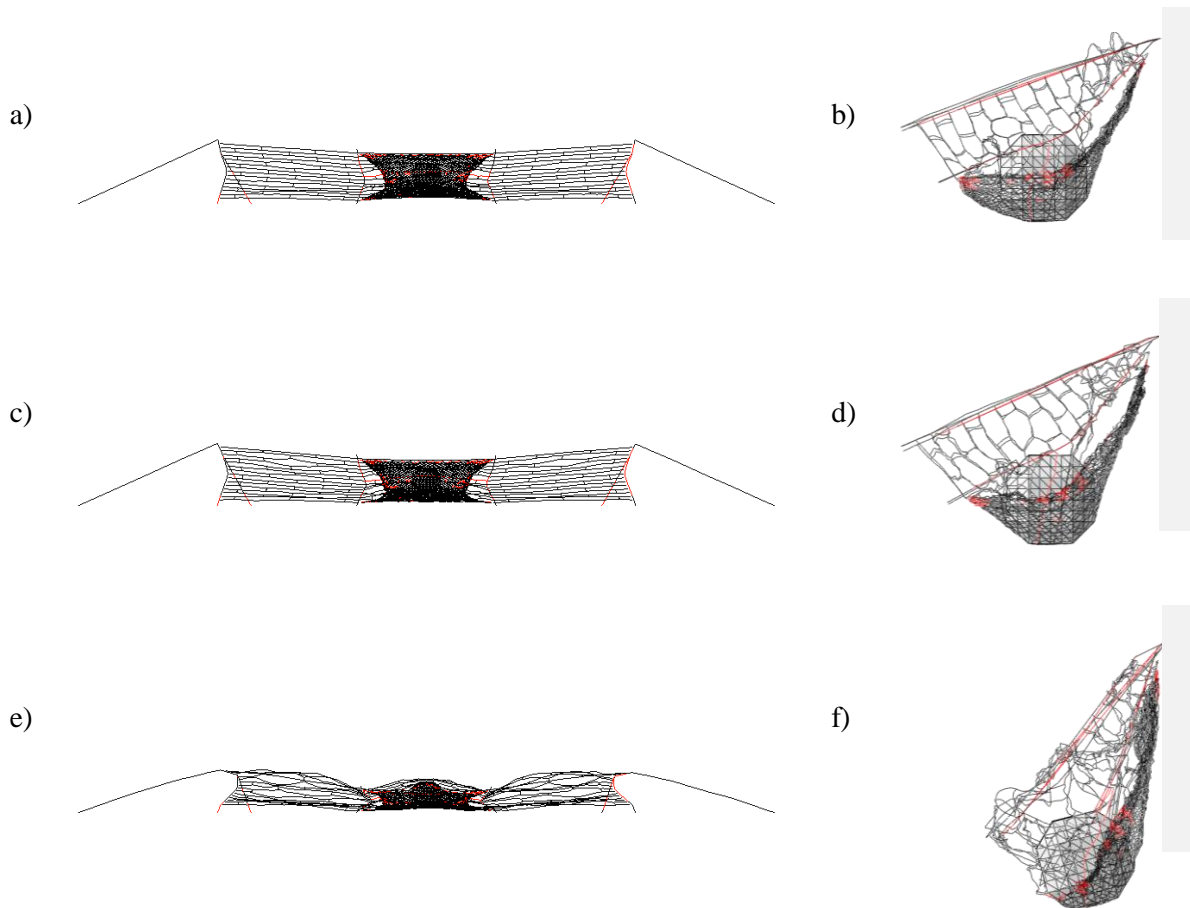


Figure 4.24 Selection of frames from failure test ($E_{kF} = 175$ kJ) on model SF3, bottom and lateral view at a) and b) 0.25 s; c) and d) 0.30 s; e) and f) 0.45 s.

For barrier model SF3, failure is achieved due to the formation of plastic hinges at the basis of the posts. The barrier response prior to failure, described with frames taken at 0.25 s and 0.3 s, are shown in Figs. 4.24a and c (with the corresponding lateral views in Figs. 4.24b and d), respectively. Again, model failure starts to occur after about 0.45 s from the test beginning as illustrated in Figs. 4.24e and f. In absence of further external constraints, the barrier posts work as cantilever beams. The formation of plastic hinges at the base makes the structure hypostatic, bringing it to collapse under an impact of intensity equal to 175 kJ.

Figure 4.25 illustrates the failure mode of barrier model SF4. In particular, pre-failure response is depicted in Figs. 4.25a and c (with the corresponding lateral views in Figs. 4.25b and d), where the deformed shapes of the model at, respectively, 0.4 s and 0.58 s of the failure test are illustrated. Failure is shown in Figs. 4.25e and f, where frames taken at 1.5 s of the test are shown. The formation of hinges at the posts is prevented

by the uphill cables and failure is reached due to the excessive deformation of the interception structure close to the barrier base under an impact of intensity equal to 250 kJ.

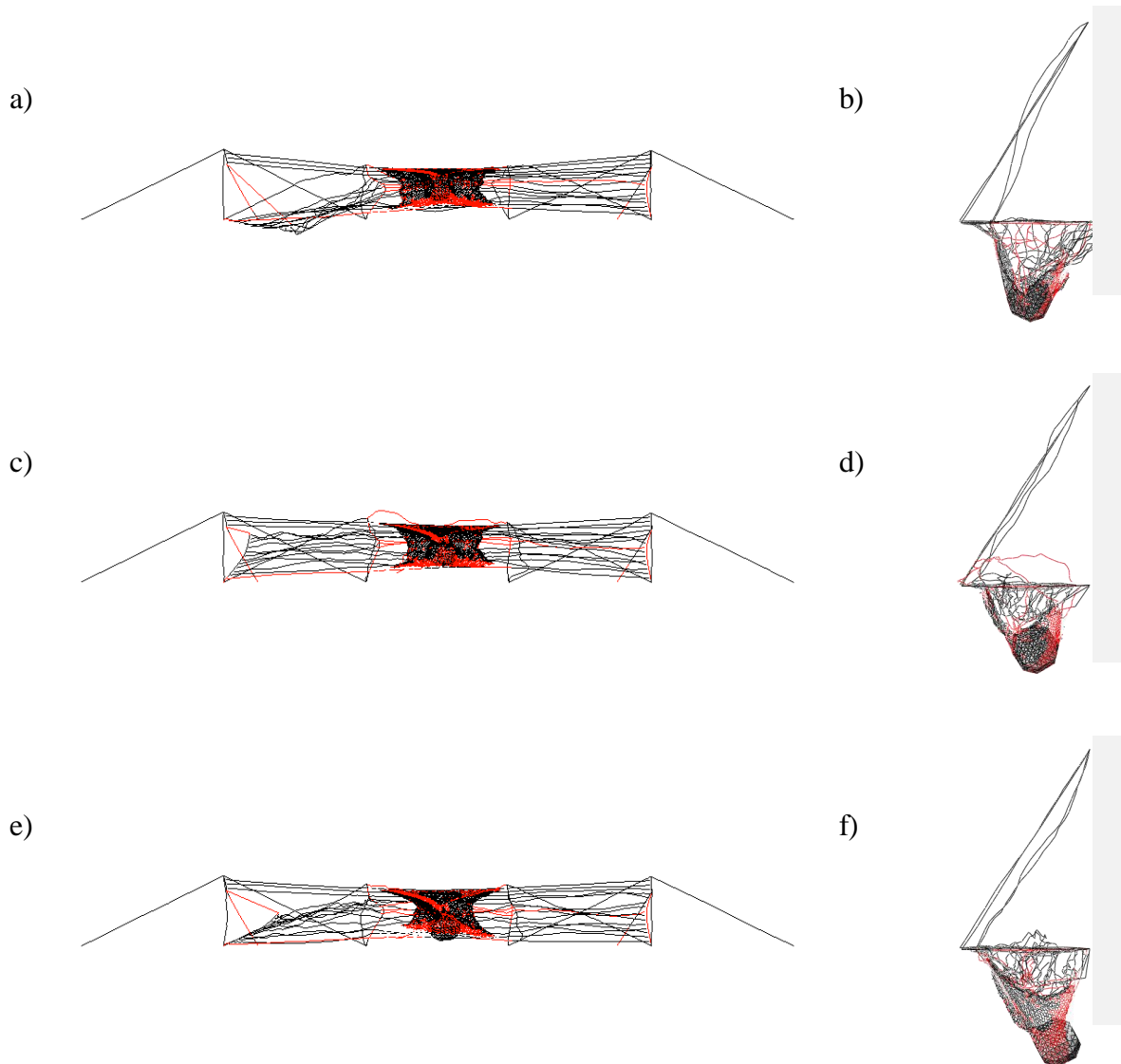


Figure 4.25 Selection of frames from failure test ($E_{kF} = 250$ kJ) on model SF4, bottom and lateral view at a) and b) 0.40 s; c) and d) 0.58 s; e) and f) 1.50 s.

In Table 4.4 details of the failure modes for all the barriers are provided. In Fig. 4.21, relevant parameters of the four barrier models during the failure tests are represented. Specifically, the time histories of the displacement and of the velocity of the test block are shown in Figs. 4.21b and d, respectively. As it can be observed, in failure tests performed onto barrier models SF1 and SF2 after the maximum displacement is attained, it continues to increase pointing out that the block goes beyond the barrier.

Barrier SF3 shows a similar behaviour even if a stationary point for the displacement is reached later. A test block rebound is evident in the test performed onto barrier SF4, due to the presence of the uphill cables, which prevent the downhill movements of the posts, allowing the interception structure to accompany the block throughout its travel. In Fig. 4.21d, the velocity curves show clearly the inability of the barrier to arrest the block. In fact, after attaining the minimum value, the block velocity increases linearly with time sharing the same slope for all the barriers. When the block passes the barrier, its motion is uniformly accelerated being governed only by the force of gravity and the velocity results linear.

Figure 4.21f depicts the evolution of the force acting on the block, Eq. (4.1), versus the vertical displacement of the test block. The response of SF1, SF2 and SF3 is essentially alike. In particular, SF1, SF2 and SF3 curves show the same slope in the first part, while SF4 curve is steeper. The difference in this behaviour is due to the presence of the uphill cables in SF4 that results in a better structural performance in arresting the falling rock. After initial fluctuations, due to the first contact between the block and the barrier, the force oscillates around a peak value, then in the last part of the diagrams, the curves display quasi-horizontal tails for increasing values of displacement. This part corresponds to the inability of the barrier to arrest the block.

Barrier name	Failure mode	Barrier component	Description
SF1	Local	Interception structure	Significant deformation of the longitudinal cables
SF2	Local	Interception structure	Failure within the central part of the secondary net
SF3	Global	Supporting structure and interception structure	Significant deformation of the interception structure and failure of the posts at the base
SF4	Local	Interception structure	Failure next to the cliff of the secondary net

Table 4.4 Failure modes for the barriers in the vertical drop testing conditions.

4.2.5 CONCLUDING REMARKS

In this paper, the structural performance of semi-rigid rockfall protection barriers has been investigated by means of finite element simulations. In particular, selected semi-rigid rockfall protection barriers, which can be commonly encountered along the Alps were considered. These barrier types are characterized by different connecting components such as secondary net, uphill cables, cross cables and clasps. The barriers have been virtually tested based on a numerical strategy recently developed by the authors. Due to the lack of guidelines and standards for barriers featuring a low capacity, the prescriptions provided by the European Guideline, ETAG 27, for high-capacity barriers were followed.

Considering that the accuracy of the results could be only assessed in presence of accurate experimental results on prototypes, data obtained from the numerical analyses allow to:

- i) investigate the structural performance of each barrier at service and limit conditions;
- ii) assign an energy capacity value to each barrier;
- iii) investigate the failure mechanisms of each barrier in vertical-drop testing condition.

Accurate definition of the energy capacity and the knowledge of the structural behaviour to rock impact can be used in rockfall hazard assessment tools and in the management of existing semi-rigid barriers, locally improving their performance by means of feasible modifications.

However, newly developed low-energy rockfall protection systems should follow standardized design procedures to avoid the presence on the territory of a multitude of low energy barrier subtypes. Then, adequately calibrated numerical models would reveal very useful to improve the design of these structures and towards the development of national design standards.

NUMERICAL ANALYSIS OF A LOW-ENERGY ROCKFALL BARRIER

Introduction

In the previous Chapters, the significance of gaining an appropriate understanding of the rigid and semi-rigid barriers response toward dynamic events was highlighted. Indeed, the current normative (EOTA 2008) does not provide any specific standard on the performance of these structures, even if they are largely used worldwide. On the contrary, high-energy systems have been increasingly studied over the last 50 years by researchers and manufacturers through full-scale tests and numerical analyses.

Recently Buzzi et al. (2013) at the University of Newcastle (NSW, Australia) have carried out a series of experiments on different prototypes of low-energy barriers to examine their behaviour under dynamic loading and to assess their limit energy absorbing capacity. The outcomes of this research were used to develop the numerical finite element model presented in this thesis. The model of one prototype of the tested barriers consists of a semi-rigid rockfall barrier built with a double-twisted hexagonal mesh as for interception structure. Constitutive models developed by Thoeni et al. (2013) were implemented to model the net's behaviour. Experimental data was used to calibrate the model and to assess its reliability. Then the numerical model was used to investigate the system performance under various impact conditions and particular attention was given to the so-called "bullet effect" analysis on this prototype. The model capacity was also exploited in order to investigate possible improvements in the system construction design.

In the following, a quick summary of data and models used to build the FE model of the barrier prototype is depicted. Additionally, an exhaustive description of the bullet effect phenomenon and of the preliminary studies conducted so far is provided. This preface is then concluded by illustrating the aims of the developed research.

Next to this introduction, a journal paper is attached as contribute of this part of the dissertation. In the paper, details about the model development and its effectiveness are provided. The model is also used to investigate the block size dependency of the barrier`s performance.

Background

Due to the nature of the geological environments in New South Wales (Australia), rockfall phenomena are often characterised by rolling of pre-detached debris and the associated hazard involve relatively low energy levels. The state Road and Traffic Authority (RTA) of NSW has therefore designed different types of low-energy rockfall barriers (i.e. energy capacity ≤ 35 kJ) trying to answer the needs of the area. The performances of some prototypes of these RTA-barrier-designs were experimentally investigated within an Australian Nationally Funded research project (Spadari et al. 2013b).

The tests were carried out at the laboratory of the Newcastle Institute for Energy and Resources (NIER) at The University of Newcastle (Buzzi et al. 2013). A pendulum system was specifically designed to reach the requested testing impact energies. The pendulum was made by a rigid arm kept in position by means of a set of five pre-tensioned chains in order to avoid the generation of transversal forces to the frame (Fig. 5.1): one chain was fixed to an overhead crane while the others to the ground floor.

In accordance with the ETAG 027 (EOTA 2008) testing procedure, a barrier with three functional modules was tested against the impact of a concrete block with polyhedral shape. During the test, the block was first lifted by the crane to the required height and then dropped to impact the central panel with a determined final horizontal velocity. An optical beam was positioned close to the barrier in order to activate a quick release system allowing the free release of the block before impacting the fence.

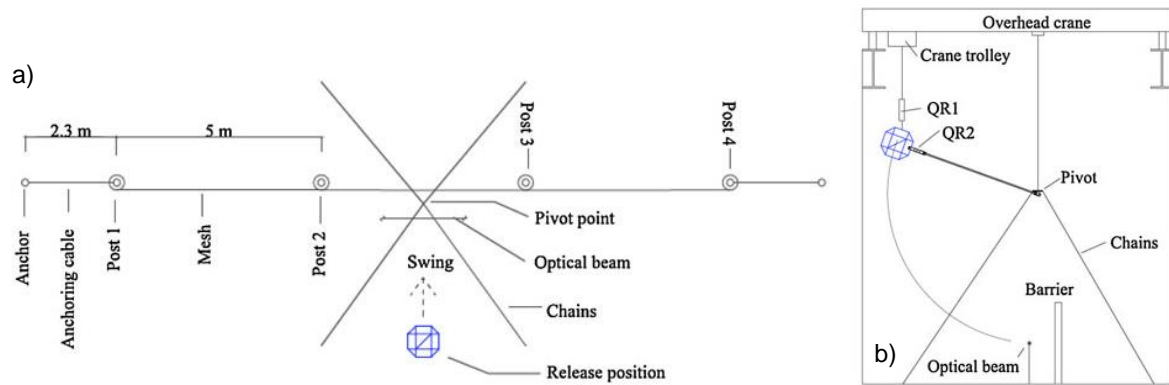


Figure 5.1 Physical model adopted for the full-scale test, the pendulum system a) sketch of the cross section and b) sketch of the plan view (after Buzzi et al. 2013).

Two high-speed cameras (500 f/sec) recorded the tests, and four load cells were installed on the longitudinal cables and at the post bases. All the tested barriers had 5m post spacing and were 2 m high. Several test configurations were considered (various positions of top, bottom and intermediate cables, and different types of mesh panels).

Experimental data showed that failure of the system always occurred at the interception structure. Therefore, in order to numerically reproduce the behaviour of the barrier, the response of the mesh upon impact must be accurately calibrated. For this purpose, a brief description of the study conducted by Bertrand et al. (2008) relevant to this type of mesh was reported in Chapter 2. More recently, Thoeni et al. (2013) further investigated the response of a double-twisted mesh with a complete set of experiments and DEM. The principal findings and results obtained by Thoeni et al (2013) are presented herein.

As for the mesh geometry, two different sections need to be considered in the mesh behaviour study: the single wire and the double twist. In order to identify their mechanical characteristics, uniaxial tensile tests were carried out on both the two section elements. The performance of a squared panel of mesh was also investigated by means of both static tensile in-plane tests and dynamic out-of-plane tests.

Above the comprehensive experimental characterisation, the authors introduced an innovative constitutive law for the mesh elements that was introduced in a DEM

numerical model. The two wire sections were modelled with an elasto-plastic stress-strain relationship.

Two parameters were introduced in the material model in order to obtain a good agreements with the experimental results. The first parameter (λ_u) considers the geometric irregularities with a shift of the force-displacement curve ($\Delta L = \lambda_u L_0$); while the second (λ_F) accounts for the mechanical irregularities of the elements by setting the first elastic yielding force ($\Delta F = \lambda_F F_1$). Fig. 5.2 shows the constitutive law obtained by applying the two parameters in terms of force-displacement. The proposed constitutive law was used to model the mesh behavior and several combinations of the parameters were considered in order to calibrate the best fitting between experimental and numerical results.

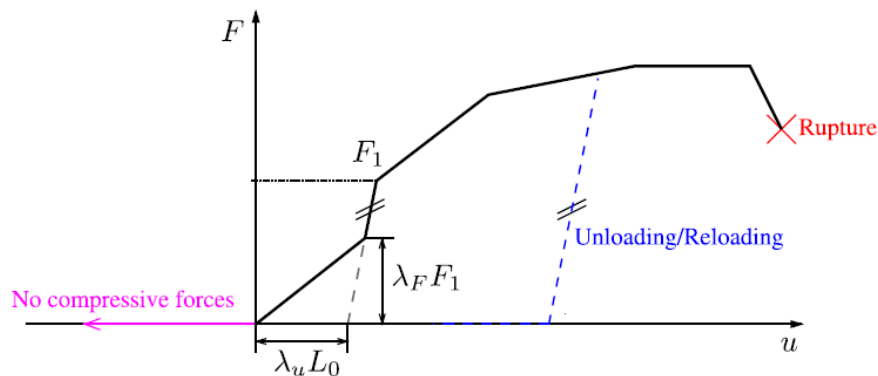


Figure 5.2 Influence of the parameters λ_u and λ_F on the material properties of the wire sections (Thoeni et al. 2013)

As previously stated, Thoeni et al. (2013) approach was used to develop the FE model of the mesh presented in this thesis. The two parameters (λ_u) and (λ_F) were opportunely re-calibrated following the same procedure followed by Thoeni et al. (2013). The best agreement by comparing results of tests and simulations, was achieved for $\lambda_u = 0.18$ and $\lambda_F = 0.8$. Further details about the model of the barrier are described in the paper reported in Section 5.1.

The bullet effect phenomenon

Historically, rockfall protection barriers are designed based on an energy criterion. The structure performance is defined as the capacity to absorb the impacting energy derived from a rock falling along a slope. The dissipation of energy is primarily achieved by elasto-plastic deformation of its components (i.e. the interception structure, the energy dissipation devices and some friction mechanisms). Therefore, even if many factors may influence the system behaviour, the criterion identifies the kinetic energy as the only parameter to be taken into account for the determination of the rockfall barrier performance. Hence, as shown in several scientific works, this value was assumed to be constant: a structure would perform equally by varying mass and speed of an impacting block, while keeping constrained the kinetic energy.

However, data obtained from real cases highlighted the mesh perforation due to the impact of rock fragments without any influence on the other components of the barrier. In fact, it was observed that, when a small block hits the barrier, only a limited area of the mesh is affected by the impact loading, and the transmission to the other elements results less effective. Thus, the dissipation of energy mostly takes place through plastic deformation of the impacted area (Volkwein et al. 2005) while the remaining elements does not contribute, leading to failure energy lower than the design value. This phenomenon was named “*bullet effect*” (Giani 1992; De Col and Cocco 1996). Even though the energy criterion to set a rockfall barrier performance has been widely assumed, its dependency to the whole spectrum of the impacting block size must be further investigated for a successful design. Up to now there is not a well-defined method to take into account for this effect.

It must be underlined that the effects taking place in a rockfall barrier can vary as function of the system construction design. The bullet effect is strictly related to the low-energy systems as their dissipation capacity is mainly affected by the plasticisation of the interception structure. The type of mesh is therefore an essential characteristic in order to evaluate the barrier response. It was also observed that semi-rigid barriers are the most prone to the bullet effect type perforation as the speed

required for a small block to punch through the net is realistic. By contrast, accordingly to the European Guideline, a flexible barrier tested at the maximum energy level requires a block of external size of one third of the nominal height impacting at 25 m/s. In this latter case, even if a loss of performance is considered for smaller blocks, the corresponding energy is given by a quite unlikely high speed at impact (> 100 m/s).

It is recognised that full-scale tests on a rockfall barrier represent the best way to investigate the block size influence at impact, however they involve significant costs and safety constrains related to the high values of impact velocity that need to be reached. Only a few numerical studies investigated the bullet effect on panels and full barriers (Cazzani et al. 2001; Spadari et al. 2012; Hambleton et al. 2013; Buzzi et al. 2014).

As mentioned in Chapter 2, Cantarelli et al. (2008) formulated a simplified analytical solution able to estimate the maximum elongation reached from a barrier represented with an elastic coefficient k calibrated through test results. The authors assumed the maximum elongation reached during the test at maximum energy level as the critical state. In order to take into account the block dimension, the coefficient k was opportunely modified. Thus, the analytical model predicted that the impact of smaller blocks having the same speed would produce a larger elongation. It may led to cause some damage on the structure or to dangerous situation in the area of interest since an intervention is planned accordingly to the maximum displacement reached from the tested prototype. The simple analytical model developed evidenced the shortcomings of an approach based only on the kinetic energy criterion as design method, suggesting that block characteristics (i.e. shape, size and mass) must also be taken into account.

Cazzani et al. (2002) first proposed to numerically study the phenomenon by using a FE model. In their study, the model of a block impacting on a rockfall barrier was run using various sizes of block diameter up to the failure of the system with the block passing through the mesh. The results, plotted in terms of kinetic energy versus block

diameter (Fig. 5.3) showed that the bullet effect can clearly be caught and it implies a significant reduction of energy capacity: up to 90% of reduction for a 77% decrease in the block dimensions.

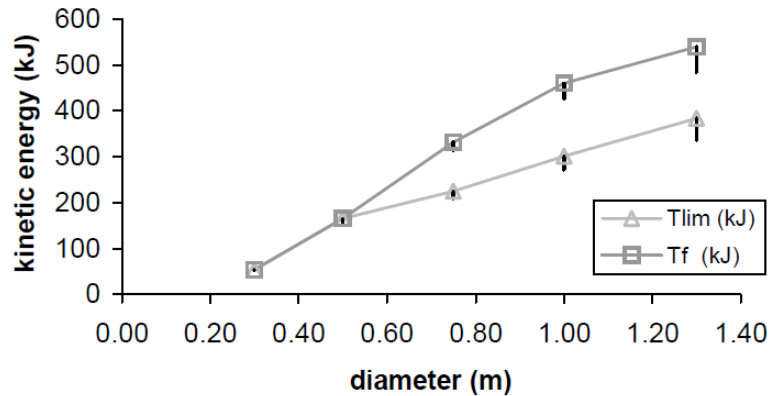


Figure 5.3 Dependency of the critical kinetic energy on the block size (Cazzani et al. 2002).

Spadari et al. (2012) proposed to study the response of the rockfall barrier upon impact of block of various sizes with a scaling approach: three independent dimensionless parameters were introduced to simplify the formulation of the physical problem under study. Among the many variables that can affect the phenomenon, four were recognised to play a major role: the dimension of the block, the strength of the steel wire, the mesh geometry and the stiffness of the system. All these variables are influenced by different factors (e.g. block size and density, opening dimension and wire diameter of the mesh, panel dimensions, etc.). The stiffness of the barrier was one of the parameters most difficult to quantify

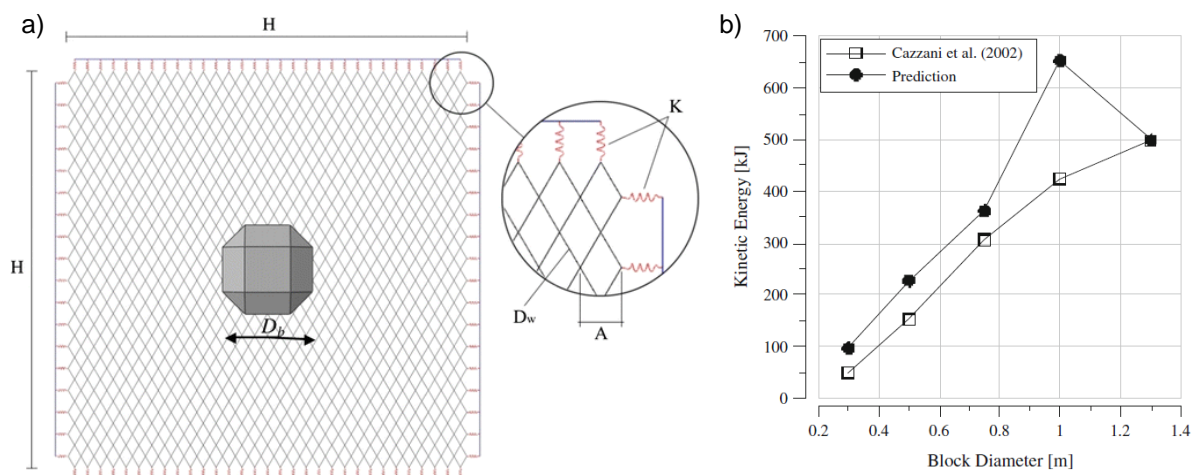


Figure 5.4 Numerical model of the chain-link mesh panel with a detail of the external springs and of the relevant dimensions (Spadari et al. 2012).

The model was validated with a simplified FE model of chain-link mesh type panel net for which the full barrier was approximated to a single mesh with a series of springs at the external nodes (Fig. 5.4a). Thus, the stiffness of the overall system (K) was introduced as the constant linear stiffness of the springs, while all of the other factors were obviously considered into the dimensionless model.

The bullet effect phenomenon was then investigated with the developed analytical model. For this purpose, details of the barrier mode of Cazzani et al (2002) were implemented in the proposed formulation in order to assess its predictive capacity. Except for one point (Fig. 5.4b) it was found a quite good agreement between the two models, especially in terms of general trend of the curve, with an almost constant overestimation of the critical energy.

Based on the assumption of Spadari et al. (2012), a different analytical model was proposed by Hambleton et al. (2013) for which the kinetic energy (E_c) is adopted as the limit criterion. The model is based on three main hypotheses. Firstly no plasticity of the mesh wire is taken into account. Thus, the total energy absorbed by the system is given by the sum of the energy contributions of the springs (E_k) and the mesh wire (E_w). A simplified FE model, allowed observing that, under the block impact at the centre of the panel, only the elements of the mesh in the two principal diagonals were stressed (Fig. 5.5 a). Hence, the considered mesh was reduced to two strips (Fig. 5.5 b) having length almost equal to the block size ($L_e \approx D_b$).

The behaviour of each strip was assumed to be independent, and finally, the model was approximated to a two-dimensional scheme (Fig. 5.5c). Consequently, through simple mechanical and mathematical calculations, the system was solved as:

$$\bar{E} = \bar{E}_w + 2\bar{E}_k = \frac{1}{2} \left(\frac{1}{\bar{K}_w} + \frac{2}{\bar{K}} \right) \bar{F}^2 \quad (5.1)$$

where \bar{K}_w and \bar{K} are the stiffness per unit length of the wire and the spring, respectively. The equation predicted the energy absorbed per unit length (\bar{E}) for a given force value (\bar{F}) in the wire. Hence, by introducing the yielding force (F_y), the critical kinetic energy could be achieved (E_c) and consequently the critical velocity (v_c) for a given block (size, mass and density).

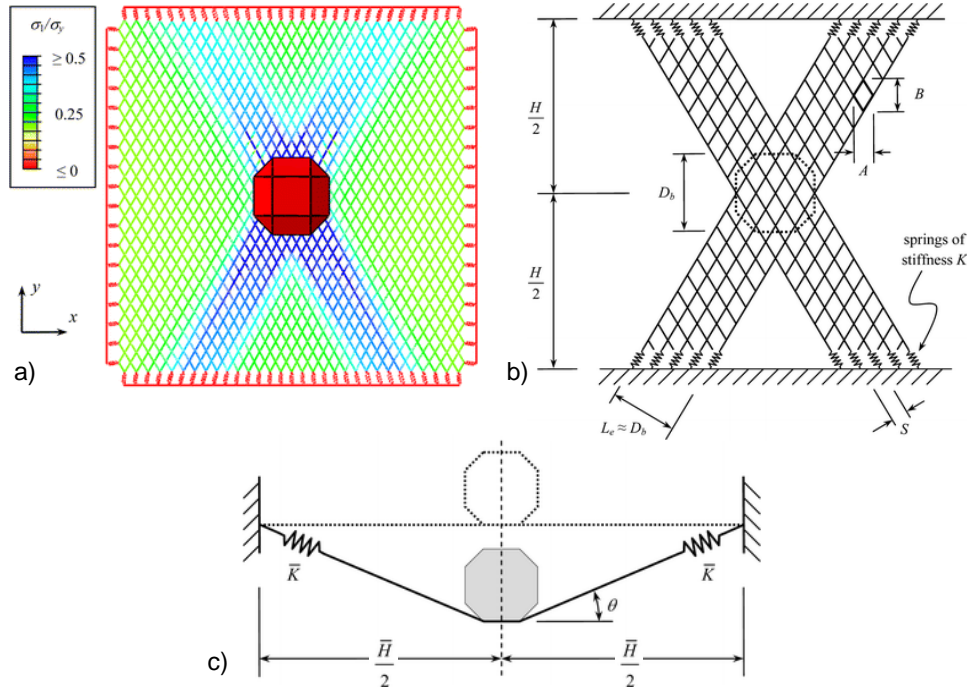


Figure 5.5 a) Distribution of stresses on the FE mesh model; b) scheme of the first approximation made; c) scheme of the final two-dimensional simplified model considered by Hambleton et al. (2013).

The behaviour of each strip was assumed to be independent, and finally, the model was approximated to a two-dimensional scheme (Fig. 5.5c). Consequently, through simple mechanical and mathematical calculations, the system was solved as:

$$\bar{E} = \bar{E}_w + 2\bar{E}_k = \frac{1}{2} \left(\frac{1}{\bar{K}_w} + \frac{2}{\bar{K}} \right) \bar{F}^2 \quad (5.1)$$

where \bar{K}_w and \bar{K} are the stiffness per unit length of the wire and the spring, respectively. The equation predicted the energy absorbed per unit length (\bar{E}) for a given force value (\bar{F}) in the wire. Hence, by introducing the yielding force (F_y), the critical kinetic energy could be achieved (E_c) and consequently the critical velocity (v_c) for a given block (size, mass and density).

At a later stage, also the bending resistance of the wire was implemented in the equation and a final formulation of the two main parameters was obtained.

A proportional dependence was predicted between the block size and the kinetic energy, while the critical velocity was inversely proportional.

In order to assess the reliability of the formulation, with particular focus on the bullet effect predictability, again, data of Cazzani et al. (2002) were used as comparison. Even though results showed a good agreement, as noted by the authors, a validation of the model by means of physical tests should be required.

More recently, Buzzi et al. (2014) carried out a series of impact tests on a chain-link mesh panel. For the first time in the scientific literature the bullet effect was analysed with a base of experimental tests. The tested geometry corresponded to the analytical model previously studied by Hambleton et al. (2013) in order to appropriately compare experimental and analytical findings. The equation was partially validated, even if it resulted a conservative tool to reproduce the bullet effect. In fact, it did not take into account for the dynamic loading mechanisms activated during the impact and a three-dimensional more realistic numerical model would be useful to further investigate the response of the whole barrier.

The experimental program was performed on a chain-link mesh but it provides a unique set of data of dynamic loading conditions on a mesh: for this reason, the study was considered in this research and used to investigate the behaviour of the double-twisted mesh. Two principal aspects of this study have been taken into account in my research:

1. The total energy at failure is more suitable than the kinetic energy at impact to capture the bullet effect phenomenon. Thus, the extra potential energy due to the maximum deformation reached by the mesh at failure ($m \cdot g \cdot D_{max}$) must be added to the initial kinetic energy (Fig. 5.6a).
2. Several domains exist in the “total energy-block dimension” plane (Fig. 5.6b). A conceptual model to recap the mesh response was proposed. The bullet effect was observed for a block with external length ranging from 50 to 80 cm. When it drops to small dimension the trend lean towards an almost constant value. This occurs for a block smaller than the aperture, impacting centrally on a node (see Buzzi et al., 2011 IACMAG). Regardless of the block size, only four wires are loaded and the energy required to break these wires remains constant. Hence, a

hypothetical horizontal trend was drawn. However, experimental data would be required to validate this domain. This is extremely challenging as small blocks required very high dropping height and deviation from the vertical (e.g. due to wind) is highly possible. The upper bound corresponds to blocks so large that the mesh cannot sustain their weight under static loading (nil kinetic energy).

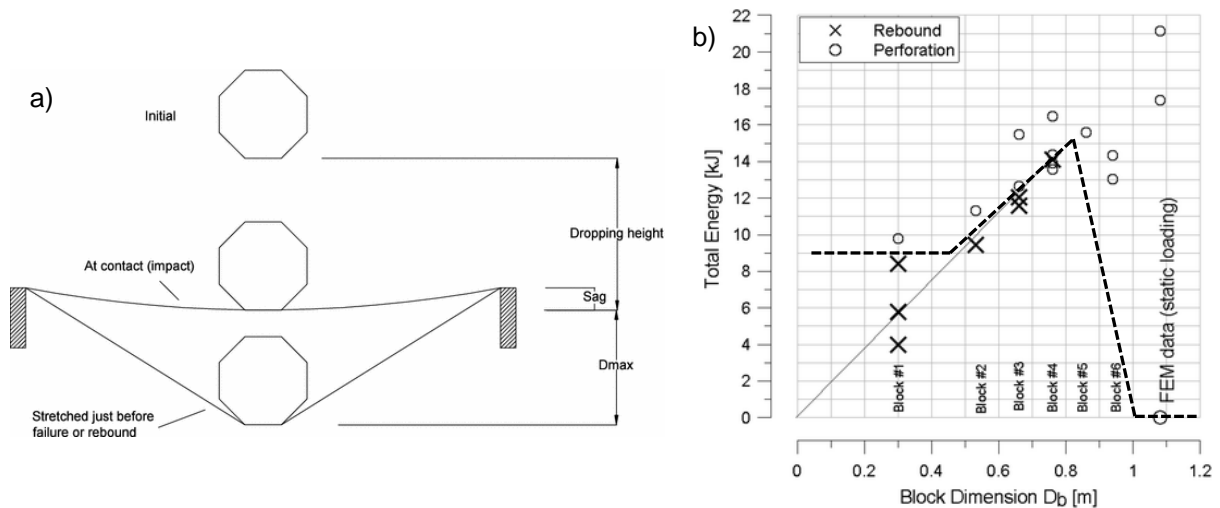


Figure 5.6 a) Sketch of the impact configurations during testing. b) Test results in terms of total energy with block size; the dotted line represents the conceptual model proposed by Buzzi et al. 2014.

The influence of the block size on the performance of a rockfall barrier was pointed out by the aforementioned works following different approaches. Particular attention was given to the energy criterion effectiveness, suggesting that other parameters can influence the overall system response and therefore, they should be taken into account. Additionally, consequences of the bullet effect cannot be underestimated, especially for low-energy barriers, where the mesh represents the main component involved in the dissipation process of the phenomenon. Due to costs and safety constraints, full-scale tests were not conducted so far to investigate this aspect, and analytical solutions and numerical simulations of simplified models only have been used.

Therefore, an exhaustive numerical research on a full barrier response upon impact, validated on experimental data, has not been provided to date.

Aims of the research

Considering the set of available data and the issues related to low-energy rockfall barrier performance dependency on the block size, the following aspects have been investigated in the paper reported in the following:

- Development of a full barrier FE model, with the calibration of the single structural components behaviour. Validation of the model effectiveness through full scale experimental results under different testing conditions (i.e. tests up to failure or not of the structure and second launch on the deformed system).
- Investigation of the barrier numerical behaviour upon impact of blocks of various dimensions. The overall performance of the barrier is studied and the bullet effect phenomenon for a double-twisted mesh type is investigated.
- Use of the model as design tool to analyse the performance of different barrier configurations: introduction of intermediate cables within the interception structure.

JOURNAL PAPER 3

5.1 NUMERICAL MODELLING OF A LOW-ENERGY ROCKFALL BARRIER PERFORMANCE: NEW INSIGHT INTO THE BULLET EFFECT

Abstract

This paper investigates the dynamic response of low energy, semi-rigid rockfall barriers. The study is based on a FE model that reproduces the geometry, components and connections of the existing systems that were previously tested at The University of Newcastle. The mechanical behaviour of the relevant barrier components was calibrated from simple mechanical tests and the response of the assembled system, i.e. 2 m high, 15 m long rockfall barrier, was validated against of full-scale tests results. Following a satisfactory validation of the model, further dynamic non-linear analyses were conducted to investigate the dependence of the full system performance to the size of impacting blocks. Interestingly, the total failure energy was found to evolve non-monotonically with block size because of dynamic effects that seem to prevail for impact speeds in excess of 20 m/s. The study also highlights the complex effects of adding intermediate longitudinal cables to the system. An improvement of the barrier performance is observed for the large blocks but the bullet effect is exacerbated for small blocks.

5.1.1 INTRODUCTION

In the last decade, most developments in terms of rockfall barriers have seen higher and higher levels of energy being catered for (Grassl et al. 2003; Peila et al. 2006; Gottardi and Govoni 2010; Volkwein et al. 2011). However, not all rockfall events have magnitudes of thousands of kilojoules. For instance, in New South Wales (located in Eastern Australia) only low to medium values of energies are typically involved (Spadari et al. 2013a).

Along with the development of rockfall protective systems, advances have been made in Europe in terms of standards for rockfall testing and the ETAG 027 recommendations (EOTA 2008) are now a milestone for rockfall barrier testing. Consistently with the current trend, ETAG 027 is geared towards medium to high-energy systems; barriers with maximum energy levels of less than 100 kJ are not explicitly considered. This is, however, the range in which a large part of the existing rockfall barriers still fall and, more specifically, for example in New South Wales the most frequently newly installed rockfall barrier has a nominal capacity of 35 kJ.

There is some information in the literature about testing of barriers of low to medium capacities, sometimes not only about performance but also maintenance (Kane and Duffy 1993; Hearn et al. 1995; Muraishi et al. 2005; Bigot et al. 2010; Van Tran et al. 2013; Bourrier et al. 2014), but a formal framework for relevant testing is still missing and one can wonder whether simply extending the ETAG 027 testing recommendations can be adequate.

Furthermore, it has been recently shown that the performance of rockfall meshes is block size dependent (Spadari et al. 2012; Hambleton et al. 2013; Buzzi et al. 2014) and this effect is likely to be predominant for low energy systems. Testing a low energy barrier at a recommended speed of 25 m/s (equivalent dropping height of 32 m) is not only experimentally challenging, since low energy systems are typically of limited height, but also it implies using a small block, which might not be the most representative or critical.

Another relevant aspect of the problem is that, unlike high-energy systems that tend to be highly deformable to enhance the capability of energy absorption, low to medium energy structures are often semi-rigid (Descoedres et al. 1997; Peila et al. 2006; Volkwein et al. 2011; Van Tran et al. 2013; de Miranda et al. 2015). For the 35kJ barriers used in New South Wales, like many other examples worldwide, such “semi-rigidity” partly originates from the use of intermediate horizontal cables placed across the mesh (see Buzzi et al. 2013). While large blocks are likely to impact the cables, small blocks could well impact a portion of mesh without cables, resulting in a completely different energy dissipation mechanism and barrier response.

This paper investigates the dynamic response of low energy barriers used in New South Wales to the impact of blocks of variable size. The study employs a dynamic and non-linear finite element model using a commercial FE code and following modelling strategies developed by the authors (Govoni et al. 2011; Gentilini et al. 2012a; Gentilini et al. 2013) and others (Peila et al. 1998; Cantarelli et al. 2008; Volkwein et al. 2009; Dhakal et al. 2011; Bertrand et al. 2012; Escallon et al. 2014). In order to build confidence on the numerical results, the mechanical behaviour of the different barrier components was first calibrated from specifically designed experimental tests and only after rigorous validation of the full barrier model, the numerical study was finally carried out. Such validation was based on experimental tests on full-scale barriers conducted at The University of Newcastle (Buzzi et al. 2013) and involved comparison of forces transmitted to the structure, elongation of the barrier, breaking time and block trajectory. The paper eventually aims at bringing new critical information about the behaviour of the low energy rockfall barriers and the combined effect of longitudinal cables and block size.

5.1.2 DETAILS OF THE EXPERIMENTS ON THE BARRIERS

A series of experimental tests on several types of rockfall barriers were conducted at The University of Newcastle, part of which has been published in Buzzi et al. (2013).

Some of these tests were selected to assess the performance of a FE model in reproducing the dynamic response of the rockfall barrier upon impact.

Barrier models selected for the study

Because symmetry applies, half the prototype considered in this research is depicted in Fig. 5.7. Insets in Figure 5.7 provide extra information about elements of the system. The barrier is 2 m high and consists of an interception structure (3 panels of 5 m mesh, resulting in a 15 m length mesh), structural steel posts and various connecting components. The mesh is made of woven and twisted steel wires forming hexagonal cells, typically referred to as a ‘double twist mesh’. Of significance when it comes to modelling are the two different wire sections that make up a cell: the single wire (SW) and the twisted double wire (DT) (see Fig. 5.7a). Steel posts (outer diameter of 133 mm) with base plates anchored to the floor form the supporting structure (Fig. 5.7b), which is connected to the mesh via two (top and bottom) longitudinal cables (diameter of 16 mm). These cables can slide relative to the mid posts but are fixed at the end posts (see Figs. 5.7d and e).

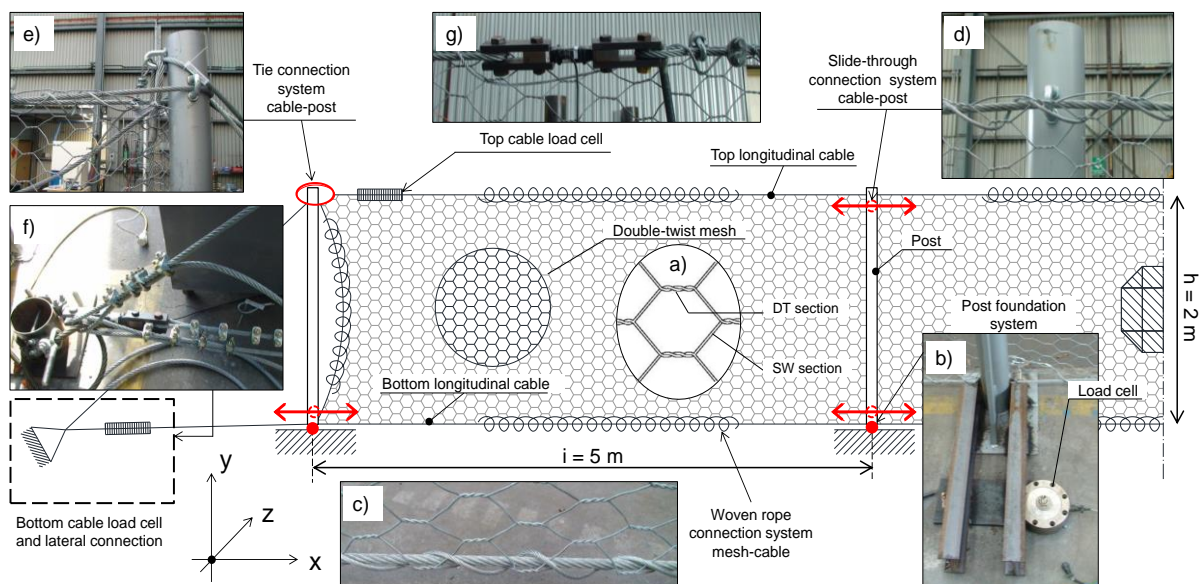


Figure 5.7 Sketch of the low energy barrier prototype tested during full-scale experiments and used in this study.

Finally, the mesh is lashed to the top and bottom cables using a 7 mm steel wire rope (Fig. 5.7c). Such an arrangement is also used at the end posts where the mesh is connected to a vertical cable, itself connected to the post. All the cables used in the barrier are wire stranded rope (consisted of seven primary strands of wire, containing further seven secondary strands). Note that, although the double twist mesh is a proprietary product by Maccaferri, the barrier prototype of Fig. 5.7 is not. Indeed, it was devised and assembled by the researchers of The University of Newcastle during their testing program.

Testing set up

Full-scale tests were carried out with the barriers installed vertically (i.e. as they are in service), bolted to the laboratory floor and subjected to the horizontal impact of test blocks of known mass and speed (Fig. 5.8). The test blocks were released from a swinging rigid arm (pendulum), lifted by an overhead crane. The combination of 5 meters of fall and a block mass of 665 kg yielded an impact energy in the order of 32 kJ. Note that only one block mass was used for these tests.

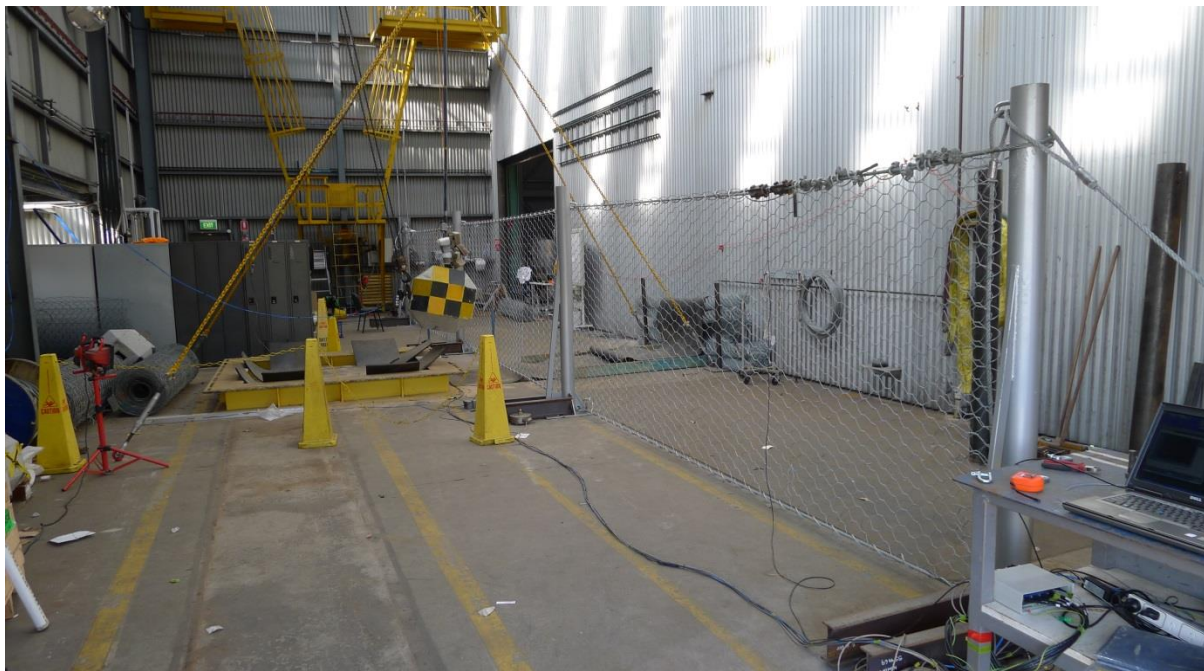


Figure 5.8 Side view of the experimental facility for the testing of low energy rockfall barriers at the University of Newcastle.

Two pneumatically-operated “quick releases” were employed: one to release the pendulum with block attached from the highest position and one to release the block from the arm on a horizontal trajectory, just before impact. The second release was automatically triggered following detection of the block by an optical beam. High-speed cameras were used to record the test, identify the exact moment of impact and track the barrier deformation and block motion. In addition, a number of load cells were inserted at different locations (in top and bottom cables, at the base of the posts) in order to record the loads generated in the structure by the impact. Reliability of measurements was ensured by a high frequency data acquisition system (2,048 samples per second). The reader is invited to refer to Buzzi et al. (2013) for more information on the testing set up.

Tests performed on the barrier

Due to space and time constraints, only three barriers of the sort presented in Section 5.1.2 were tested and the block was launched four times (i.e. there was one repeated impact). Note that there was a slight change in wire diameter used after the first test (as indicated in Table 5.1). All relevant details and test outcomes are given in Table 5.1. In particular, tests T1 and T3 were single impact tests at 31.1 kJ and 25.8 kJ, respectively. Test T2 consisted of two impacts on the same barrier: T2-1 at 16.1 kJ and T2-2 at 19.8 kJ. The second launch (i.e. T2-2) was performed without changing any element of the barrier that had sustained the first impact (T2-1).

Time-history results of the full-scale tests are reported for each test in Figs. 5.14 to 17 in terms of displacement and speed of the block along the z-axis, load recorded at cable in the x-axis and at post in the y-axis, accordingly to the reference system of Fig. 5.7.

Test	Diameter of SW [mm]	Block speed at impact [m/s]	Kinetic energy at impact [kJ]	Max. displacement [m]	Outcome of the test
T1	3	9.7	31.1	1.64	Failure
T2-1	2.7	6.9	16.1	1.46	No failure
T2-2	2.7	7.7	19.8	1.58	Failure
T3	2.7	8.8	25.8	1.51	Failure

Table 5.1 Summary of tests parameters and outcome. SW: single wire of the double twist mesh. Failure of the barrier occurred by failure of the mesh.

5.1.3 NUMERICAL MODELLING

The finite element commercial code Abaqus version 6.11 (Abaqus 2011) was used to develop the model of the low energy barrier and run the simulations. Attention was paid to create a numerical model whose geometry is as close as possible to the real system (as described in Section 5.1.2). The barrier model is three-dimensional but includes one-dimensional elements (trusses), in order to reduce the computational time.

Structural elements of the barrier

The only relevant structural elements here are the longitudinal and side cables and the posts as all anchors and/or foundations were modelled as boundary conditions. Longitudinal and side cables are modelled with 2-node linear truss elements. These have a solid circular cross section with an area equivalent to that of the wire rope. The mechanical behaviour of the cables was determined using one-dimensional tensile tests at different loading rates (v_c), from 0.01 mm/s to 30 mm/s (with an initial length of specimens of 300 mm). It was found that the strain rate had no noticeable influence on the stress-strain response, as showed in Fig. 5.9.

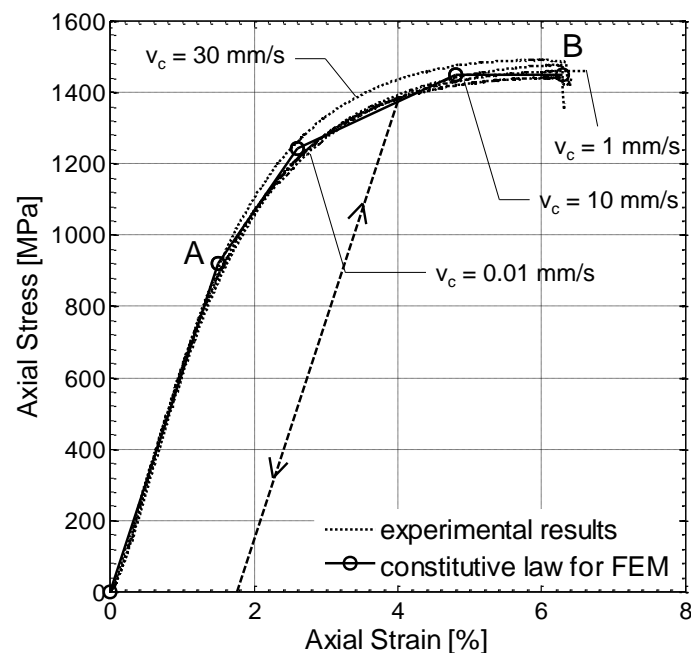


Figure 5.9 Experimental stress-strain curves of the cables and corresponding constitutive law for the FEM elements. A is the elastic limit, B the failure point.

The experimental response was approximated in a piecewise linear evolution that defined the response of all the finite element cables. The model behaves as linear elastic until point A (Young's modulus of 60GPa) and non-linear plastic from A to B. Point B is characterised by a strain of 6.2% and a stress of 1450 MPa, at which failure occurs.

The barrier posts were modelled using a simple elastic-perfectly plastic law with a Young's modulus of 210 GPa and a yield stress of 235 MPa was assigned to the relevant beam elements.

Double twist hexagonal wire mesh

The double twist hexagonal wire mesh is modelled with two-node beam elements connected through spherical hinges and were assigned the constitutive law depicted in Fig. 5.10. Note that it is necessary to define constitutive laws for the single wire (Fig. 5.10a) and double twisted wire (Fig. 5.10b).

These curves were proposed by Thoeni et al (2013), following a comprehensive experimental and DEM study on a double twist hexagonal wire mesh. From A to D, they reproduce the experimental behaviour observed in tensile tests on single and double twisted wires.

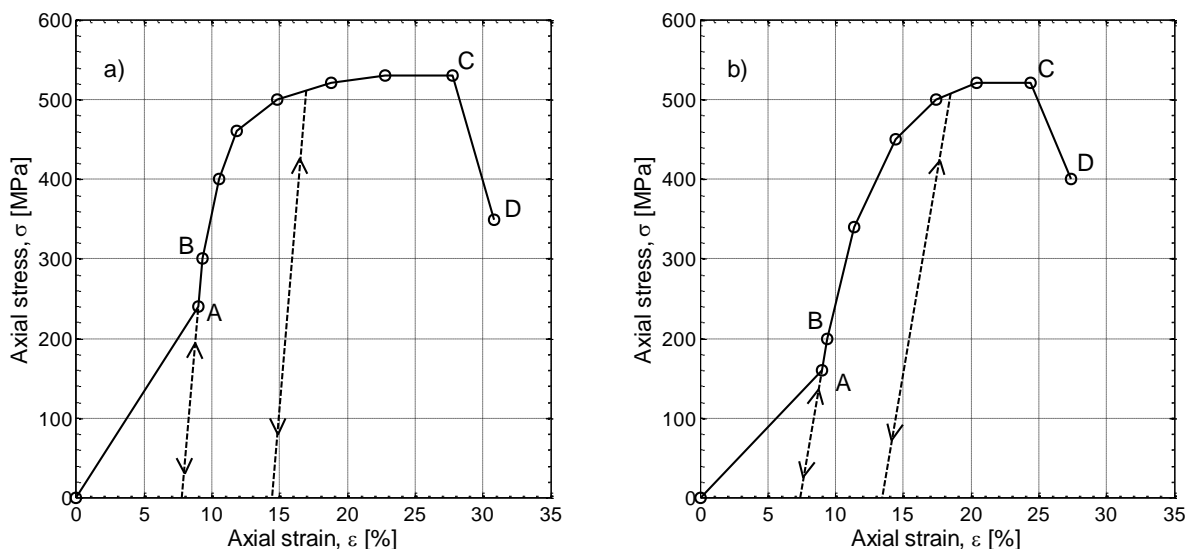


Figure 5.10 One-dimensional constitutive law for the FE wire elements: a) single wire and b) double twisted. A is the first elastic limit to capture irregularities of the mesh, B is the elastic limit, C is the plastic hardening limit, D is the failure point. Dotted lines represent the elastic unloading path.

The behaviour is elastic but non-linear from A to point B, followed by progressive yielding all the way to C, which is the onset of softening. At point D, the wire fails. The branch O-A was introduced to capture the geometrical and mechanical irregularities within the mesh that result in some initial compliance before all contributing cells within the mesh panel are fully loaded.

The parameters used to define the point A should be calibrated based on the observation of the experimental response of net samples to static and dynamic tests. Refer to Thoeni et al (2013) for further details about this aspect of the constitutive law.

This check included a static in-plane tensile test and a dynamic out-of-plane test. The numerical models required for this verification step were consistent with the experimental setup, geometry and dimensions (see Fig. 5.11). In particular, Fig. 5.11a provides information on the static in-plane finite element test. The specimen was 36 cm wide and 95 cm long. As for the laboratory experiment (DISTART, 2006), in the numerical simulation, the specimen is stretched in the horizontal plane (u_y) with a constant vertical speed of 10 mm/min, while the corresponding in-plane reaction force (R_y) is measured. The horizontal displacement (u_x) is restrained at four nodes on each side.

Figure 5.11b pertains to the dynamic out-of-plane test (Thoeni et al. 2013). In the numerical test, the specimen, a square panel of 2 m by 2 m, fully restrained on two opposite sides and partially restrained by connection to a cable on the other two sides, is subjected to the vertical impact of a test block of characteristic dimension of 300 mm. During the numerical test, the vertical displacement (d_z) of the block is monitored with time. The dynamic analysis was performed by adding some artificial damping, using the Rayleigh matrix approach in order to capture the successive rebounds post impact.

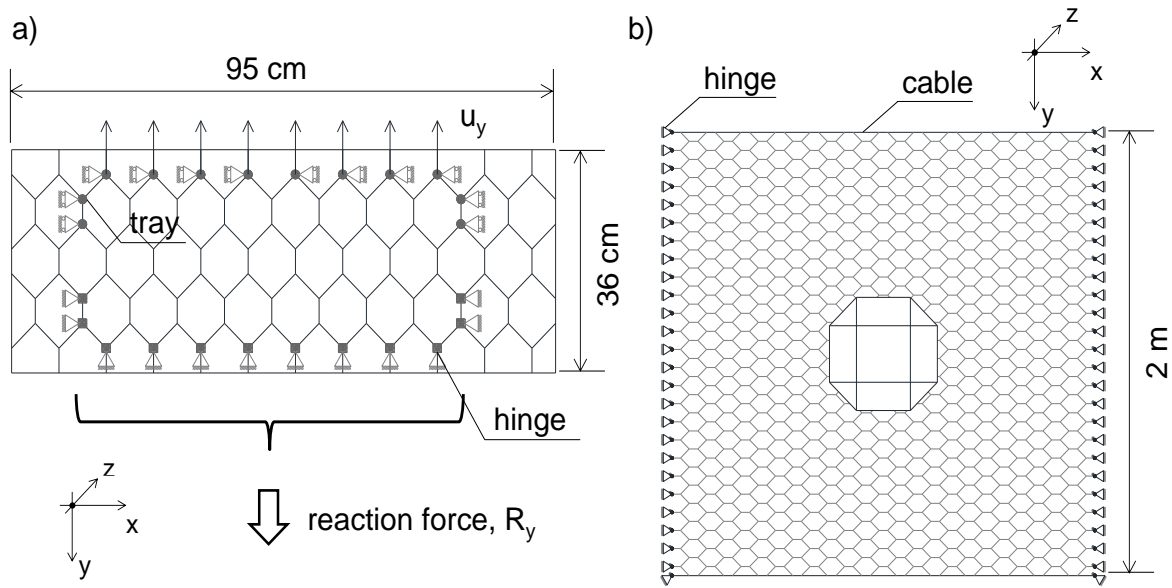


Figure 5.11 Schematic representation of the net samples for the experimental and numerical tests in: a) static in-plane (DISTART 2006) and b) dynamic out-of-plane conditions (Thoeni et al. 2013).

Results of these two tests are shown in Fig. 5.12. In both cases, the numerical results are found to match the experimental trends to a satisfactory degree, confirming the definition of the constitutive law adopted for the wire strands (single and double).

In Fig. 5.12a, the numerical in-plane force-displacement curve is plotted in black along with the corresponding experimental results (in grey). Although the numerical inflexion point does not quite match the experimental one, failure occurs at comparable values of force and displacement. The model slightly overestimates the failure load.

In Fig. 5.12b, the numerical vertical displacement of the block (in black) is compared to the corresponding experimental data (in grey). The first impact is well captured and the model also reproduces the successive rebounds although its magnitude is slightly overestimated. This could be further tuned by increasing the damping but it was found that adding too much mass proportional damping can modify the motion of the block during its interaction with the barrier. Overall, the model can adequately reproduce the static and dynamic response of the mesh for the testing conditions considered.

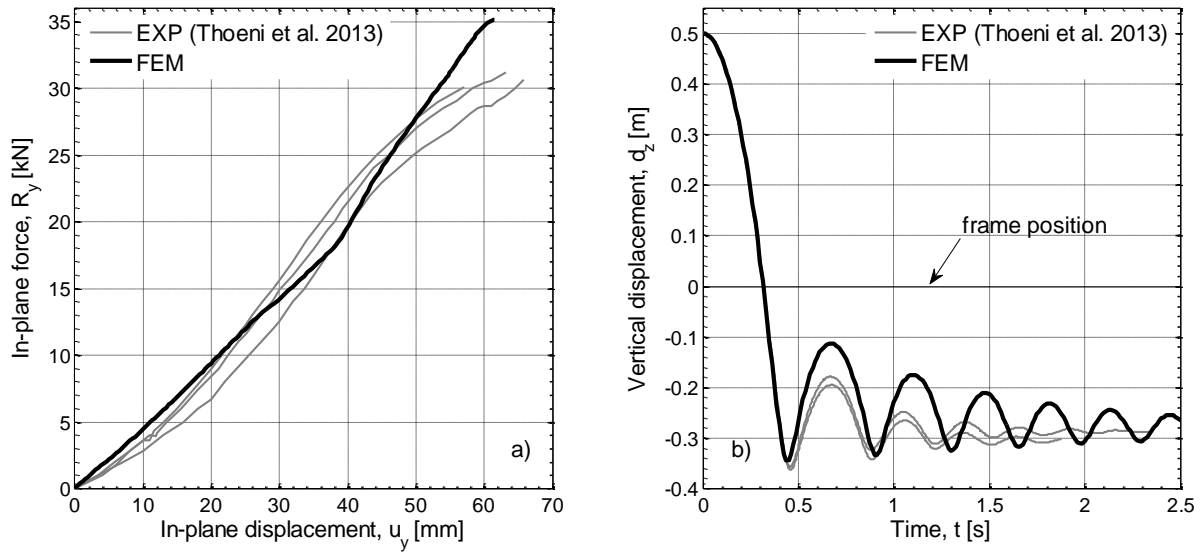


Figure 5.12 Results of numerical and experimental tests in: a) static and b) dynamic conditions.

Internal constraints and boundary conditions

A number of connectors have been used in the model in order to best reproduce the existing connections of the physical system and associated degrees of freedom. These connectors are based on a research previously conducted by Gentilini et al. (2012a, 2013). For example, the behaviour of the braided rope connecting the mesh to the longitudinal cables can be conveniently modelled using axial connectors (Fig. 5.13). This one-dimensional element is characterized by a force-displacement relationship (similar to that of Fig. 5.13) between the two connected nodes. Note that a similar connector is used between the mesh and the vertical cables (at the external posts). Another relevant connection is that between the longitudinal cables and the posts: the upper longitudinal rope is fixed with respect to the head of the external posts; however, a slot connector with penalty friction coefficient of 0.4 is used at the head of the internal posts. This offers a slide-through mechanism between the posts and the cables. In other words, vertical movements are restrained but the cable can slide longitudinally. In terms of external boundary conditions, spherical hinges were placed at lateral anchorages while the posts are cantilevered.

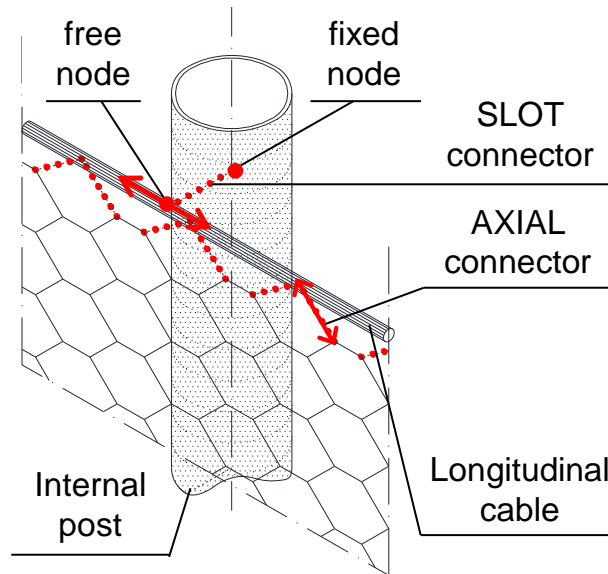


Figure 5.13 Representation of the longitudinal cable/post connection and the longitudinal cable/mesh connection.

Test block

In the numerical simulations, all the barriers are subjected to the central impact of a test block having a polyhedral shape, modelled with 10-node quadratic tetrahedron elements. This is in accordance with the testing recommendation by ETAG 027 (EOTA 2008). Consistent with the physical block, its numerical counterpart has a density of 2225 kg/m^3 , a dimension of 750 mm and a mass of 665 kg. The interaction between the block and the mesh is handled via a master-slave contact algorithm using the Coulomb friction model (friction coefficient of 0.4) involving node-based surfaces.

Analyses

All the simulations involved non-linear explicit dynamic analyses. Note that rather than modelling the physical fall, the block was placed in contact with the mesh and with a suitable initial speed. In other words, the initial time of the simulation ($t_0 = 0 \text{ s}$) corresponds to the moment of impact. Consistently with the test conditions, gravity was applied perpendicular to the block trajectory. The simulations were conducted at the level of energy highlighted in Table 5.1.

5.1.4 VALIDATION OF THE MODEL

In this Section, the results of the simulations are compared to the experimental data in order to demonstrate that the relatively simple FE model described in Section 5.1.3 can capture the dynamic response of the full barrier. Attention is focused on the displacement and speed of the block post impact (reflecting failure and post failure behaviour) as well as the time history of forces in the cables and at the base of the posts.

In order to interpret the results, it should be remembered that $t = 0$ s is the instant of impact, from which the speed of the block progressively drops while the barrier deforms with the block. The impact energy for T1 was 31.1 kJ and subjected to this energy, the barrier displacement peaked at about 1.64 m (Fig. 5.14a, for $t = 0.2$ s). In the experiment, the block displacement plateaus after maximum deformation, reflecting the barrier failure and the fact that the block has fell on the ground. The values of block speed showed in Figure 8b are non-filtered and show the oscillations generated by the derivation of displacement with time, as done by the tracking software. The residual speed of the block obtained by the simulation is still of about 3 m/s and consequently, the block keeps moving after failure. This is the only test where there is a significant difference between experiment and simulation in terms of residual speed.

In considering the forces, the experimental values are more scattered and, consequently, accurate comparison with the numerical model is more difficult. The maximum value of force in the cables is observed in the bottom cable (57 kN), reached at about 0.15 s. A rapid decrease in the force within the cable follows, accompanied by a sudden increase in the force recorded at the internal post, which reaches a peak value of 65 kN at about 0.20 s. These forces reflect tension in the cables and bending of the posts. Again, the numerical model generally captures the trend and magnitude of the forces recorded experimentally.

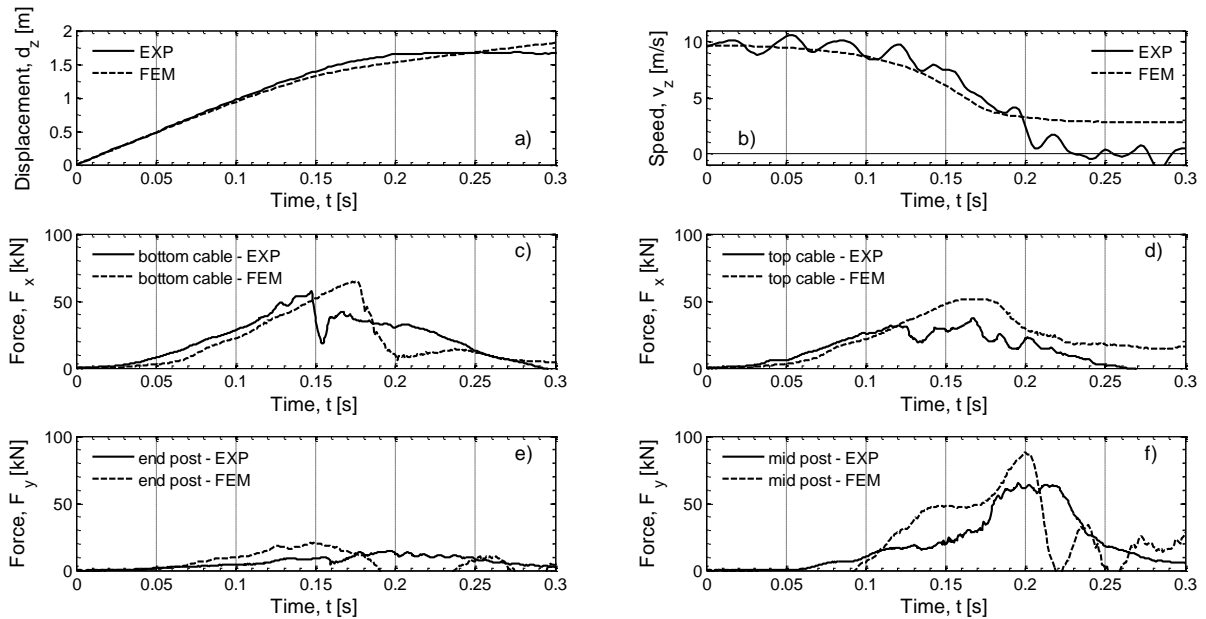


Figure 5.14 Comparison of experimental and numerical results for test T1: a) horizontal displacement of the block; b) horizontal speed of the block; c) force within the bottom cable; d) force within the top cable; e) force at the end post and f) force at the mid post.

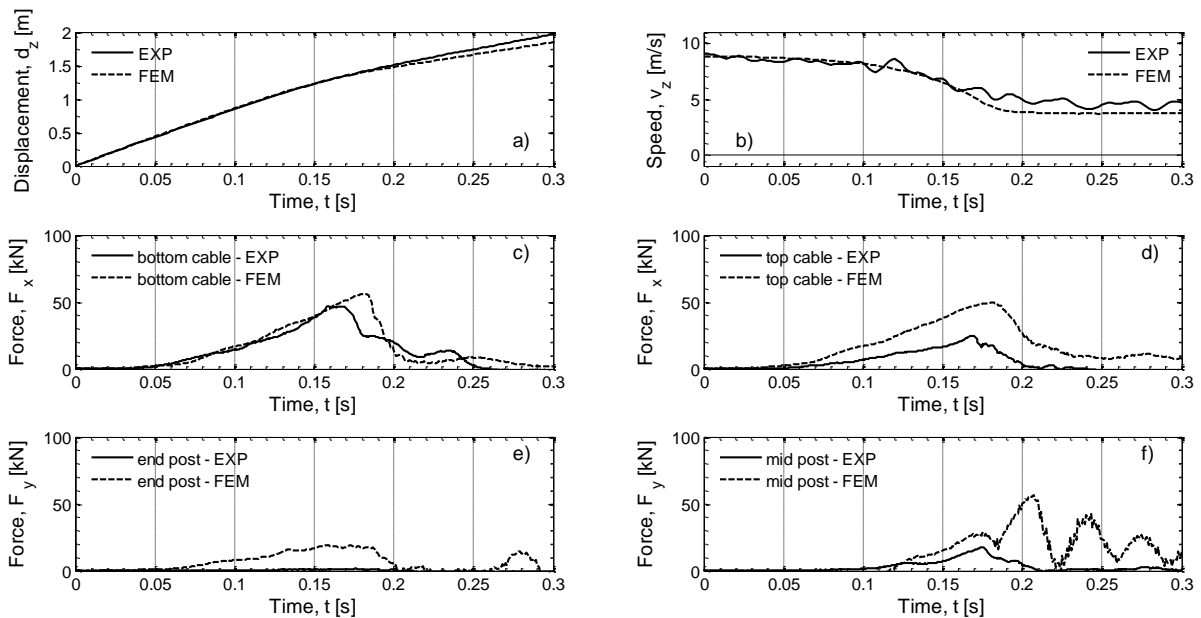


Figure 5.15 Comparison of experimental and numerical results for test T3: a) horizontal displacement of the block; b) horizontal speed of the block; c) force within the bottom cable; d) force within the top cable; e) force at the end post and f) force at the mid post.

Test T3 presents similar outcomes than test T1 and is hence presented next (Fig. 5.15). The time evolution of deformation, speed and forces are very similar to test T1 except for two things: the block speed profiles after failure now match but the model slightly overestimates the forces developing at the base of the posts. Soil-structure interaction is however beyond the scope of the paper.

T2 is the test where failure did not occur in the first place and where the impact was repeated. Note that both experimentally and numerically, this meant removing the block while leaving the barrier untouched and re-launching the block. In other words, nothing was adjusted or changed on the deformed system. The first impact (test T2-1, Fig. 5.16) occurred with an energy of 16.1 kJ. It is clear from Figs. 5.16a and b that the barrier caught the block: there is a rebound in the deformation profile and the block speed switches from positive to negative reflecting the rebound.

The braking time is 0.28 s and the value of maximum displacement is 1.46 m. Again, the numerical results closely follow the experimental trends but for a slight overestimation of the forces developing at the cables and at the base of the posts.

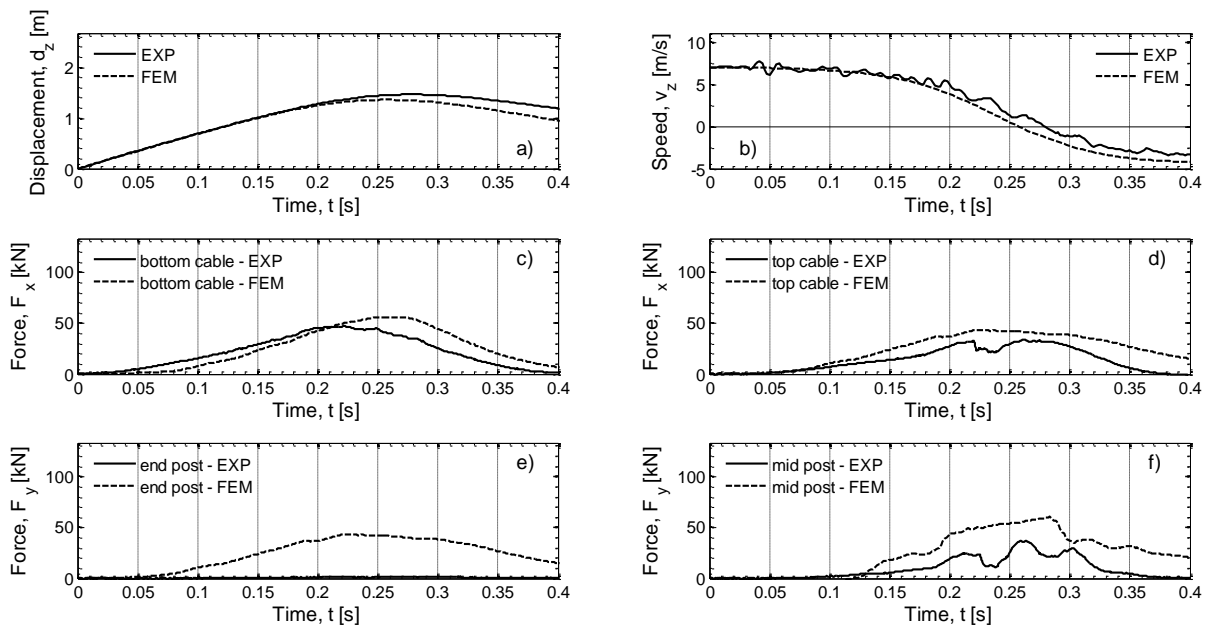


Figure 5.16 Comparison of experimental and numerical results for the first launch of test T2-1: a) horizontal displacement of the block; b) horizontal speed of the block; c) force within the bottom cable; d) force within the top cable; e) force at the end post and f) force at the mid post.

The second launch (test T2-2) was carried under an energy of 19.8 kJ. This time, the block went through the barrier and the evolutions of barrier deformation and block speed are very similar to those pertaining to tests T1 and T3 (Fig. 5.17). Again, the numerical predictions are in very good agreement both in terms of trend and quantities, demonstrating the model ability in reproducing the barrier response to repeated impacts.

In conclusion, the model appears to be able to well capture the dynamic behavior of the barrier under single or repeated impacts, opening the door for further research on the performance of low energy barriers based on numerical simulations that are far less expensive than real full-scale tests. Such a validation step is crucial to ensure confidence in the results for the bullet effect that will be presented in the coming Sections.

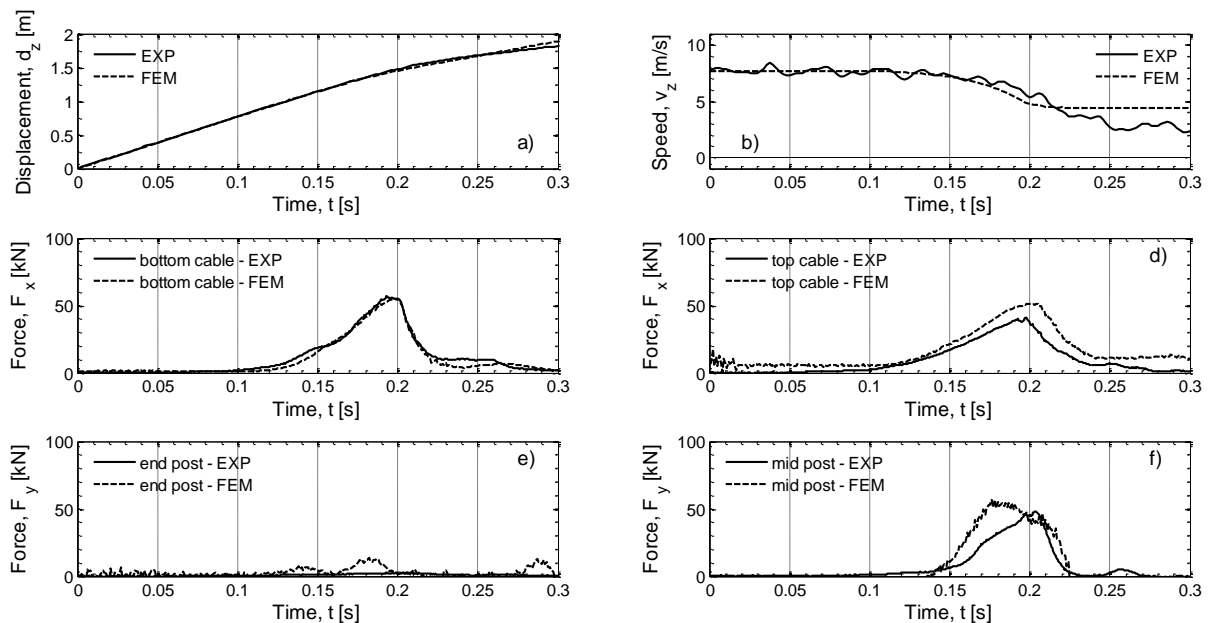


Figure 5.17 Comparison of experimental and numerical results for the first launch of test T2-2: a) horizontal displacement of the block; b) horizontal speed of the block; c) force within the bottom cable; d) force within the top cable; e) force at the end post and f) force at the mid post.

5.1.5 INVESTIGATIONS ON THE BULLET EFFECT

The bullet effect pertains to the phenomenon where a mesh is perforated by a small block travelling at high speed but having a kinetic energy lower than the nominal capacity of the barrier. In this Section, the bullet effect is investigated numerically, first on single panels of double twist mesh followed by simulations on the full barrier.

Response of the double twist hexagonal mesh

Due to its hexagonal cell shape and the existence of single and double wires, the mechanism of load distribution and energy dissipation in a double twist mesh is quite complex. In order to provide more information on the energy dissipation mechanisms, four panels of double-twist hexagonal mesh (denoted S1 to S4; S for specimen) having a single wire diameter of 2.7 mm were tested. These panels are 2 m wide with a variable length (2, 3, 4 and 5 m) and the tests were conducted in a similar manner than the dynamic out-of-plane tests detailed in Section 5.1.3 (see Fig. 5.11b, with the mesh positioned horizontal and the block in free fall) but this time, seven test blocks (size ranging from 200 mm to 800 mm.) were used to impact the mesh. 200 mm corresponds to the smallest object that is likely to cause a safety hazard on a road (Austroads 2010). For each block, several simulations were run to find the failure kinetic energy (E_{kf}), defined as the minimum kinetic energy at which the block breaks one element of the mesh. This failure energy is defined for increments of 100 J. In other words, the mesh was found to fail at E_{kf} but not at $E_{kf}-100$ J.

Finally, as discussed in Buzzi et al. (2014), the total energy at failure is the sum of the kinetic energy at impact plus a potential energy associated to the maximum deformation of the mesh:

$$E_f = E_{kf} + mgD_{max} \quad (5.2)$$

where E_{kf} is the failure kinetic energy, m is the block mass, g is the earth's gravity and D_{max} is the maximum deformation of the mesh. It was found that D_{max} varies very little

with block size. Values of 0.59 m, 0.84 m, 0.98 m and 1.08 m were found for the S1, S2, S3 and S4 meshes respectively.

Figure 5.18 clearly illustrates the bullet effect where the block energy to cause mesh failure decreases by about 50% when the boulder diameter decreases from 800 mm to 200 mm (Fig. 5.18a).

Note that the correlation between total failure energy and block dimension differs from that found analytically for a chain-link mesh (Hambleton et al. 2012; Buzzi et al. 2014), possibly due to the difference in mesh structure: the simplified loading mechanism devised in Hambleton et al. (2012) does not apply to the double twist mesh. Consequently, the direct proportionality between energy at failure and block size is not necessarily expected.

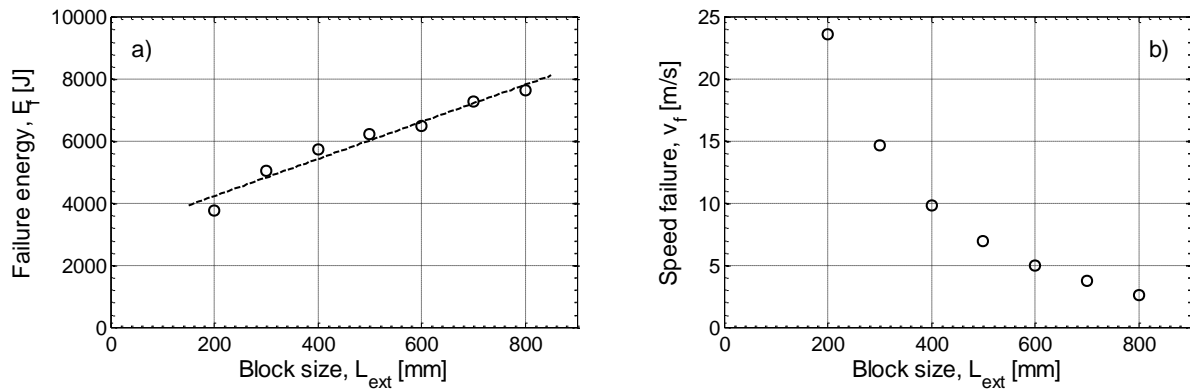


Figure 5.18 Simulation results pertaining to mesh S1 (2 m by 2 m): a) evolution of total energy at failure with block size and b) evolution of block speed with block size.

In the following, comparison is made between the energy required to fail meshes of different size. To facilitate the comparison, the normalised energy (E_f^*) was introduced:

$$E_f^* = \frac{E_{fi}}{E_{fmax}} \quad (5.3)$$

where, for each panel, E_{fi} is the failure energy associated to a block of dimension L_i , and E_{fmax} is the failure energy for a 800 mm block.

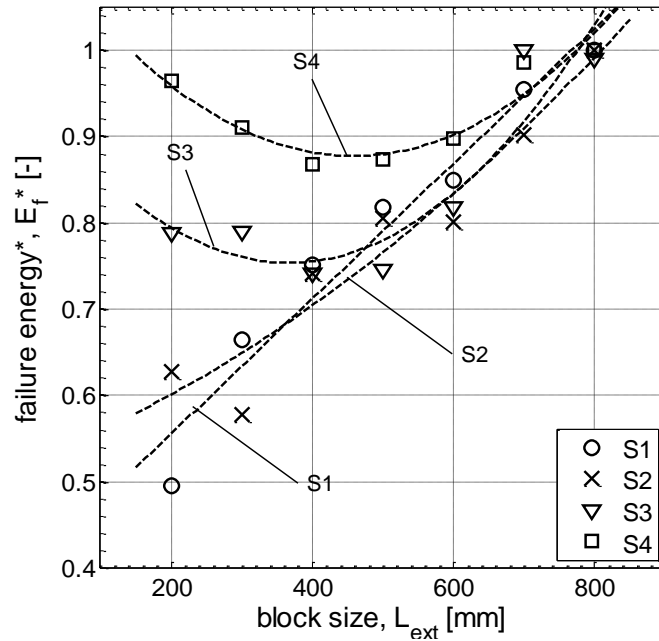


Figure 5.19 Results of FEM simulation of double twist mesh panels: evolution of total failure energy with block size for mesh S1 (2 m by 2 m), S2 (2 m by 3 m), S3 (2 m by 4 m) and S4 (2 m by 5 m).

Figure 5.19 exposes an interesting phenomenon that was not observed before: although the 2m×3m panel (S2) behaves very similarly to the 2m×2m panel (S1), as the mesh gets longer the failure energy becomes non monotonic with decreasing block size. The transition occurs for blocks of 400 mm, below which more energy is then required to perforate the mesh. This is in contradiction with the observations made so far on the bullet effect.

This change in behaviour can be explained by the dynamic response of the mesh. As the block size (and hence mass) reduces, the speed required to perforate the block increases significantly (from 3 m/s for a 800 mm block to more than 20 m/s for a 200 mm block). All values of speed corresponding to failure are reported in Table 5.2.

The large increase in speed accompanying the reduction in block size from 800 mm to 200 mm changes the dynamics of the impact and the way the mesh is loaded. In particular, it appears that for a small mesh, as the block size decreases, the portion of the mesh that enters into plasticity is reduced (see Fig. 5.20a). For example, for mesh S1, about 57% of the panel is at plastic state for the 500 mm block (at failure), a figure that drops to 46% for a 300 mm block. This effect contributes to the monotonic drop

in failure energy (at least in the range of block size under consideration) expected from the bullet effect.

Block size (L_{ext}) [mm]	Block speed at failure (v_f) [m/s]			
	Mesh S1 (2mx2m)	Mesh S2 (2mx3m)	Mesh S3 (2mx4m)	Mesh S4 (2mx5m)
200	23.6	32.2	38.8	37.4
300	14.7	16.5	20.9	22.4
400	9.8	11.8	12.7	13.8
500	6.9	8.4	8.6	9.3
600	5	5.8	6.3	6.6
700	3.8	4.4	5.1	4.8
800	2.6	3.2	3.2	2.9

Table 5.2 Block speed at failure for different block and mesh size. In bold are the values of speed for which an increase of energy is observed.

However, as the mesh gets larger, the full height of the mesh reaches the plastic state in the vicinity of the impact and such area extends laterally. For a 300 mm block travelling at 22.4 m/s, the plastic zone extends further, resulting in about 66% of the mesh as opposed to only 55% for the 500 mm block (Fig. 5.20b).

Although the change of mechanisms of energy dissipation and load transmission within the barrier with increasing speed is not yet fully explained, the larger plastic zone means more capacity to absorb energy and hence, more energy required to perforate the mesh. This explains the additional energy required for failure at the low end of block size in Fig. 5.19 for the 4 m (S3) and 5m (S4) meshes. Note that meshes S1 and S2 are not large enough (2 m by 2 m and 2 m by 3 m) to allow the development of a larger lateral plasticized zone, in a similar manner than meshes S3 and S4, when the block speed increases. This explains the monotonic reduction in failure energy with diminishing block size.

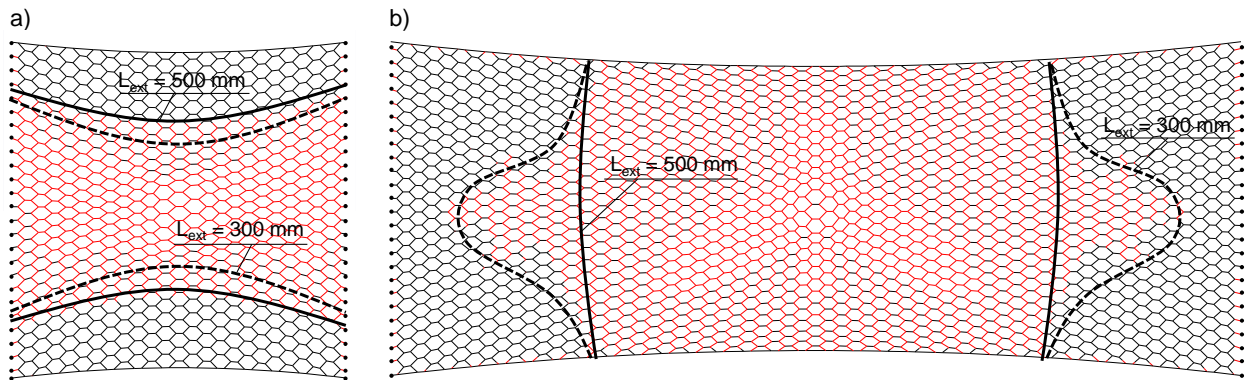


Figure 5.20 View of the mesh area having undergone full plasticity highlighted in red for: a) 2 m by 2 m mesh and b) 2 m by 5 m mesh.

Performance of the full barrier in relation to the bullet effect

So far, most of the research conducted by the authors on the bullet effect pertained to meshes alone but not a full system, whose response needs to be investigated. In the following, a finite element model of low energy barrier similar to that presented in Sections 5.1.3 and 5.1.4, is considered. Here again, the double twist hexagonal mesh is 2 m high and 15 m long and the virtual barrier is subjected to a central impact by a block of known mass and speed. Consistent with numerical simulations on the single mesh, the virtual tests on the full barrier are conducted with the barrier positioned horizontal with the blocks in free fall.

Eighteen blocks were considered for the analyses, with a size ranging from 200 mm to 1100 mm. For each block, the failure energy (E_f) was identified by iterations with 1 kJ increments. Results are reported in Fig. 5.21 in terms of failure speed ($v_{z,f}$) (Fig. 5.21a) and failure energy (E_f) (Fig. 5.21b), both being expressed as a function of the block size.

As discussed previously, 200 mm was considered an appropriate lower bound of block size in the Australian context but the absolute upper limit for the barrier under consideration is still to be defined. To do so, the virtual barrier was subjected to quasi-static loading in order to find the smallest block the barrier could simply not carry.

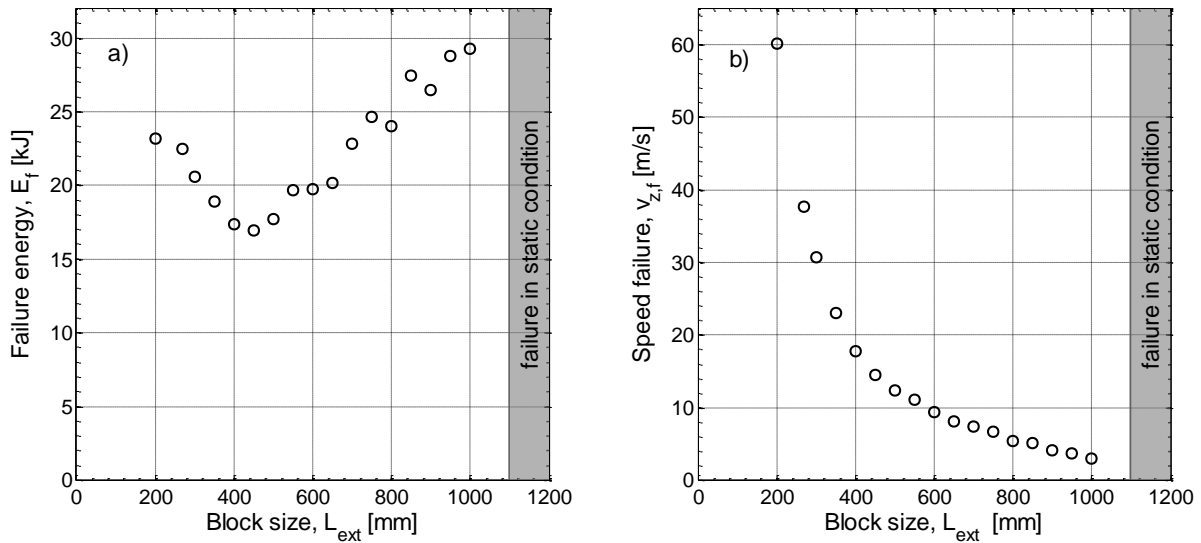


Figure 5.21 a) Failure impact energy and b) speed at impact, with dimension of block.

This was modelled in two steps where the block was first lowered in the barrier in a quasi-static manner until the onset of plasticity and then gravity loading was applied. It appears that the barrier fails in quasi static loading for any block larger than 1100 mm (Fig. 5.21). It was also found that the highest capacity (close to 30 kJ) was reached for a block of 1000 mm, which suggests that the transition from maximum capacity to failure under quasi-static loading is fairly sharp.

Now, as expected for blocks in the range 450-1000 mm, the bullet effect takes place (Fig. 5.21a) but the opposite effect occurs in that range 200 mm- 450 mm, similar to that observed for large meshes in Section 5.1.5. In the range 450-1000 mm, there is a twofold variation in barrier performance (from about 30 kJ to about 17 kJ). The data scattering is low and, most points fall close to a linear trend. The 450 mm block appears to be a critical dimension (at least for this barrier) and represents a minimum point of failure energy, corresponding to a block speed failure of 15 m/s (Fig. 5.21b), a realistic value recorded by Spadari et al. (2012, 2013a) during field experiments.

Reducing the block size further from 450 mm yields a better performance with a notable increase from 17 kJ to 23 kJ. As explained previously, this is attributed to a larger portion of the mesh reaching the plastic state and thus contributing to the energy dissipation (see Fig. 5.22).

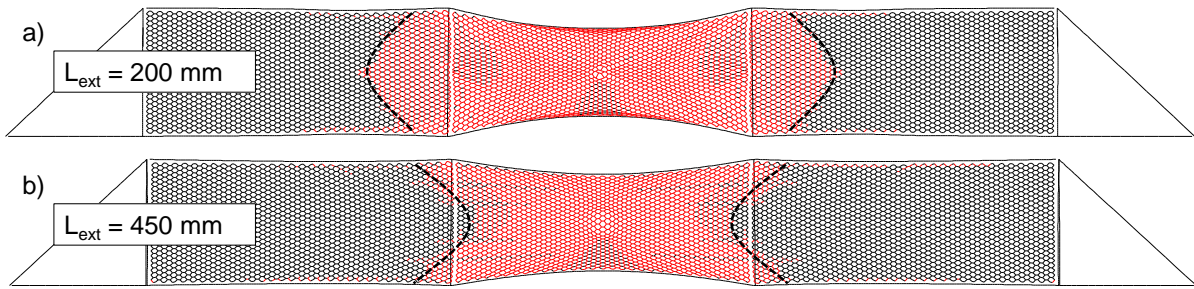


Figure 5.22 View of the mesh with the area having undergone full plasticization prior to failure highlighted in red (at the centre). Results for impacting block of: a) 200 mm and b) 450 mm. Dotted line shows the approximate extent of the plasticized area.

Further analysis of the simulations pertaining to the meshes only and the full barrier suggests that the dynamic effects leading to a larger plastic area seem to prevail for impact speed around 18 m/s (Fig. 5.23). This corroborates the experimental observations by Buzzi et al. (2014) on a chain-link mesh. It also suggests that such low energy systems should be tested at an impact speed corresponding to the onset of these improving dynamic effects, i.e. about 18 m/s, in order to test for the critical case.

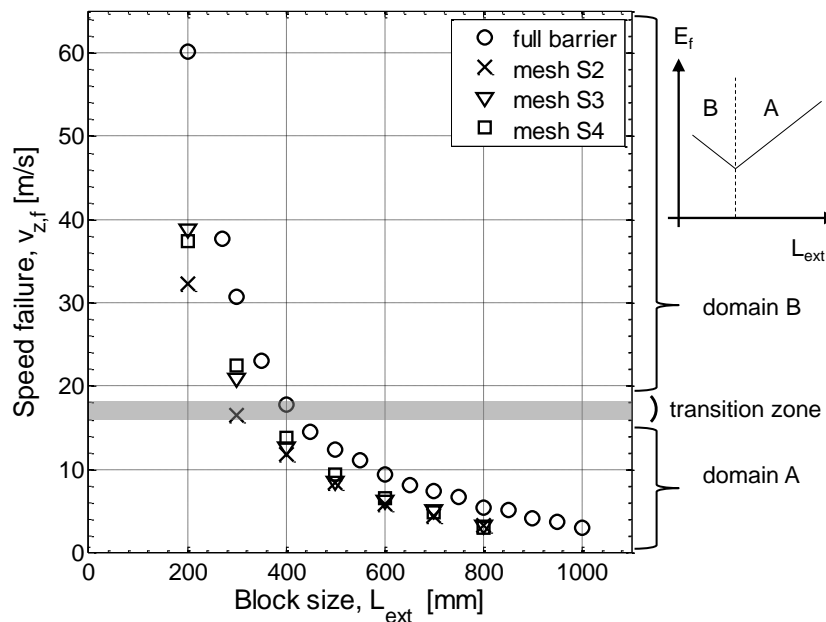


Figure 5.23 Speed failure at impact with dimension of block pertaining simulations on full barrier and meshes, grey area highlight the transition between a bullet effect and dynamic effect leading to a larger plastic area of the mesh. The grey area shows an approximate boundary between points pertaining to domain A and domain B.

This Section highlights the significance of the bullet effect for low energy barriers: a loss of capacity in the order of 50% possibly occurs when the block size drops from 1000 mm to 450 mm, with a realistic speed required to get barrier perforation. The issue would possibly materialize in a rockfall assessment scenario where attention is focused on the presence of large blocks along the slope while much smaller blocks, located at a much higher elevation, are overlooked.

Effect of intermediate longitudinal cables on the barrier response

The barrier modelled in Section 5.1.3 corresponds to a modification of the 35kJ barrier of the New South Wales Road and Maritime Services, formerly known as Road and Traffic Authority (see Buzzi et al. 2013). The original design includes intermediate longitudinal cables placed downhill from the mesh (as illustrated in Fig. 5.24). The rationale for including these cables is to reduce the deflection upon impact and improve the energy absorption capacity of the system. Section 5.1.5 focused on the behaviour the barrier without intermediate cables in order to define a baseline dynamic behaviour. This Section will highlight the effect of the intermediate cables on the performance of the barrier with an emphasis on the bullet effect.

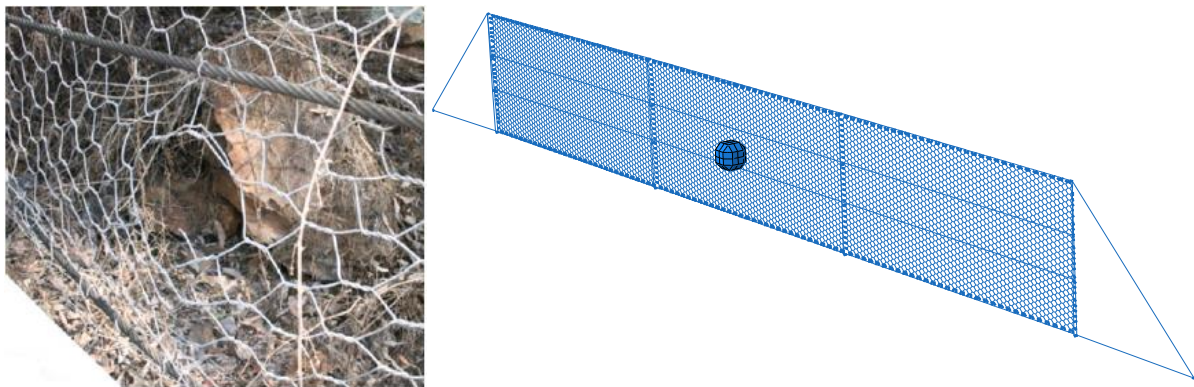


Figure 5.24 Low energy barrier with intermediate additional longitudinal cables: a) photograph of local failure of an installed barrier in New South Wales (after Spadari et al. 2012) and b) model of the barrier with intermediate cables.

Note that only two intermediate cables were used herein while three are typically mounted on the physical barrier, the reason being that with three cables, the central impact occurs on the mid cable, hence suppressing the bullet effect. To overcome this

for a 3 cable barrier, a non-centered impact is required but Cazzani et al. (2002) showed a correlation between energy at failure and impact location. So, for consistency of the results, only two cables were used as shown in Fig. 5.18b, which leaves a central portion of mesh for the impact by blocks of variable size.

The intermediate cables have a diameter of 16 mm at a spacing of 600 mm. Their restraints are similar to those of top and bottom cables, i.e. tied to the two external posts but allowed to slide with respect to the internal posts. Here again, gravity is applied perpendicular to the barrier.

Figure 5.25 compares the evolution of total energy at failure with and without the intermediate cables. Three domains seem to appear. For blocks of 600 mm and above, the intermediate cables are impacted by the blocks and the performance of the barrier is improved, which is quite intuitive. Interestingly, the larger the block, the wider the gap between the performance of the two systems. This highlights the effectiveness of the cables. The downside of a direct impact on the cables is that less energy is dissipated by the mesh and more forces are transmitted to the structure.

The second domain of response lies between block sizes of 300 mm to 500 mm where there is not any noticeable difference in barrier response due to the cables. For both systems, 400 mm is the critical dimension below which the failure energy increases again.

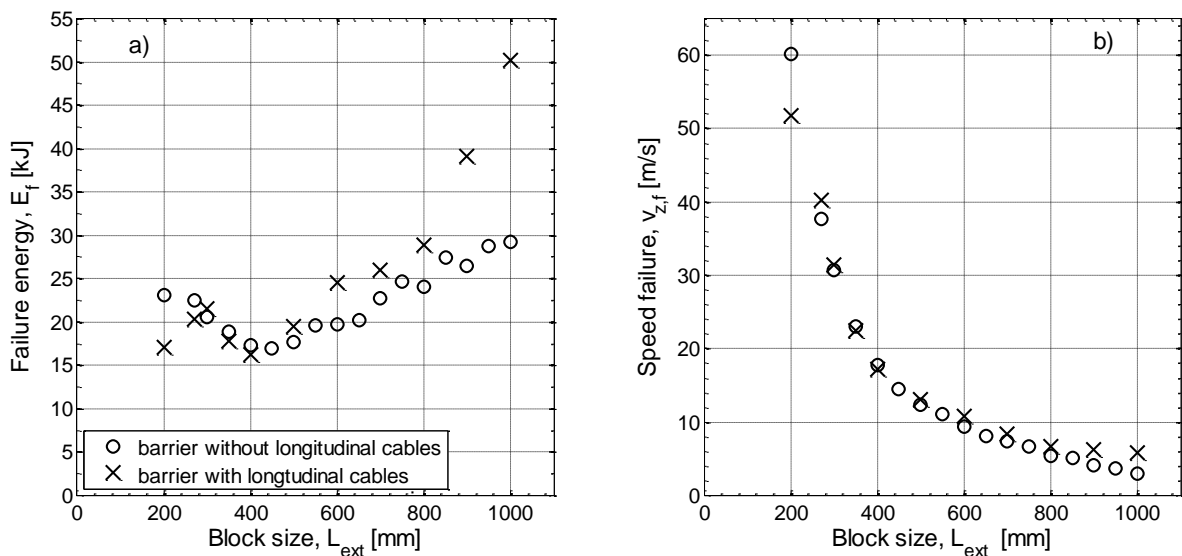


Figure 5.25 a) Total failure energy and b) speed at impact as a function of block size for system with and without intermediate cables.

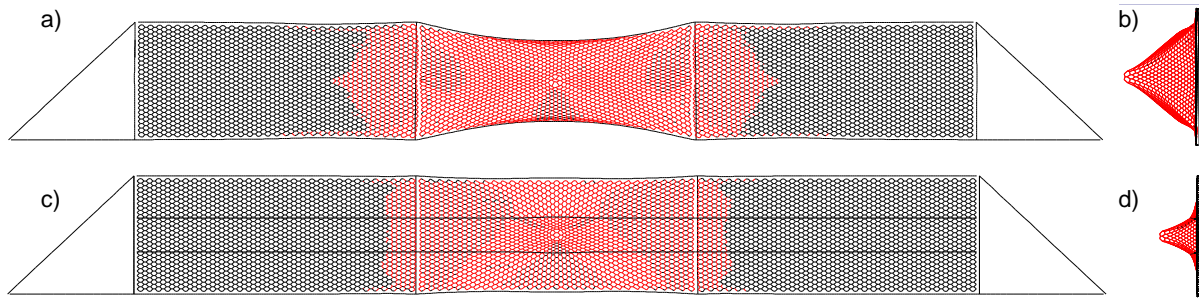


Figure 5.26 View of the part of the mesh having undergone full-plasticization (at the centre, in red) prior to failure, for an impacting block of 200 mm. a) and b) pertain to the barrier without cables while c) and d) represent the barrier with intermediate cables.

Finally, a block size of 300 mm marks a new transition in the response of the barrier with cables: unlike its un-reinforced counterpart, the failure energy drops again for very small blocks (200 mm to 300 mm). This is attributed to the combination of high impact speeds and a restraining effect provided by the cables (see Fig. 5.26), hindering the plasticization of the mesh in a large extent.

5.1.6 CONCLUDING REMARKS

This paper presents new findings pertaining to the response of full barriers to the so-called bullet effect. The study focuses on low energy barriers that are the most common type deployed in New South Wales, Eastern Australia.

The study is mainly numerical and, in order to build confidence in the results and improve their reliability, the numerical model has been validated against a series of experiments that were previously conducted at The University of Newcastle, on individual components and full barriers. It was checked that the relatively simple model could reproduce the outcomes of the tests and in particular the time evolution response of the system in terms of displacement, failure and forces.

The validated model was used to assess the dynamic response of the double twist mesh alone. A loss mesh performance in the order of 50% was observed when diminishing the block size from 800 mm to 400 mm. In addition, a new effect was unveiled: the decrease of failure energy with block size is not monotonic, as dynamic effects seem to appear for impact speed in the order, or in excess of, 18 m/s,. This seems to be due to different loading mechanisms of the mesh, resulting in different extensions of plastic zone. All these aspects were corroborated on the full system.

Finally, the consequence of adding intermediate longitudinal cables was investigated (as per standard low energy barrier design, see Buzzi et al. 2013). It was found that, although these cables are beneficial for large blocks, they actually exacerbate the susceptibility to the bullet effect at the low end of the spectrum.

It should be appreciated that low-energy systems are very prone to the bullet effect type perforation because the speed required for the small block to punch through is realistic (16 m/s for the lowest failure energy). The results presented here further highlight the need to consider the whole spectrum of block sizes for a successful design of a low energy barrier instead of focusing on one simple block dimension, typically large, thus allowing to mitigate possible local failures.

CONCLUDING REMARKS

6.1 INTRODUCTION

This thesis is concerned with understanding the dynamic response of rockfall protection barriers in order to significantly advance the analysis option available for the numerical simulation of realistic on-site installations toward falling rock events. The work combines the outcomes of extensive experimental tests with numerical techniques to arrive at a modelling package that has been shown to achieve good quality prediction of the rockfall barriers behaviour as measured in full-scale tests.

This final chapter summarises the major contributions that have been made, including the achieved developments and the main findings arising from the research

6.2 ORIGINAL CONTRIBUTIONS AND MAIN FINDINGS

6.2.1 Development of advanced three-dimensional finite element models of high-energy rockfall protection barriers

A three-dimensional FE modelling strategy for high-energy rockfall protection barriers was proposed by Gentilini et al (2012a). The authors devised a set of solutions for modelling the structural elements involved and their interaction properties. Notwithstanding the validation with experimental outcomes of full-scale tests, in order to enable the use of the model as a predictive tool some uncertainties and approximations were still observed that needed to be further enhanced. Due to the complexity of the dynamic and high non-linear phenomenon, the trustworthiness of numerical models as design tools relies upon a preliminary and accurate procedure of calibration (Gottardi et al. 2014).

In the model presented in Chapter 3, the numerical approach previously conceived has been further developed, analysing the response of a flexible rockfall barrier having high-energy absorption capacity (i.e. 3000 kJ). A thorough study of all the structural components of the system in dynamic condition is carried out, based on experimental evidences rather than numerical methods. Special emphasis is focused to modelling the dynamic response of the interception structure and the energy dissipating devices. The model is calibrated by exploiting a rich set of experiments performed with different energy levels at impact. High quality experimental data obtained from full-scale tests carried out in a vertical test site are employed to validate the numerical approach. Thus, the weaknesses highlighted in the pre-existing tools are solved through a more consistent assessment of the whole model effectiveness.

Several results such as maximum elongation and corresponding braking time, residual heights, shortenings of energy dissipating devices, forces mobilised at the anchorages and at the post-foundations, are evaluated from the simulations and compared to the experimental data. An excellent match is exhibited for the different test conditions analysed, confirming the reliability of the numerical choices made.

The validated model is then usefully employed to investigate the ability of the barrier to withstand different impact configurations. The relevant results are investigated, enabling to identify the structure performance under more realistic scenarios and to propose some design optimization.

6.2.2 Evaluation of performance of existing protective structure by means of a numerical approach to support rockfall risk assessment

In a rockfall risk assessment procedure, which is able to account for countermeasures, the main parameter to contemplate for existing rockfall barriers is the capacity of absorption energy. This crucial parameter is usually evaluated through full-scale testing of prototypes but this data is not provided for most of the existing systems

within the Alps territory. To fill this lack of information, in Chapter 4, the numerical approach already defined for flexible barriers is exploited to produce reliable data integration.

An inventory of the protection systems installed in the province area has been carried out along with the Autonomous Province of Bolzano (PAB). The database supplies information about the main features of the existing barriers. Each barrier type is described reporting the geometrical details of the system and its components. In addition, the characteristics about the material used and the general state of maintenance are illustrated. Based on these data, a comprehensive numerical study of a set of rockfall barrier types is developed. The selected barriers represent the most common typologies installed within the Province. They are semi-rigid structure with low-energy capacity.

The FE models are developed in order to define a reliable behavioural characterisation of the considered barriers. In absence of a standardised procedure to assess the energy parameter of semi-rigid barriers, the essential prescriptions of ETAG are essentially followed.

The FE analyses enable to determine the limit energy level and to evaluate the response in service condition. The limit energy is defined as the maximum energy possessed by a block the prototype is still able to arrest, while the service level is considered as one third of the limit value and the test is repeated twice on the barrier. At the end of the process an energy capacity is assigned to each studied structure providing an important parameter for a rockfall risk assessment in the area where these structures are installed. Details about the test results, like the maximum elongation reached and forces mobilised at the foundation structures are also supplied, allowing an interpretation of the barrier behaviour.

Further, the failure mode is analysed to give understand of the rupture mechanism and to provide suggestion for improving the low-energy barriers design.

6.2.3 Development of a numerical model of a low-energy rockfall barrier and investigation about the effectiveness of the energy criterion

Despite many researches in the last few years have encouraged the improvements of high-energy rockfall barriers effectiveness through both experimental and numerical modelling analysis, low-energy systems received only little attention up to now. Conversely, many rockfall events develop only small amount of energy due to the characteristic of the unstable slope, hence low-energy barriers are more suitable solutions.

In Chapter 5 the data of a comprehensive experimental campaign, carried out to investigate the response of a barrier prototype having low-energy capacity, are used to develop a FE model. The whole model is assembled after assessing the mechanical behaviour of the structural components through experimental evidences. The barrier model is calibrated by comparing with the outcomes of full-scale tests carried out both in service condition than up to failure of the system. Hence, the reliability of the model is fully-validated by considering the results of several impact conditions. Results of all the simulated tests are monitored and compared to the experimental evidences of forces and barrier elongation produced.

The calibrated model is then used to highlight critical remarks about the influence of the block size on the rockfall barrier performance. The so-called bullet effect is examined for this barrier type. It refers to a reduction of the barrier energy absorption capacity with decreasing size of the impacting block. Due to the structures design, this issue is typical for low-energy systems rather than flexible barriers. In the studied semi-rigid barrier, built with a double-twisted mesh type, the reduction of energy capacity with the block size has shown to be not linearly constant. A lower threshold of the block size is shown below which the barrier performance seems to improve, due to the greater extension of the engendered plastic area which contribute to the dissipation of energy.

Finally, the study is also carried out to highlight the effectiveness of adding intermediate longitudinal cables to the interception structure to enhance the barrier capacity. It is proved that an improvement can be observed in terms of prototype capacity when large blocks are colliding the net, while a drop in the barrier's ability is reached for smaller blocks. Thus, a benefit of the barrier performance cannot be achieved just adding elements to the structure and a wide spectrum of block dimension should be considered when investigating a low-energy rockfall barrier experimentally.

6.4 CONCLUSION

Modelling the behaviour of rockfall barrier systems poses a variety of complex challenges. In this thesis, complementary physical and numerical modelling has been utilised in the development of a novel three-dimensional analysis package, providing confidence in the predictions to be realistic for rockfall barriers response in the field.

REFERENCES

- Agliardi, F., Crosta, G.B, Frattini, P. (2009). Integrating rockfall risk assessment and countermeasure design by 3D modelling techniques. *Natural Hazard and Earth System Sciences*, 9: 1059-73.
- Anderheggen, E., Volkwein, A., Grassl, H. (2002). Numerical simulation of highly flexible rockfall protection systems, in *Proc. Fifth World Congress on Computational Mechanics (WCCM V)*. Vienna University of Technology, 2002.
- Arndt, B., Ortiz, T., Turner, A.K. (2009). Colorado's full-scale field testing of rockfall attenuator systems. *Transportation Research E-Circular*, Issue E-C141, 130p.
- Austrroads (2010) *Guide to Road Design Part 3: Geometric Design No. AGRD03/10*, 295 pages
- Bertolo, P., Oggeri, C., Peila, D. (2009). Full-scale testing of draped nets for rock fall protection. *Canadian Geotechnical Journal*, 46(3): 306–317.
- Bertrand, D., Nicot, F., Gotteland, P., Lambert, S. (2008). Discrete element method (DEM) numerical modeling of double-twisted hexagonal mesh. *Canadian Geotechnical Journal*, 45(8): 1104–1117.
- Bertrand, D., Trad, A., Limam, A., Silvani, C. (2012). Full-scale dynamic analysis of an innovative rockfall fence under impact using the discrete element method: from the local scale to the structure scale. *Rock Mechanics and Rock Engineering*, 45(8):885-900. DOI 10.1007/s00603-012-0222-5.
- Bigot, C., Berger, F., Lambert, S. (2010). Treenet: an innovative type of rockfall protection fence on forested slopes specially designed for low energy events. In: *Interpraevent 2010, International Symposium in Pacific Rim*. Taipei (TWN): 366-371.
- Bourrier, F., Lambert, S., Heymann, A., Gotteland, P., Nicot, F. (2011). How multi-scale approaches can benefit the design of cellular rockfall protection structures. *Canadian Geotechnical Journal*, 48: 1803-16.
- Bourrier, F., Lambert, S., Baroth, J. (2014). A reliability-based approach for the design of rockfall protection fences. *Rock Mechanics and Rock Engineering*, 48(1): 247-259. doi: 10.1007/s00603-013-0540-2.

- Buzzi, O., Spadari, M., Giacomini, A., Fityus, S., Sloan, S.W. (2013). Experimental testing of rockfall barriers designed for the low range of impact energy. *Rock Mechanics and Rock Engineering*, 46: 701-712.
- Buzzi, O., Leonarduzzi, E., Krummenacher, B., Volkwein, A., Giacomini, A. (2014). Performance of high strength rockfall mesh: effect of block size and mesh geometry. *Rock Mechanics and Rock Engineering*. doi:10.1007/s00603-014-0640-7
- Cantarelli, G., Giani, G.P., Gottardi, G., Govoni, L. (2008). Modelling rockfall protection fences. Proc. of the 1st World Landslide Forum, Tokyo, 18-21 November 2008: 103-108.
- Cargnel, G. (2011) Tests on steel wire and cable net meshes. *Rivista GEAM* 132, 65-74.
- Castro-Fresno, D., del Coz Díaz, J.J., López, L.A., García Nieto, P.J. (2008). Evaluation of the resistant capacity of cable nets using the finite element method and experimental validation. *Engineering Geology*, 100: 1–10.
- Castro-Fresno, D., del Coz Díaz, J.J., Alonso Martínez, M., Blanco-Fernandez, E., Polanco Madrazo, J.A. (2012). Numerical and experimental study of a new type of clip for joining cables. *Engineering Structures*, 44: 107-121.
- Cazzani, A., Mongiovì, L., Frenez, T. (2002). Dynamic finite element analysis of interceptive devices for falling rocks. *International Journal of Rock Mechanics and Mining Sciences*, 39: 303–321.
- Corominas, J., Copons, R., Moya, J., Vilaplana, J.M., Altimir, J., Amigó, J. (2005). Quantitative assessment of the residual risk in a rockfall protected area. *Landslides*, 2: 343-57.
- de Miranda, S., Gentilini, C., Gottardi, G., Govoni, L., Ubertini, F. (2010). A simple model to simulate the full-scale behaviour of falling rock protection barriers. Proc. of the 7th ICPMG 2010, Zurich, 28 June-1 July 2010, vol. 2. London: CRC Press, Taylor & Francis Group: 1247-1252.
- de Miranda, S., Gentilini, C., Gottardi, G., Govoni, L., Mentani, A., Ubertini, F., (2011). On the structural response of falling rock protection barriers, in: Atti XX Congresso dell'Associazione Italiana di Meccanica Teorica e Applicata – AIMETA 2011, Conselice (RA), Publi&stampa, pp. 1-10.

-
- Descoeurdes, F. (1997). Aspects geomécaniques des instabilités de falaises rocheuses et des chutes de blocs. *Société Suisse de mécanique des sols et des roches* 135: 3-11.
- Descoeurdes, F., Montani-Stoffel, S., Boll, A., Gerber, W., Labiouse, V. (1999). Coping study on disaster resilient infrastructure. Chapter 4: 37–46.
- Dhakal, S., Bhandary, N.P., Yatabe, R., Kinoshita, N. (2011). Experimental, numerical and analytical modelling of a newly developed rockfall protective cable-net structure. *Natural Hazards and Earth System Sciences*, 11: 3197–3212. doi:10.5194/nhess-11-3197-2011.
- Dorren, L., Berger, F. (2006). Stem breakage of trees and energy dissipation at rockfall impacts. *Tree Physiology*, 26: 63–71.
- Dorren, L., Berger, F., Jonsson, M., Krautblatter, M., Moelk, M., Stoffel, M., and Wehrli, A. (2007). State of the art in rockfall – forest interactions. *Schweizerische Zeitschrift für Forstwesen*, 158: 128–141.
- Duffy, J.D., Haller, B. (1993). Field tests of flexible rockfall barriers. Proc. of the Conference on Transportation Facilities Through Difficult Terrain, Aspen Snowmass, Colorado, USA: 465-473.
- Duncan, C.W. (2014). *Rock Fall Engineering*. CRC Press 2014, p. 270. ISBN: 9781482219975.
- Escallon, J.P., Wendeler, C., Chatzi, E., Bartelt, P. (2014). Parameter identification of rockfall protection barrier components through an inverse formulation. *Engineering Structures*, 77: 1-16. doi:10.1016/j.engstruct.2014.07.019.
- EOTA (2008). Guideline for European technical approval of falling rock protection kits (ETAG 027), Brussels.
- Fityus, S.G., Giacomini, A., Buzzi, O. (2012). The significance of geology for the morphology of potentially unstable rocks. *Engineering Geology*, 162: 43-52.
- Fontanari, V., Monelli, B.D., Degasperi, F. (2009) Experimental and numerical analysis of full-locked coil ropes fire behaviour. Proceedings of SEM 2009 Annual Conference & Exposition on Experimental & Applied Mechanics, Bethel, CT: SEM Society for Experimental Mechanics; June 1–4, 2009.
- Gentilini, C., Govoni, L., de Miranda, S., Gottardi, G., Ubertini, F. (2012a). Three-dimensional numerical modelling of falling rock protection barriers. *Computer and*

Geotechnics, 44: 58-72.

Gentilini, G., Gottardi, G., Govoni, L., Mentani, A., Ubertini, F. (2012b). Dynamic analysis of flexible falling rock protection barriers. In Proceedings of: 7th International Conference on Computational Mechanics for Spatial Structures (IASS-IACM 2012), Sarajevo, Bosnia and Herzegovina, April 2-4, 2012: 112-115.

Gentilini, C., Gottardi, G., Govoni, L., Mentani, A., Ubertini, F. 2013. Design of falling rock protection barriers using numerical models. Eng. Struct. 50: 96-106.

Gerber, W. (2001) Guideline for the approval of rockfall protection kits. Swiss Agency for the Environment, Forests and Landscape (SAEFL) and the Swiss Federal Research Institute WSL, Berne.

Giani, G.P. (1992). Rock slope stability analysis. Balkema, Rotterdam.

Gorlato, A. (2011). Numerical non linear modelling of the response of a rockfall protection barrier, Master Thesis, Bologna 2010 (in Italian).

Gottardi, G., Govoni, L. (2010). Full scale modelling of rockfall protection barriers, Rock Mechanics and Rock Engineering, 43: 261-274.

Gottardi, G., Govoni, L., Mentani, A., Ranalli, M., Strada, C. (2011). The effectiveness of protection systems toward rockfall risk mitigation. In Proceedings of: 3rd Geotechnical Safety and Risk (ISGSR 2011). Munich, Germany, June 2-3, 2011: 157-164.

Gottardi, G., Govoni, L., Mentani, A., Gentilini, C., Ubertini, F. (2014). Modelling for the design of passive protection measures against rockfall. In Proceedings of: 8th International Conference on Physical Modelling in Geotechnics (ICPMG 2014), Perth, Australia, January 14-17, 2014, 2: 1179-85.

Govoni, L., de Miranda, S., Gentilini, C., Gottardi, G., Ubertini, F. (2011). Modelling of falling rock protection barriers. International Journal of Physical Modelling in Geotechnics, 11: 126-137.

Grassl, H., Volkwein, A., Anderheggen, E., Ammann, W.J. (2002). Steel-net rockfall protection – Experimental and numerical simulation. Proceedings of: Seventh International Conference on Structures Under Shock and Impact, SUSI VII, Montreal, Canada, 27-29 May 2002. Structures and Materials, 11, pp. 143-153.

Grassl, H., Bartelt, P.A., Volkwein, A., Wartmann, S. (2003). Experimental and

-
- numerical modeling of highly flexible rockfall protection barriers, in: Culligan, P.J., Einstein, H.H., Whittle, A.J. (Eds.), Proc. Soil and Rock America 2003, Cambridge, Massachusetts.
- Hearn, G. (1991). CDOT Flex-post rockfall fence. Colorado Highway Department. Report: CDOH-R-UCB-91-6, Denver, Colorado, p. 109.
- Hearn, G., Barret, R.K., McMullen, M.L. (1992). Flexpost rockfall fence development, testing and analysis. Rockfall prediction and control and landslide case histories. Transportation Research Record 1343. National Academy Press, Washington, DC: 23-29.
- Hearn, G., Barrett, R.K., Henson, H.H. (1995). Developing of effective rockfall barriers. Journal of transportation Engineering, 121: 507-516.
- Hibbitt, Karlsson and Sorensen Inc. (1998) Abaqus Theory Manual, 1998.
- Jonsson, M. (2007). Energy absorption of trees in a rockfall protection forest, Ph.D. thesis, ETH, Zurich.
- Kane, W.F., Duffy, J.D. (1993). Brugg low energy wire rope rockfall net field tests. Technical Research Report 93-01. Department of Civil Engineering, The University of the Pacific.
- Kwan, J.S.H., Chan, S.L., Cheuk, J.C.Y., Koo, R.C.H. (2014). A case study on an open hillside landslide impacting on a flexible rockfall barrier at Jordan Valley, Hong Kong. Landslides, 11: 1037-1050. doi: 10.1007/s10346-013-0461-x
- Lambert, S., Nicot, F. (2011). Rockfall Engineering. Wiley-ISTE.
- Lambert, S., Bourrier, F., Toe, D. (2013). Improving three-dimensional rockfall trajectory simulation codes for assessing the efficiency of protective embankments. International Journal of Rock Mechanics and Mining Sciences, 60: 26-36.
- Mignelli, C., Peila, D., Lo Russo, S., Ratto, S. M., & Broccolato, M. (2014). Analysis of rockfall risk on mountainside roads: Evaluation of the effect of protection devices. Natural Hazards, 73(1): 23-35. doi: 10.1007/s11069-013-0737-4
- Moon, T., Oh, J., Mun, B. (2014) Practical design of rockfall catchfence at urban area from a numerical analysis approach. Engineering Geology, 172: 41-56.
- Muhunthan, B., Shu, S., Sasiharani, N., Hattamleh, O.A., Badger, T.C., Lowell, S.M.,

- Duffy, J.D. (2005). Analysis and design of wire mesh/cable net slope protection. Washington State Transportation Center (TRAC) Report No. WA-RD 612.1, Seattle, Washington, p. 267.
- Muraishi, H., Samizo, M., Sugiyama, T. (2005). Development of a flexible low-energy rockfall protection fence. Quarterly Report of RTRI, 46(3):161-66.
- Neri, M. (1986). Barriere paramassi deformabili ad elevato assorbimento di energia. Quarry and Construction, PEI, Padova, May 1986: 79–85.
- Nicot, F., Cambou, B., Mazzoleni, G. (2001). From a constitutive modelling of metallic rings to the design of rockfall restraining nets. International Journal for Numerical and Analytical Methods in Geomechanics, 25: 49–70.
- Oggeri, C., Tosco, P. (2005). Identificazione del rischio per fenomeni di caduta massi. GEAM, 2005, 1, 23-32.
- Oggeri C., Peila D., Valfré A. (2006), Dimensionamento di barriere paramassi a rete. Le Strade 10, pp. 158–164.
- Paronuzzi, P., Cocco, A. (1998). Modelli di calcolo per la valutazione dell'energia dissipabile da reti paramassi poco deformabili. GEAM 2008, 2-3, 189-196.
- Peila, D., Pelizza, S., Sassudelli, F. (1998). Evaluation of behaviour of rockfall restraining nets by full scale tests. Rock Mechanics and Rock Engineering. 31(1): 1-24.
- Peila, D., Oggeri, C., Baratono, P. (2006) Barriere paramassi a rete, interventi e dimensionamento. GEAM, Quaderni di studio e documentazione 25, Torino.
- Peila, D., Guardini, C. (2008). Use of the event tree to assess the risk reduction obtained from rockfall protection devices, Natural Hazards Earth System Science 8, 1441–1450.
- Peila, D., Ronco, C. (2009). Technical note: design of rockfall net fences and the new ETAG 027 European guideline. Natural Hazards and Earth System Sciences, 9: 1291–1298.
- Ritchie, A. (1963). Evaluation of rockfall and its control. Highway research record, 17: 13–28.
- Roth, A., Ranta-Korpi, R., Volkwein, A., Wendeler, C. (2007) Numerical modeling

- and dynamic simulation of high-tensile steel wire mesh for ground support under rockburst loading. Proceedings of the 1st Canada-US Rock Mechanics Symposium - Rock Mechanics Meeting Society's Challenges and Demands. Vancouver, Canada; 27-31 May 2007, 2: 1505-1509.
- Sasiharan, N., Muhunthan, B., Badger, T.C., Shu, S., Carradine, D.M. (2006). Numerical analysis of the performance of wire mesh and cable net rockfall protection systems. *Engineering Geology*, 88: 121–132.
- Shi, S.Q., Wang, M., Peng, X.Q., Yang, Y.K. (2013). A new-type flexible rock-shed under the impact of rock block: initial experimental insights. *Natural Hazard and Earth System Sciences*, 13: 3329–38.
- Smith, D.D., Duffy, J.D. (1990). Field Tests and evaluation of rockfall restraining nets. No. CA/TL-90/05, Final Report, CALTRAN, California Department of Transportation, San Luis Obispo, Ca.
- Spadari, M., Giacomini, A., Buzzi, O., Hambleton, J. (2012). Prediction of the bullet effect for rockfall barriers: a scaling approach. *Rock Mechanics and Rock Engineering*, 45(2): 131-144. doi:10.1007/s00603-011-0203-0
- Spadari, M., Kardani, M., De Carteret, R., Giacomini, A., Buzzi, O., Fityus, S., Sloan, S.W. (2013a). Statistical evaluation of rockfall energy ranges for different geological settings of New South Wales, Australia. *Engineering Geology*, 158: 57-65. doi:10.1016/j.enggeo.2013.03.007
- Spadari, M., Giacomini, A., Buzzi, O., Fityus, S. (2013b). Barriers for Cost Effective Rockfall hazard mitigation, Industry Report LP0989965, pag. 360.
- Thoeni, K., Lambert, C., Giacomini, A., Sloan, S.W. (2013). Discrete modelling of hexagonal wire meshes with a stochastically distorted contact model. *Computer & Geotechnics*, 49: 158-69.
- Trad, A., Limam, A., Bertrand, D., Robit, P. (2011). Multi-scale analysis of an innovative flexible rockfall barrier, in *Rockfall engineering* S. Lambert, F. Nicot eds., HOBOKEN: Wiley.
- Turner, A.K., Schuster, R.L. (2013). *Rockfall: characterisation and control*. Transportation Research Board (TRB), pag. 400. ISBN: 0309223121.
- Van Tran, P., Maegawa, K., Fukada, S. (2013). Prototype of a wire-rope rockfall

protective fence developed with three-dimensional numerical modeling. *Computer and Geotechnics*, 54: 84–93.

Volkwein, A. (2004). *Numerische Simulation von flexiblen Steinschlagschutzsystemen*. Ph.D. Diss, Swiss Federal Institute (ETH Zurich), 134 pp., ISBN 3-7281-2986-0F.

Volkwein, A. (2005). Numerical simulation of flexible rockfall protection systems. In *Proceedings of the 2005 ASCE International Conference on Computing in Civil Engineering*, Cancun, Mexico: 1285-95.

Volkwein A., Roth A., Gerber W., Vogel A. Flexible rockfall barriers subjected to extreme loads, *Structural Engineering International* 19 (2009) 327–331.

Volkwein, A., Schellenberg, K., Labiouse, V., Agliardi, F., Berger, F., Bourrier, F., Dorren, L.K.A., Gerber, W., Jaboyedoff, M. (2011). Rockfall characterisation and structural protection - A review. *Natural Hazard and Earth System Sciences*, 11: 2617-2651.